seria wydawnicza:

PRACE

KATEDRY MATERIAŁÓW

INŻYNIERSKICH i BIOMEDYCZNYCH

MIĘDZYNARODOWA

KONFERENCJA NAUKOWA

MATERIAL TECHNOLOGIES IN SILESIA'2022

12-15 CZERWCA 2022, WISŁA

Redaktor naukowy:
dr hab. inż. Mirosław Bonek, Prof. PŚ

Gliwice, 2022

Katedra Materiałów Inżynierskich i Biomedycznych
Wydział Mechaniczny Technologiczny
Politechnika Śląska
ul. Konarskiego 18a, 44-100 Gliwice tel. +48 (32) 2371322

Redakcja techniczna i skład komputerowy:
dr hab. inż. Mirosław Bonek, prof. PŚ

Materiały są opublikowane na podstawie oryginałów dostarczonych przez Autorów, zaopiniowanych przez Zespół Recenzentów.

Wydano za zgodą:
Kierownika Katedry Materiałów Inżynierskich i Biomedycznych
Wydziału Mechanicznego Technologicznego
Politechniki Śląskiej

Wydawca:
Katedra Materiałów Inżynierskich i Biomedycznych
Wydział Mechaniczny Technologiczny
Politechnika Śląska
Gliwice 2022

Seria wydawnicza:
Prace Katedry Materiałów Inżynierskich i Biomedycznych
Wydział Mechaniczny technologiczny
Politechnika Śląska
Publikacja czerwiec 2022

ISBN 978-83-65138-32-3

Spis treści

MIĘDZYNARODOWA KONFERENCJA NAUKOWA

MATERIAL TECHNOLOGIES IN SILESIA

12-16 CZERWCA 2022, WISŁA

Konferencja MATERIAL TECHNOLOGIES IN SILESIA 2020 ma na celu zintegrowanie środowiska naukowego i przemysłowego jak również młodej kadry śląskich ośrodków naukowych zajmujących się tematyką dotyczącą technologii materiałowych. Konferencja daje możliwość wymiany doświadczeń, wiedzy, umiejętności oraz prezentacji dotychczasowego dorobku naukowego, najnowszych rozwiązań technologii materiałowych, projektów prowadzonych z przemysłem, projektów realizowanych w ramach Programów Operacyjnych Inteligentny Rozwój i innych. Ważnym elementem konferencji jest dyskusja nad zagadnieniem planowania jakości wyrobów i technologii wytwarzania, inżynierii jakości procesów wytwórczych, technologicznych aspektów jakości w tym miedzy innymi: materiału, konstrukcji, produktu, jakości badań laboratoryjnych, zarządzania jakością wyrobów i procesów, w tym również w zakresie badań i rozwoju. Konferencja będzie inicjować dyskusję na temat koordynacji badań i wdrożeń technologii materiałowych najbardziej istotnych gospodarczo oraz systemu kształcenia dualnego i oczekiwań przemysłu w stosunku do współczesnego absolwenta uczelni technicznych.

PATRONAT KONFERENCJI

Prof. dr hab. inż. Arkadiusz Mężyk

Rektor Politechniki Śląskiej

ORGANIZATOR KONFERENCJI

Stowarzyszenie Wychowanków Politechniki Śląskiej, Koło Inżynierii Materiałowej przy Oddziale Wydziału Mechanicznego Technologicznego.

WSPÓŁORGANIZATOR

Katedra Materiałów Inżynierskich i Biomedycznych, Wydział Mechaniczny Technologiczny Politechnika Śląska, Gliwice

Katedra Technologii Materiałowych, Wydział Inżynierii Materiałowej, Politechnika Śląska, Katowice,

Sieć Badawcza Łukasiewicz – Instytut Metali Nieżelaznych, Gliwice,

Sieć Badawcza Łukasiewicz – Instytut Metalurgii Żelaza im. Stanisława Staszica, Gliwice,

Sieć Badawcza Łukasiewicz – Instytut Spawalnictwa, Gliwice.

KOMITET NAUKOWY

prof. dr hab. inż. Arkadiusz Mężyk – Politechnika Śląska

dr hab. inż. Anna Timofiejczuk, prof. PŚ – Politechnika Śląska

dr hab. inż. Tomasz Tański, prof. PŚ – Politechnika Śląska

dr hab. inż. Dariusz Bartocha, prof. PŚ – Politechnika Śląska

dr hab. inż. Jacek Górka, prof. PŚ – Politechnika Śląska

dr hab. inż. Bogusław Mendala, prof. PŚ – Politechnika Śląska

prof. dr hab. inż. Adam Zieliński – Sieć Badawcza Łukasiewicz – Instytut Metalurgii Żelaza

dr inż. Barbara Juszczyk– Sieć Badawcza Łukasiewicz – Instytut Metali Nieżelaznych

dr inż. Adam Pietras – Sieć Badawcza Łukasiewicz – Instytut Spawalnictwa

prof. dr hab. inż. Jerzy Wysłocki – Politechnika Częstochowska

dr hab. inż. Tomasz Goryczka, prof. UŚ – Uniwersytet Śląski

KOMITET PROGRAMOWY

dr hab. inż. Mirosław Bonek, prof. PŚ – Politechnika Śląska

dr hab. inż. Marcin Adamiak, prof. PŚ – Politechnika Śląska

dr hab. inż. Grzegorz Matula, prof. PŚ – Politechnika Śląska

dr hab. inż Marek Sroka, prof. PŚ – Politechnika Śląska

dr inż. Wojciech Głuchowski – Sieć Badawcza Łukasiewicz – Instytut Metali Nieżelaznych

dr hab. inż. Jarosław Marcisz – Sieć Badawcza Łukasiewicz – Instytut Metalurgii Żelaza

dr hab. inż. Zygmunt Mikno – Sieć Badawcza Łukasiewicz – Instytut Spawalnictwa

dr inż. Marek Węglowski – Sieć Badawcza Łukasiewicz – Instytut Spawalnictwa

dr inż. Agnieszka Szczotok – Politechnika Śląska

dr hab. inż. Grzegorz Golański, prof. PCz – Politechnika Częstochowska

dr hab. inż. Marcin Nabiałek, prof. PCz – Politechnika Częstochowska

KOMITET ORGANIZACYJNY

dr hab. inż. Mirosław Bonek, prof. PŚ – Stowarzyszenie Wychowanków Politechniki Śląskiej

dr hab. Agata Śliwa, prof. PŚ – Stowarzyszenie Wychowanków Politechniki Śląskiej

mgr inż. Ksenia Czardyban – Stowarzyszenie Wychowanków Politechniki Śląskiej

KOMITET TECHNICZNY

dr hab. inż Marek Sroka, prof. PŚ

dr inż. Rafał Honysz

mgr inż. Weronika Smok

mgr inż. Anna Woźniak

mgr inż. Marta Zaborowska

ZAKRES TEMATYCZNY KONFERENCJI

Materiały inżynierskie

- Stopy metali, materiały narzędziowe, kompozyty, ceramika i szkło, materiały amorficzne, nanomateriały, biomateriały, polimery

Badania własności materiałów inżynierskich

- Własności mechaniczne, zmęczenie materiałów, odporność na pękanie, badania korozyjne i erozyjne, własności trybologiczne

Metodologia badawcza

- Metalografia i analiza obrazu, mikroskopia elektronowa, rentgenowska analiza fazowa

Modelowanie własności materiałów

- Techniki numeryczne, metody statystyczne, CAD/CAM

Procesy wytwarzania

- Odlewanie, metalurgia proszków, spawanie, spiekanie, obróbka cieplna, obróbka powierzchniowa, powłoki i cienkie warstwy, skrawanie, obróbka plastyczna

Jakość w inżynierii materiałowej

- Inżynieria jakości, jakość materiału, jakość procesów wytwórczych, technologiczność, kontrola jakości, kontrola jakości badań laboratoryjnych, zarządzanie jakością wyrobów i procesów

Współpraca z przemysłem w realizacji projektów badawczych

Wdrożenia przemysłowe.

WYDARZENIA TOWARZYSZĄCE

SESJA NAUKOWA:

INNOVATIVE AND ADDITIVE MANUFACTURING TECHNOLOGY – NEW TECHNOLOGICAL SOLUTIONS FOR 3D PRINTING OF METALS AND COMPOSITE MATERIALS

Celem projektu jest stworzenie unikalnej platformy badawczej w zakresie "Innowacyjnych addytywnych technologii produkcji" zajmującej się zagadnieniami interdyscyplinarnymi, które

będą wspierać i wzmacniać długofalową współpracę międzysektorową. Główną ideą projektu jest rozwój współpracy między jednostkami badawczymi i sektorem przemysłowym w ramach wspólnej działalności badawczo-rozwojowej. Cel realizowanego projektu koncentruje się na pracach badawczych w zakresie druku 3D z proszków metali za pomocą technologii selektywnego stapiania wiązką lasera (SLM) i technologii osadzania topionego materiału (FDM). Kluczowe działania w ramach projektu mają na celu zapewnienie dwustronnego transferu unikalnej wiedzy, doświadczeń i know-how zaangażowanych podmiotów, przygotowanie i rozwój długoterminowej strategii współpracy między jednostkami badawczymi a sektorem przemysłowym, prowadzenie wspólnych prac badawczych, wzmocnienie istniejącej współpracy i rozwój nowej współpracy z sektorem przemysłowym - podmiotów z siedzibą w aglomeracji ITI Ostrava oraz utworzenie i rozwój wspólnego ośrodka badawczego. Wartość dodana projektu polega na opracowaniu nowych rozwiązań technologicznych (druk 3D metali i materiałów kompozytowych) oraz innowacyjnych technologii z uwzględnieniem aktualnych wymagań technicznych i technologicznych w przemyśle maszynowym. Projekt umożliwi stworzenie unikalnego zespołu badawczego zdolnego do realizacji konkretnych zadań praktycznych i przeprowadzenie dwukierunkowego transferu wiedzy, doświadczeń i wyników badań do sektora przemysłowego i aplikacji końcowych.

W skład konsorcjum realizującego projekt wchodzą jednostki badawcze: VŠB–Technical University of Ostrava (Czechy) – lider projektu, Klastr aditivní výroby, z. s. (Czechy), Fraunhofer Institut für Werkzeaugmaschinen und Umformtechnik IWU (Niemcy), Politechnika Śląska, University of Žilina (Słowacja) i partnerzy przemysłowi: V-NASS, a. s., Vítkovice – výzkum a vývoj – technické aplikace a. s., BREBECK Composite s. r. o., dk metal prominent s.r.o., Advanced Metal Powders, s. r. o. Projekt jest finansowanych ze środków Unii Europejskiej Republiki Czeskiej w ramach Operational Programme Research, Development and Education w latach 2018-2021.

SESJA NAUKOWA:

INTEGRACJA ZAAWANSOWANYCH METOD BADAWCZYCH, OBLICZENIOWYCH ORAZ PRZETWARZANIA DANYCH DLA INNOWACJI TECHNOLOGII SPAWANIA STALI NIERDZEWNEJ TYPU DUPLEX

W ramach realizowanego projektu utworzono międzynarodowy zespół badawczy, posiadający szeroki zakres wiedzy i doświadczeń praktycznych w dziedzinie spawania, charakterystyki materiałów, komputerowego wspomagania prac inżynierskich, modelowania predykcyjnego opartego na zjawiskach fizycznych/chemicznych oraz przetwarzania dużych zbiorów danych (big data), aby sprostać nadchodzącym wyzwaniom, przed którymi staje obecnie zarówno przemysł jak i świat nauki w zakresie badań naukowych i prac badawczo-rozwojowych, dotyczących stali nierdzewnych typu duplex. Wymaga to specjalistycznej wiedzy i innowacji, zaawansowanego sprzętu i metod oraz opłacalnych rozwiązań, które można rozwinąć dzięki międzynarodowej współpracy. Prace naukowe prowadzone w ramach projektu obejmują badania podstawowe w zakresie spawania stali nierdzewnych typu duplex w jedno- i różnoimiennych konfiguracjach materiałowych, a także opracowanie nowych technologii i rozwiązań materiałów z tym związanych. Projekt prowadzony jest w ramach akcji RISE przez zespół 8 partnerów, w tym pięciu z krajów europejskich i trzech z krajów azjatyckich, przy szeroko zakrojonej akcji wymiany naukowców (33 naukowców i 110 osobomiesięcy) przez okres 4 lat, tak aby w pełni wydobyć komplementarną siłę i synergię działań w ramach powstałego konsorcjum badawczego. Projekt obejmuje wspólne badania nad spawaniem stali nierdzewnej typu duplex przy użyciu nowoczesnego systemu wymiany danych, wyników eksperymentalnych i predykcyjnego modelowania fizycznego, w celu opracowania nowych materiałów i procesów przetwarzania tych stali. W ramach projektu zostanie opracowany uporządkowany system danych dla kluczowych składników strukturalnych/fazowych powstających w trakcie spawania i korozji stali typu duplex. Kolejnym etapem realizacji projektu będzie ustalanie optymalnych warunków spawania zapewniających wysokie własności mechaniczne i odporność korozyjną przy pomocy hybrydowej metodyki komputerowego wspomagania (CAD/CAM) i modelowania fizycznego materiałów. Uzyskane dane i zaawansowane techniki badawcze zostaną wykorzystane do opracowania nowej

technologii wytwarzania zapewniającej kontrolę struktury, występujących faz wtórnych oraz wad spawalniczych, w szczególności w strefie wpływu ciepła (SWC), która stanowi najbardziej krytyczny/ograniczający czynnik w trakcie przetwarzania i stosowania stali nierdzewnych typu duplex oraz innych materiałów metalowych. Prowadzone prace będą zorientowane na zastosowaniu nowoczesnych technologii przetwarzania danych i modelowania predykcyjnego w opracowaniu nowych/hybrydowych systemów materiałowych dla znaczącej redukcji ich wagi oraz kosztów. Powstały w ten sposób zaawansowany system danych, nowych materiałów, procesów spawania i hybrydowych lekkich materiałów przyczynią się do zwiększenia potencjału badawczego i innowacyjnego w Europie i na świecie w zakresie stali nierdzewnych typu duplex oraz związanych z nimi systemów o długoterminowym wpływie na aspekty gospodarcze i społeczne. Opracowany w ramach projektu zaawansowany system danych będzie służyć jako platforma bazowa dla przyszłych badań naukowych i innowacji przemysłowych, przyspieszając cykl opracowania nowych materiałów, technologii lub produktów, z zasadniczym wkładem w badania naukowe i przemysłowe prace badawczo-rozwojowe. Zwiększy to również potencjał badawczy i innowacyjny w zakresie interdyscyplinarnych i międzysektorowych działań partnerów projektu umożliwiając wspólne opracowanie przełomowych rozwiązań technologicznych. Prowadzone prace będą łączyć nowatorskie podejście w zakresie innowacji i prac badawczo-rozwojowych, co przyczyni się do rozwoju nowoczesnego Przemysłu 4.0 w zakresie spawania i znacznie przyspieszy rozwój umiejętności badawczych, wiedzy oraz kariery młodych naukowców w zakresie łańcuch dostaw zorientowany na klienta (ECR) z trwałym wpływem w UE i poza nią.

W projekt są zaangażowane: Liverpool John Moores University (Wielka Brytania) jako koordynator projektu, międzynarodowe jednostki naukowo-badawcze: Politechnika Śląska (Polska), Hogskolan Vast (Szwecja), Electric Welding Institute of the National Academy of Sciences of Ukraine (Ukraina), Yanshan University (Chiny), University of Malaya (Malezja) oraz partner przemysłowy Ermetal Otomotiv Ve Esya Sanayi Tic. A.S. (Turcja).

MIĘDZYNARODOWA STUDENCKA KONFERENCJA NAUKOWA

TALENTDETECTOR2022_SUMMER

Tempo zmian cywilizacyjnych, głównie w wyniku postępu technologicznego, sprawia, że uczelnia i osoby przez nią kształcone muszą elastycznie reagować na pojawiające się zmiany na rynku pracy i dostosowywać się do nowych wyzwań i wymagań. Studentów oraz nauczycieli akademickich charakteryzuje ciekawość poznawcza i determinacja w podejmowaniu działań w zakresie własnych zainteresowań i nie rzadko dla własnej przyjemności, w oparciu o wiedzę oraz doświadczenie zawodowe oraz stopniowo uzyskiwane dodatkowe umiejętności, które w efekcie pozwalają na osiągnięcie zamierzonego celu. Wychodząc naprzeciw wyżej wspomnianym oczekiwaniom studentom proponuje się dodatkową aktywność w ramach działalności studenckich kół naukowych oraz realizacji zajęć w firmie PBL. Zaangażowanie w prace naukowe daje studentom możliwość pełniejszej i szerszej realizacji prac przejściowych i dyplomowych w zakresie tematyki związanej z kierunkiem studiów. Ponadto działalność taka stwarza różnorodne możliwości organizacyjne np. opracowywanie wyników badań i ich prezentacji zarówno podczas spotkań naukowych, jak również w trakcie zjazdów integracyjnych czy wizyt w przedsiębiorstwach wykorzystujących nowoczesne technologie produkcyjne. Jedną z form działalności dydaktycznej nowoczesnych uczelni, rozszerzającą możliwości pozyskiwania wiedzy, jest uczestnictwo w konferencjach naukowych. Jedną z takich propozycji jest Międzynarodowa Studencka Konferencja Naukowa TalentDetector2022_Summer mająca na celu zintegrowanie środowiska studenckiego i naukowego oraz młodej kadry śląskich ośrodków naukowych zajmujących się tematyką dotyczącą technologii materiałowych. Jest to miejsce dające możliwość wymiany doświadczeń, wiedzy, umiejętności oraz prezentacji dotychczasowego dorobku naukowego rozwijające i poszerzające zainteresowania studentów w zakresie inżynierii materiałowej, inżynierii powierzchni, biomateriałów i inżynierii biomedycznej, nanotechnologii, technologii proekologicznych oraz komputerowej nauki o materiałach. Konferencja pozwala przedstawienie projektów prowadzonych z przemysłem, w ramach działalności Studenckich Kół Naukowych, doktoratów wdrożeniowych oraz projektów realizowanych w formie PBL – Project Based Learning.

MTS CONFERENCE
MATERIAL TECHNOLOGIES IN SILESIA

12-15.06.2022
Crystal Mountain***** Hotel, Wisła, Poland

The anticorrosion properties of entropy stabilized $Al_{85}(Ni,Fe,Cr,Cu)_{10}Y_5$ amorphous and nanocrystalline alloys

R. Babilas[a], K. Młynarek-Żak, A. Radoń, W. Łoński

[a] Silesian University of Technology, Faculty of Mechanical Engineering, Department of Engineering Materials and Biomaterials
email: rafal.babilas@polsl.pl

Abstract: An entropy stabilized $Al_{85}(Ni,Fe,Cr,Cu)_{10}Y_5$ alloys were synthesized by induction melting, copper mold casting, and melt-spinning. The chemical compositions of the alloys were proposed in the optimization of thermodynamic parameters. The formation of a fully amorphous structure was possible for three alloys $Al_{85}Ni_{10}Y_5$, $Al_{85}(Ni, Fe)_{10}Y_5$, and $Al_{85}(Ni, Fe, Cu)_{10}Y_5$ in a form of melt-spun ribbons. Samples in the form of induction melted ingots and copper mold casted plates showed multiphase crystalline structures, which were confirmed by XRD and Mössbauer spectroscopy. A crystallization mechanism was proposed on the DTA heating and cooling curves. Additionally, electrochemical corrosion resistance tests were performed, which demonstrated the beneficial effect of the addition of copper and chromium to the alloys studied. In the case of plates, the $Al_{85}Ni_5Fe_5Y_5$ alloy was characterized by the best corrosion resistance in a 3.5% NaCl solution.

Keywords: Al-based alloys, thermodynamics, X-ray diffraction, electrochemical measurements

1. INTRODUCTION

Al-based alloys with an amorphous and nanocrystalline structure are characterized by favourable mechanical properties and corrosion resistance compared to those of crystalline Al-based alloys. Relatively better properties resulted, among others, from chemical homogeneity and the absence of defects in the structure [1,2]. Structural changes affect the properties of alloys and depend on the chemical composition and cooling rate of the liquid state [3]. Rapid solidification techniques provide one with the ability to obtain bulk metallic glasses (BMGs). These technologies include high-pressure casting and the melt-spinning method [2]. Data from the literature indicate chemical compositions with fully amorphous structure, such as Al-Ni-Y [4], Al-Ni-Fe [5], and Al-Y-Fe [6]. Al-based alloys with the addition of rare-earth and transition metals indicate many beneficial effects such as grain fragmentation (Fe, Cr), high corrosion resistance (Cr, Cu), high strength (Cu, Y), high hardness (Cr, Ni, Cu), good mechanical properties at higher temperatures (Fe, Cr), which determine a promising application of this group of materials, i.e. in aerospace engineering [3].

2. MATERIALS AND METHODS

Master alloys with nominal compositions were prepared by induction melting pure metals (more than 99.9%) in an a ceramic crucible in argon atmosphere. Ribbons and plates were prepared by remelting the master alloys in quartz crucibles and injection-casting onto a rotating Cu wheel or into a Cu mold, respectively.
Phase identification was performed using X-ray diffraction (XRD). XRD patterns were recorded using a diffractometer equipped with a copper tube as an X-ray radiation source. To determine how the composition and casting method influenced the structure and local Fe environment, we used Mössbauer spectroscopy (MS) as a complementary technique.

To determine the crystallization mechanism, differential thermal analysis (DTA) of the master alloys was performed. The DTA curves were recorded at a cooling rate of 20 K/min under a protective argon atmosphere. Electrochemical measurements were carried out in 3.5% NaCl solution using an Autolab 302N potentiostat equipped with a three-electrode cell. A saturated calomel electrode was used as the reference electrode, and a platinum rod was used as the counter electrode. The corrosion resistance was evaluated by recording the variation

of the open circuit potential (E_{OCP}). Samples were measured after 3600 s of open-circuit potential stabilization at a scan rate of 1 mV s^{-1}.

3. RESULTS

The effect of the chemical composition on the corrosion properties was described, which demonstrated the beneficial effect of the addition of copper to the master alloys. However, the $Al_{85}Ni_5Fe_5Y_5$ alloy in the form of plates showed high corrosion resistance in 3.5% NaCl solution. The best anticorrosion properties were also achieved for amorphous $Al_{85}(Ni, Fe)_{10}Y_5$ ribbons. The surface morphology of the $Al_{85}Ni_{10}Y_5$, $Al_{85}Ni_5Fe_5Y_5$, and $Al_{85}Ni_{3.33}Fe_{3.33}Cr_{3.33}Y_5$ alloys in the form of ingots and plates after the corrosion process is shown in Figure 1 using a light microscope. The phenomenon of pitting corrosion can be observed. The mechanism of corrosion revealed the fragmentation of the structure of the plates, which is the result of rapid solidification technology.

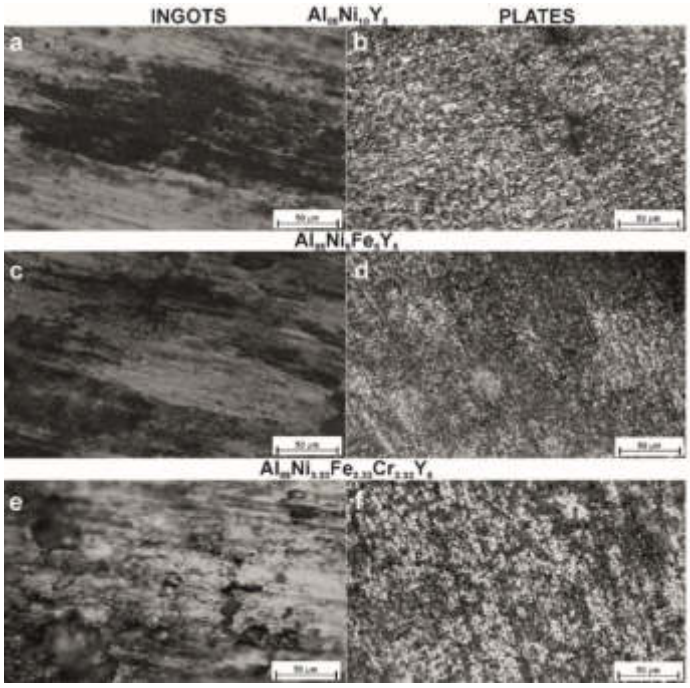

Figure 1. Surface morphology of master alloys and plates $Al_{85}Ni_{10}Y_5$ (a,b), $Al_{85}Ni_5Fe_5Y_5$ (c,d), $Al_{85}Ni_{3.33}Fe_{3.33}Cr_{3.33}Y_5$ (e,f) after electrochemical measurements in a 3.5% NaCl solution at 25 °C

Acknowledgments: The work was supported by the National Science Centre of Poland under research project no. 2018/29/B/ST8/02264.

BIBLIOGRAPHY

1. R. Jindal, V.S. Raja, M.A. Gibson, M.J. Styles, T.J. Bastow, C.R. Hutchinson, Effect of annealing below the crystallization temperature on the corrosion behavior of Al-Ni-Y metallic glasses, Corros. Sci. 84 (2014) 54–65.
2. A. Inoue, H. Kimura, Fabrications and mechanical properties of bulk amorphous, nanocrystalline, nanoquasicrystalline alloys in aluminum-based system, J. Light Met. 1 (2001) 31–41.
3. Y. Shen, J.H. Perepezko, Al-based amorphous alloys: Glass-forming ability, crystallization behavior and effects of minor alloying additions, J. Alloys Compd. 707 (2017) 3–11.
4. L.M. Zhang, S.D. Zhang, A.L. Ma, H.X. Hu, Y.G. Zheng, B.J. Yang, J.Q. Wang, Thermally induced structure evolution on the corrosion behavior of Al-Ni-Y amorphous alloys. Corros. Sci. 144 (2018) 172–183.
5. A. Inoue, Y. Horio, T. Masumoto, New Amorphous Al-Ni-Fe and Al-Ni-Co Alloys. Mater. Trans. JIM. 34 (1993) 85–88.
6. R. Babilas, M. Spilka, K. Młynarek, W. Łoński, D. Łukowiec, A. Radoń, M. Kądziołka-Gaweł, P. Gębara, Glass-forming ability and corrosion resistance of $Al_{88}Y_{8-x}Fe_{4+x}$ (x= 0, 1, 2 at.%) alloys. Materials (Basel). 14 (2021) 1–12.

MTS CONFERENCE
MATERIAL TECHNOLOGIES IN SILESIA

12-15.06.2022
Crystal Mountain***** Hotel, Wisła, Poland

Influence of annealing conditions on changes of the structure and selected properties of $Al_{88}Y_7Fe_5$ and $Al_{88}Y_6Fe_6$ alloys

R. Babilas, M. Spilka[a], W. Łoński, A. Radoń, M. Kądziołka-Gaweł, P. Gębara

[a] Silesian University of Technology, Faculty of Mechanical Engineering, Department of Engineering Materials and Biomaterials
email: monika.spilka@polsl.pl

Abstract: The article describes the influence of heat treatment on the structural changes and selected properties of Al-Y-Fe metallic glasses in the form of ribbons. The structure of the $Al_{88}Y_7Fe_5$ and $Al_{88}Y_6Fe_6$ alloys was examined by X-ray diffraction (XRD) and Mössbauer spectroscopy (MS). The corrosion resistance of the samples was investigated using polarization tests. The magnetic properties of Al-based alloys were also explored.

Keywords: Al-Y-Fe metallic glasses, heat treatment, structural tests, corrosion resistance, magnetic properties

1. INTRODUCTION

Low density, high strength, anti-wear and anticorrosion alloys are widely desired in aerospace, automobile, home appliances and architecture. Al-based amorphous alloys are characterized by the higher strength-to-weight ratio, better wear and corrosion resistance, and more flexible alloy composition than many conventional crystalline aluminum alloys, which makes this material attractive for practical applications [1,2].

The properties of metallic glasses, including those based on Al, are directly related to the metastable amorphous structure of the glasses. During thermal activation, the amorphous structure decomposes, which affects changes in mechanical, magnetic and electrochemical properties of metallic glasses [3-5].

Heat treatment of amorphous alloys may consist of structural relaxation annealing, partially devitrified annealing and fully crystallized annealing. Fully crystallized annealing leads to the deterioration of the intrinsic high corrosion resistance of amorphous alloys. Structural relaxation annealing and partially devitrified annealing, in some cases, can retain the good mechanical and electrochemical properties of the amorphous alloys. Sometimes, by heat treatment, even more superior properties by choosing appropriate temperature and duration time of annealing. However, the reasons for the improved corrosion resistance and other properties after structural relaxation annealing are still being discussed, and therefore further research is needed in this area [1,4,6].

2. MATERIALS AND METHODS

Studies were carried out on $Al_{88}Y_7Fe_5$ and $Al_{88}Y_6Fe_6$ alloys in the form of ribbons. The master alloy was prepared by induction melting the mixtures of commercially pure elements in a ceramic crucible in an argon atmosphere. The samples were obtained by melt spinning at a wheel speed of 30 m/s. The ribbons were annealed for 30 minutes at 200, 250 and 300 °C and then cooled under an argon atmosphere.

The structure of $Al_{88}Y_7Fe_5$ and $Al_{88}Y_6Fe_6$e6 alloys in the cast state and in the annealed state was tested using the X-ray diffraction (XRD) method and Mössbauer spectroscopy (MS). Electrochemical corrosion investigations were conducted in 3.5% NaCl solution at room temperature in 1 hour. The corrosion resistance of samples in the cast state and in the annealed state was examined by polarization tests. The surface morphology of the samples after electrochemical tests was analyzed using scanning electron microscopy (SEM). Furthermore, investigations of magnetic properties of $Al_{88}Y_7Fe_5$ and $Al_{88}Y_6Fe_6$ alloys after annealing were carried out on a vibrating sample

magnetometer (VSM). The analysis was carried out over the magnetic field range of 6 T to 6 T, and included coercive force and saturation magnetization, which were determined from hysteresis loops.

3. RESULTS

The electrochemical results obtained from measurements in 3.5% NaCl solution at 25 °C for $Al_{88}Y_7Fe_5$ and $Al_{88}Y_6Fe_6$ alloys in the form of ribbons in as-cast state and as-annealed are presented in Figure 1. The open circuit potential (E_{OCP}) of all samples during the whole immersion time showed unstable behavior. After 3,600 s, the better E_{OCP} values were recorded for the $Al_{88}Y_6Fe_6$ and $Al_{88}Y_7Fe_5$ alloys after annealing at 300 °C and 200 °C, respectively, than in as-cast state.

Based on the polarization tests (Figure 1a,b), it was concluded that the electrochemical properties are better for $Al_{88}Y_6Fe_6$ alloys after annealing at 300 °C.

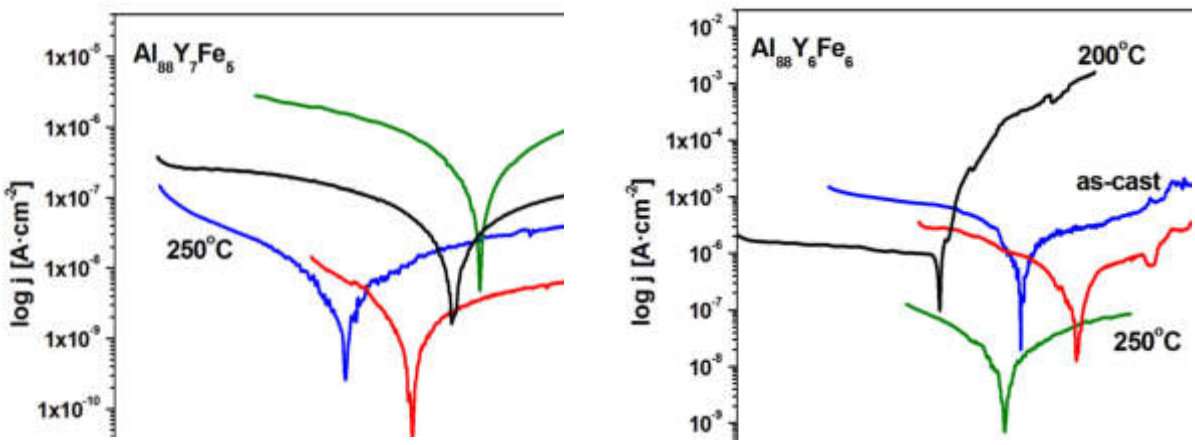

(a) (b)

Figure 1. Variation of the polarization curves in 3.5 % NaCl solution at 25 °C of $Al_{88}Y_7Fe_5$ alloy (a) and $Al_{88}Y_6Fe_6$ alloy (b)

Acknowledgments: The work was supported by National Science Centre, Poland under research project no.: 2018/29/B/ST8/02264.

BIBLIOGRAPHY

1. L.M. Zhang, S.D. Zhang, A.L. Ma, H.X. Hu, Y.G. Zheng, B.J. Yang, J.Q. Wang, Thermally induced structure evolution on the corrosion behavior of Al-Ni-Y amorphous alloys, Corrosion Science 144 (2018) 172-183.
2. S.Y. Kim, G.Y. Lee, G.H. Park, H.A. Kim, A.Y. Lee, S. Scudino, K. Gokuldoss Prashanth, D.H. Kim, J. Eckert, M.H. Lee, High strength nanostructured Al-based alloys through optimized processing of rapidly quenched amorphous precursors, Scientific Reports 8 (2018) 1090.
3. R. Jindal, V.S. Raja, M.A. Gibson, M.J. Styles, T.J. Bastow, C.R. Hutchinson, Effect of annealing below the crystallization temperature on the corrosion behavior of Al–Ni–Y metallic glasses, Corrosion Science 84 (2014) 54-65.
4. J.H. Perepezko, M. Gao, J.Q. Wang, Nanoglass and nanocrystallization reactions in metallic glasses, Frontiers in Materials 8 (2021) 663862.
5. C. Fan, X. Yue, A. Inoue, C.T. Liu, X. Shen, P.K Liaw, Recent topics on the structure and crystallization of Al-based glassy alloys, Materials Research 22 (2019) e20180619.
6. A. Aronin, D. Matveev, E. Pershina, V. Tkatch, G. Abrosimova, The effect of changes in Al-based amorphous phase structure on structure forming upon crystallization, Journal of Alloys and Compounds 715 (2017) 176-183.

MTS CONFERENCE
MATERIAL TECHNOLOGIES IN SILESIA

12-15.06.2022
Crystal Mountain***** Hotel, Wisła, Poland

Structure and properties of M300 maraging steel fabricated by SLM for cold work tools application

M. Benedyk*, M. Król, T. Tański

Silesian University of Technology, Faculty of Mechanical Engineering, Department of Engineering Materials and Biomaterials
*email: marcin.benedyk@polsl.pl

Abstract:

In the presented work, maraging steel, classified as cold work tools, was used in the Selective Laser Melting process for die-cutting components. As participating hardening steel, a one and two stages heat treatment i.e. solution annealing at 820°C for 1 h, followed by aging at 490°C for soaking time 6 h, was utilised to improve mechanical properties and wear resistance. Research was conducted to determine the influence of heat treatment microstructure, impact resistance, tensile strength and hardness. The tensile strength of M300 increased from 1078 MPa (solution annealed) to 2020 MPa after the aging process. Tensile strength of 2090 MPa was obtained after a full heat treatment at 490 °C/6 h. After the SLM process, the component fabricated from M300 steel was characterised by a tensile strength of 1175 MPa.

Keywords: maraging steel, structure, mechanical properties, additive manufacturing, SLM

1. INTRODUCTION

Additive manufacturing (AM), namely selective laser melting (SLM) technology, allows to create complex components that can be customised in different ways (topological optimization, lightweight construction, lattice structures, etc.). Components manufactured by SLM are near full density and have mechanical properties almost the same as bulk material. SLM technology works on the basis of melting the individual layers to each other (layer-by-layer) directly from metallic powder, which creates thermal gradients that permeate the previously molten layer.

The presented results indicate that the SLM technique and properly selected heat treatment gives a possibilities for to receive cold work tools with high accuracy, high speed and at low costs and own outlays. Moreover, this technique gives the constructors possibilities to design very complicated shapes of profiles with more than one of the working areas.

Figure 1. Punch and matrix produced by SLM.

Acknowledgments: The research is co-financed under the Program of the Ministry of Science and Higher Education "Implementation Doctorate". The presented results were developed within the framework of the project: Innovative and additive manufacturing technology—new technological solutions for 3D printing of metals and composite materials, reg. No. CZ.02.1.01/0.0/0.0/17_049/0008407 financed by Structural Funds of the European Union.

BIBLIOGRAPHY

1. Thompson, S.M.; Bian, L.; Shamsaei, N.; Yadollahi, A. An overview of Direct Laser Deposition for additive manufacturing; Part I: Transport phenomena, modeling and diagnostics. Addit. Manuf., 8, 36–62. (2015)
2. Król, M.; Snopinski, P.; Czech, A. The phase transitions in selective laser-melted 18-NI (300-grade) maraging steel. J. Therm. Anal. Calorim, 1–8 (2020)

MTS CONFERENCE
MATERIAL TECHNOLOGIES IN SILESIA

12-15.06.2022
Crystal Mountain***** Hotel, Wisła, Poland

Laserowo wspomagane formowanie związków międzymetalicznych Ti_xAu_y do zastosowań biomedycznych

O. Bialas[a], K. Buczek [b], M. Adamiak[c]

[a] Politechnika Śląska, Wydział Mechaniczny Technologiczny, Katedra Materiałów Inżynierskich i Biomedycznych
[b] Międzynarodowe Centrum Słuchu i Mowy Medincus,
[c] Politechnika Śląska, Wydział Mechaniczny Technologiczny, Laboratorium Badania Materiałów

email: oktawian.bialas@polsl.pl

Abstract: Celem niniejszej pracy było sprawdzenie możliwości otrzymania międzymetalicznych związków Ti oraz Au, przy pomocy powierzchniowej obróbki laserowej. Międzymetaliczne związki takie jak Ti3Au charakteryzują się znacznie polepszonymi własnościami mechanicznymi, elektrycznymi oraz mniejszą podatnością na działanie czynników korozyjnych, co przekłada się na rozszerzenie cyklu życia implantu w środowisku biologicznym takim jak żywy organizm. W obszarze szczególnego zainteresowania autorów połączenie tytanu oraz złota przedstawia się jako obiecujący materiał dla implantów układu sercowo-naczyniowego takich jak pompy wspomagania pracy serca, w ortopedii – endoprotezy czy w otolaryngologii – w zabiegach na uchu środkowym. W toku badań Ti jako materiał bazowy został pokryty elektrochemicznie mikrometryczną warstwą złota a następnie został poddany obróbce laserowej w szeregu parametrów. Zmienność obejmowała zarówno moc wiązki lasera jak i szybkość posuwu wiązki. Otrzymane wyniki pozwoliły na ocenę stopnia oraz rodzaju połączenia materiału powłoki z materiałem bazowym. Wyniki eksperymentu potwierdzają, że wytworzenie stałego, międzymetalicznego połączenia jest możliwe oraz powinno zostać zoptymalizowane w kierunku maksymalizacji powstawania specyficznej fazy Ti_3Au, która zapewnia najlepsze własności mechaniczne. W trakcie badań została przeprowadzona analiza mikroskopii świetlnej, skaningowej mikroskopii elektronowej SEM, analiza EDS a także analiza XRD.

Keywords: TiAu, Tytan, złoto, mikroobróbka laserowa

1. INTRODUCTION

Choroby układu krążenia są nadal główną przyczyną zgonów w Polsce i na świecie, jak wynika z najnowszych danych WHO [1], stanowiąc około 30% umieralności. Mimo upływu lat stan ten nie ulega zadowalającej poprawie. Nie każdy pacjent z chorobami układu sercowo-naczyniowego kwalifikuje się do przeszczepu lub przeżyje wystarczająco długo, aby poddać się zabiegowi transplantacji. Istnieje potrzeba tworzenia/ulepszania i projektowania materiałów i urządzeń, które umożliwiają czasowe lub stałe funkcjonowanie w stanie osłabienia funkcji pracy serca lub układu krążenia [2]. Instrumenty zaprojektowane głównie w celu zwiększenia wydajności pompowania serca w przypadku jego nieprawidłowego działania to urządzenia wspomagające pracę komór (VAD - Ventricular Assist Devices) oraz urządzenia do całkowitej sztucznej protezy serca (TAH - Total Artificial Heart)[3]. Zastosowanie układu TiAu wydaje się również możliwe w przypadku innych dziedzin medycyny. W ortopedii – endoprotezy, w otolaryngologii – w zabiegach na uchu środkowym - protezy stosowane w stapedotomii; protezy typu PORP lub TORP. W toku badań Autorzy podjęli próbę modyfikacji warstwy wierzchniej Tytanu (Ti) – najczęściej stosowanego materiału biomedycznego we współczesnej medycynie, wzbogacając go w metal szlachetny – Złoto (Au)[4]. Naniesiona elektrochemicznie warstwa została poddana obróbce laserowej w celu przetopienia powłoki z materiałem podłoża, które pozwoliło na uzyskanie połączenia międzymetalicznego oraz wytworzenie materiału o korzystniejszych własnościach w stosunku do materiału rodzimego. Badania wykazują, że otrzymany materiał charakteryzuje się zwiększoną odpornością na korozję, hydrofilowym charakterem

powierzchni, oraz odmiennym – bardziej korzystnym osadzaniem się oraz konsolidacją biofilmu w środowisku tkankowym, co zapewni dłuższy cykl życia produktu w miejscu swojego przeznaczenia – organizmie żywym[5].

1.1. Przebieg eksperymentu

Próbki wykonane z komercyjnie czystego Tytanu (Ti grade 2) (Wolften, Wrocław, Polska) w formie krążków zostały poddane mechanicznej obróbce za pomocą szlifowania i polerowania w celu otrzymania jednorodnie płaskiej powierzchni, zgodnie z metodyką prezentowaną we wcześniejszych artykułach [4,6]. Następnie, na próbki została naniesiona elektrochemicznie mikrometryczna warstwa złota. Tak przygotowany materiał został poddany obróbce laserowej w szeregu parametrów mających na celu dobór najbardziej korzystnych dla tworzenia się warstw TiAu, zarówno pod kątem składu chemicznego, fazowego jak i głębokości przetopu. Zmienność parametrów realizowana była zarówno w aplikowanej mocy wiązki, jak i prędkości posuwu oraz sposobie ogniskowania. Całość była realizowana w atmosferze gazu ochronnego. Schemat przebiegu obróbki laserowej został zaprezentowany na Rysunku nr 1.

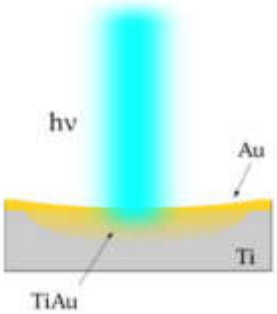

Rysunek 1 Schemat eksperymentu, obróbka laserowa tytanu z naniesioną warstwą złota

Gotowy materiał pocięto w przekrojach oraz poddano analizie przy pomocy mikroskopii świetlnej, SEM wraz ze wstępną analizą składu EDS, oraz badaniom rentgenowskiej analizy fazowej XRD. Wyniki badań pozwoliły na dobór najlepszych parametrów oraz wstępną analizę składu fazowego otrzymanego materiału. Wykazano, że uzyskanie międzymetalicznych związków Ti oraz Au jest możliwe w zadanych parametrach. Obecność struktury dendrytycznej oraz zmienność składu procentowego dla najbardziej korzystnego wariantu waha się w zakresie użytecznym od 50% do 30% Au wagowo w funkcji odległości od powierzchni co pozwala na dalszą identyfikację procesów zachodzących w układzie TiAu, stopowanym wiązką lasera. Szybkość nagrzewania oraz intensywność powodowanych w trakcie procesu ruchów konwekcyjnych wydaje się mieć kluczowe znaczenie dla charakteru finalnie uzyskiwanych warstw oraz kinetyki przemian fazowych.

Acknowledgments: Co-financed by the European Union through the European Social Fund (grant POWR.03.05.00-00-Z305).

BIBLIOGRAPHY

1. Https://Www.Who.Int/Healthinfo/Statistics/En/ (25.05.2020).
2. Szczeklik, A.; Gajewski, P.; Wydawnictwo Medycyna Praktyczna *Interna Szczeklika 2018*; Medycyna Praktyczna: Kraków, 2018; ISBN 978-83-7430-547-1.
3. Chaanine, A.H.; Pinney, S.P. Mechanical Circulatory Support as a Bridge to Heart Transplantation. In *Heart Failure*; Eisen, H., Ed.; Springer London: London, 2017; pp. 639–663 ISBN 978-1-4471-4218-8.
4. Bialas, O.; Poloczek, T.; Lis, M.; Skowronek, A.; Górka, J.; Adamiak, M. Laser Assisted Size Reduction of Gold (Au) Particles onto a Titanium (Ti) Substrate Surface. *Applied Sciences* **2021**, *11*, 8755, doi:10.3390/app11188755.
5. Gu, X.; Xu, Z.; Gu, L.; Xu, H.; Han, F.; Chen, B.; Pan, X. Preparation and Antibacterial Properties of Gold Nanoparticles: A Review. *Environ Chem Lett* **2020**, doi:10.1007/s10311-020-01071-0.
6. Woźniak, A.; Staszuk, M.; Reimann, Ł.; Bialas, O.; Brytan, Z.; Voinarovych, S.; Kyslytsia, O.; Kaliuzhnyi, S.; Basiaga, M.; Admiak, M. The Influence of Plasma-Sprayed Coatings on Surface Properties and Corrosion Resistance of 316L Stainless Steel for Possible Implant Application. *Archiv.Civ.Mech.Eng* **2021**, *21*, 148, doi:10.1007/s43452-021-00297-1.

MTS CONFERENCE
MATERIAL TECHNOLOGIES IN SILESIA

12-15.06.2022
Crystal Mountain***** Hotel, Wisła, Poland

Wpływ gęstości mocy przetapiania laserowego na jakość powłoki Au osadzanej elektrochemicznie na podłożu Ti

O. Bialas[a], M. Wala[c], T. Poloczek[d], M. Adamiak[d]

[a] Politechnika Śląska, Wydział Mechaniczny Technologiczny, Katedra Materiałów Inżynierskich i Biomedycznych
[b] Politechnika Śląska, Wydział Chemiczny, Katedra Chemii Nieorganicznej, Analitycznej i Elektrochemii
[c] Politechnika Śląska, Wydział Mechaniczny Technologiczny, Katedra Spawalnictwa
[d] Politechnika Śląska, Wydział Mechaniczny Technologiczny, Laboratorium Badania Materiałów

email: oktawian.bialas@polsl.pl

Abstract: Celem niniejszej pracy była analiza wpływu parametrów powierzchniowej obróbki laserowej na jakość powierzchni układu TiAu stopowanego laserowo. Powierzchnia materiału, będąc miejscem kontaktu detalu ze środowiskiem, jest najbardziej newralgicznym obszarem, warunkującym możliwy czas prawidłowego działania urządzenia. W przypadku metalicznych materiałów biomedycznych, pracujących w silnie korozyjnym środowisku płynów ustrojowych, ma to tym większe znaczenie, w związku z koniecznością (w przypadku niewłaściwego działania) reoperacji obarczonej ryzykiem powikłań. W obszarze szczególnego zainteresowania autorów niniejszej pracy znajduje się wykorzystanie połączenia tytanu oraz złota do zastosowań wewnątrzustrojowych - do urządzeń mających permanentny kontakt z krwią. Badany materiał wykonany z Tytanu (Ti) został pokryty elektrochemicznie mikrometryczną warstwą złota, a następnie został poddany obróbce laserowej w szeregu parametrów procesowych. Zmienność obejmowała zarówno moc wiązki lasera jak i szybkość wiązki oraz jej ogniskowanie. Otrzymane w konsekwencji takiej obróbki materiału powierzchnie zostały poddane analizie przy pomocy mikroskopii świetlnej. Zauważono wyraźną zależność otrzymanych mikrostruktur od parametrów obróbki laserowej. Analiza mikroskopowa pozwoliła na ocenę udziału strefy wpływu ciepła, stopnia dendrytyczności materiału oraz obecności kumulowania wad hartowniczych. Uzyskane wyniki pozwoliły przeprowadzić dobór parametrów obróbki laserowej i przejść do analizy składu fazowego w przekrojach.

Keywords: obróbka laserowa, TiAu, Ti, Au, złoto, tytan

1. INTRODUCTION

We współczesnej medycynie złoto w postaci nanocząstek zyskuje coraz większą popularność ze względu na możliwość wykorzystania go jako skutecznego systemu dostarczania leków/genów [1]. Odpowiednio związane cząstki złota w postaci soli służą do obrazowania guzów nowotworowych oraz jako nośniki leków w terapiach przeciwnowotworowych. Ponadto, badania wykazują, że powierzchnia złota w odróżnieniu od powierzchni tytanowej, tworzy skonsolidowaną, gęstą i stałą w czasie warstwę biofilmu, co ma istotne znaczenie dla stabilności implantu [2,3]. Próba wytworzenia wielowarstwowego układu TiAu na materiale bazowym dzięki przetopieniu wiązką laserową doprowadzi do wytworzenia cienkiej powłoki, która dzięki wytworzeniu się połączenia międzymetalicznego będzie prezentowała kombinację zalet konwencjonalnie stosowanego tytanu oraz złota na ściśle wybranej głębokości od powierzchni materiału, stosownie do przewidywanej potrzeby stosowania. Poza ściśle określonym składem fazowym, jednorodność powierzchni, brak pęknięć czy lokalnej zmiany składu powierzchni materiału jest czynnikiem warunkującym prawidłowe osadzenie się warstwy biofilmu, bez tworzenia się korozji lokalnej i wżerowej. W niniejszej pracy dokonano przeglądu otrzymanych mikrostruktur powierzchni w zależności od zestawu parametrów stosowanych do obróbki powierzchniowej materiału Ti z elektrochemicznie nałożoną powłoką Au z wykorzystaniem mikroskopii świetlnej.

1.1. Przebieg eksperymentu

Próbki wykonane z komercyjnie czystego Tytanu (Ti grade 2) (Wolften, Wrocław, Polska) w formie krążków zostały poddane mechanicznej obróbce za pomocą szlifowania i polerowania w celu otrzymania jednorodnie płaskiej powierzchni, zgodnie z metodyką prezentowaną we wcześniejszych artykułach [4,5]. Następnie, na próbki została naniesiona elektrochemicznie mikrometryczna warstwa złota. Tak przygotowany materiał został poddany obróbce laserowej w szeregu parametrów mających na celu dobór najbardziej korzystnych dla tworzenia się warstw TiAu, ze szczególnym uwzględnieniem wyglądu mikrostruktury powierzchni po procesie. Zmienność parametrów realizowana była zarówno w aplikowanej mocy wiązki, jak i prędkości posuwu oraz sposobie ogniskowania. Całość była realizowana w atmosferze gazu ochronnego. Schemat przebiegu obróbki laserowej został zaprezentowany na Rysunku nr 1.

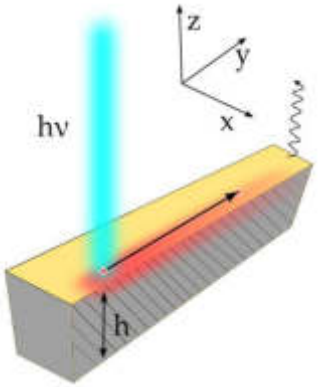

Rysunek 1 Schemat procesu obróbki laserowej układu TiAu

Gotowy materiał poddano analizie przy pomocy mikroskopii świetlnej. Wyniki badań pozwoliły na dobór najlepszych parametrów oraz analizę morfologii, mikrostruktury oraz charakteru powierzchni otrzymanego materiału. Wykazano, że uzyskanie międzymetalicznych związków Ti oraz Au jest możliwe w zadanych parametrach. Obecność struktury dendrytycznej w wybranych próbkach świadczy o dużym wpływie parametrów na otrzymywaną mikrostrukturę oraz na kinetykę przemian napędzanych czasem oddziaływania wiązki na materię oraz intensywnością ruchów konwekcyjnych.

Acknowledgments: Co-financed by the European Union through the European Social Fund (grant POWR.03.05.00-00-Z305).

BIBLIOGRAPHY

1. Fan, J.H.; Hung, W.I.; Li, W.T.; Yeh, J.M. Biocompatibility Study of Gold Nanoparticles to Human Cells. In *13th International Conference on Biomedical Engineering*; Lim, C.T., Goh, J.C.H., Eds.; IFMBE Proceedings; Springer Berlin Heidelberg: Berlin, Heidelberg, 2009; Vol. 23, pp. 870–873 ISBN 978-3-540-92840-9.
2. Ajdari, N.; Vyas, C.; Bogan, S.L.; Lwaleed, B.A.; Cousins, B.G. Gold Nanoparticle Interactions in Human Blood: A Model Evaluation. *Nanomedicine: Nanotechnology, Biology and Medicine* **2017**, *13*, 1531–1542, doi:10.1016/j.nano.2017.01.019.
3. Shah, M. Gold Nanoparticles: Various Methods of Synthesis and Antibacterial Applications. *Front Biosci* **2014**, *19*, 1320, doi:10.2741/4284.
4. Bialas, O.; Poloczek, T.; Lis, M.; Skowronek, A.; Górka, J.; Adamiak, M. Laser Assisted Size Reduction of Gold (Au) Particles onto a Titanium (Ti) Substrate Surface. *Applied Sciences* **2021**, *11*, 8755, doi:10.3390/app11188755.
5. Woźniak, A.; Staszuk, M.; Reimann, Ł.; Bialas, O.; Brytan, Z.; Voinarovych, S.; Kyslytsia, O.; Kaliuzhnyi, S.; Basiaga, M.; Admiak, M. The Influence of Plasma-Sprayed Coatings on Surface Properties and Corrosion Resistance of 316L Stainless Steel for Possible Implant Application. *Archiv.Civ.Mech.Eng* **2021**, *21*, 148, doi:10.1007/s43452-021-00297-1.

MTS CONFERENCE
MATERIAL TECHNOLOGIES IN SILESIA

12-15.06.2022
Crystal Mountain***** Hotel, Wisła, Poland

Fracture observation and mechanical properties of PLA and PET samples obtained by fused deposition modelling with filling type 45/45

M. Bilewicz, M. Gąsiorek

Silesian University of Technology, Faculty of Mechanical Engineering, Department of Engineering Materials and Biomaterials
email: marcin.bilewicz@polsl.pl

Abstract:
The article presents results of tensile test of PP and PET printed samples obtained by FDM technology with the same type of filling 45/45. Material profiles for printing in FDM technology are selected depending on the purpose, because 3D printing is mainly dedicated to the creation of prototypes or small-lot production. Device manufacturers choose printing parameters to optimize the process time and material cost while maintaining appropriate mechanical strength of the detail.

Keywords: 3D printing, FDM, polymers

1. INTRODUCTION

Currently, one of the most common and widespread 3D printing methods is the FFF (Fused Filament Fabrication) technology, also known as FDM (Fused Deposition Modeling). The devices intended for printing from thermoplastics available on the market are very diverse in terms of functionality, construction and price. Starting from cheap RepRap devices for self-assembly, to industrial machines with large working areas and additional functionalities. The use of 3D printing is mainly associated with prototyping parts and devices. Thanks to low financial outlays, the FDM technology has found a lot of interest in the entire industry, e.g. food, automotive, military, aviation, medical, design, architecture, etc. 3D printing technology is developing at a very fast pace and is constantly being improved and modified. Therefore, there is a need to investigate how the final detail is printed in FDM technology and what are the differences in the performance of particular materials. The main characteristic parameters and materials used in FDM technology are described in this article [1-3]. Main parameters of 3D printing are the temperature of printing (temperature of printing nozzle), temperature of the plate and working chamber, size of the nozzle, height of the layer, speed of printing, retraction and type of filling and its percentage. Types of filling are presented below (fig. 1).

Figure 1. Types of filling: broken line, parallel lines, contour, honeycomb, spiral.

2. MATERIALS AND METHODS

In the experiment were used two types of filaments – PET and PP. Characteristics given by suppliers are described below.

Table 1. Material characteristics provided by supplier.

Product parameter	PET	PP
Diameter	1,75 ±0,05 mm	1,75 ±0,05 mm
Density	1,34 g/cm^3	0,89 g/cm3
Softening point	214 °C	115°C
Elongation	9%	>200%

Samples were printed on printer type Industry F340 from 3DGence. The printer is equipped with an actively heated temperature chamber and a Wade extruder. Heating chamber avoid absorption of water by filament, so materials with high hygroscopicity can be printed as well.

3. RESULTS

Mechanical results from tensile test are presented below (fig. 2).

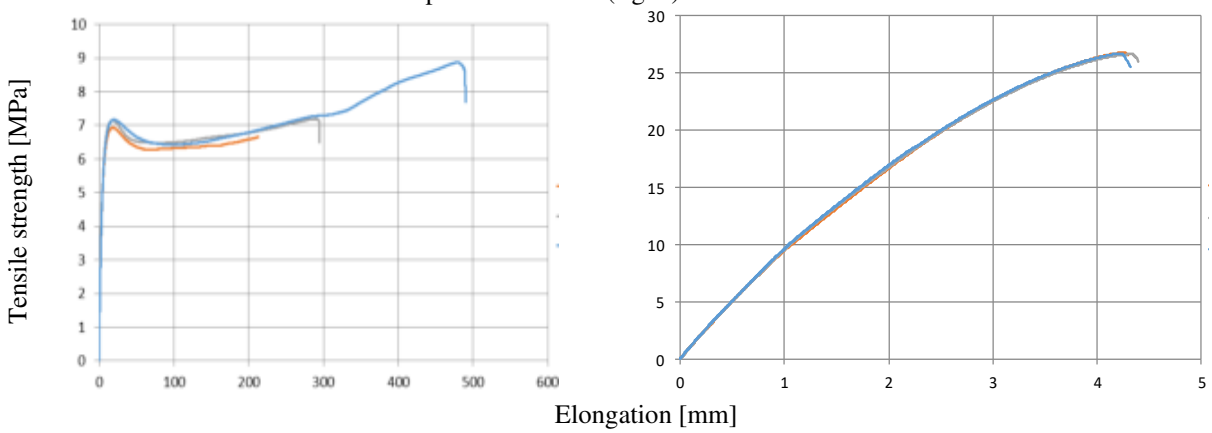

Figure 2. Curves after tensile test of PP (left) and PET (right) printed samples

Elongation of samples is highly different. PET as a rigid material reached elongation of little bit more than 4 mm, while PP reached even 500 mm. Observation of fracture after tensile test is presented below (fig. 3)

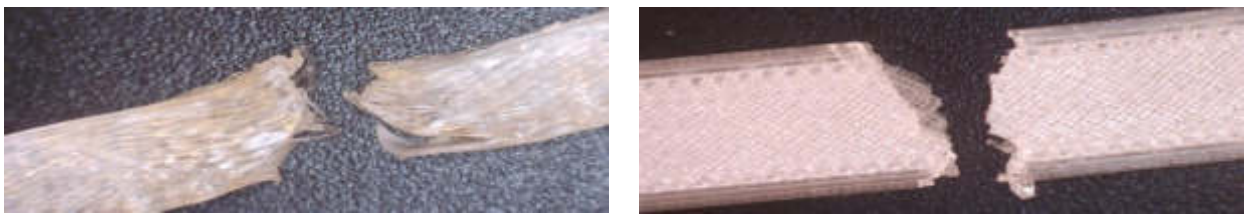

Figure 3.Fracture characteristics after tensile test of PP (left) and PET (right) printed samples.

BIBLIOGRAPHY

1. K. France, A. Make: 3D Printing: The Essential Guide to 3D Printers Helion 2014
2. P. Siemiński i G. Budzik, Techniki Przyrostowe 3D, Warszawa, Oficyna Wydawnicza Politechniki Warszawskiej, 2015 *(in polish)*
3. *Winnam C. D. 3D Printers- The Next Technology Goldrush, CreateSpace Independent Publishing Platform*

MTS CONFERENCE
MATERIAL TECHNOLOGIES IN SILESIA

12-15.06.2022
Crystal Mountain***** Hotel, Wisła, Poland

Influence of isothermal annealing on relaxations and defects of structure in bulk amorphous rods

K. Błoch[1]

[a] Institute of Physics, Czestochowa University of Technology, 19 Armii Krajowej Av., 42-200 Czestochowa, Poland

email: katarzyna.bloch@pcz.pl

Abstract: This paper presents studies relating to the influence heat treament on structural relaxations of the bulk $Fe_{65}Co_{10}Y_5B_{20}$ alloy. The investigated sample was prepared by injection-suction method in the form of rod. The amorphicity of the investigated alloy, in the as-quenched state and after annealing process in a temperature below the crystallization temperature was verified using X-ray diffractometry and Mössbauer spectroscopy. Using completely automated set up the disaccommodation of the magnetic susceptibility were determined . The disaccommodation curve was decomposed into three elementary processes described by Gaussian distribution of relaxation times. The obtained results indicate that the disaccommodation phenomenon in studied alloy is related with directional ordering of atom pairs near the free volumes. This paper also presents the results of numerical analysis of the primary magnetization curves, which were obtained under the assumptions of the theory of approach to ferromagnetic saturation described in by H. Kronmüller. On the basis of the obtained results, the type of structural defects having influence on magnetization in high magnetic fields were determined and the calculation of the spin wave stiffness parameter. It was observed that the heat treatment, carried out below crystallization temperature leads to irreversible structural relaxations, specifically reorganizing the atomic configuration with in the volume of the alloy into an amorphous structure

Keywords: bulk amorphous alloy, magnetic relaxations, disaccommodation phenomenon, approach to ferromagnetic saturation

1. INTRODUCTION

The bulk amorphous alloys are a new group of functional materials, characterised with unique magnetic properties which result in the first place from their structure [1]. The structure of amorphous alloys is formed already in the process of their production. Structural relaxations taking place during the production of amorphous alloys occur due to small displacements of atoms. They can accompany either the displacement of a single atom or a number of atoms, or the collective movement of a large quantity of atoms. Relaxations cannot be treated as processes taking place in the isolated two-level systems of continuous energy distribution. If one process is activated, then the resulting change of local material structure influences other relaxation processes. Structural relaxations affect both the chemical and the topological short range order of atoms. The chemical short-range order of atoms is related to the arrangement of atoms of a given type, and this process can be either reversible or irreversible. Changes in the topological short-range order of atoms are irreversible, the process being related to the reduction and redistribution of free volumes.

Structural relaxations occurring in amorphous alloys finally lead to their crystallization. The crystallization which leads to the generation of nanometric-size grains is called nanocrystallization. The nanocrystalline structure of an alloy can be achieved by either conventional or impulse heat treatment. The conventional treatment is most frequently applied in constant temperature close to the crystallization point. Also the impulse treatment carried out by means of either electric current or laser light can result in generation of nanocrystalline structure. If it is the case, the alloy crystallization proceeds at the temperature much exceeding the one maintained during the conventional treatment, but for very short periods of time (of the millisecond order).

Structural relaxations are microscopic processes which lead to the change of both the structure and some macroscopic properties of amorphous materials. A proper tool to examine changes in an amorphous structure is Mössbauer spectroscopy. Structural relaxations can also be investigated by measuring magnetic properties of amorphous materials. As far as amorphous alloys are concerned, the direct observation of their structure is hardly possible. Therefore employed some measurements of structurally sensitive quantities. One of the possible methods is the measurement of the magnetic susceptibility and its disaccommodation in weak magnetic fields, in the so-called Rayleigh law range. It is well known that the non-uniform arrangement of atoms occurs in amorphous alloys, resulting in the presence of structural defects which shall be understood as the departure from thermodynamic equilibrium of atom arrangement in liquid phase. These defects are sources of short-range or long-range stresses. Regarding magnetic susceptibility, the significant defects are those which produce long-range stresses. Relaxation processes with respect to magnetic susceptibility are directly related to the time-dependent stabilization potential of domain wall. After demagnetization of a specimen with alternating current of amplitude decreasing to zero, the positions of domain walls are determined by the potentials of their static anchoring. This potential results from the presence of structural defects and surface irregularities. Thanks to magnetic interactions between spontaneous magnetization and mobile configurations of defects within domain walls, the reduction of the total magnetic energy of interaction between domain wall s and the structural defects can be achieved by the rearrangement of defects. This leads to the time-dependent so-called 'stabilization potential' within which the domain walls can move.

The measure of temporary stability of the magnetic susceptibility is its disaccommodation *(DPM)*, which can be observed within the range of weak magnetic fields, the so-called Rayleigh law range. Disaccommodation of magnetic susceptibility is one of magnetic after-effects occurring during magnetization of amorphous ferromagnetics and consists in time-dependent decrease of magnetic susceptibility of a specimen previously demagnetized with alternating current of amplitude decreasing to zero [2].

In strong magnetic fields, within the region known as the approach to the ferromagnetic saturation, the specimen does not reach the full saturation due to structural defects. These defects are sources of short-range and middle-range stresses. As a result of magneto-elastic interaction between stress and magnetization, a non-collinear magnetic structure occurs. Magnetization (*M*) of an amorphous alloy in a strong magnetic field (*H*), according to H. Kronmüller's theory, can be described by the equation called 'the law of the approach to ferromagnetic saturation'[3]:

$$\mu_0 M(H) = \mu_0 M_S \left(1 - \sum_{n=1}^{4} a_{n/2} \Big/ \mu_0 H^{n/2} \right) + \chi \mu_0 H + b(\mu_0 H)^{1/2} \quad , \qquad 1$$

where: M_S – saturation magnetization, $a_{n/2}, b$ – coefficients, χ – magnetic susceptibility, μ_0 – magnetic permeability of the vacuum, $a_{n/2} \big/ \mu_0 H^{n/2}$ – the term expressing the influence of structural defects, $\chi \mu_0 H$ – the term resulting from paramagnetism of electron band and diamagnetism of complete atomic shells, $b(\mu_0 H)^{1/2}$ – expression determining an increase in magnetization due to damping of the spin-waves by the magnetic field

For high values of magnetic fields, near the magnetic saturation point, when structural defects no longer influence the magnetization process, further magnetization increase proceeds according to the term $b(\mu_0 H)^{1/2}$, describing the Holstein–Primakoff paraprocess [4]. This process is related to the damping of the thermally induced spin waves by the magnetic field.

BIBLIOGRAPHY

1. A. Inoue,. Mater. Sci. Eng. A 1997, 226–228,357–363.
2. M. Borrous, N. Moser, H. Kronmüller, Phys. Stat. Sol. (a) 112 (1989) 181–188.
3. H. Kronmüller, Micromagnetism in Amorphous Alloys. IEEE Trans. Magn. 1979, 15, 1218.
4. T. Holstein, H. Primakoff, Phys. Rev. 58, 1940, 1098-1113.

MTS CONFERENCE
MATERIAL TECHNOLOGIES IN SILESIA

12-15.06.2022
Crystal Mountain***** Hotel, Wisła, Poland

Laser surface treatment of tool materials

M. Bonek[a], E. Tillova[b]

[a] Silesian University of Technology, Faculty of Mechanical Engineering, Department of Engineering Materials and Biomaterials, Gliwice, Poland
[b] University of Zilina, Department of Materials Engineering, Faculty of Mechanical Engineering, Slovak Republic

1. INTRODUCTION

Many applications of laser radiation are due to the spatial coherence and monochromaticity of the laser light. The spatial coherence enables extreme concentration of radiation and thus the generation of very high power densities that can be used for thermal and chemical surface modification. The monochromaticity of the laser beam allows, through the wavelength, i.e. the type of laser and the operating time, to set the penetration depth of the thermal treatment and to break the chemical bonds on the surface of the material or in the particles of the surrounding gas phase. In addition, the treatment process is controlled in terms of location and time by moving the laser pulses or continuous laser beams in relation to the target.

Laser surface modification processes can be divided into those in which the surface properties of the workpieces change, and others, in which their shape changes. The first category of these processes includes transformation hardening, remelting hardening, production of coating layers by fusing, melting and laser-induced chemical reactions, laser glazing, i.e. the formation of amorphous (glassy) surfaces, deep hardening with laser induced shock waves, laser annealing and laser recrystallization. The second category includes material removal processes such as drilling, cutting and etching, as well as joining processes by welding and laser beam soldering.

There are mainly three types of lasers used for material processing: neodymium-doped solid-state (Nd-YAG) lasers, CO2 gas lasers and excimer lasers. Doped lasers and CO2 lasers emit in the IR range at 1.06 µm and 10.6 µm, and excimer lasers in the UV range at wavelengths from 193 to 351 nm. Ruby lasers and lasers based on noble gas ions (e.g. argon ions, krypton ions) are used less frequently.

2. ADVANTAGES AND DISADVANTAGES OF USING LASERS

Although widely believed to be expensive, laser techniques offer several distinct advantages over other conventional surface modification processes. All variants of laser surface modification are characterized by very high heating and cooling rates, which results in a rapid solidification of the layer, in which both the microstructure and the distribution of alloying elements can be adapted to the needs by appropriate control of operating parameters. The metastable and non-equilibrium phases that can arise as a result of quick quenching, make it possible to create layers with innovative microstructures and better properties than in the case of traditional processes. The laser energy is highly directional and can be precisely controlled, and using the appropriate optics, the beam can also be shaped into a point, line or area beam depending on the needs. Due to the directivity of the laser light, it is possible to use the laser beam to modify hard-to-reach places. The laser light can also be of a very short duration, allowing a large amount of energy to be deposited in a very narrow area. In addition, laser processes are chemically clean, extremely environmentally friendly and generally do not require any additional treatment. The fact that the process can be easily automated is a significant additional benefit.

However, there are also disadvantages: relatively high investment costs, integration and depth of melting are limited, and all precautions must be taken.

3. SUMMARY

The latest scientific reports on modern steels (corrosion-resistant, tool steels) focus on the growing need to increase their durability in aggressive environments. New, innovative methods of improving the steel surface are constantly being sought. Research conducted today more and more often concerns the modification of surface properties by means of laser processing. The popularity of these methods results not only from the increase of corrosion resistance, but also from a significant increase in the tribological properties of the surface.

The innovativeness of laser surface treatment methods results from the wide possibilities of optimizing the process parameters by modifying the composition of protective atmospheres, the speed of surface layer remelting and the laser power. It is also important that laser techniques allow the processing of small surfaces, which translates into a reduction in operating costs and a significant increase in processing precision. Combined with a wide range of applications for stainless steels and tool steels, these laser treated materials represent a very promising alternative for today's industry.

ACKNOWLEDGMENT

The article was created as a result of the project at the Department of Materials Engineering, Faculty of Mechanical Engineering, University of Zilina within the National Scholarship Programme of the Slovak Republic and project KEGA 016ŽU-4/2020 "Improving the quality and innovation of education in bachelor study at the Faculty of Mechanical Engineering, University of Žilina".

REFERENCES

[1] R. Haefer, Modifizierung von Oberflächen durch Laserstrahl-Verfahren, in: R. Haefer, Oberflächen- und Dünnschicht-Technologie. Teil II: Oberflächenmodifikation durch Teilchen und Quanten, Springer-Verlag Berlin Heidelberg, 1991
[2] S. V. Joshi, M. Roy, Laser Surface Modification For Protection Against Wear, in: M. Roy (ed.), Surface Engineering for Enhanced Performance against Wear, Springer-Verlag, Wiedeń, 2013
[3] R. Vilar, Laser Alloying and Laser Cladding, Materials Science Forum, Vol. 301, 1999, 229-252.
[4] Woldan, J. Kusiński, E. Tasak, S. Kąc, Wpływ laserowego stopowania stali węglowej chromem na strukturę i własności warstwy wierzchniej, Inżynieria Materiałowa, nr 6, 2000, 478-481.
[5] H. Pokhmurska, Z. Mucha, W. Kalita, J. Hoffman, O. Kamiński, Wpływ laserowej obróbki na zmęczenie korozyjne stali węglowych i nierdzewnych, Inżynieria Materiałowa, nr 6, 2000, 397-399.
[6] A.K. Nath, S. Sarkar, Laser Transformation Hardening of Steel, Advances in Laser Materials Processing (Second Edition), 2018
[7] L. Li, The Challenges Ahead for Laser Macro, Micro and Nano Manufacturing, Advances in Laser Materials Processing (Second Edition), 2018

MTS CONFERENCE
MATERIAL TECHNOLOGIES IN SILESIA

12-15.06.2022
Crystal Mountain***** Hotel, Wisła, Poland

Symulacja odkształcenia plastycznego na gorąco stopu tytanu z chromem

W. Borek[a]

[a] Politechnika Śląska, Wydział Mechaniczny Technologiczny, Katedra Materiałów Inżynierskich i Biomedycznych
email: wojciech.borek@polsl.pl

Streszczenie: Do zastosowań biomedycznych zaprojektowano nowy biomateriał, stop tytanu z chromem. Proces wytwarzania stopów Ti poprzez zastosowanie odkształcania plastycznego na gorąco ma kluczowe znaczenie dla kontrolowania struktury i właściwości mechanicznych wytwarzanych stopów. W ramach niniejszej pracy wykonano prób ściskania na gorąco próbek osiowosymetrycznych w zakresie temperatury od 850 do 1000°C ze zmienną szybkością odkształcenia w zakresie od wartości 0,01 do 10 s^{-1}. Badania ściskania na gorąco wykonano z wykorzystaniem symulatora do obróbki cieplno-plastycznej Gleeble-3800, który jest na wyposażeniu Laboratorium Naukowo-Dydaktycznego Nanotechnologii i Technologii Materiałowej Politechniki Śląskiej. Na podstawie wyznaczonych krzywych naprężenie rzeczywiste-odkształcenie rzeczywiste opracowano mapy procesowe badanego stopu tytan-chrom, które zostały wyznaczone w oparciu o model materiałów dynamicznych, aby ocenić ich podatność na odkształcenie plastyczne na gorąco oraz mechanizm deformacji w różnych zakresach temperatury i szybkości odkształcenia. W ramach niniejszej pracy zbadano również strukturę badanych stopów i dokonano korelacji z otrzymaną mapą procesową. Na podstawie otrzymanych map stwierdzono, że adiabatyczne pasma ścinania mogą tworzyć się w niższych wartościach temperatury 850 - 950°C i przy umiarkowanych do wysokich wartościach szybkości odkształcania od 1 do 10 s^{-1}, podczas gdy zarodkowanie pęknięć klinowych prawdopodobnie następuje na granicy ziaren w wysokiej temperaturze i przy niskich szybkościach odkształcania 950-1000/0,01 s^{-1}.

Słowa kluczowe: symulator Gleeble, symulacja fizyczna, stopy β-tytanu, odkształcenie plastyczne na gorąco, mapy procesowe, struktura

1. WPROWADZENIE

Tytan i jego stopy znalazły zastosowanie w kilku zastosowaniach biomedycznych ze względu na ich bardzo dobre właściwości mechaniczne, doskonałą odporność na działanie środowiska korozyjnego oraz wysoką biokompatybilność. Najszerzej stosowany stop Ti w wielu zastosowaniach biomedycznych Ti64 (Ti-6Al-4 V), który jest typu α+β, ma wysoki moduł Younga 110 GPa, który jest o połowę niższy niż w przypadku stali nierdzewnej 316L ~200 GPa. Stop T64 jest nadal używany na implanty. Innym przykładem stopów tytanu stosowanych w różnych zastosowaniach biomedycznych jest stop Ti-15Mo-5Zr-3Al, który jest typu β. Stop ten charakteryzuje się wysoką wytrzymałością <1400 MPa przy dopuszczalnej ciągliwości oraz niskim modułem sprężystości 44,4 GPa. Jednak problem uwalniania jonów Al ma perspektywiczny wpływ neurologiczny, który powoduje różnego rodzaju choroby w tym przede wszystkim chorobę Alzheimera. Z tego powodu dla naukowców kluczowe jest opracowanie nowoczesnych stopów tytanu wolnych od Al i V. Stopy dwuskładnikowe Ti-Cr były przedmiotem nadmiernej uwagi badawczej ze względu na ich wysoką odporność na zużycie, znakomitą wysoką wytrzymałość w podwyższonej temperaturze, doskonałą odporność na utlenianie i biokompatybilność. Ostatnio prowadzone są zintensyfikowane badania nad biokompatybilnością i właściwościami mechanicznymi binarnego układu Ti-Cr, na podstawie których stwierdzono, że dodatek Cr do 14% wag. daje wysoką wytrzymałość i wysoką biokompatybilność w porównaniu do stali nierdzewnej 316L. Ponadto wykazano, że wytrzymałości na rozciąganie dla wszystkich badanych stopów są wyższe niż 700 MPa. Cr ma również zdolność do manipulowania aktywnością anodową stopu i zwiększania tendencji Ti do pasywacji, a ta pasywna warstwa na stopach Ti, sekwencyjnie,

zwiększa odporność na korozję. Odkształcenie plastyczne na gorąco jest istotnym i znaczącym krokiem w procesie wytwarzania materiałów metalicznych, co pociąga za sobą szereg badań wymagających zaawansowanych badań teoretycznych i eksperymentalnych. W przypadku stopów tytanu obróbka plastyczna na gorąco traktowana jest jako podstawowy element kontroli ich właściwości mechanicznych. W ramach obróbki termomechanicznej istotną rolę odgrywa odkształcenie plastyczne na gorąco i bezpośrednio związane z tym kontrolowanie mikrostruktury badanego stopu. W przypadku stopów beta-tytanu β-Ti mikrostruktura jest bardzo wrażliwa na czynniki procesu formowania na gorąco i należy zwracać szczególną uwagę na zrozumienie wpływu poszczególnych parametrów zainicjowanych w procesie odkształcenia na gorąco na zmianę mikrostruktury stopów β-Ti, tak aby uzyskać idealną mikrostrukturę oraz optymalne właściwości mechaniczne. Fizyczna symulacja termiczna i mapa procesowe są dość korzystnymi technikami charakteryzowania zachowania materiałów podczas odkształcania plastycznego na gorąco. Warto również podkreślić że stopy tytanu β mają szczególne znaczenie w wielu zastosowaniach nie tylko w biomedycznym ale także w przemyśle lotniczym i chemicznym, ze względu na wysoki stosunek wytrzymałości do gęstości i wyjątkową odporność na korozję.

2. WYNIKI BADAŃ I ICH OMÓWIENIE

Dane eksperymentalne w postaci krzywych naprężenia rzeczywistego w funkcji odkształcenia rzeczywistego zostały zebrane dla próbek osiowosymetrycznych ze stopu tytan-chrom w testach izotermicznego ściskania na gorąco przy użyciu symulatora Gleeble 3800, w zakresie temperatury 850-1000°C) i szybkości odkształcenia w zakresie od 0,01–10 s^{-1} i wartości odkształcenia rzeczywistego równego 0,6. W każdym stanie naprężenie płynięcia rosło wraz ze spadkiem temperatury odkształcenia przy stałej szybkości odkształcenia i ze wzrostem szybkości odkształcenia w stałej temperaturze. Struktura stopu tytanu w stanie wyjściowym składała się z równoosiowych ziaren fazy β, co wskazuje, że 14% wag. Cr stabilizuje fazę β w temperaturze pokojowej. Na podstawie wyzanczonych map procesowych stwierdzono adiabatyczne pasma ścinania które tworzą się w nższej temperaturze i przy wysokich szybkościach odkształcania, podczas gdy zarodkowanie pęknięć klinowych prawdopodobnie rozwija się na granicy ziaren w wysokiej temperaturze i przy niskich szybkościach odkształcenia. Dlatego też obróbka na gorąco w tych regionach map procesowych nie jest zalecana.

MTS CONFERENCE
MATERIAL TECHNOLOGIES IN SILESIA

12-15.06.2022
Crystal Mountain***** Hotel, Wisła, Poland

Low temperature corrosion resistance in C_2H_5OH solution of plasma diffusion treated 316L steel

T. Borowski, J. Kamiński, M. Tarnowski, K. Kulikowski, J. R. Sobiecki, T. Wierzchoń

Warsaw University of Technology, Faculty of Materials Science and Technology
email: tomasz.borowski@pw.edu.pl

Abstract:
One of the most commonly used diffusion processes are glow discharge treatments, such as nitriding, nitrocarburizing or oxynitriding. This methods have number of advantages, including the possibility of full control of the phase and chemical composition, thickness, surface roughness of the produced layers, as well as functional properties such as: hardness, wear and corrosion resistance. Another advantage is the possibility of processing austenitic steels, where light elements show slower diffusion into austenitic structure compared to ferritic or martensitic steels. The study attempts to apply diffusion layers in the aspect of improving the durability of the austenitic steel elements of the centrifugal extractor operating at subzero temperatures. The layers produced on the austenitic AISI 316L steel in the processes of nitriding (450, 480, 520 °C) and oxynitriding (450 °C) glow discharge were investigated. The layers were tested for microstructure, morphology and surface roughness (optical profilometer) and corrosion resistance (potentiodynamic method) in 99% ethyl alcohol solution at room temperature and -30 ° C. The results showed a large influence of the applied glow discharge treatments on the functional properties of AISI 316L steel, in particular on its corrosion resistance in the C_2H_5OH environment.

Keywords: 316L steel, glow discharge nitriding, oxynitriding, low temperature corrosion, morfology,

1. INTRODUCTION

Austenitic steels are very popular metallic materials used in the chemical, food, automotive, nuclear and medical industries, to name a few [1]. The corrosion resistance of austenitic alloys results from their high chromium content and the single-phase structure of paramagnetic austenite. Better corrosion resistance results can be obtained by the application of low-temperature nitriding (<450 °C) [2-6] or oxynitriding [7].The main aim of a work was to present properties and characterization of nitrided and oxynitrrided AISI 316L steel in the aspect of improving the corrosion resistance of the austenitic steel elements of the centrifugal extractor operating at subzero temperatures., what is not yet reported in the worldwide literature.

2. EXPERIMENTAL METHOD

The investigations were conducted on AISI 316L austenitic steel with the following chemical composition in wt.%: C < 0.03, Si < 0.08, Mn < 2, P < 0.045, S < 0.03, Cr 16–18, Mo 2–2.5, Ni 12–15, the rest being Fe. The flat surfaces of cylindrically shaped φ25 mm x 3 mm samples were ground using 240 to 800-grit SiC sandpapers and then cleaned in an ultrasonic cleaner with acetone. The prepared samples were subjected to glow discharge nitriding at 450, 480 and 520 °C for 6 h at a working chamber pressure of 230 Pa, while the working mixture composition was as follows: N_2 and H_2 at a ratio of 1:1, while in the case of oxynitriding: temperature of 450 °C, 6h, pressure 230 Pa, N_2, H_2 and air at a ratio of 2:2:1.The processes were conducted via a semi-industrial device produced by the Institute of Precision Mechanics in Warsaw, Poland. The surfaces of the samples prepared for microscopic analysis were polished along the cross-sections of the layers using SiC abrasive papers up to 1200 grit and then with a 1 µm diamond suspension. Etching of AISI 316L steel was carried out using a reagent consisting of 50% HCl + 25% HNO_3 + 25% H_2O. The microstructures were imaged using a Hitachi S-3500N scanning

electron microscope. The roughness and morphology of the surface layers was analysed by means of a Wyko NT9300 optical profilometer. The corrosion resistance of AISI 316L steel at an initial state and after nitriding and oxynitriding processes was measured in a solution of C_2H_5OH at temperature of -30 °C by means of the potentiodynamic method using an Atlas-Sollich 0531 EU&IA device. A three-electrode setup was used in the tests comprising a test electrode, a saturated calomel electrode (SCE), i.e., the reference electrode and a platinum gauze as a counter electrode. Before the tests, the samples were kept in the measurement array for 2 h to stabilise open circuit potential (OCP). The anodic polarisation curves of the tested materials were then registered via the potentiodynamic method. The samples were polarised from a potential 0.2 V lower than the OCP, to a potential of 1V. In the potential range of +/-200 mV from the OCP, a polarisation rate of 0.2 mV/s was used, whereas in the remaining potential range the rate was 0.8 mV/s. The corrosion current density icorr and corrosion potential Ecorr were determined using the Tafel extrapolation method.

3. RESULTS

Nitrided and oxynitrided layers differed in thickness depending on the applied temperature of the process. The highest thickness was shown by the nitrided layer at the temperature of 520 °C. The highest hardness of 1613 HV0.05 was also recorded for this layer. The lowest thickness was found for the produced layers at 450 °C, and they were also characterized by the lowest hardness: 1361 HV0.05 for nitrided and 864 HV0.05 for oxynitrided layers.

The roughness of the layers increased with the temperature of the processes. The lowest parameters are observed for the nitrided layer at 450 °C and the highest for 520 °C. The increase of Ra and Rq parameters is influenced by cathode sputtering, which is most intense at the highest temperature. In the case of the oxynitrided layer, we can observe slight increase in roughness compared to the nitrided layer at the same temperature of 450 °C. This is due to the formation of oxides on the surface of the oxynitrided layer.

The best corrosion resistance in the environment of C_2H_5OH at -30 °C was demonstrated by AISI 316L steel as well as nitrided and oxynitrided layers at 450 °C. They showed the lowest corrosion current density and the highest corrosion potential. The worst corrosion properties were presented by nitrided layers at 480 and 520 °C and they were characterized by the lowest corrosion potential and the highest corrosion current density. The influence of the process temperature on the corrosion parameters can also be noticed. As the temperature increased, the corrosion current density increased and the corrosion potential decreased.

Acknowledgments: The financial support of the National Center fo Research and Development, Poland, is gratefully acknowledged, grant no. MAZOWSZE/0070/19-00.

BIBLIOGRAPHY

1. Lo, K.H.; Shek, C.H.; Lai, J.K.L. Recent developments in stainless steels. Mater. Sci. Eng. R Rep. 2009, 65, 39–104.
2. Orellana, L.M.; Pérez, F.J.; Gómez, C. The effect of nitrogen ion implantation on the corrosion behaviour of stainless steels in chloride media. Surf. Coat. Technol. 2005, 200.
3. Celik, O.; Baydogan, M.; Atar, E.; Kayali, E.S.; Cimenoglu, H. Fatigue performance of low temperature nitrided AISI 321 grade austenitic stainless steel. Mater. Sci. Eng. A 2013, 565.
4. Biehler, J.; Hoche, H.; Oechsner, M. Corrosion properties of polished and shot-peened austenitic stainless steel 304L and 316L with and without plasma nitriding. Surf. Coat. Technol. 2017, 313.
5. Rajendran, P.; Devaraju, A. Experimental Evaluation of Mechanical and Tribological Behaviours of Gas Nitride treated AISI 316LN Austenitic Stainless Steel. Mater. Today Proc. 2018, 5.
6. Lu, S.; Zhao, X.; Wang, S.; Li, J.; Wei, W.; Hu, J. Performance enhancement by plasma nitriding at low gas pressure for 304 austenitic stainless steel. Vacuum **2017**, 145.
7. Skolek-Stefaniszyn E., Kaminski J., Sobczak J., Wierzchon T. Modifying the properties of AISI 316L steel by glow discharge assisted low-temperature nitriding and oxynitriding, Vacuum 2010, 164.

MTS CONFERENCE
MATERIAL TECHNOLOGIES IN SILESIA

12-15.06.2022
Crystal Mountain***** Hotel, Wisła, Poland

Microstructure and wear resistance of aluminium bronzes printed using Wire Arc Additive Manufacturing Technology

A. Brudny[a], J. Kulasa[a], A. Kowalski[a], A. Kawecki[b]

[a] Łukasiewicz Research Network - Institute of Non-Ferrous Metals, Centre of Advanced Materials Technologies
email: anna.brudny@imn.lukasiewicz.gov.pl
[b]AGH University of Science and Technology, Faculty of Non-Ferrous Metals

Abstract:

This paper presents the results of microstructure and wear resistance tests of elements made of CuAl9Ni5Fe3Mn2 alloy by means of Wire Arc Additive Manufacturing (WAAM) 3D printing technology. Tribological tests (Pin-on-Disk) and microstructure analysis were conducted on cross-sectional and longitudinal sections of the printed objects. Microstructure changes and wear resistance evaluation of multi-component aluminium bronze samples printed by 3DMP® process are shown and analysed.

Keywords: WAAM, Additive Manufacturing, microstructure, wear resistance, aluminium bronzes

1. INTRODUCTION

Additive manufacturing technologies are currently the fastest growing manufacturing methods and involve depositing material layer by layer until the final form of an object is achieved. One of these technologies is Wire Arc Additive Manufacturing (WAAM), which uses a variation of the MIG/MAG welding process for printing, which involves welding with an electric arc produced between a consumable electrode and the material to be welded. The consumable electrode is a continuously fed wire, while the arc and the liquid metal are protected by a shielding gas stream.

The observed continuous increase in the use of copper alloys in the maritime industry is directly related to their excellent properties, including high static strength, resistance to elevated temperatures and abrasion, as well as high corrosion resistance. In this industry copper alloys often used are Cu-Al bronzes, the chemical composition of which also includes other alloying elements (Ni, Mn, Fe, Si), and the amount of these elements is of particular importance in designing the final properties such as strength and resistance to corrosion and wear of the finished products.

Compared to conventional production methods of components from these alloys, additive manufacturing technologies allow for complete automation of the process from object modelling to manufacturing, which significantly affects the efficiency of the manufacturing process. The optimization of 3DMP® process parameters enables the production of objects characterized by a structure with high homogeneity, and changes in parameters cause a significant impact on the microstructure, as well as on the functional properties of the printed objects [1-6].

In this work, a multi-component aluminium bronze wire, CuAl9Ni5Fe3Mn2, was used to print three-dimensional objects in the form of a cuboid (Fig. 1). Tribological tests and microstructure analysis were carried out on the cross-section and longitudinal section of the objects starting from the base plate to the top of the samples. Microstructure changes and wear resistance evaluation of multicomponent aluminium bronze samples printed by means of 3DMP® process are shown and analysed. The printing process was conducted on a 3D printer type Arc403 from Gefertec.

Examination of the microstructure of the produced elements on samples taken from the cross-section and longitudinal section to the direction of deposition of individual material layers were carried out on a Keyence VHX-7000 digital microscope. Identification of the chemical composition in the micro-areas was performed using

a Zeiss Evo MA10 microscope equipped with a Bruker XFlash® 5010 EDS spectrometer using energy dispersive analysis (EDS). Tribological properties including mean value of coefficient of friction and wear rate were determined in accordance with ASTM G99-05 norm using a CSM Instruments THT pin-on-disk high-temperature tribotester. The tests were performed at ambient temperature with a constant contact pressure of 10N and a sliding speed of 50 cm/s over a wear track of 2000 m. The counter sample was a ball made of 100Cr6 grade steel with a diameter of 6 mm.

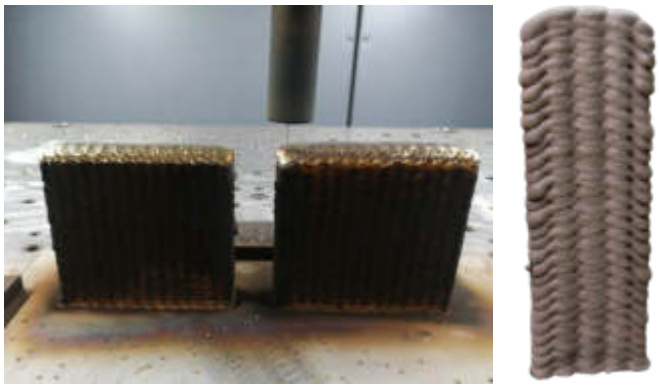

Figure 1. View of printed objects for testing

Acknowledgments: The research was conducted as part of the Implementation Doctorate programme at Łukasiewicz Research Network – Institute of Non-Ferrous Metals in Gliwice.

BIBLIOGRAPHY

1. B. P. Pisarek, B. Kowalski, H. Atapek, Ş. Polat, T. Tüfekçi, Microstructural and Tribological Characterization of Aluminium Bronzes with Additions of Si and Cr, Archives of Foundry Engineering, 2018, Vol. 18, iss. 1 93-98
2. Jisun Kim, Jaewoong Kim Changmin PyoComp of Mechanical Properties of Ni-Al-Bronze Alloy Fabricated through Wire Arc Additive Manufacturing with Ni-Al-Bronze Alloy Fabricated through Casting, Metals 2020, 10, 1164
3. Mukti Chaturvedi, Elena Scutelnicu, Carmen Catalina Rusu, Luigi Renato Mistodie, Danut Mihailescu, Arungalai Vendan Subbiah, Wire Arc Additive Manufacturing: Review on Recent Findings and Challenges in Industrial Applications and Materials Characterization, Metals 2021, 11, 939
4. C.Dharmendra, A. Hadadzadeh, B.S.Amirkhiz, G.D.Janaki Ram, M.Mohammadi, Microstructural evolution and mechanical behavior of nickel aluminum bronze Cu-9Al-4Fe-4Ni-1Mn fabricated through wire-arc additive manufacturing, Additive Manufacturing, Volume 30, December 2019, 100872
5. Donghong Ding, Zengxi Pan, Stephen van Duin, Huijun Li, Chen Shen, Fabricating Superior NiAl Bronze Components through Wire Arc Additive Manufacturing, Materials 2016, 9, 652
6. Project 3DMPWIRE. Material-efficient Cu wire-based 3D printing technology, EIT RawMaterials, 2019-2021 (http://3dmpwire.com).

MTS CONFERENCE
MATERIAL TECHNOLOGIES IN SILESIA

12-15.06.2022
Crystal Mountain***** Hotel, Wisła, Poland

Analysis of interfacial phenomena during liquid-phase fabrication of ultra-high temperature materials from Mo-Si-B system

G. Bruzda[a,b], W. Polkowski[a], A. Polkowska[a], R. Nowak[a], A. Kudyba[a], M. Książek[b], S. Lech[c], K. Karczewski[d], D. Giuranno[e]

[a] Łukasiewicz Research Network – Krakow Institute of Technology, Zakopiańska 73 Str., 30-418 Cracow, Poland
[b] AGH University of Science and Technology, Faculty of Non-Ferrous Metals, Mickiewicza 30 Av., 30-059 Krakow, Poland
[c] AGH University of Science and Technology, International Centre of Electron Microscopy for Materials Science and Faculty of Metals Engineering and Industrial Computer Science, Mickiewicza 30 Av., 30-059 Krakow, Poland
[d] Faculty of Advanced Technologies and Chemistry, Military University of Technology, gen. S. Kaliskiego 2 Str., 01-476 Warsaw, Poland
[e] CNR - Institute of Condensed Matter Chemistry and Technologies for Energy, Via E. De Marini, 6- 16149 Genova, Italy
email: grzegorz.bruzda@kit.lukasiewicz.gov.pl.

Abstract: In the present work, interfacial phenomena taking place at high temperature between a molten Si-B alloy and molybdenum, were experimentally evaluated in terms of a possible new approach for a fabrication of Mo-Si-B ultra-high temperature materials. For this purpose, series of sessile drop experiments were performed at temperature of 1385-1550°C, a holding time up to 30 minutes and by using various technical procedures. During each experiments images of Si-B drop/Mo substarte were in-situ recorded with a high speed camera, and further used for computing wetting kinetics. After sessile drop tests, the solidified samples were subjected to a complex structural characterization (by using SEM/EDS; TEM and XRD techniques) in order to reveal microstructural phenomena reactively induced at the interface.

Keywords: Mo-Si-B alloys; Sessile drop method; Liquid assisted processing; Interfaces; Intermetallic compounds

1. INTRODUCTION

Since 1950's a continuous increase of operational temperatures in internal combustion engines (i.e. gas turbines) has been accomplished through introducing new generations of heat resistant Ni superalloys. Although subsequent classes of wrought, as-cast, directionally solidified and single crystalline alloys have provided a prominent increase of working temperatures (from ~800°C to 1120°C), it seems that metallic alloys have reached their limits [1]. These limitations are justified by both (i) insufficient mechanical strength (as most of strengthening precipitates in superalloys are destabilized or dissolved at temperature >1000°C) and; (ii) relatively low melting points of superalloys (even<1300°C).

Therefore, in order to move forward the efficiency of land and aircraft gas turbine engines, it is necessary to introduce new materials with a much better physical and performance properties at high temperatures. Much attention has been given to advanced ceramics (e.g. SiC/C composites) or to refractory metals (RM) based materials. Among the latter group, a great interest was raised by so called silicides, that are intermetallic-based materials from RM-Si systems [2]. They exhibit a number of physicomechanical properties making them attractive candidates for breaking the superalloys' limits, namely: melting points above 2000°C, and high strength combined with low density (6-7 gcm^{-3} vs. 7-8 gcm^{-3} of superalloys)[3]. As the main disadvantage of simple binary silicides is insufficient oxidation resistance at intermediate temperatures, this issue has been already improved by a microalloying with boron (1-3 wt%). Such modification of chemical composition provides an excellent enhancement of the oxidation behavior by inducing the formation of surface borosilicate glass layer showing a "self-healing" behavior. Moreover, the alloying with boron induces new binary (borides) or ternary (borosilicides) phases having high hardness and creep resistance. Consequently, it has been also proven that boron

enhanced Mo-based silicides offers ~150°C increase in airfoil material operating temperature in aircraft engines over the most advanced Ni-based single-crystalline superalloys [4]. Although having very good results of lab-scale experiments on Mo-Si-B alloys, it should be noted that their wide industrial development is still being hindered by very complex and expensive fabrication method based on high-temperature/high-pressure powder metallurgy based methods.

Therefore, the main purpose of our work is to design a new technological approach for a fabrication of multiphase Mo-Si-B based materials, by using a direct reactive interaction of Si-B melt with Mo „templates". The method adopts practical findings of works reported by Zhang et al. [5] on „hot-dipping" synthesis of either functionally graded coatings or self-standing components made of Mo-$MoSi_2$ composites. The main difference between reported works of team led by Zhang, and thus the novelty of our approach, is that we introduce boron directly from the Si-B melt to produce *boron enhanced silicides*. In such a case, the effect of variables of liquid-assisted process, namely: temperature, time and a structure of „Mo template" on the course of the reactive interaction with Si-B melt, must be experimentally evaluated.

2. MATERIALS AND METHODS

Materials investigated were::

a. polycrystalline near eutectic Si-3.2B (wt %) alloy produced by melting a mixture of elemental powders in h-BN ceramics.
b. polycrystalline molybdenum either in bulk form or as a porous sinters produced by Spark Plasma Sintering

The materials were subjected to sessile drop experiments by using a *contact heating* (Fig. 1a) or *capillary purification* procedures (Fig. 1b). In both cases, temperature of 1385-1550°C, a holding time up to 30 minutes, were applied.

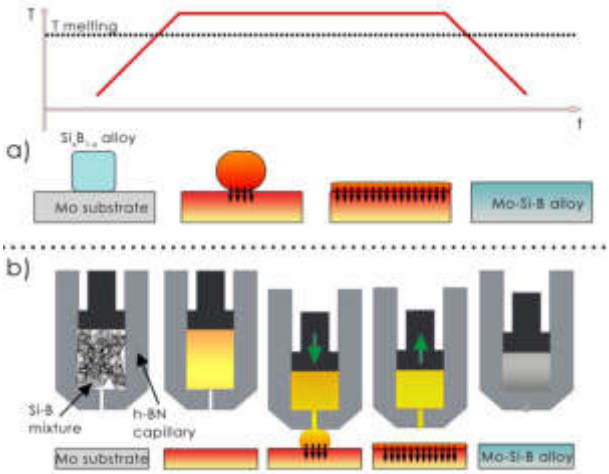

Figure 1. Sessile drop experiments on wettability and reactivity between Si-B alloy and Mo substrates in accordance to contact heating (a) and capillary purification (b) procedures.

The solidified Mo-Si-B samples were subjected to structural characterization by using SEM/EDS; TEM and XRD techniques, while the obtained results were discussed in terms of recorded wetting kinetics and involved structural phenomena.

Acknowledgments: The financial support given by the National Science Centre, Poland under the project no. 2018/31/N/ST8/01513 (PRELUDIUM 16) is gratefully acknowledged.

BIBLIOGRAPHY

1. J. H. Perepezko, The hotter the engine, the better. Science 326 (2009) 1068-1069
2. S. Drawin, J. F. Justin, Advanced lightweight silicide and nitride based materials for turbo-engine applications. Journal of AerospaceLab 3 (2011) 1–13
3. J. A. Lemberg, R. O. Ritchie, Mo-Si-B alloys for ultrahigh-temperature structural applications, Advanced Materials 24 (2012) 3445–3480.
4. S. Drawin S, The European ULTMAT project: Properties of new Mo- and Nb-silicide based materials, Materials Research Society Symposium Proceedings 1128 (2009) (1128-U07-11).
5. Y.Y. Zhang, J. Zhao, J.H. Li, J. Lei, X.K. Cheng, Effect of hot-dip siliconizing time on phase composition and microstructure of Mo–$MoSi_2$ high temperature structural materials. Ceramics International 44 (2019) 5588–5593.

MTS CONFERENCE
MATERIAL TECHNOLOGIES IN SILESIA

12-15.06.2022
Crystal Mountain***** Hotel, Wisła, Poland

The corrosion resistance of 3D printed M789 maraging steel in various post-printing heat treatment states

Z. Brytan[a], M. Król[a], M. Benedyk[b], T. Tański[a]

[a] Silesian University of Technology, Faculty of Mechanical Engineering, Department of Engineering Materials and Biomaterials, ul. Konarskiego 18a, 44-100 Gliwice, Poland
[b] Paks'D Sp Zoo, Strzelecka 74, 43-100 Tychy, Poland; mbenedyk@paksd.co

Abstract: The purpose of the present work is to evaluate the corrosion behavior of additively printed Co-free M789 maraging steel in a chloride-rich environment. The correlation between the state of heat treatment of 3D printed steel, its microstructure, and suspensibility to corrosion was assessed. The AM M789 subjected to an age hardening process after 3D printing realized as an independent heat treatment process shows better corrosion resistance (R_p = 24.1 kΩ·cm^2) compared to materials heat treated as a subsequent step directly after printing (R_p = 16.1 kΩ·cm^2). Furthermore, the corrosion resistance in the age-hardening states realized in different ways is quite similar, while a strong improvement in corrosion resistance is revealed when the material undergoes only the solution annealing (R_p = 289.8 kΩ·cm^2).

Keywords: SLM; LPBF; M789 steel; heat treatment; microstructure; corrosion resistance.

1. INTRODUCTION

The data available in the literature on additively manufactured (AM) Co-free M789 maraging steel powder are very limited. The M789 powder was launched within the last 3 years, and detailed research in its field is still in progress. Most of the available research focuses on maraging steel with the addition of Co, such as 8% Ni maraging steel EN: 1.2709, also known as 18Ni(300) or Maraging 300 steel [1,2], while Co-free grades are a novelty. The main mechanical properties of the printed elements are analysed, along with the subsequent heat treatment. Post-processing heat treatment of AM maraging steel is a crucial issue in optimisation of the final mechanical properties of 3D printed parts. According to the manufacturer's recommendations, the maximum effect of precipitation strengthening for Co-free M789 steel can be obtained at a temperature of about 500◦C for 3 h. However, for classic grade 1.2709 with Co addition, ageing treatment of 3–6 h and even 10 h is recommended. 3D printed parts from maraging steels can be supplied in different processing conditions, like as-printed (without any further heat treatment), solution annealed, solution annealed and aged, which will result in which affect the different degree of hardening, plastic properties, and stress relaxation.

The recent study of the authors [3] shows that the AM M789 maraging steel is composed of a martensitic microstructure with retained austenite (6-8%) depending on the solution annealing time (3–9 h). The mechanical properties obtained (that is, the yield point and tensile strength of 1500–1600 MPa) are below (~10%) the maximum values available in the literature (that is, 1800 MPa), keeping in mind that these are data for optimized printing conditions [4]. The maraging steel under heat treated conditions, regardless of the ageing time, includes the presence of combined oxide inclusions of Ti and Al (TiO_2:Al_2O_3) along the grain boundaries and secondary porosity. These are considered metallurgical defects that can act as preferential zones for the initiation of cracks and may increase the brittleness of the AM steel under-aged conditions. The effects of such oxide inclusions are visible in the form of relatively low plastic properties (elongation after fracture,A5< 2%) of the printed parts, both under solution annealed and annealed and aged conditions.

The scope of the presented research is to evaluate the corrosion behavior of AM M789 maraging steel in various post-printing heat treatment conditions, i.e. in the as-printed state, solution annealed and solution annealed and aged. The correlation between the state of heat treatment, the microstructure of the material, and the tendency to corrosion in a chloride-rich environment was briefly presented.

2. MATERIALS AND METHODS

In the experiment, M789 steel powder (0.02% C, 12.2% Cr, 10% Ni, 1% Mo, 0.06% Al,1% Ti, Fe), was printed in LPBF process with the following parameters: laser power = 200 W, laser speed = 340 mm/s, and hatch distance = 120μm, described in detail in [3]. In the present study, samples were studied in print conditions, aged (500°C/3h) directly after printing, solution annealed (1000°C/1h), solution annealed (1000°C/1h) and aged (500°C/3h) conditions. The corrosion resistance was evaluated in 3.5% NaCl solution using a standard electrochemical method and Tafel analysis.

3. RESULTS

The microstructure of AM 789 maraging steel is composed of a martensitic microstructure with retained austenite. In a printed condition typical for printing, melt pool boundaries were visible and directional martensitic grains. Direct ageing treatment results in the relaxation of the microstructure, the annihilation of dislocations, and the formation of secondary precipitates (η-phase) responsible for the age-hardening effect. The solution annealing after printing strongly influenced microstructure homogenisation and elimination of residual stresses, while subsequent ageing resulted in an age-hardening effect.

The corrosion resistance of AM 789 maraging steel in 3.5% NaCl (Table 1) depends on the post-printing heat-treatment applied. When polarisation resistance (R_p) it can be seen that solution annealed condition causes a significant improvement in corrosion resistance. Bearing in mind that the optimal state for this steel in terms of mechanical properties is age hardening (solution annealing plus ageing), it can be concluded that better corrosion resistance will occur when, after printing, the material is subjected to solution annealing in the next step and then ageing, and not the ageing process immediately after printing. This is due to the greater heterogeneity of the composition and phase structure as well as the concentration of defects in the crystal structure in the state after printing and subsequent ageing. However, solution annealing causes homogeneity of the chemical composition, which reduces the formation of active-passive areas in the steel microstructure, and thus improves corrosion resistance.

Table 1. Electrochemical parameters of AM 798 in a 3.5% NaCl solution

AM 789 maraging steel	E_{cor}, V	I_{cor}, μA ·cm^{-2}	b_a, V	b_c, V	R_p, kΩ·cm^2	E_b, kΩ·cm^2
as printed	-0.33	1.11	0.088	0.079	16.3	-0.048
aged (500°C/3h)	-0.42	4.02	0.068	0.117	4.7	-0.263
solution annealed (1000°C/1h)	-0.149	0.04	0.145	0.030	289.8	0.172
solution annealed (1000°C/1h) and aged (500°C/3h)	-0.276	1.29	0.228	0.096	24.1	0.117

4. CONCLUSIONS

The corrosion resistance of additively manufactured 789 maraging steel is related to post-processing heat treatment and resulting microstructure. Materials subjected to an age-hardening process after 3D printing performed as an independent heat-treatment process show better corrosion resistance (R_p = 24.1 kΩ·cm^2) compared to materials heat treated as a subsequent step directly after printing (R_p = 16.1 kΩ·cm^2). Furthermore, the corrosion resistance in the age-hardening states realized in different ways is quite similar, while a strong improvement in corrosion resistance is revealed when the material undergoes only the solution annealing process (R_p = 289.8 kΩ·cm^2).

BIBLIOGRAPHY

1. Kucerova, L.; Burdova, K.; Jenícek, S.; Chena, I. Effect of solution annealing and precipitation hardening at 250◦C–550◦C onmicrostructure and mechanical properties of additively manufactured 1.2709 maraging steel.Mater. Sci. Eng. A2021,814, 141195.
2. Piekło, J.; Garbacz-Klempka, A. Use of maraging steel 1.2709 for implementing parts of pressure mold devices with conformalcooling system.Materials2020,13, 5533.
3. Tian, Y.; Palad, R.; Jiang, L.; Dorin, T.; Chadha, K.; Aranas, C., Jr. the effect of heat treatments on mechanical properties of M789steel fabricated by laser powder bed fusion.J. Alloys Comp.2021,885, 161033.

MTS CONFERENCE
MATERIAL TECHNOLOGIES IN SILESIA

12-15.06.2022
Crystal Mountain***** Hotel, Wisła, Poland

Production technology of the liners intended for the shaped charges used in the mining industry

W. Burian[a], A. Kowalski[a], J. Kulasa[a], K. Wiśniewski[a], B. Jóźwik[b], M. Pytlik[c], J. Janiszewski[d], J. Lachmajer[e], D. Szmania[e], M. Mazurkiewicz[e]

[a] Łukasiewicz Research Network – Institute of Non-Ferrous Metals, Centre of Advanced Materials Technologies
email: aleksander.kowalski@imn.lukasiewicz.gov.pl
[b] Łukasiewicz Research Network – Institute of Non-Ferrous Metals, Centre of Functional Materials
email: bartosz.jozwik@imn.lukasiewicz.gov.pl
[c] Central Mining Institute
email: mpytlik@gig.eu
[d] Military University of Technology
email: jacek.janiszewski@wat.edu.pl
[e] Chemical Works „NITRO-CHEM" S.A.
email: lachmajer@nitrochem.com.pl

Abstract: The technology of liners manufacturing is presented. The conical and semi-spherical liners made of Cu and Cu-based alloys were manufactured by means of conventional technology – die stamping or machining, and also 3D printing technology – Selective Laser Melting. Moreover, the results of the grains size measurements are presented.

Keywords: liners technology, copper alloys, die stamping, 3D printing, SLM

1. INTRODUCTION

The analysis of the market of blasting services in Poland proves that there is a great demand for shortening the time of making blast holes, as well as for limiting the time spent by the crew in the longwall. The directions of exploitation in underground mining plants are heading towards deposits lying in difficult conditions, where the possibility of drilling is significantly limited by mining, geological, climatic conditions, and natural hazards. Currently, the crew performing preparatory work in blasting works in underground mining plants is exposed to accidents resulting from high temperature, rock ejection or falling into the excavation, gas outbursts, and rock bursts. One of the frequent causes of "blast" accidents is drilling into explosives or their remains, as a result of which rock fragments and a detonation wave often cause severe accidents for the drilling crew.

The main goal of the project "Nanocrystalline and amorphous materials for shaped charge liners used in mining industry" was the development of new, finely fragmented materials for the production of cumulative inserts used in the mining industry, including charges for blast hole drilling. The large fragmentation of the structure allows to achieve a high level of mechanical properties while maintaining high ductility, which is particularly desirable in the case of materials used for the liners for shaped charges because they guarantee a long, continuous cumulative stream with high penetrating properties [1-3].

Acknowledgments: The financial support of The National Centre for Research and Development in the frame of the TECHMATSTRATEG program, Poland, is gratefully acknowledged, grant no. TECHMATSTRATEG1/349156/13/NCBR/2017.

BIBLIOGRAPHY

1. J. Janiszewski, E. Włodarczyk, Rola materiału wkładki w formowaniu strumienia kumulacyjnego, [in:] "Biuletyn WAT," No. 3/2002.
2. J. Janiszewski, Badania materiałów inżynierskich w warunkach obciążenia dynamicznego, Wydawnictwo WAT, Warszawa 2012.
3. M. Magier, W. Burian, M. Rotkegel, J. Szymala, Experimental analysis of the concrete penetration by using warheads from demobilized ammunition, Key Engineering Materials, Vol. 715, pp. 243-248, 2016.

MTS CONFERENCE
MATERIAL TECHNOLOGIES IN SILESIA

12-15.06.2022
Crystal Mountain***** Hotel, Wisła, Poland

The influence of prior-precipitated carbides on kinetic, microstructure and properties of bainite in 100CrMnSi6-4 bearing steel

K. Chmielarz

Warsaw University of Technology, Faculty of Materials Engineering
email: krzysztof.chmielarz.dokt@pw.edu.pl

Abstract:

100CrMnSi6-4 steel is a popular bearing steel characterized by good mechanical properties and which can be subject to bainitic transformation. Due to the low silicon content, however, it is impossible to obtain carbide-free bainite in this steel. For this reason, series of tests were conducted to determine whether and how the carbides present in the initial state affect the kinetics of the bainite transformation, the microstructure of the formed bainite and the final properties of the steel. For this purpose, three variants of the treatment preceding the bainite transformation were used - ordinary austenitizing, double austenitizing, aimed at fragmenting the existing carbides, and double austenitizing with additional spheroidization, aimed at growing the existing carbides. The banitization stage was carried out at three temperatures, corresponding to the lower and upper bainite formation temperatures as well as granular bainite formation. In order to determine the influence of carbides, the kinetics of bainite formation, the produced microstructure and the mechanical properties after individual processes were investigated.

Keywords: bainite, transformation kinetic, carbides, 100CrMnSi 6-4, steel

1. INTRODUCTION

The heat treatment develops extremely quickly. Modern heat treatments allows to change the properties of steels that are often already available on the market or only with minor changes of chemical composition, which significantly simplifies the implementation process and reduces costs. Examples of this type of development are nanostructuring, QP and BQP processes - all of them allow to improve the properties of commercially available steels only by changing the heat treatment [1]

In the majority of modern designed heat treatments, precipitation of carbides is avoided. This is related to their high brittleness and the fear of formation of a mesh of particles at the grain boundaries, which leads to the brittleness of the material. At the same time, the importance of austenite present in the structure is growing due to its high ductility and the possibility of improving the properties of the material with the TRIP or TWIP effect. However, as some more recent studies show, the presence of carbides in a material does not necessarily mean a deterioration of the mechanical properties. The combination of precipitation hardening with nanobainite allowed to increase the yield point and strength in X37CrMoV 5-1 steel [2], as well as to increase the hardness in steel with increased silicon content [3]. It follows that spherical precipitations of carbides can positively affect the mechanical properties of bainite steel. In this work, an attempt was made to investigate the influence of the size of carbide precipitates on the kinetics of the bainite transformation and on the properties obtained after heat treatment. To determine that, a series of different treatments was attempted, following by austempreing in three different temperatures. To identify influence of prior-precipitated on kinetics of bainitic transformation, dilatometric measurements were made, and compared via usage of two different models of transformation. A series of microscopic observation was attempted to determine influence of carbides on prior austenite grains and microstructure. Finally, mechanical properties after each treatment were checked and described.

2. RESULTS AND DISCUSSION

Two different treatments of carbides precipitation was chosen to control precipitation of carbides. First was double austenitization (DA)– process where steel is first austenitizated, then quenched, and austenitizated again in temperature lower than previous austenitization. This process allows to decrease size and homogenize it's distribution in matrix [4]. Second treatments adds a additional step between quenching and second austenitization, which is spheroidisation (DA+S). This allows to increase size and decrease a number of present cardbides, with a preservation of uniform distribution [5]. Third treatment was a normal, single austenitization (SA), to compare results of previously described treatment.

Also three different temperatures of austemepring where chosen, which was 250, 320 and 430°C, what should allow to obtain respectively lower, upper and granular bainite.

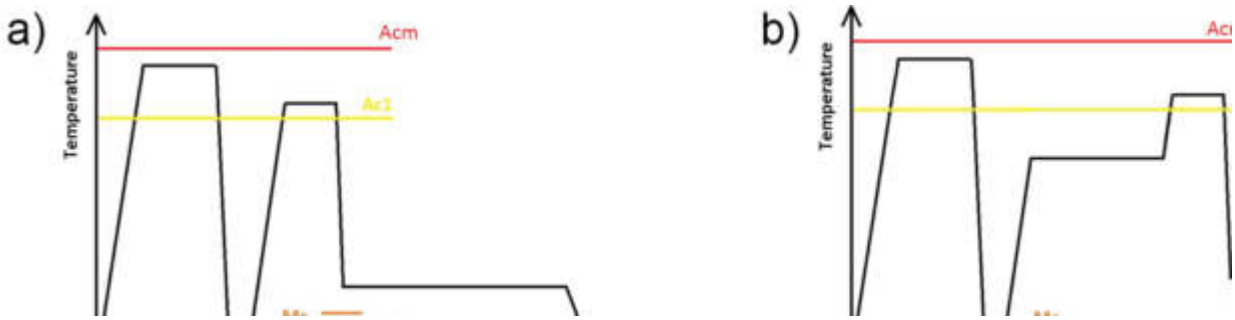

Fig 1 diagram of described heat treatment. a) – double austenitisaton (DA); b) - double austenitizaton + spheroidisation (DA+S).

After each austenitization variant – DA, DA+S, SA, samples were quenched to and Ms temperature was measured to check if it have effect on content of carbon in austenite. That samples were later observed on TEM and SEM to determine size of carbides present in that structures.

The Ms temperature remain within close range after designed treatment treatments. As it is mainly dependent on carbon content in the austenite, and the deviation between the treatments is close, we may assume that the changes in the content of carbon in austenite wont be meaningful to the kinetics of bainitic transformation. Also strong dependence with the treatment, grain size and kinetics of the transformation was observed. Finally, after double austenitization (DA), a strong increase in mechanical properties was observed when compared to the single austenitization (SA) – as a result of precipitation strengthening. Overall, controlled precipitation of carbides increased kinetic of bainitic transformation, and increased some of its mechanical properties.

Acknowledgments: The results presented in this work have been obtained within the project NanoCarbain (contract no. LIDER/12/0040/L-9/17/NCBR/2018). The project is financed by the National Centre for Research and Development under the LIDER IX program

BIBLIOGRAPHY

1 Y. Li, Y. Lu, C. Wang, S. Li, and L. Chen, "Phase Stability of Residual Austenite in 60Si2Mn Steels Treated by Quenching and Partitioning," *Journal of Iron and Steel Research International*, vol. 18, no. 2, pp. 70–74, Feb. 2011, doi: 10.1016/S1006-706X(11)60026-5.

2 Chmielarz Krzysztof and Marciniak Szymon, "Changes of microstructure and mechanical properties of nano crystalline steel X37CrMoV5-1 subjected to heat treatment as is used during nitriding," in *ISCAME 2017 conference proceedings*, 2017, pp. 90–95.

3 M. Zorgani, C. Garcia-Mateo, and M. Jahazi, "Microstructural evolution during tempering of an ausformed carbide-free low temperature bainitic steel," *Materials & Design*, vol. 210, p. 110082, Nov. 2021, doi: 10.1016/j.matdes.2021.110082.

4 B. Ögel and E. Tekin, "The effect of double austenitization on the microstructure and toughness of AISI M2 high speed steel," Steel Research, vol. 69, no. 6, pp. 247–252, 1998, doi: 10.1002/srin.199805544.

5 SZWEJKOWSKA, K., BAGROWSKA, M., WASIAK, K., SKOŁEK, E., MARCINIAK, S., & ŚWIĄTNICKI, W. (2019). The effect of carbides on the kinetics of bainitic transformation and the resulting nanobainitic microstructure in 90SiCrMn6-4 steel. In *METAL Conference Proeedings. METAL 2019*. TANGER Ltd. https://doi.org/10.37904/metal.2019.720

MTS CONFERENCE
MATERIAL TECHNOLOGIES IN SILESIA

12-15.06.2022
Crystal Mountain***** Hotel, Wisła, Poland

Synergia między stadium Przemysłu 4.0 rewolucji przemysłowej oraz rozwojem nowoczesnej stomatologii – wykład specjalny

Prof. Leszek A. Dobrzański [a, b]

[a] Centrum Projektowo – Badawczo – Produkcyjne Inżynierii Medycznej i Stomatologicznej ASKLEPIOS w Gliwicach
[b] Politechnika Koszalińska w Koszalinie, Wydział Mechaniczny, Katedra Inżynierii Biomedycznej
email: leszek.dobrzanski@centrumasklepios.pl; leszek.dobrzanski@tu.koszalin.pl

TEZY WYKŁADU:

Przed ludnością Świata, która ok. 2050 roku najpewniej osiągnie 10 miliardów stoją bardzo poważne wyzwania, głównie dotyczące żywności, energii, wody oraz ochrony zdrowia i dobrostanu ludzi. ONZ po Deklaracji z Rio de Janeiro oraz po wznowieniu przez tzw. Agendę 2030 ustanowiła 17 Celów Zrównoważonego Rozwoju DSG, skupionych w pięciu zasadniczych grupach z języka angielskiego oznaczonych przez „P", tzn. ludzie, dobrobyt, partnerstwo, pokój i planeta. Spośród nich w wykładzie uwagę skupiono na dwóch dotyczących dobrego zdrowia oraz aktywności przemysłowej, z próbą znalezienia korelacji między tymi z pozoru odległymi sferami działania. Warto jednak zwrócić uwagę, ze wiele współczesnych osiągnięć medycyny, stało się możliwych wyłącznie dzięki inżynierskiemu wspomaganiu.

Podstawą rozważań zajmujących pierwszą główną cześć wykładu jest analiza prawidłowości rozwoju cywilizacji, opisanego przez dwa komplementarne modele: japoński ujmujący fazy od kultury łowieckiej po rozwinięte społeczeństwo informatyczne Społeczeństwo 5.0 oraz niemiecki i szeroko rozpowszechniony w Świecie skupiający się wyłącznie na rozwoju cywilizacji przemysłowej, począwszy od wykorzystania pary po w pełni zinformatyzowany, zrobotyzowany i zautomatyzowany współczesny przemysł w stadium Przemysłu 4.0. Począwszy od tezy głównego twórcy tej koncepcji Prof. H. Kagermana, że brak jakiejkolwiek alternatywy, szczegółowo przeanalizowano założenia modelu 4.0, badając zarówno jego adekwatność, jak i kompleksowość. Okazuje się, model jest jednostronny i niekompletny i w istocie dotyczy wyłącznie zagadnień informatycznych tzw. systemów cyber-fizycznych CPS. Wykazano niekompletność takiego podejścia, zagrażającą załamaniem rozwoju przemysłu, w razie braku świadomości konieczności zrównoważonego rozwoju pozostałych istotnych elementów składowych tego systemu, tzn. materiałów, procesów wytwarzania oraz maszyn i urządzeń technologicznych. Wykazano, że wytwarzanie jakiegokolwiek produktu od zarania naszej cywilizacji i z istoty wymaga użycia materiałów technicznych, u zarania w dużej mierze naturalnych, a z czasem w przeważającej mierze materiałów inżynierskich. I odwrotnie, produkcja bez materiałów nie ma racji bytu. Na tym tle przedstawiono historyczny rozwój materiałów oraz zmianę podejścia od metody prób i błędów ich doboru w stadium Materiałów 1.0 po aktualnie rozwijające się projektowanie materiałowe i weryfikację w przestrzeni wirtualnej z wykorzystaniem idei „wirtualnego bliźniaka", by ostatecznie zbadać produkt wytworzony w optymalny sposób w stadium Materiały 4.0. Przedstawiono mnogość współczesnych technologii wymagających bardzo szerokiego udziału komputerowego wspomagania wytwarzania, ale również zapewnienie jakości, niezawodności i innych istotnych aspektów wytwarzania ogólnie określanych jako komputerowe wspomaganie wytwarzania CAM. W świetle tych rozważań w żadnej mierze nie broni się teza stawiana w pierwotnym modelu Przemysłu 4.0, że wyłącznie preferowaną technologią jest wytwarzanie przyrostowe. Tak postawiona teza jest fałszywa, pomimo niezaprzeczalnych walorów takiego rozwiązania technologicznego, chociaż o znaczeniu komplementarnym, a konkurencyjnego jedynie w relatywnie nielicznych przypadkach. Zwrócono uwagę na rozwinięte technologie zdigitalizowane ADT, opanowane przez ok. 10 państw i perspektywy osiągnięcia takiego poziomu najwyżej przez kolejnych 30 i to w perspektywie kolejnych kilkudziesięciu lat.

W warunkach gospodarki rynkowej inżynierowie są odpowiedzialni jedynie za część pełnego cyklu wprowadzania produktów na rynek, co dotyczy modelowania przemysłowego, projektowania inżynierskiego, przygotowania produkcji i wytwarzania, po części obsługi serwisowej i eksploatacji oraz usuwania odpadów. Zwrócono uwagę na nierozdzielność projektowania materiałowego, technologicznego i konstrukcyjnego, jak również na paradygmat inżynierii materiałowej dotyczący zasady sześciu oczekiwań 6xO (z j. angielskiego 6xE). Cykl trwania oraz ślad

środowiskowy (węglowy i wodny) oraz minimalizacja odpadów we wszystkich fazach projektowania i użytkowania produktów zostały przedstawione jako ważne determinanty projektowania inżynierskiego i realizacji zasady integracji ludzi z naturą. W kontekście nowoczesnego spojrzenia na zagadnienia zapewnienia jakości i niezawodności produktów przedstawiono relację wymagań ludzi oraz potencjalnych możliwości tkwiących w materiałach, co zbiega się w wytwarzanych produktach dostępnych na rynku. Trendy rozwojowe materiałów inżynierskich kończą rozważania ogólne nad koncepcją aktualnego stadium rozwoju przemysłu i jego perspektyw.
Zagadnienia znaczenia zachowania zdrowia oraz możliwości wspomagania w tym zakresie ograniczono do przykładów z zakresu stomatologii. Zagadnienie dotyczy bowiem 3-5 miliardów ludzi na ziemi, a powikłania wynikające z chorób zębów i bezzębia, które jest nieuchronnym następstwem, są przyczyną co najmniej 500 chorób i powikłań ogólnoustrojowych. Polska należy do sześciu krajów na świecie o największej skali zaniedbań w tym zakresie oraz o najwyższych wskaźnikach DALY wśród grupy najmłodszych. Zagadnienie ma odniesienia etyczne, a wdrażanie koncepcji Zrównoważonego Rozwoju Stomatologii DSD wymaga praktycznej realizacji modelu Stomatologii (Dentistry) 4.0, który w pełni odpowiada pryncypiom koncepcji Przemysłu 4.0. Co do podejścia projektowanie i wytwarzanie stomatologicznych uzupełnień protetycznych w niczym nie odbiega od produkcji elementów samochodu lub samolotu. Przedstawiono pełny cykl projektowo-wytwórczy uzupełnień protetycznych z istoty spersonalizowany, począwszy od obrazowania medycznego, poprzez komputerowo wspomagane projektowanie i wytwarzanie CAD/CAM wraz z licznymi przykładami praktycznymi. Przedstawiono komputerowo wspomagany proces leczenia implanto-protetycznego wraz z fazą projektowania zabiegu komputerowo-wspomaganego przez inżynierów stomatologicznych wraz z projektowaniem i wytwarzaniem szablonów chirurgicznych. Przedstawiono klasyczną koncepcję implantu stomatologicznego wkręcanego według Branemarka z przełomu lat siedemdziesiątych XX wieku oraz oryginalne własne opatentowane konstrukcje implanto-skafoldów porowatych lub porowatych z litym rdzeniem oraz implanto-skafoldów z wypustkami, zapewniającymi znacznie silniejsze mocowanie w kościach szczęk, umożliwiających wbijanie implantów przy pomocy oryginalnego akcesorium objętego patentem, a co najważniejsze umożliwiających skrócenie leczenia do jednej wizyty zabiegowej po szczegółowym diagnozowaniu z użyciem tomografu rentgenowskiego podczas wizyty wstępnej, zamiast wielozabiegowego leczenia w okresie co najmniej pół roku, jak to dotychczas ma zwykle miejsce. Przedstawiono również szczegółowo zastosowanie technologii przyrostowych selektywnego spiekania laserowego SLS do wytwarzania implanto-skafoldów oraz stomatologicznych uzupełnień protetycznych, technologii obróbki skrawaniem z wykorzystaniem centrum sterowanego numerycznie CNC o pięciu osiach oraz stereolitografii SLA do wytwarzania szablonów chirurgicznych z materiałów fotopolimerowych. Przeanalizowano istotne znaczenie doboru warunków wytwarzania na strukturę, głównie porowatość, wynikającą z niespełnienia warunków spiekania z udziałem fazy ciekłej oraz struktury szkieletowe i z wypustkami, a także porównano własności mechaniczne, odporność na zużycie i na korozję tak wytworzonych materiałów na przykładzie stopów tytanu, zamiast głównie stosowanych stopów kobaltu o znacznie większej masie. Wykonano badania struktury z wykorzystaniem wysokorozdzielczego transmisyjnego mikroskopu elektronowego. Przeanalizowano znaczenie warstw powierzchniowych zarówno na implantach jak i uzupełnieniach protetycznych (mostach i koronach) wytwarzanych jedyną dostępną metodą „nie dającą cienia" osadzania warstw atomowych ALD. Przedstawiono również wybrane wyniki badan biologicznych, w tym proliferacji żywych komórek ludzkich w zależności od stosowanych technologii i ich warunków.

WNIOSKI:

Wnioski wskazują na konieczność rozwoju podejścia Przemysłu 4.0 z uwzględnieniem zrównoważonego rozwoju wszystkich czterech elementów składowych, tj. materiałów, technologii, urządzeń technologicznych i systemów cyber-fizycznych. Wskazano na zasadność wykorzystywania technologii przyrostowych, tam gdzie to jest możliwe i uzasadnione. Przedstawiono, jako dojrzały przykład aplikacyjny całego podejścia, rozwój inżynierii stomatologicznej w ramach koncepcji Zrównoważonego Rozwoju Stomatologii, zawierającej jako ważny komponent Stomatologię 4.0 jako pełne wdrożenie idei Przemysłu 4.0 w obszarze inżynierii stomatologicznej.

BIBLIOGRAFIA:

1. Dobrzański, L.A.; Dobrzańska-Danikiewicz, A.D.; Dobrzański, L.B. Effect of Biomedical Materials in the Implementation of a Long and Healthy Life Policy. Processes 2021, 9, 865. https://doi.org/10.3390/pr9050865
2. Dobrzański, L.A.; Dobrzański, L.B.; Dobrzańska-Danikiewicz, A.D.; Dobrzańska, J. The Concept of Sustainable Development of Modern Dentistry. Processes 2020, 8, 1605. https://doi.org/10.3390/pr8121605
3. Dobrzański, L.A.; Dobrzański, L.B. Dentistry 4.0 Concept in the Design and Manufacturing of Prosthetic Dental Restorations. Processes 2020, 8, 525. https://doi.org/10.3390/pr8050525
4. Dobrzański, L.A.; Dobrzański, L.B. Approach to the Design and Manufacturing of Prosthetic Dental Restorations According to the Rules of Industry 4.0. Mater. Perform. Charact 2020, 9, 394–476.
5. Dobrzański, L.A.; Dobrzańska-Danikiewicz, A.D. Why Are Carbon-Based Materials Important in Civilization Progress and Especially in the Industry 4.0 Stage of the Industrial Revolution. Mater. Perform. Charact 2019, 8, 337–370.

MTS CONFERENCE
MATERIAL TECHNOLOGIES IN SILESIA

12-15.06.2022
Crystal Mountain***** Hotel, Wisła, Poland

Influence of Laser Surface Alloying with CrWC on microstructure of copper

J. Domagała-Dubiel[a,*], K. Bilewska[b], D. Janicki[c], M. Pawlyta[d]

[a] Łukasiewicz Research Network – Institute of Non-Ferrous Metals, Centre of Advanced Materials Technologies, Sowinskiego Street 5, 44-100 Gliwice, Poland

[b] Łukasiewicz Research Network – Institute of Non-Ferrous Metals, Centre of Powder and Composite Materials, Sowinskiego Street 5, 44-100 Gliwice, Poland

[c] Silesian University of Technology, Faculty of Mechanical Engineering, Welding Departments, Konarskiego Street 18A, 44-100 Gliwice, Poland

[d] Silesian University of Technology, Faculty of Mechanical Engineering, Materials Research Laboratory, Konarskiego Street 18A, 44-100 Gliwice, Poland

email*: justyna.d.dubiel@imn.lukasiewicz.gov.pl

Abstract: The influence of laser surface alloying (LSA) of Cu on microstructure was investigated. The paper presents microstructure of the composite Cu surface layer alloyed with a mixture of CrWC powders. Copper alloying was performed using high power diode laser HPDL. In the tests three mixtures of powders with different percentage contents (75%Cr 25%WC, 50%Cr 50%WC, 25%Cr 75%WC) were injected into the melt pool during laser surface alloying. Structural investigations were performed using light microscopy, scanning electron microscopy (SEM, TEM) and X-ray diffraction (XRD). The copper top layer after laser treatment consists of uniform distribution of the particles of applied powders in the shaped layer and nanoscale precipitates in the Cu matrix. Also microhardness of the modified surface layer was examined. The copper surface layer after laser alloying with CrWC powders shows increased microhardness compared to pure copper.

Keywords: copper, laser surface alloying, microstructure, microhardness

1. INTRODUCTION

Copper and its alloys are widely used as electric contact materials, such as electronic devices, lead frame materials for integrated circuits, welding electrodes, overhead contact wires, mainly due to their high electrical and thermal conductivities [1,2]. However, in many cases, the use of copper is limited by the unsatisfactory properties of the surface layer, i.e. its low hardness and wear resistance. Therefore, some attractive techniques are used in surface engineering to increase the performance of components and to reduce their wear. Significant improvement of anticorrosive properties and increase of resistance to abrasive wear can be achieved by application of methods of surface metal layer shaping. The laser alloying, also known as the Laser Surface Alloying - LSA, is based on introduction of alloying elements into the alloyed material [3]. Mutual intense mixing of materials occurs in the melt pool as a result of convection and gravitational movements, and a laser beam. The liquid metal rapidly cools down and solidifies as a result of a large temperature gradient at the boundary of the melted surface layer and the substrate.

Copper and its alloys are characterized by high laser radiation reflection coefficients, which is a serious problem in the processes of laser surface treatment of these materials [4,5].

The paper presents the investigation results of copper after laser surface alloying using three mixtures of powders with different percentage contents (75%Cr 25%WC, 50%Cr 50%WC, 25%Cr 75%WC).

2. MATERIAL AND METHODOLOGHY FOR STUDIES

Commercially pure copper (cp Cu) of 50 mm diameter and 5 mm high plates were used as the substrate. Laser alloying of the surface layer of copper, using Cr and WC powder with various percentage contents of 75%Cr 25%WC, 50%Cr 50%WC, 25%Cr 75%WC was carried out using a HPDL Rofin DL 020 high power diode laser. The WC powder contained amounts of Mo and Ni (~1%). Before the laser surface treatment, the samples were sandblasted and then rinsed in an ultrasonic bath. Ni powder was mixed with ethyl alcohol and then was applied in the form of a paste onto the sandblasted copper surface. In the second step, CrWC powder of different percentage concentration was fed in the gas stream to the melt pool area.

3. RESULTS

The article presents the microstructure of the copper surface layer after laser alloying with mixtures of CrWC powders (with various concentrations). Laser surface alloying of cp Cu with different content CrWC in the alloyed zones has been successfully achieved using a HPDL The copper top layer after laser treatment consists of uniform distribution of the particles of applied powders in the shaped layer and nanoscale precipitates in the Cu matrix. Several characteristic types of precipitations were observed - different in terms of morphology, structure and chemical composition. The phase composition of the analyzed samples was determined. The highest intensity of chromium reflexes was observed for a copper specimen alloyed with Cr75WC25 powder, and the smallest for a copper sample after alloying with Cr25 WC75 powder. In all samples apart from the dominant copper-structure phase several other phases were identified. Most apparent is the cubic A2 structure of α-chromium.

The increase in microhardness in the Cu surface layer after laser alloying with CrWC is attributed to solution and dispersion hardening. Microhardness of the surface layer of copper after alloying with CrWC powder with different powder concentration shows large scatter of its value at the cross-section of the melted zone. This is due to the numerous fluctuations in the chemical composition in the laser treated zone.

Acknowledgments: The study was carried out as part of the project LIDER/33/0091/L-7/NCBR/2016 "Laser surface treatment of selected copper alloys on high-current constructional elements" financed by NCBiR and Statutory Work of Łukasiewicz Research Network - Institute of Non-Ferrous Metals „Study of the possibility of regeneration of high-current structural elements in the laser surface treatment process”.

BIBLIOGRAPHY

1. Z. Rdzawski, Copper alloy. Monograph 229, Silesian University of Technology, Gliwice, 2009.
2. J.R. Davis, ASM Specialty Handbook. Copper and Copper Alloys.; ASM International, 2001.
3. J. Kusiński, Lasers and their application in material engineering, Scientific Publisher "Akapit", Cracow, 2000.
4. M. Li, M. Chao, E. Liang, J. Yu, J. Zhang, D. Li,” Improving wear resistance of pure copper by laser surface modification,” Applied Surface Science, 258 (4) (2011) 1599 - 1604.
5. C.T. Kwok, P.K. Wong, H.C. Man, Laser surface alloying of copper with titanium: Part I. Electrical wear resistance in dry condition. Part II. Electrical wear resistance in wet and corrosive condition, Surface & Coatings Technology 297 (2016) 58–73.

MTS CONFERENCE
MATERIAL TECHNOLOGIES IN SILESIA

12-15.06.2022
Crystal Mountain***** Hotel, Wisła, Poland

Performance analysis of dye-sensitized solar cells with TiO_2 photoanode deposited using screen printing and ALD method

A. Drygała[a], M. Szindler[b]

[a] Silesian University of Technology, Faculty of Mechanical Engineering, Department of Engineering Materials and Biomaterials, 18a Konarskiego Str., 44-100 Gliwice, Poland
[b] Silesian University of Technology, Faculty of Mechanical Engineering, Scientific and Didactic Laboratory of Nanotechnology and Material Technologies, Towarowa 7 Str., 44-100 Gliwice, Poland
email: aleksandra.drygala@polsl.pl

Abstract: In this study, dye-sensitized solar cells based on titanium oxide films with different printing layers were fabricated by screen printing method. Moreover, TiO_2 blocking layers with different thickness were deposited between the transparent conductive oxide and the mesoporous screen-printed TiO_2 layer using atomic layer deposition (ALD). The topography, absorption/transmission spectra of the deposited layers were studied using scanning electron microscope (SEM), atomic force microscope (AFM) and UV-Vis spectrophotometer. Electrical properties of manufactured DSSCs were characterized by I-V illuminated characteristics under standard AM 1.5 radiation.

Keywords: photovoltaics, dye-sensitized solar cell, titanium dioxide, atomic layer deposition, blocking layer

1. INTRODUCTION

Solar power is an important resource because of its inexhaustibility and pollution-free character. Moreover, solar energy is the cleanest and most abundant renewable energy source available in the world. New technologies are being explored and refined to enable solar power to become a reliable, stable power source for the future. Photovoltaics PV is a simple method of harnessing the sun's energy [1,2].

Dye-sensitized solar cells (DSSCs) are attractive as simple and low cost renewable energy source. This type of solar cell is considered to be one of the most promising, current technological developments that meets the requirement of cost-effective green energy technology. The DSSC is an alternative to standard solar cells operating thanks to the p-n junction, they consist of a photoanode, an electrolyte and a counter electrode. Photoanode is an important element in DSSC. It functions as a scaffold for dye molecules adsorption. The working electrode acts as medium for collection and transportation of photo-exited electrons from dye to external electric circuit. Usually the photoanode consists of nanoporous semiconductor (e.g. metal oxide) with wide band gap. In this work the TiO_2 films were formed by the screen printing method which is relatively easy, inexpensive and can be used for mass production [3-5].

Electron recombination in dye-sensitized solar cells results in significant electron loss and performance degradation. Prevention of this occurrence can be achieved through appropriate design of the device and incorporation of a thin film that blocks the back-transfer reaction of the photoelectrons [5, 6]. In this study, TiO_2 blocking layers with different thickness (controlling by the different number of ALD cycles) were deposited between the transparent conductive oxide and the mesoporous titanium oxide layer using atomic layer deposition method ALD. The prepared samples were characterized by scanning electron microscopy SEM, atomic force microscope (AFM) and UV–Vis absorption spectroscopy. The effects of film thickness on the electrical properties of DSSCs were also investigated.

These studies revealed that the photovoltaic properties of DSSCs significantly depend on the TiO_2 film thickness. The DSSCs with porous TiO_2 film thickness of 13 μm (this corresponds two printed layers) achieved the maximum efficiency value. The blocking layer deposited by atomic layer deposition is much denser than the

mesoporous screen-printed TiO_2 layer. Therefore, it reduces the contact surface area between FTO/electrolyte and increased electron pathways. The best electrical properties have been obtained for DSSCs with ALD-TiO_2 thin film after 600 cycles of deposition.

a) b)

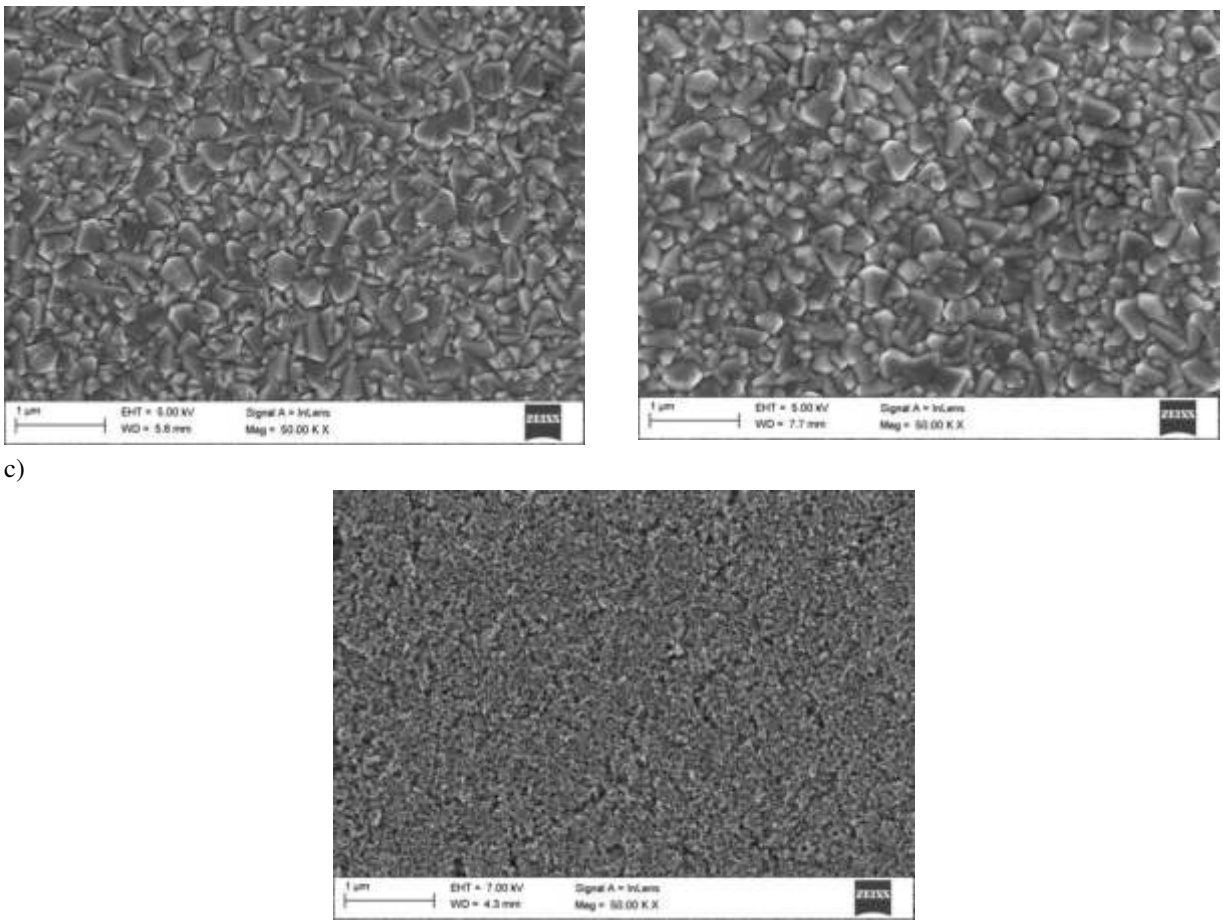

c)

Figure 1. SEM images of the surface topography of a) substrate (FTO coated glass), b) TiO_2 blocking layer deposited on the FTO coated glass by ALD method, c) screen-printed TiO_2 layer

BIBLIOGRAPHY

1. D. Gielen, F. Boshell, D. Saygin, M.D. Bazilian, N. Wagner, R.Gorini: The role of renewable energy in the global energy transformation. Energy Strategy Reviews, 24 (2019) 38-50.
2. J.A. Luceno-Sanchez, A.M. Diez-Pascual and R.P. Capilla, Materials for photovoltaics: state of art and recent developments, International Journal of Molecular Sciences, 20/4 (2019) 976.
3. F. Babar, M. Umer, A. Hafza, M.H. Mehdi, A. Ul Haq Khan, H. Khalid, N. Ul Huda, Z. Fatima, Nanostructured photoanode materials and their deposition methods for efficient and economical third generation dye-sensitized solar cells: a comprehensive review, Renewable & Sustaiable Energy Reviews, 129 (2020) 1-13.
4. S. Seo, S. Jeong, H. Park, H. Shin, N.G. Park, Atomic layer deposition for efficient and stable perovskite solar cells, Chemical Communications, 55/17, (2019) 2403-2416.
5. P. Cheng, P. Banerjee, Few monolayer atomic layer deposition (ALD) on surfaces and interfaces for energy applications, Material Matters, 13/2 (2018) 65-69.
6. Y. Li, L. Ma, Y. Yoo, G. Wang, X. Zhang, M.J. Ko, Atomic layer deposition: A versatile method to enhance TiO_2 nanoparticles interconnection of dye-sensitized solar cell at low temperature", Journal of Industrial and Engineering Chemistry, 73/25 (2019) 351-356.

MTS CONFERENCE
MATERIAL TECHNOLOGIES IN SILESIA

12-15.06.2022
Crystal Mountain***** Hotel, Wisła, Poland

Silanization of spherical aluminosilicates using tetraethoxysilane (TEOS) and graphene oxide (GO), taking into account the process variables i.e. temperature and thermal treatment atmosphere.

A. Dubiel[a], W. Walke[a], D. Nakonieczny[a], M. Antonowicz[a], G. Dzido[b], S. Holesova[c]

[a] Silesian University of Technology, Faculty of Biomedical Engineering, Department of Biomaterials and Medical Device Engineering
email: agnieszka.dubiel@polsl.pl
[b] Silesian University of Technology, Faculty of Chemistry, Department of Chemical Engineering and Process Design
[c] VŠB-Technical University of Ostrava, Nanotechnology Centre

Abstract: The aim of this research work was to produce COOH and OH groups on the aluminosilicate surface allowing the attachment of biomolecules acting as drug carriers. To ensure appropriate physicochemical properties, spherical aluminosilicates were silanized using tetraethoxysilane (TEOS), while graphene oxide was prepared using a modified Humers method. For comparison purposes, the sample group was divided into two types: in the initial state (after silanization) and with graphene oxide. Samples of different sizes (fraction: 90 µm,150 µm and 220µm) were evaluated. In this work, studies were carried out to determine the behavior of graphene oxide on the aluminosilicate surface in the formation of functional groups using Fourier Transform Infrared Spectroscopy (FTIR). Scanning electron microscopy (SEM-EDS) observations, X-ray analysis (XRD) and particle size distribution (PSD) studies were additionally carried out to more fully characterize the proposed modification type.

Keywords: aluminosilicates, TEOS, graphene oxide

1. INTRODUCTION

Following the current health statistics have clearly shown that as the population ages, there is an increasing percentage of bone fractures due to weakening of their structure, in particular the occurrence of osteoporosis. Decreasing density of bone structure also has an impact on injuries resulting from traffic accidents, which translates into the number of people hospitalized, treated surgically and requiring rehabilitation. In the treatment of bone fractures, mainly surgical methods with the use of implants supporting the adhesion process or less invasive methods in the form of plaster dressings are used. There is a wide range of synthetic materials including metals, ceramics, polymers and cements are available to treat damaged bone. Despite the variety of solutions available, a material with properties similar to those of bone is still being sought. One such solution is spherical aluminosilicate. It is a material that is formed from the combustion of hard coal in pulverized furnaces. As a result of high temperature and under the influence of surface tension forces (change in surface energy), aluminosilicates take on a spherical shape, and gases released at an earlier stage of combustion form a cavity inside the newly formed spherical grains. In this way, an ultralight filler is formed. The use of microspheres as a filler will allow to obtain a composite material not only with a significantly lower density but also with higher stiffness, stability and surface smoothness, which will translate into strength of the produced filler for polymers used in biomedical engineering. Additionally, the use of graphene oxide will allow for the production of carbosyl and hydroxyl groups in order to produce a drug carrier.

1.1. Materials and methods

The modification process was divided into three steps. First, the aluminosilicates were etched in fresh hot Piranha solution, which was prepared from H2SO4 and 30% H2O2 in a volume ratio of 3:1. The acid was mixed in a beaker with a flat bottom on a magnetic stirrer (time, 10 min; speed, 350 rpm). After 10 min, microspheres were added and treated with Piranha solution for 30 min (speed, 350 rpm). After 30 min, the Piranha solution was decanted into a separate beaker. To remove residual acid, the powders were percolated (4 x 1000 cm3 wash) with deionized water under reduced pressure using a water pump and then washed with 2-propanol. The second step of the modification process was silanization using tetraethoxysilane (TEOS) in (1:1) and (1:2) ratios. 1g of graphene oxide (GO) was added to the solution and allowed to stand for 6 h at 400 rpm at 25°C and 40°C. The powders were then washed and dried in an oven for 24 h at 60°C. The test was also conducted in a glove box under a vacuum atmosphere. Scanning electron microscopy-energy dispersive X-ray spectroscopy (SEM-EDS), X-ray diffraction (XRD), Fourier transform infrared spectroscopy (FTIR) analysis are planned to verify the process.

1.2 Results and Discussion

In the present study, aluminosilicate microspheres were subjected to surface modification to develop it by using silanization process and doping with graphene oxide.FTIR analysis revealed the presence of carboxyl and hydroxyl groups resulting from the silanizing agent and graphene oxide. The shown groups may become drug carrier in further modification of the composite. X-ray analysis revealed peaks typical of cenospheres containing mainly aluminosilicate phases such as mullite and silimanite and other smaller phases such as quartz. The analysis revealed several characteristic peaks including a broad peak near 9° representing the occurrence of GO. The structure of the microspheres in the SEM study showed surface development due to the application of etching and silanization process.

Acknowledgments: The project was funded by the Department of Biomaterials and Medical Devices Engineering, Faculty of Biomedical Engineering, Silesian University of Technology, Zabrze, Poland.

BIBLIOGRAPHY

1. I.Dayana, T.Sembiring, A.P. Tetuko, K.Sembiring, N.Maulida, Z.Cahyarani, E. A. Setiadi, N.S. Asri, M. Ginting, P. Sebayang, The effect of tetraethyl orthosilicate (TEOS) additions as silica precursors on the magnetite nano-particles (Fe3O4) properties for the application of ferro-lubricant, Journal of Molecular Liquids, 294 (2019)
2. C.Kunyao , Y.Zongxue, Y.Di, C.Legang, J.Yong, Z.Lijuan, Fabrication of BTA-MOF-TEOS-GO nanocomposite to endow coating systems with active inhibition and durable anticorrosion performances, Progress in Organic Coatings,143 (2020)

MTS CONFERENCE
MATERIAL TECHNOLOGIES IN SILESIA

12-15.06.2022
Crystal Mountain***** Hotel, Wisła, Poland

Steam oxidation studies of Additive Manufactured (AM) Monel 400 alloy

T. Dudziak[a], W. Polkowski[a], T. Kruml[b], Jan-Philipp Roth[c], P. Wieliczko[a], E. Rząd[a], Ł. Boroń, F.J. Perez Trujillo[d], I. Milasant[d]

[a] Łukasiewicz – Krakow Institute of Technology, Zakopiańska 73, 30-418 Krakow, Poland
email: tomasz.dudziak@kit.lukasiewicz.gov.pl, wojciech.polkowski@kit.lukasiewicz.gov.pl, piotr.wieliczko@kit.lukasieiwcz.gov.pl, ewa.rzad@kit.lukasieiwcz.gov.pl, Lukasz.boron@kit.lukasiewicz.gov.pl
[b] Institute of Physics of Materials AS CR, Czech Academy of Science, Žižkova 513/22 616 00 Brno
Czech Republic
kruml@ipm.cz
[c] Faculty of Engineering and Computer Science, Hochschule Osnabrück / Osnabrück University of Applied Sciences
j.roth@hs-osnabrueck.de
[d] Research group Surface Engineering and Nanostructured Materials, Dept. Chemical and Materials Engineering Faculty of Chemical Sciences Universidad Complutense de Madrid, Spain
milasant@ucm.es, fjperez@ucm.es

Abstract: Aim of this work was to investigate the results of additive manufactured Monel 400 alloy exposed to steam oxidation test at 650 and 750 ºC for 500 hours. The process was carried out in 100% steam rig where deionised water is transferred throughout the hot zone of the furnace and condensate in a reservoir. During the process, nitrogen is constantly running to purge the reservoir in order to minimise oxygen concentration in water. The steam was flown with 2.833 ml/min using 1 rotation per minute (rpm) speed. Both tests were carried out in the same way, the samples were exposed for 24, 72, 168, 250 and finally 500 hours. The mid exposure investigations were carried out after 250 hours, the final analyses were carried out after 500 hours, comparison of data confirmed degradation of the exposed samples. The materials were printed using Laser Powder Bed Fusion (LPBF) using commercial available Monel 400 powder (Ni – Cu alloy). The material was investigated using XRD and finally SEM/EDS techniques to analyse: phase constituents, microstructure and chemical composition. The results revealed much higher mass gain of the Monel 400 exposed at 750 ºC in comparison to the Monel 400 exposed at 650 ºC, further mass gain of no scale spallation, flaking or delamination of the oxide scale was observed.

Keywords: materials, additive manufacturing, hot isostatic press, oxidation, high temperature

Introduction

Importance of the high temperature materials resistance is crucial for modern industry where a higher efficiency is required. Among a wide list of the Fe based, Ni – based materials with a Cr content that show a high resistance to corrosion in oxidising atmospheres, recently a new class of the materials are become more fascinating for scientist and engineers. The additive manufactured (AM) alloys currently are the materials of interest since the materials can be fabricated in any shape using specific powder with a restricted dimension [1]. The AM materials are a new generation of materials that can be used in energy sector where high temperature steam is used or other gas mixtures are present including aggressive atmosphere. Nevertheless, to deliver the material with appropriate properties, a new material must be investigated in lab scale process to understand the fundamental processes such as mechanical properties and oxidation resistance. In this work additively manufactured alloys Ni-Cu Monel 400 printed using Laser Powder Bed Fusion was exposed in steam atmosphere at 650 ºC for 500 hours. The exposed materials latterly were investigated using XRD, SEM coupled with EDS.

2. Experimental procedure

The LPBF was used to fabricate Monel 400 alloy, the method is the most prevalent method currently being utilized for AM and is a layer-by-layer process in which a high-powered laser is used to melt a thin layer of powdered material in the desired net-shape of a part. [2, 3]. The research in steam atmosphere was carried out in the steam oxidation rig shown in Figure 1 [4,5,6].

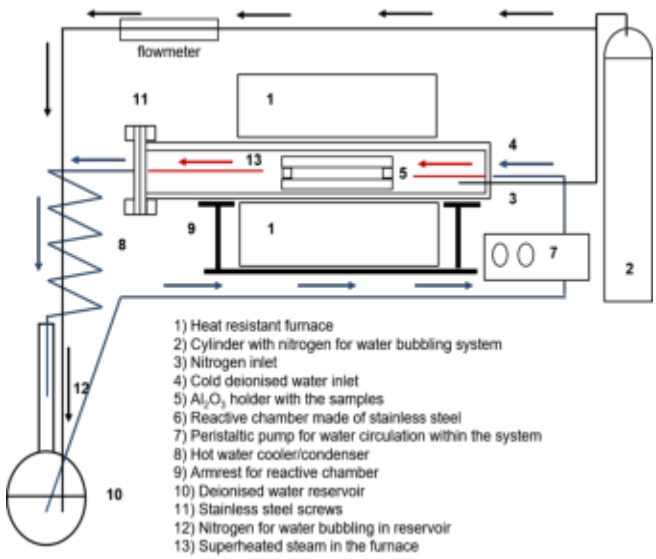

Figure 1 Steam oxidation rig used in this work

Acknowledgements: The work presented in this study was carried out in within the scope of project entitled: "*Tailoring ODS materials processing routes for additive manufacturing of high temperature devices for aggressive environments*" topAM. This project has received funding from the European Union's Horizon 2020 research and innovation programme under grant agreement No 958192.

BIBLIOGRAPHY

[1] C. Magnin, Z. Islam, M. Elbakhshwan, A. Brittan, D. J. Thoma, M. H. Anderson, The performance of additively manufactured Haynes 282 in supercritical CO2, Materials Science and Engineering: A, Volume 841, 2022, 143007

[2] T. DebRoy, H.L. Wei, J.S. Zuback, T. Mukherjee, J.W. Elmer, J.O. Milewski, A.M. Beese, A. Wilson-Heid, A. De, W. Zhang Additive manufacturing of metallic components – process, structure and properties Prog. Mater. Sci., 92 (2018), pp. 112-224,

[3] S. Sanchez, P. Smith, Z. Xu, G. Gaspard, C.J. Hyde, W.W. Wits, A.T. Clare, Powder bed fusion of nickel-based superalloys: a review, Int. J. Mach. Tool Manufact., 165 (2021), 103729

[4] T. Dudziak et al., Phase Investigations under Steam Oxidation Process at 800 ºC for 1000 h of Advanced Steels and Ni-Based Alloys, Oxid. Met., 2018, 139–158

[5] T. Dudziak, et al. Steam oxidation behaviour of advanced steels and Ni based alloys at 800 ºC, J. Mater. Eng. Perform.: 26, 2017, 1044–1056

[6] T. Dudziak, et al. Neural Network Modelling Studies of Steam Oxidised Kinetic Behaviour of Advanced Steels and Ni-based alloys at 800 ºC for 3000 hours, Corros. Sci: 133(1), 2018, 94–111. doi.org/10.1016/j.corsci.2018.01.013

MTS CONFERENCE
MATERIAL TECHNOLOGIES IN SILESIA

12-15.06.2022
Crystal Mountain***** Hotel, Wisła, Poland

Implants in Traumatology and Orthopaedics

K. Frydrýšek[a,c], D. Čepica[a,c], T. Halo[a,c], F. Sejda[a,c], K. Šimečková[a,c], O. Skoupý[a,c], L. Pleva[b,c], J. Hlinka[d], M. Sadílek[e], M. Havlíček[f], P. Krpec[g], D. Stančeková[h], P. Eiba[a,c]

[a] Department of Applied Mechanics, Faculty of Mechanical Engineering, VSB—Technical University of Ostrava, 17. Listopadu 2172/15, 708 00 Ostrava, Czech Republic, e-mail: karel.frydrysek@vsb.cz, daniel.cepica@vsb.cz, tomas.halo@vsb.cz, frantisek.sejda@vsb.cz, katerina.simeckova@vsb.cz, ondrej.skoupy@vsb.cz, patrik.eiba@vsb.cz.
[b] Trauma Center, University Hospital Ostrava, 17. listopadu 1790, 708 52 Ostrava-Poruba, Czech Republic: leopold.pleva@fno.cz.
[c] Institute of Emergency Medicine, Faculty of Medicine, University of Ostrava, Syllabova 19, 703 00 Ostrava-Vítkovice, Czech Republic.
[d] Center of Advanced Innovation Technologies, VSB—Technical University of Ostrava, 17. listopadu 15/2172, 708 00 Ostrava-Poruba, Czech Republic, e-mail: josef.hlinka@vsb.cz.
[e] Department of Machining, Assembly and Engineering Metrology, Faculty of Mechanical Engineering, VSB—Technical University of Ostrava, 17. listopadu 2172/15, 708 00 Ostrava, Czech Republic, e-mail: marek.sadilek@vsb.cz.
[f] V-NASS, a.s., Halasova 2938/1a, 703 00 Ostrava-Vítkovice, Czech Republic, e-mail: pavel.krpec@v-nass.cz.
[h] Department of Machining and Manufacturing Technologies, Faculty of Mechanical Engineering, University of Žilina, Univerzitná 8215/1, 010 26 Žilina, Slovakia, e-mail: dana.stancekova@fstroj.uniza.sk.

Abstract: This paper is a review and represents a multidisciplinary approach to biomechanics (medicine, engineering, technology and mathematics) in the field of design of the implants for traumatology and orthopaedics. These implants are applied in osteosyntheses for treatment of bone fractures of humans and animals.

Keywords: biomechanics, traumatology, orthopadedics, engineering design, technology

1. INTRODUCTION

External fixators and internal fixators are used for the treatments of complicated fractures in traumatology and orthopaedics. They can be produced by catting technology and in some cases by aditive technology in combination with catting teghnology. This paper is a review of some designs of implants solved by our team and produced of biocompatible materials via catting and aditive technologies.

In Fig. 1, there is headless (Herbert) screw made of Ti6Al4V material as an application for osteosynthesis of the 5th metatarsal bone, see references [1] and [2]. There are presented analytical (deterministic), stochastic (probabilistic, Monte Carlo Method), experimental (measurements) and numerical (Finite Element Method) approaches.

In Fig. 2, there are strength and deformation analyses of screws for femoral neck fractures, see references [3] and [4]. There are presented analytical (deterministic), stochastic (probabilistic, Monte Carlo Method), and numerical (Finite Element Method) approaches. Screws are made of Ti6Al4V and stainless steel material.

There are experiments about the mechanical behaviour of frontal part of human skull, i.e. splachnocranium, linked with an external loads and damages caused mainly via brachial violence. Practical focuses are mainly on orbita, os frontale and os zygomaticum. As a first approach, the brachial violence is simulated via quasi-static compression laboratory tests. Cadaveric skulls are attached in testing machine and loaded till fractures occurs. The

goals of experiements are about the biomechanical testings and future design of implants made of of Ti6Al4V, stainless steel material and plastics.

Other biomechanical applications are presented in [5] and [6].

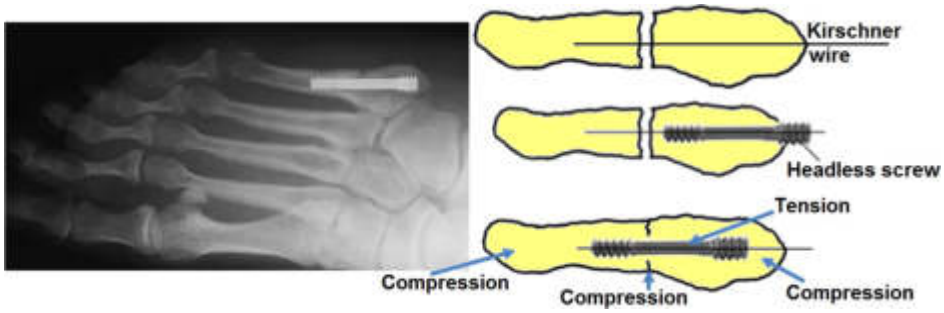

Figure 1. Application of a headless screw to the 5th metatarsal bone

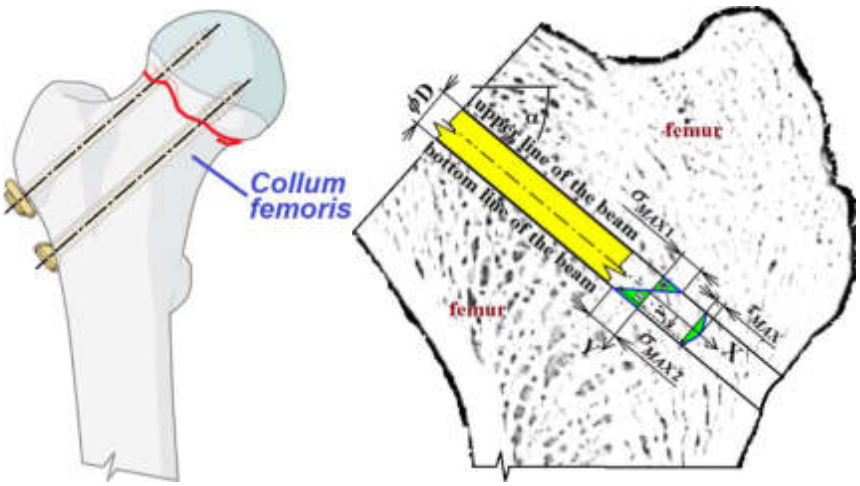

Figure 2. Application of a femoral screw to the femur

Acknowledgments: This article was supported by Czech project SP2022/2 and by projects CZ.02.1.01/0.0/17_049/0008407 and CZ.02.1.01/0.0/0.0/17_049/0008441 within the Operational Programme Research, Development and Education financed by the European Union and from the state budget of the Czech Republic.

BIBLIOGRAPHY

1. Bajtek, V.; Frydrýšek, K.; Pleva, L. Stochastic Strength Analysis of Compression Headless Screw. MM Science Journal, March, 2020, pp. 3837-3840, ISSN: 18031269, DOI: 10.17973/MMSJ.2020_03_2019133.
2. Šimečková, K.; Frydrýšek, K.; Machalla, V.; Demel, J.; Pleva, L.; Bajtek, V. Osteosynthesis of the Fractured Fifth Metatarsus with Headless Screw. Engineering Mechanics, 2019, pp. 355-358, DOI: 10.21495/71-0-355.
3. Frydrýšek, K.; Šír, M.; Pleva, L. Strength Analyses of Screws for Femoral Neck Fractures. J. Medical and Biological Engineering, 2018, pp. 1-19, ISSN 2199-4757, DOI: 10.1007/s40846-018-0378-x.
4. Frydrýšek, K.; Šír, M.; Pleva, L.; Szeliga, J.; Stránský, J.; Čepica, D.; Kratochvíl, J.; Koutecký, J.; Madeja, R.; Dědková, K.P.; Stančeková, D. Stochastic Strength Analyses of Screws for Femoral Neck Fractures. Appl. Sci. 2022, 12, 1015. https://doi.org/10.3390/app12031015
5. Frydrýšek, K.; Čepica, D.; Halo, T.; Skoupý, O.; Pleva, L.; Madeja, R.; Pometlová, J.; Losertová, M.; Koutecký, J.; Michal, P.; Havlas, V.; Kraus, Š.; Ďurica, D.; Dědková, K.P.; Pagáč, M.; Krpec, P.; Osemlak, P. Biomechanical Analysis of Staples for Epiphysiodesis. Appl. Sci. 2022, 12, 614. https://doi.org/10.3390/app12020614
6. Čada, R.; Frydryšek, K.; Sejda, F.; Demel, J.; Pleva, L. Analysis of Locking Self-Taping Bone Screws for Angularly Stable Plates. J. Med. Biol. Eng., 37, 2017, pp. 612–625, DOI: 10.1007/s40846-017-0279-4

MTS CONFERENCE
MATERIAL TECHNOLOGIES IN SILESIA

12-15.06.2022
Crystal Mountain***** Hotel, Wisła, Poland

Wpływ długotrwałej eksploatacji wirników turbin parowych na zmiany struktury i właściwości niskostopowej stali Cr-Mo-V

J. Furmanek[a], J. Dobrzański[a]

[a] Sieć Badawcza Łukasiewicz – Instytut Metalurgii Żelaza im. Stanisława Staszica, Grupa Badawcza: Badania Materiałów dla Energetyki
email: joanna.furmanek@imz.pl

Streszczenie: Celem pracy była ocena stanu i stopnia wyczerpania materiałów ze stali 21HMF po długotrwałej eksploatacji o wybranych stanach struktury i stopniu rozwoju procesów wydzieleniowych. Wybrane stany struktury zdefiniowano na podstawie ujawnionych obrazów w skaningowym mikroskopie elektronowym oraz stopnia rozwoju procesów wydzieleniowych w oparciu o przeprowadzoną rentgenowską analizę składu fazowego osadów węglików wyizolowanych elektrolitycznie. Dla wyznaczenia szybkości pełzania wykonano próby pełzania z pomiarem wydłużenia w czasie próby, prowadzone w stałej temperaturze badania i dla różnych poziomów naprężenia. Dla wyznaczenia trwałości resztkowej, wykonano skrócone próby pełzania przy stałym poziomie naprężenia, odpowiadającym eksploatacyjnemu i w kilku poziomach temperatury badania.

Abstract: The aim of the study was the assessment of the state and degree of depletion of 21HMF steel materials after long-term operation with selected states of structure and degree of development of precipitation processes. Selected structure states were identified on the basis of scanning electron microscopy images and the degree of development of precipitation processes based on X-ray analysis of electrolytically-isolated carbide deposit phase composition. To determine creep rate, creep tests were carried out with measurement of elongation during the test, conducted at a constant test temperature and for different stress levels. To determine residual life, shortened creep tests were performed at a constant stress level corresponding to the operational one and at several test temperature levels.

Słowa kluczowe: wirnik, turbina, stal 21HMF, próby pełzania, mikrostruktura

1. WPROWADZENIE

Problematyka oceny trwałości długo eksploatowanych elementów ciśnieniowych bloków energetycznych i wydłużania czasu bezpiecznej ich eksploatacji ma niezwykle istotne znaczenie dla funkcjonowania gospodarki kraju. Eksploatowane jednostki są często poddawane procesowi modernizacji, którego celem jest zwiększenie ich sprawności i efektywności przy uwzględnieniu rosnących wymagań w zakresie wydłużenia czasu bezpiecznej eksploatacji znacznie poza obliczeniowy. Wymaga to podejmowania decyzji o przedłużeniu eksploatacji elementów i instalacji na podstawie obiektywnych informacji na temat stanu materiału i elementu. W tym celu niezbędna jest ocena stanu technicznego tych jednostek. Praca obejmuje zagadnienia oceny przydatności materiału wirników do eksploatacji po przekroczeniu obliczeniowego czasu pracy, oceny ich stanu mikrostruktury i zespołu właściwości użytkowych [1-4].

2. WYNIKI BADAŃ

W pracy przedstawiono wyniki badań przeprowadzone na reprezentatywnych wycinkach pobranych z części SP (średnioprężnej) i WP (wysokoprężnej) wirnika turbiny 18K360 bloku energetycznego o mocy nominalnej 360 MW po 220 000 godzin eksploatacji. Materiał do badań dobrano tak, aby różnił się strukturą i odpowiadającym jej stopniowi wyczerpania. Wybrane wyniki badań pokazano na rys. 1.

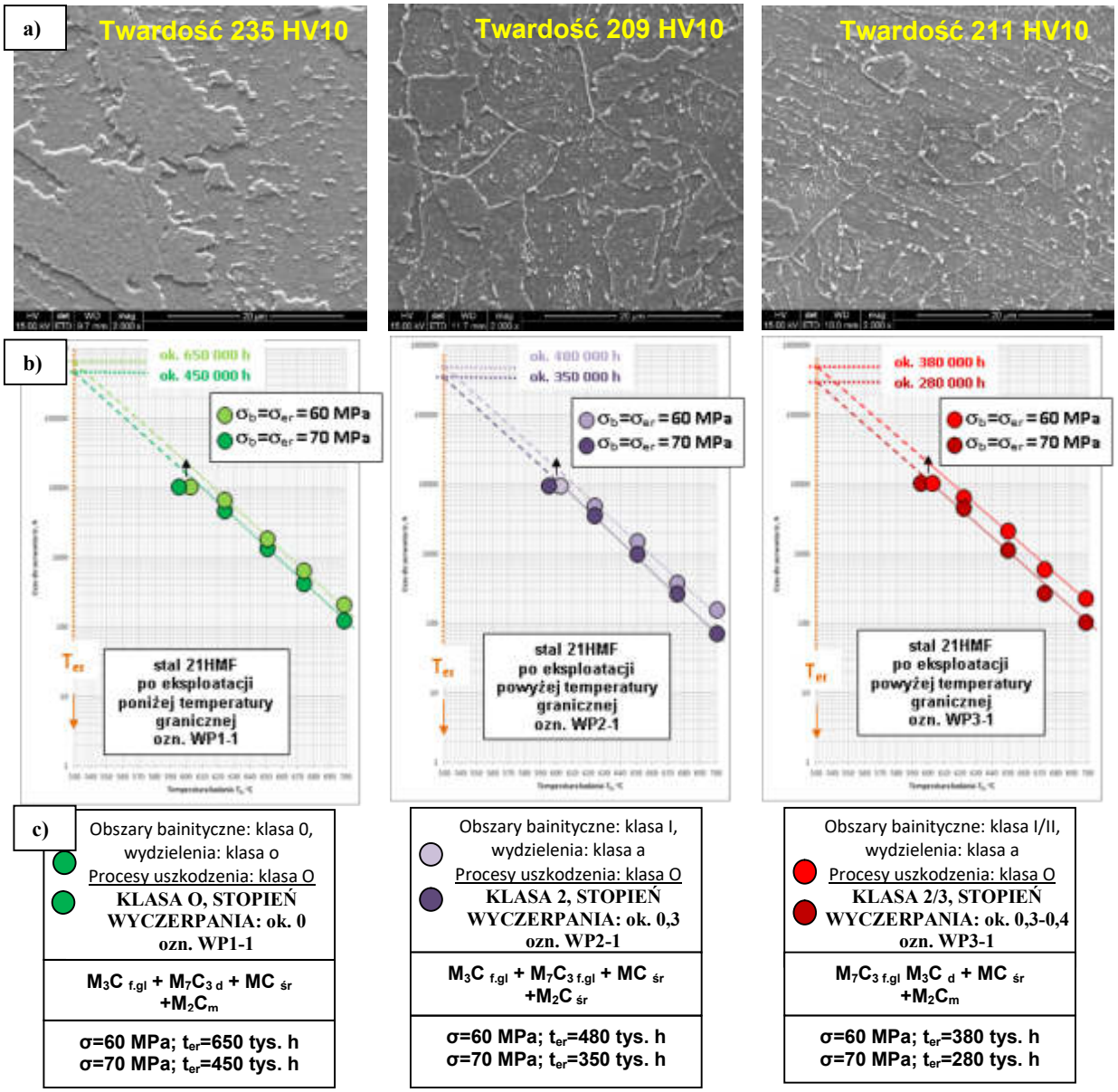

Rysunek 1. Struktura, resztkowa wytrzymałość na pełzanie t_{er} i skład fazowy wydzieleń w odniesieniu do klasy struktury i stopnia wyczerpania materiału części wysokoprężnej WP wirnika turbiny parowej bloku 360 MW wykonanego ze stali 21HMF po długotrwałej eksploatacji: a) obraz struktury obserwowanej w SEM, b) skrócone próby pełzania i wyznaczenie trwałości resztkowej, c) klasa struktury i skład fazowy wydzieleń

LITERATURA

1. J. Dobrzański, Trwałość elementów ciśnieniowych bloków energetycznych, Wydawnictwo Instytutu Metalurgii Żelaza, 2019.
2. J. Dobrzański, H. Purzyńska, Badania materiałowe w ocenie stanu i prognozowaniu dalszej bezpiecznej eksploatacji wirników turbin parowych po przekroczeniu obliczeniowego czasu pracy, Energetyka 11 (2015) 761-764.
3. J. Dobrzański, A. Rusin, H. Purzyńska, A. Zieliński, Wysokochromowe stale nowej generacji na wirniki turbin parowych bloków energetycznych o nadkrytycznych parametrach pracy. W: Maszyny i urządzenia energetyczne węglowych bloków na wysokie parametry pary, Wydawnictwo Politechniki Śląskiej, 2015, 95-124.
4. J. Furmanek, J. Dobrzański, Structure and mechanical properties of 21HMF steel steam turbine rotor materials after long-term operation for a time significantly exceeding the design time, Journal of Metallic Materials 73 (2) (2021) 40–55.

MTS CONFERENCE
MATERIAL TECHNOLOGIES IN SILESIA

12-15.06.2022
Crystal Mountain***** Hotel, Wisła, Poland

Characteristics of $Mg_{63}Zn_{30}Ca_4Au_3$ alloy produced by mechanical alloying

A. Gabryś[a], S. Lesz[a], J. Popis[a], B. Hrapkowicz[a], M. Karolus[b], K. Gołombek[c]

[a] Silesian University of Technology, Faculty of Mechanical Engineering, Department of Engineering Materials and Biomaterials
[b] Institute of Materials Engineering, University of Silesia
[c] Silesian University of Technology, Faculty of Mechanical Engineering, Materials Research Laboratory
Email: adrian.gabrys@polsl.pl, julia.popis@polsl.pl

Specific porosity, fine-grained structure and isotropic properties characterize the magnesium-based alloys produced by mechanical alloying. In addition, alloys containing magnesium, zinc, calcium, and the noble element - gold are biocompatible, so they can be used for biomedical implants. Gold has bactericidal and fungicidal properties and the addition of it to the mentioned alloys has a positive effect. In this paper selected mechanical properties and the structure of the $Mg_{63}Zn_{30}Ca_4Au_3$ alloy produced by mechanical alloying as a powder and a sinter obtained with the use of the Spark Plasma Sintering (SPS) method, were characterized. The results of the X-ray diffraction (XRD) method, density, scanning electron microscopy (SEM), determining particle size distributions with laser measuring, and Vickers microhardness for milling and sintering samples were presented. $MgZn_2$ and $AuZn_3$ phases, as well as pure elements of Mg, Zn, Au were stated in sintered samples.

Keywords: magnesium alloys, mechanical alloying, spark plasma sintering

1. INTRODUCTION

Mechanical Alloying (MA) is the process of milling a substance in a solid-state to obtain a powder. The input material comprises pure elements in appropriately selected proportions or alloys that are subjected to the milling process in high-energy mills. The material is placed in steel or ceramic containers filled with milling media made of appropriate materials, i.e., tungsten carbides, hardened steel or ceramics, etc. The result of the process is the formation of particles of similar size. This method is used for alloy amorphization, but as well as base material grinding and to change the order of the intermetallic phases microstructure. Because of the ongoing process, the input material is crushed and agglomerated. Due to the cyclic deformations, i.e. welding, crushing, and re-welding, the grain size is reduced and new grain boundaries are created. The structure of the material is not stable, the alloy may exist as a solid solution, intermetallic phase, mixture of components, or amorphous material [1 - 3].

The ingredients used in the mechanical alloying process are in a solid-state. During its duration, a mechanically induced reaction takes place between the powdery components of the alloy. This results in a change in the phase composition and microstructure. A special feature that distinguishes the mechanical alloying process from the many ball milling processes is the occurrence of both crushing and melting processes. Depending on the properties of the starting powders, we can distinguish different processes [4].

When both powders are plastic and collide with the spheres and the walls of the container, deformation occurs, resulting in which the grains overlap, creating a very developed lamellar structure (Figure 1.). A simultaneous process is powerful strengthening, which leads to cracking of the powder grains. Their surfaces do not oxidize because the process is carried out in an atmosphere of protective gases, such as argon or helium, and they can melt. Particles with a new chemical composition are formed [5].

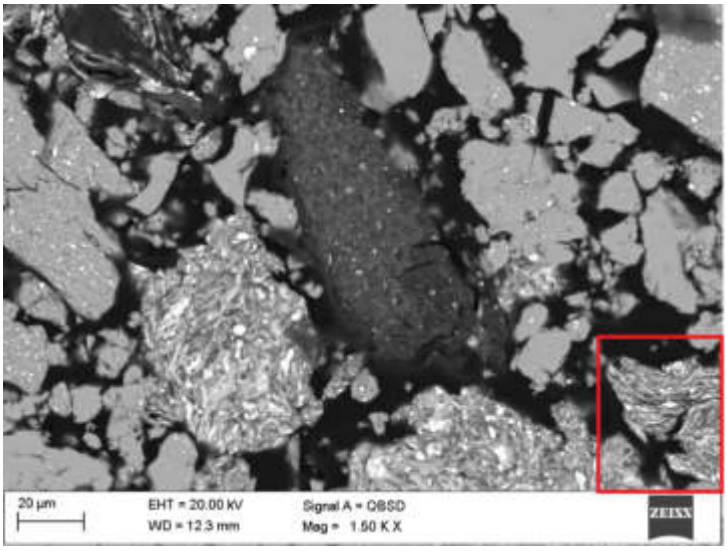

Figure 1. The lamellar structure formed during MA is marked in red, SEM photo

Depending on the size of the starting particles, the particle diameter changes two or three times. There is also a process of strong deformation strengthening. The particle breaks when it reaches the critical diameter and becomes hardened, repeating the cycle. Large particles break more frequently because the occurrence of a nucleus is proportional to the particle size. There are no crack nuclei in small particles, thanks to which they are more resistant to deformation and can combine with other, equally small particles. Over time, the small particles reach their maximum hardening point and break. The powder grains are disintegrating and show a crystalline or amorphous structure while maintaining a similar size and hardness [6].

Mechanical alloying enables a very high rate of phase transformations related to a low rate of diffusion in metals taking place at a temperature of several dozen degrees Celsius. A significant contact area, which increases during thinning of the component layers of the plate structure, facilitates the process overlap. The diffusion rate also increases due to the increased dislocation density and higher than equilibrium vacancy concentrations. Another advantageous feature is the local temperature increase caused by friction and plastic deformation of the powders. The size of the resulting grains also depends on the type of grinder in which they were produced. Each of the grinders has its own specific grinding energy. The grain size and deformation depend on the grinding intensity. The greater the grinding intensity, the smaller the grain and the greater the deformation. The mass of the ground powder also plays a significant role. The greater amount of powder, which behaves like a viscoelastic layer, reduces the impact force, increasing along with the grinding frequency [5].

Thanks to mechanical alloying, it is possible to produce materials that are inaccessible to traditional methods, such as casting, and it is also possible to obtain materials with a strictly defined chemical composition and high purity. The process of mechanical synthesis with the above-mentioned features enables the production of components, including biomedical implants with complex shapes, as well as high-entropy alloys [4].

BIBLIOGRAPHY

1. J. Rakowska, K. Radwan, Z. Ślosorz, Problems of estimation the size and shape of grain solids, 2012, Chemical and Fire Research Laboratories, Poznań University of Technology.
2. R.W. Kelsall, I.W. Hamley, M. Geoghegan, Nanotechnologies, Warsaw, Polish Scientific Publishers PWN, 2008. ISBN 978-83-01-15537-7.
3. S. Lesz, T. Tański, B. Hrapkowicz, M. Karolus, J. Popis, K. Wiechniak, „Characterisation of Mg-Zn-Ca-Y powders manufactured by mechanical milling", Journal of Achievements in Materials and Manufacturing Engineering 103 (2) 2020 49-59.
4. Y.P. Wang, B.S. Li, M.X. Ren, C. Yang, H.Z. Fu, ―Microstructure and compressive properties of AlCrFeCoNi high entropy alloy‖, Materials Science and Engineering A 491 (2008) 154–158.
5. M. Jurczyk, Mechanical synthesis, 2003, Publishing House of the Poznań University of Technology, Poznań.
6. K. Kowalski, A. Miklaszewski, M. Jurczyk, Obtaining and properties of solid magnesium-based alloys with ultra-fine-grained microstructure, Metal Forming Vol. XXVII No. 3 (2016) 195 - 210.

MTS CONFERENCE
MATERIAL TECHNOLOGIES IN SILESIA

12-15.06.2022
Crystal Mountain***** Hotel, Wisła, Poland

Influence of ageing on microstructure and mechanical properties of TP347HFG austenitic stainless steel

G. Golański[a], H. Purzyńska[b]

[a] Częstochowa University of Technology, Department of Engineering Materials, Częstochowa, Poland
email: grzegorz.golanski@pcz.pl

[b] Łukasiewicz Research Network – Institute for Ferrous Metallurgy, Department of Materials for Power Engineering, Gliwice, Poland

Abstract: The paper presents the results of microstructural and mechanical tests of long-term aged TP347HFG steel. The ageing was performed at time of up to 30 000 hours and the temperature of 600 and 650°C. Ageing was proved to lead to the precipitation of secondary phase particles not only inside grains, but also on the boundaries of grains and twins. The changes in the microstructure of the examined steel translated into the mechanical properties, i.e. initially observed growth and then the fall of the strength properties, and a gradual decrease in the fracture energy. The rate of changes in the microstructure and mechanical properties depended on the ageing temperature.

Keywords: austenitic stainless steel, precipitates, microstrcuture, mechanical properties

1. INTRODUCTION

Steel TP347HFG belongs to a group of heat-resisting austenitic steels used in the power industry, among other things for the steam superheaters. This type of steel was designed on the basis of steel TP347H by obtaining fine-grained structure through applying properly selected parameters of thermoplastic treatment. Because of fine grain, the TP347HFG steel shows better resistance to corrosion and oxidation compared to the base steel with similar creep resistance [1].

Austenitic steels were introduced in the power industry as construction materials because of low microstructure stability of martensitic steels of the 12%Cr type (HCM12A, VM12), and due to large susceptibility to dispersive transitions, the favourable MX precipitates into Z phase. It results in a fast degradation of creep resistance of the steel, which translates into a considerable reduction of the time of its safe service [2, 3].

Previous studies on the creep-resisting austenitic steel were mostly concentrated on the steel grades of HR3C and Super 304H, or focused on the investigation of material after service. These studies proved that the dominant mechanism of both the strengthening and the degradation of miscrostructure of austenitic steel are the processes connected with precipitation and coagulation of secondary phases [4, 5]. However, there is a lack of comprehensive data concerning the influence of the effect of temperature and time of ageing, simulating the actual service, on the processes of degradation of microstructure and mechanical properties of TP347HFG steel.
The paper presents the influence of temperature and time of ageing on the microstructure and mechanical properties of TP347HFG steel.

2. MATERIAL AND METHODOLOGY OF RESEARCH

The investigated material was test pieces taken from a pipe fragment made of TP347HFG steel of the chemical composition presented in table 1.

Table 1. Chemical composition of the examined steel, % wt

C	Mn	Si	P	S	Cr	Ni	Nb	N
0.10	1.42	0.38	0.022	0.001	18.71	11.88	0.60	0.10

The examined test pieces were after long-term ageing for up to 30 000 hours at the temperature of 600 and 650°C. The scope of the performed research included microstructural tests with the scanning and transmission electron microscopy, as well as the tests of mechanical properties, including: hardness test, static test of tension and impact strength test.

3. RESEARCH RESULTS

In the as-received state the TP347HFG steel had an austenitic microstructure with twins and numerous primary precipitates rich in niobium. The proces of ageing contributed to the precipitation of many particles of secondary phases not only inside grains but also on the grain boundaries. The precipitation processes in the initial phase of ageing contributed to a relatively significant growth of the strength properties and hardness, and then to the overageing of the alloy. At the same time, a decrease in the crack resistance of the examined steel was observed. This decrease was expressed in crack energy and was more substantial for the higher temperature of ageing.

4. SUMMARY

The investigated material was test pieces taken from TP347HFG steel, subject to long-term ageing at the temperature of 600 and 650°C and soaking time of up to 30 000 hours. In the as-received state, the examined steel had a fine-grained austenitic structure with twins and numerous primary precipitates. The process of ageing at the temperature close to the expected temperature of service contributed mostly to the precipitation of secondary phase particles inside grains and on the boundaries of grains and twins. The process of degradation of the analyzed steel microstructure resulted in a change in the mechanical properties, i.e. initially observed growth and then the fall of the strength properties and the progressive fall of fracture energy. The rate of change in the microstructure and reduction of mechanical properties depended on the temperature of ageing. The more advanced processes of microstructure degradation and the effect of overageing and growth of brittleness were visible for the material aged at a higher temperature.

BIBLIOGRAPHY

1. K. Yoshikawa, H. Teranishi, K. Tokimasa, H. Fujikawa, M. Miura, K. Kubota, Fabrication and properties of corrosion resistant TP347H stainless steel, Journal of Materials Engineering 10 (1988) 69-84.
2. H.K. Danielsen, Review of Z phase precipitation in 9-12%wt. Cr steels, Materials Science and Technology 32 (2015) 126-137.
3. R. O. Kaibyshev, V. N. Skorobogatykh, I. A. Shchenkova, Formation of the Z-phase and prospects of martensitic steels with 11%Cr for operation above 590°C, Metal Science and Heat Treatment 52 (2010) 90-99.
4. A. Zieliński, G. Golański, M. Sroka, Evolution of the mircrostructure and mechanical properties of HR3C austenitic stainless steel after ageing for up 30000 h at 650-750°C, Materials Science and Engineering 796A (2020) 139944.
5. K. Sawada, T. Hatakeyama, K. Sekido, K. Kimura, Microstructural changes and creep-strength degradation in 18Cr-9Ni-3Cu-Nb-N steel, Materials Characterization 178 (2021) 111286.

MTS CONFERENCE
MATERIAL TECHNOLOGIES IN SILESIA

12-15.06.2022
Crystal Mountain***** Hotel, Wisła, Poland

The influence of biodegradable polymer coatings containing nanohydroxyapatite on the corrosion resistance of a titanium alloy

K. Goldsztajn[a], J. Szewczenko[a], M. Sowa[b], K. Nowińska[c], A. Hercog[d], J. Jaworska[d], K. Jelonek[d], W. Simka[b], M. Basiaga[a]

[a] Silesian University of Technology, Faculty of Biomedical Engineering, Department of Biomaterials and Medical Device Engineering
[b] Silesian University of Technology, Faculty of Chemistry, Department of Inorganic Chemistry, Analytical Chemistry and Electrochemistry
[c] Silesian University of Technology, Faculty of Mining, Safety Engineering and Industrial Automation, Department of Applied Geology
[d] Polish Academy of Sciences, Centre of Polymer and Carbon Materials
email: karolina.goldsztajn@polsl.pl

Abstract: The aim of the study was to determine the influence of PLGA biodegradable polymer coatings containing hydroxyapatite on the corrosion resistance of titanium alloy. Polymer coating was applied by the ultrasonic spray method. To determine corrosion resistance, the potentiodynamic polarization method and electrochemical impedance spectroscopy were chosen. The amount of metal ions released to the solution was also investigated. Tests were carried out for metal substrate, PLGA coating and PLGA coating enriched with hydroxyapatite in the initial state, as well as, after 3, 6 and 9 weeks of exposure to Ringer's solution. The results show beneficial effect of polymer coatings on the corrosion resistance of titanium alloy. Moreover, the PLGA coatings reduce release of metallic ions from the surface. The obtained results indicate the suitability of the applied coatings in biomedical applications.

Keywords: biodegradable polymer coatings, hydroxyapatite, corrosion resistance, electrochemical impedance spectroscopy, titanium alloy, biomaterials

1. INTRODUCTION

Titanium alloys are widely used in medical applications, especially in orthopedics, due to their corrosion resistance in the tissue environment, biocompatibility, and the value of Young's modulus similar to the bone elasticity modulus [1]. However, the undesirable reactions caused by the aluminum and vanadium ions present in the most commonly used titanium alloys (Ti6Al4V and Ti6Al7Nb) make it necessary to propose a surface modification method to further improve biocompatibility [2]. The most commonly used method is anodic oxidation, which provides high corrosion resistance, but does not eliminate the presence of aluminium and vanadium ions [3,4].

One of the methods of surface modification of titanium alloys may be the use of biodegradable polymer coatings. Polymer coatings can improve biocompatibility by limiting the penetration of metal ions into the tissue environment [5]. Moreover, biodegradable coatings can also be a matrix for the release of mineral substances, such as hydroxyapatite.

The aim of the work was to determine the influence of PLGA biodegradable polymer coatings containing hydroxyapatite on the corrosion resistance of titanium alloy. The scope of the research included the potentiodynamic studies, electrochemical impedance spectroscopy tests and investigation of metal ion's release.

2. MATERIAL AND METHODS

Ti6Al7Nb alloy samples were taken from a rod of 25 mm in diameter. The surface of metal substrate was ground, sandblasted and anodically oxidated with the use of the electrolyte based on phosphorus and sulphuric acid at the voltage 97 V. Polymer coating based on poly(D,L-lactide-coglycolide) PLGA(85/15) was synthesized in bulk by the ring opening polymerization of glycolide (Purac) and D,L-lactide (Purac) (130 °C for 24 hours and 120 °C for 48 hours) at argon atmosphere. Solution of 1% PLGA in CH_2Cl_2 was enriched with 20% synthetic hydroxyapatite powder (<200 nm particle size) (Merck). Coatings was applied by ultrasonic spray system ExactaCoat (Sono-Tek) with Impact nozzle with following parameters: ultrasound frequency 60 kHz, ultrasound power 1,5 W, speed of nozzle motion 10 mm/s and liquid's flow rate 1 cm^3/min. Coatings was composed of 15 layers. The non-coated and coated samples were immersed in Ringer's solution at 37°C for 3, 6 and 9 weeks.

Resistance to pitting corrosion was tested by the potentiodynamic method with the use of AUTOLAB PGSTAT 302N (Metrohm). Electrochemical Impedance Spectroscopy was carried out with PARSTAT 4000 (Ametek). Metal ion's release was measured by inductively coupled plasma-atomic emission spectrometry (ICP-AES), using JY 2000 spectrometer (Yobin-Yvon).

3. RESULTS

The performed tests showed a beneficial influence of biodegradable polymer coatings on corrosion resistance of titanium alloy. Moreover, mass density of metal ions in Ringer's solution released from PLGA coated surface is lower than metal ion concentration released from uncoated surface.

4. CONCLUSION

The PLGA biodegradable polymer coating containing hydroxyapatite could improve the biocompatibility of titanium alloy by increasing corrosion resistance and limiting the release of degradation products of metallic substrate to tissue environment.

Acknowledgments: Research funded by statutory activities of Department of Biomaterials and Medical Devices Engineering, Faculty of Biomedical Engineering, Silesian University of Technology, no. 07/020/BK_22/0073

BIBLIOGRAPHY

1. I. Gotman, Characteristics of Metals Used in Implants, Journal of Endourology, 11(6), 2009.
2. Y. Okazaki, E. Gotoh, Comparison of metal release from various metallic biomaterials in vitro, 26(1), 2005.
3. X. Yan, W. Cao, H. Li, Biomedical Alloys and Physical Surface Modifications: A Mini-Review, Materials (Basel), 15(66), 2022.
4. R. Asri, W. Harun, M. Samykano, N. Lah, S. Ghani, F. Tarlochan, M. Raza, Corrosion and surface modification on biocompatible metals: A review, Materials Science and Engineering: C, 77, 2017.
5. J. Szewczenko, W. Kajzer, M. Grygiel-Pradelok , J. Jaworska, K. Jelonek, K. Nowińska, M. Gawliczek, M. Libera, A. Marcinkowski, J. Kasperczyk, Corrosion resistance of PLGA-coated biomaterials, Acta of Bioengineering and Biomechanics, 19(1), 2017.

MTS CONFERENCE
MATERIAL TECHNOLOGIES IN SILESIA

12-15.06.2022
Crystal Mountain***** Hotel, Wisła, Poland

Metaloznawcze i technologiczne aspekty wytwarzania karoseryjnych stali średniomanganowych

A. Grajcar[a]

[a] Politechnika Śląska, Wydział Mechaniczny Technologiczny, Katedra Materiałów Inżynierskich i Biomedycznych
email: adam.grajcar@polsl.pl

Streszczenie: W pracy opisano metaloznawcze zasady projektowania składu chemicznego stali średniomanganowych z uwzględnieniem czynników mikrostrukturalnych, projektowanie profili temperaturowych obróbki cieplnej oraz najbardziej istotne technologiczne aspekty ich wytwarzania. Skupiono się na analizie zapewnienia odpowiedniej czystości metalurgicznej ciekłego metalu i analizie wtrąceń niemetalicznych w stalach zawierających znaczne stężenia Mn, Si i Al oraz ich lejności w procesie COS. Dokonano analizy odkształcalności blach ze szczególnym uwzględnieniem odkształcalności krawędzi blach. Przeanalizowano wpływ składu chemicznego stali na spawalność metalurgiczną oraz podatność taśm stalowych na cynkowanie ogniowe.

Słowa kluczowe: stal średniomanganowa, blacha karoseryjna, odkształcalność blach, czystość metalurgiczna, spawalność, cynkowanie ogniowe

1. WPROWADZENIE

Nowoczesne, wielofazowe stale karoseryjne łączą wysoką wytrzymałość, plastyczność oraz zdolność absorpcji energii w warunkach obciążeń dynamicznych. Najbardziej zaawansowane technologicznie są stale średniomanganowe o ultradrobnoziarnistej mikrostrukturze ferrytyczno-austenitycznej lub bainitycznej z austenitem szczątkowym. Wytwarzane są one w nowoczesnych liniach wyżarzania ciągłego, a w przypadku taśm gorącowalcowanych na walcowni gorącej z zaawansowanym system kontrolowanego chłodzenia laminarnego. Wymienione cykle cieplne pozwalają wygenerować w strukturze duży udział austenitu szczątkowego, który podczas przetwarzania blach na zimno wnosi wkład w jednoczesne umocnienie i zwiększenie plastyczności dzięki efektowi TRIP (TRansformation Induced Plasticity).

Mimo znakomitego połączenia własności wytrzymałościowych i plastyczności aplikacja przemysłowa tych stali jest na razie ograniczona, głównie do partii testowych. Powodem tego są liczne problemy technologiczne, które muszą być rozwiązane, aby w pełni wykorzystać potencjał wasności mechanicznych oferowanych przez te stale wielofazowe. Problemy technologiczne są związane z podwyższonym stężeniem następujących pierwiastków: Si, Al, Mn, czasami w połączeniu z Cr, Mo oraz mikrododatkami Ti, Nb, V. Obecnie prowadzone są intensywne badania nad polepszeniem: czystości metalurgicznej ciekłego metalu związanej z ograniczeniem udziału wtrąceń niemetalicznych, lejności ciekłego metalu, odkształcalności blach ze szczególnym uwzględnieniem odkształcalności krawędzi blach, spawalności oraz cynkowalności. Głównym wyzwaniem jest zapewnienie tych kluczowych własności technologicznych bez pogorszenia własności mechanicznych.

2. METALOZNAWCZE ASPEKTY WYTWARZANIA STALI KAROSERYJNYCH

W stalach średniomanganowych dąży się do maksymalizacji udziału austenitu szczątkowego, który kształtuje się zazwyczaj na poziomie od 20 do 40%. Stabilizację tak znacznego udziału fazy γ uzyskuje się w wyniku dodania od 3 do 12% manganu (najczęściej między 5 a 8%) oraz poprzez rozdrobnienie ziarn (rośnie wówczas stabilność austenitu szczątkowego – spada temperatura początku przemiany martenzytycznej). Ich obróbka cieplna polega na wytrzymaniu taśm stalowych w zakresie międzykrytycznym (wyżarzanie kołpakowe – długi czas,

wyżarzanie w liniach ciągłych – krótki czas), po czym następuje ochłodzenie stali do temperatury pokojowej. Ze względu na silne rozdrobnienie mikrostruktury (mieszanina $\alpha+\gamma$ tworzy się z drobnopłytkowego martenzytu listwowego) oraz dużą zawartość Mn, temperatura M_s jest niższa od temperatury pokojowej, co stabilizuje austenit szczątkowy.

3. TECHNOLOGICZNE ASPEKTY WYTWARZANIA STALI KAROSERYJNYCH

3.1. Czystość metalurgiczna i wtrącenia niemetaliczne

Ze względu na podwyższoną zawartość pierwiastków takich jak: Mn, Al, Si oraz Ti w składzie chemicznym stali średniomanganowych, wykazują one tendencję do tworzenia wtrąceń niemetalicznych o charakterze siarczkowym, tlenkowym oraz złożonym. Skład chemiczny tych stali skutkuje także zwiększonym udziałem wtrąceń niemetalicznych w strefie przetopu podczas spawania.

3.2. Lejność ciekłego metalu

Stale średniomanganowe zawierają często do 1,5% Al (czasem do 3%). Tak duże stężenie tego pierwiastka skutkuje dużym udziałem wtrąceń niemetalicznych w postaci tlenków aluminium. Ze względu na ich wysoką temperaturę topnienia pozostają one w stanie stałym podczas przelewania ciekłej stali z kadzi pośredniej do krystalizatora. Powoduje to często problemy z zatykaniem dysz. Zapobiega się temu przez obróbkę ciekłej stali związkami wapnia.

3.3. Podatność na cynkowanie

Krzem jest jednym z najbardziej istotnych składników stali średniomanganowych, gdyż zapobiega wydzielaniu się cementytu. Problem zapewnienia odporności korozyjnej blach ze stali o podwyższonej zawartości krzemu wynika z braku odpowiedniej zwilżalności powierzchni taśm stalowych przez ciekły cynk w wyniku tworzenia się na powierzchni cienkiej warstwy tlenków oraz kruchej powłoki międzymetalicznej. Poprawę podatności na cynkowanie oraz uzyskanie pożądanego udziału austenitu szczątkowego uzyskuje się dzięki częściowemu lub całkowitemu zastąpieniu Si przez Al. Ten pierwiastek ma jednak mniejszy potencjał umocnienia roztworowego oraz tworzy liczne wtrącenia tlenkowe.

3.4. Odkształcalność blach

Odkształcalność technologiczna blach rośnie wraz ze zmniejszeniem ich wytrzymałości i zwiększeniem wydłużenia. W pewnych przypadkach odkształcalność technologiczna blach jest zaskakująco mała. Jest tak dlatego, że w niektórych operacjach formowania blachy istotna jest tzw. duża plastyczność lokalna, niekoniecznie jednoznaczna z wydłużeniem. Jedną z najbardziej istotnych własności technologicznych blach stosowanych na karoserie samochodowe jest ich podatność do zaginania obrzeży blach, a także do wywijania kołnierzy wokół otworów. Cecha ta wskazuje na odkształcalność krawędzi blach, szczególnie krawędzi uzyskanych w wyniku wykrawania. Przycięte krawędzie podczas zaginania, kształtowania kołnierzy itp. podlegają dużym naprężeniom rozciągającym. Najlepiej podatność blachy do zaginania obrzeży oraz do wywijania otworów charakteryzują lokalna ciągliwość oraz współczynnik anizotropii normalnej. Odkształcalność krawędzi blach wyraża się współczynnikiem powiększania otworu.

3.5. Spawalność i zgrzewalność blach

Stale średniomanganowe są spawalne oraz zgrzewalne. Mimo podwyższonego stężenia Mn nie obowiązują tutaj klasyczne zasady stosowalności równoważnika węgla, gdyż spawaniu podlegają zazwyczaj mieszane struktury ferrytyczno-austenityczne. Stale te mają większy opór elektryczny, wymagane jest zwiększenie nacisku elektrody o ok. 20% lub więcej (ze względu na większe $R_{p0,2}$), większa średnica końcówki elektrod oraz dłuższy czas zgrzewania. W celu redukcji twardości w strefie spoiny/zgrzeiny często stosuje się wieloimpulsowy przebieg zgrzewania lub wyżarzanie końcowe, a w przypadku spawania laserowego – spawanie w układzie tandem.

MTS CONFERENCE
MATERIAL TECHNOLOGIES IN SILESIA

12-15.06.2022
Crystal Mountain***** Hotel, Wisła, Poland

Wpływ odkształcenia wysokotemperaturowego oraz parametrów wytrzymania izotermicznego na mikrostrukturę stali wielofazowych zawierających 3-5% Mn

A. Grajcar[a], M. Opiela[a,*], W. Pakieła[a]

[a] Politechnika Śląska, Wydział Mechaniczny Technologiczny, Katedra Materiałów Inżynierskich i Biomedycznych
email: *marek.opiela@polsl.pl

Streszczenie: W pracy przedstawiono charakterystyki naprężenie - odkształcenie zarejestrowane podczas czteroetapowego ściskania próbek osiowosymetrycznych w symulatorze termomechanicznym Gleeble. Porównano odkształcalność trzech stali o stężeniu Mn wynoszącym 3, 4 oraz 5%. Dokonano analizy wpływu odkształcenia plastycznego oraz zawartości Mn na mikrostrukturę stopów. Parametry wytrzymania izotermicznego dobrano na podstawie wykresów CTP oraz OCTP (dla austenitu odkształconego plastycznie). Udział austenitu szczątkowego wyznaczono metodą rentgenowską. Stwierdzono, że zawartość Mn w zakresie od 3 do 5% nie ma znaczącego wpływu na oporność wysokotemperaturową podczas prób ściskania, natomiast ma istotny wpływ na mikrostrukturę stali oraz udział austenitu szczątkowego. Najlepsze warunki dla maksymalizacji udziału austenitu szczątkowego uzyskano w temperaturze 400°C, przy czym malał on wraz ze wzrostem stężenia Mn w stali. Wykazano, że jest to związane z wypieraniem węgla z pozostałej frakcji austenitu wraz ze wzrostem zawartości manganu. Własności mechaniczne określono na podstawie pomiarów twardości.

Słowa kluczowe: odkształcenie na gorąco, symulator termomechaniczny, przemiana bainityczna, austenit szczątkowy, wpływ manganu

1. WPROWADZENIE

Stale średniomanganowe o mikrostrukturze wielofazowej są wyznacznikiem bieżących osiągnięć metaloznawstwa stopów żelaza w zakresie projektowania stali na karoserie samochodowe, łączące wysoką wytrzymałość, plastyczność i zdolność do pochłaniania energii przez odpowiednio zaprojektowane strefy kontrolowanego zgniotu. Taśmy zimnowalcowane są wytwarzane w wyniku wyżarzania międzykrytycznego po walcowaniu na zimno. Pozwala to na uzyskanie w mikrostrukturze równowagi ferrytu oraz austenitu, który na drodze stabilizacji C i Mn może zostać zachowany do temperatury pokojowej. Obniżeniu temperatury przemiany martenzytycznej sprzyja dyfuzja węgla z ferrytu / ferrytu bainitycznego do fazy γ, podwyższone stężenie manganu w stali oraz rozdrobnienie mikrostruktury. Austenit szczątkowy w tych stalach to metastabilna faza znacznie poprawiająca plastyczność materiału, ze względu na tzw. efekt TRIP (TRansformation Induced Plasticity) związany z indukowaną odkształceniem na zimno przemianą martenzytyczną. W przypadku blach gorącowalcowanych o większej grubości (przeznaczonych np. na elementy samochodów ciężarowych lub na elementy podwozia) konieczne jest kontrolowane, kilkuetapowe chłodzenie bezpośrednio po zakończeniu walcowania na gorąco. Jego zasadniczym etapem jest izotermiczna przemiana bainityczna (w warunkach przemysłowych np. zwijanie blach w kręgi), podczas której tworzeniu ferrytu bainitycznego towarzyszy zwiększenie zawartości węgla w pozostałej frakcji fazy γ. Odkształcenie plastyczne austenitu przyspiesza te procesy dyfuzyjne, a obecność w stali krzemu i/lub aluminium ogranicza / zapobiega wydzielaniu się węglików w bainicie. Odkształcenie wysokotemperaturowe (wartości stopnia gniotu, szybkość odkształcenia, czasy przerw między odkształceniami, temperatura końca odkształcenia) oraz warunki chłodzenia z zakresu istnienia austenitu do izotermicznej przemiany bainitycznej mają istotny wpływ na kinetykę tej przemiany oraz końcową

mikrostrukturę i własności mechaniczne stali wielofazowych. Decydujące znaczenie mają temperatura oraz czas wytrzymania izotermicznego.

2. WYNIKI BADAŃ I ICH OMÓWIENIE

Wartości naprężeń uplastyczniających uzyskane w próbie ściskania czteroetapowego istotnie rosną wraz ze zmniejszeniem temperatury odkształcenia, przy czym są zbliżone do naprężeń uzyskanych w próbie ściskania ciągłego. W całym zakresie temperatury odkształcenia procesem kontrolującym przebieg umocnienia odkształceniowego jest zdrowienie dynamiczne. Wpływ Mn w zakresie od 3 do 5% na wartości naprężenia uplastyczniającego jest pomijalnie mały. Mikrostruktury uzyskane po kontrolowanym chłodzeniu wskazują, że stale mają taki sam skład fazowy, jak w stanie wyjściowym. Jednak realizacja przemian fazowych austenitu przechłodzonego odkształconego poniżej temperatury rekrystalizacji fazy γ skutkuje znaczącym rozdrobnieniem wszystkich składników strukturalnych. Odnosi się to zarówno do obszarów bainityczno-martenzytycznych, jak i do austenitu szczątkowego. Udział austenitu szczątkowego w stali typu 3MnNb wynosi od 12 do 18%. Austenit jest równomiernie rozmieszczony, zarówno na byłych graniach ziarn fazy γ, a także wewnątrz ziarn – zgodnie z kierunkiem wzrostu listew ferrytu bainitycznego.

Można wyróżnić dwie główne formy morfologiczne austenitu szczątkowego: drobne ziarenka oraz austenit warstwowy. Austenit o różnej grubości warstw zlokalizowanych pomiędzy listwami ferrytu bainitycznego dominuje szczególnie w temperaturze 350°C, gdzie listwy bainityczne mają wybitnie listwową morfologię. Wraz ze wzrostem temperatury wytrzymania izotermicznego stali do 400 i 450°C rośnie udział austenitu szczątkowego, który przyjmuje formę drobnych ziarenek.

Ze względu na większą hartowność stale o zawartości 4 i 5% Mn mają wyraźnie listwowe struktury bainityczno-martenzytyczne w całym zakresie temperatury wytrzymania izotermicznego od 350 do 450°C. Występuje w nich austenit warstwowy oddzielający listwy ferrytu bainitycznego. Blokowe ziarna o większej wielkości zlokalizowane pomiędzy poszczególnymi pakietami bainityczno-martenzytycznymi przemieniają się częściowo w martenzyt podczas chłodzenia stali do temperatury pokojowej.

3. WNIOSKI

Wartości naprężenia płynięcia stali średniomanganowych z grupy AHSS są nieco wyższe niż dla stali HSLA. Zawartość Mn w zakresie 3-5% nie wpływa istotnie na naprężenie płynięcia, a przemiany fazowe realizowane są w warunkach silnego odkształcenia austenitu niezrekrystalizowanego. Warunki wytrzymania izotermicznego w zakresie 350-450°C sprzyjają wytwarzaniu struktur bainityczno-austenitycznych dla stali 3MnNb oraz bainityczno-martenzytycznych z austenitem szczątkowym dla stali 4MnNb oraz 5MnNb. Najwyższy udział austenitu szczątkowego (18%) uzyskano dla stali o najmniejszym stężeniu Mn i spada on do ok. 9% dla stali 5MnNb. W temperaturze wytrzymania 450°C dominuje austenit blokowy, który zmienia morfologię na listwową wraz z obniżeniem temperatury do 350°C.

Podziękowania: Praca wykonana i finansowana w ramach grantu Narodowego Centrum Nauki, nr 2017/27/B/ST8/02864.

MTS CONFERENCE
MATERIAL TECHNOLOGIES IN SILESIA

12-15.06.2022
Crystal Mountain***** Hotel, Wisła, Poland

Symulacja fizyczna walcowania wieloprzepustowego obrabianych termomechanicznie stali średniomanganowych

A. Grajcar[a], B. Grzegorczyk[a,*], W. Borek[a], A. Skowronek[a]

[a] Politechnika Śląska, Wydział Mechaniczny Technologiczny, Katedra Materiałów Inżynierskich i Biomedycznych
email: *barbara.grzegorczyk@polsl.pl

Streszczenie: W pracy przeprowadzono symulację fizyczną walcowania wieloprzepustowego z temperaturą końca walcowania 850°C w symulatorze procesów metalurgicznych Gleeble. Badano stopy o zawartości Mn wynoszącej 3 oraz 5% oraz zawierające mikrododatek Nb oraz stale referencyjne bez mikrododatku. Po odkształceniu 7-etapowym zastosowano zmienne warunki temperaturowo-czasowe wytrzymania izotermicznego w zakresie temperatury od 300 do 500°C. Przeprowadzono identyfikację strukturalną ze szczególnym uwzględnieniem wyznaczenia udziału austenitu szczątkowego (metodą rentgenowską). Własności mechaniczne wyznaczono w statycznej próbie rozciągania z użyciem sub-wymiarowych próbek. Temperatura wytrzymania izotermicznego oraz zawartość Mn mają istotne znaczenie dla mikrostruktury oraz własności mechanicznych badanych stali wielofazowych. Dla większości stopów uzyskano wytrzymałość na rozciąganie powyżej 1 GPa oraz zadowalające wydłużenie.

Słowa kluczowe: walcowanie termomechaniczne, austenit szczątkowy, symulator Gleeble, symulacja fizyczna, przemiana bainityczna, stal średniomanganowa

1. WPROWADZENIE

Stale średniomanganowe należą do najbardziej perspektywicznych materiałów przeznaczonych na karoserie samochodowe. Ich obróbka cieplna polega na wyżarzaniu rekrystalizującym (w piecach kołpakowych lub w linii ciągłego wyżarzania) realizowanym po walcowaniu na zimno. Po takiej obróbce cieplnej posiadają one mikrostrukturę ultradrobnoziarnistego ferrytu i austenitu, która tworzy się w trakcie wyżarzania w zakresie temperatur krytycznych A_{c1} i A_{c3}. Alternatywnie blachy o większej grubości mogą być wytwarzane jako gorącowalcowane w procesie walcowania termomechanicznego połączonego z kontrolowanym chłodzeniem po jego zakończeniu. Właściwy dobór przebiegu i szybkości chłodzenia, często z wytrzymaniem izotermicznym stabilizującym austenit, zapewniają struktury wielofazowe z kilkunastoprocentowym udziałem austenitu szczątkowego. Takie stale średniomanganowe mają osnowę martenzytyczną, bainityczną lub ferrytyczną oraz austenit szczątkowy jako składnik strukturalny pozwalający na kontrolę balansu pomiędzy wytrzymałością i plastycznością taśm stalowych. W zakresie stężenia Mn poniżej 5% jest możliwe zastosowanie walcowania termomechanicznego pozwalającego na uzyskanie blach o grubości 2-3 mm. Elementy stalowe o tej grubości znajdują zastosowanie na najbardziej odpowiedzialne elementy wzmacniające karoserię oraz elementy podwozia.

2. WYNIKI BADAŃ I ICH OMÓWIENIE

Wynikiem symulacji fizycznej wieloprzepustowego walcowania termomechanicznego są krzywe naprężenie-odkształcenie. Stopniowe obniżenie temperatury odkształcenia z 1150 do 850°C powoduje stopniowy wzrost naprężenia uplastyczniającego. Ciągły wzrost naprężenia związany jest ze stopniowym obniżaniem temperatury odkształcenia oraz relatywnie małym stopniem zaniku umocnienia pomiędzy poszczególnymi odkształceniami. W stalach z mikrododatkiem Nb w końcowym etapie odkształcenia dochodzi czasem do rekrystalizacji dynamicznej w wyniku akumulacji odształcenia, a w stalach wielofazowych typu Al-Nb istnieje niebezpieczeństwo

niekontrolowanych zmian w warunkach płynięcia z powodu utworzenia ferrytu w warstwie powierzchniowej blach. Przebieg krzywych nie świadczy o zajściu powyższych zjawisk z powodu zwiększonej zawartości Mn w badanych stalach.

Porównując przebiegi krzywych σ-ε dla stali 3Mn i 5Mn oraz 3Mn-Nb i 5Mn-Nb można stwierdzić, że wpływ Mn jest pomijalnie mały, gdyż wartości naprężenia uplastyczniającego są bardzo zbliżone. Począwszy od temperatury 950°C widoczny jest natomiast istotny wzrost naprężenia dla stali z mikrododatkiem Nb. Większe zadane odkształcenie sumaryczne objawia się zwiększeniem wartości naprężeń w porównaniu do prób czteroetapowego odkształcenia. Kumulacja odkształcenia oraz większe szybkości odkształcenia w końcowym etapie ściskania mogą spowodować zapoczątkowanie wydzielania węglikoazotków w stalach z mikrododatkiem Nb. Jednak wzrost naprężenia dla stali 3MnNb i 5MnNb w porównaniu do stali nie zawierających Nb nie jest znaczący i wynosi około 30 MPa. W całym zakresie temperatury odkształcenia procesem kontrolującym przebieg umocnienia odkształceniowego jest zdrowienie dynamiczne, a rozdrobnienie struktury austenitu możliwe jest przez częściowy przebieg rekrystalizacji statycznej w przerwach pomiędzy kolejnymi odkształceniami.

Konsekwencją zakończenia odkształcenia plastycznego stali w temperaturze 850°C, tj. poniżej temperatury końca rekrystalizacji austenitu i kilkuetapowego chłodzenia są drobnoziarniste produkty przemian fazy γ. Duże odkształcenie sumaryczne powoduje, że uzyskane mikrostruktury wielofazowe są bardziej drobnoziarniste w porównaniu do uzyskanych po zastosowaniu czteroetapowego odkształcenia. Udział ferrytu w stalach o mniejszej zawartości Mn jest znikomy (poniżej 5%), a osnowę stali stanowią drobnoziarniste obszary bainityczno-martenzytyczne. Największy udział austenitu szczątkowego dla stali 3Mn i 3MnNb obserwuje się po wytrzymaniu izotermicznym próbek w temperaturze 400 i 450°C, natomiast optymalny czas wytrzymania stali w tej temperaturze wynosi 300s. Nie zaobserwowano wyraźnego wpływu mikrododatku Nb na mikrostrukturę stali i udział fazy γ.

Podziękowania: Praca wykonana i finansowana w ramach grantu Narodowego Centrum Nauki, nr 2017/27/B/ST8/02864.

MTS CONFERENCE
MATERIAL TECHNOLOGIES IN SILESIA

12-15.06.2022
Crystal Mountain***** Hotel, Wisła, Poland

Comprehensive research of heat treatment on additively manufactured stainless steel 316L in connection on mechanical properties

J. Hajnys[a], P. Nevrly[a], J. Mesicek[a], M. Pagac[a]

[a] VSB-Technical University of Ostrava, Faculty of Mechanical Engineering
email: jiri.hajnys@vsb.cz

Abstract: The present article deals with extensive research into the heat treatment of additively produced 316L stainless steel. In the introductory part, a research of heat treatment in connection with conventionally produced steel and additively produced steel is performed. Furthermore, an experiment was performed, which aimed to investigate a wide range of temperatures and times of heat treatment and based on this to evaluate the mechanical properties. At the end of the article, the most suitable heat treatment to achieve optimal values of yield strength, tensile strength, elongation and hardness is presented.

Keywords: SLM, Heat Treatment, Mechanical properties, 3D metal print

1. INTRODUCTION

Additive manufacturing (AM) is a technology that allows the creation of structurally complex components that are very difficult to manufacture or even impossible in a conventional way, one of the AM methods is the Selective Laser Melting (SLM) technique, which works with metal powder and transforms into a solid material [1]. The combination of good mechanical properties, good machinability, corrosion resistance and abrasion resistance makes 316L the ideal metal for SLM research and printing [2]. Optimization of laser parameters such as laser power, scanning speed, hatch distance, scanning strategy and layer height is a topic that is very well researched in several publications [3, 4, 5]. A less explored topic is the optimization of heat treatment after printing, which aims to correct this study. In general, it is possible to apply hardening, tempering, annealing and normalizing [6]. Hardening and tempering are commonly used to increase strength and wear resistance [6]. After reaching the hardening stage, the steel reaches its maximum yeild strenght, thanks to the formation of martensite on the other hand it becomes very brittle.

Based on a study [6], it is clear that the mechanical properties of austenitic steels depend on their microstructure, which determines the transformation phases, precipitation and recrystallization. It follows from this statement that heat treatment does not have a significant effect on hardness and strenhgt, due to the fact that strengthening depends mainly on the austenite-martensite transformation phase. This transformation is not possible or very difficult to achieve due to the very low carbon content [7].

2. MATERIALS AND METHODS

For experimental purposes, several sets of samples were printed (see Table 1) and tested. All samples were heat treated in the same furnace, under different conditions. Samples for heat treatment were produced in one building in order to eliminate as many errors as possible. The mechanical properties were then examined by tensile testing and hardness measurement. Furthermore, the microstructure of the samples was investigated.

Table 1. Sets of samples for testing

Sample No.	Temperature [° C]	Time [h]	Cooling
1	550	2	Water

2	650	2	Water
3	500	2	Water
4	700	2	Water
5	600	2	Air
6	500	1	Air
7	550	1	Water
8	600	1	Water
9	550	2	Air
10	700	2	Air
11	650	2	Air
12	650	1	Water
13	500	2	Air
14	550	1	Air
15	700	1	Air
16	650	1	Air
17	700	1	Water
18	600	2	Water
19	500	1	Water
20	600	1	Air
21	550	2	Air
22	600	2	Water
23	600	1	Water
24	650	2	Water

BIBLIOGRAPHY

1. Berman, B. 3-D Printing: The New Industrial Revolution. Business Horizons 2012, 55 (2), 155–162. https://doi.org/10.1016/J.BUSHOR.2011.11.003.
2. Choi, J.-P.; Shin, G.-H.; Brochu, M.; Kim, Y.-J.; Yang, S.-S.; Kim, K.-T.; Yang, D.-Y.; Lee, C.-W.; Yu, J.-H. Densification Behavior of 316L Stainless Steel Parts Fabricated by Selective Laser Melting by Variation in Laser Energy Density. MATERIALS TRANSACTIONS 2016, 57 (11), 1952–1959. https://doi.org/10.2320/matertrans.M2016284.
3. Hajnys, J.; Pagáč, M.; Měsíček, J.; Petru, J.; Król, M. Influence of Scanning Strategy Parameters on Residual Stress in the SLM Process According to the Bridge Curvature Method for AISI 316L Stainless Steel. Materials 2020, 13, 1659. https://doi.org/10.3390/ma13071659
4. Cegan, T.; Pagac, M.; Jurica, J.; Skotnicova, K.; Hajnys, J.; Horsak, L.; Soucek, K.; Krpec, P. Effect of Hot Isostatic Pressing on Porosity and Mechanical Properties of 316 L Stainless Steel Prepared by the Selective Laser Melting Method. Materials 2020, 13, 4377. https://doi.org/10.3390/ma13194377
5. Saxena, P.; Gajera, H.; Shah, D.; Pancholi, N. Effect of SLM Process Parameters on Hardness and Microstructure of Stainless Steel 316 Material. Materials Today: Proceedings 2022, 50, 1653–1659. https://doi.org/10.1016/J.MATPR.2021.09.144.
6. Bhadeshia, H. K. D. H.; Honeycombe, S. R. The Bainite Reaction. Steels 2006, 129–154. https://doi.org/10.1016/B978-075068084-4/50008-X.
7. Kumar, B. R.; Sharma, S. Recrystallisation Characteristics of Cold Rolled Austenitic Stainless Steel during Repeated Annealing. Materials Science Forum 2013, 753, 157–162. https://doi.org/10.4028/www.scientific.net/MSF.753.157.

Acknowledgments: ***This paper has been completed in connection with project Innovative and additive manufacturing technology – new technological solutions for 3D printing of metals and composite materials, reg. no. CZ.02.1.01/0.0/0.0/17_049/0008407 financed by Structural Funds of the European Union and project.***

MTS CONFERENCE
MATERIAL TECHNOLOGIES IN SILESIA

12-15.06.2022
Crystal Mountain***** Hotel, Wisła, Poland

Cyclic Plasticity and Low-Cycle Fatigue Properties of AlSi10Mg Manufactured from Recycled Powder

R. Halama[a], F. Sari, J. Hajnyš

[a] VŠB-Technical University of Ostrava, Faculty of Mechanical Engineering, Department of Applied Mechanics
email: radim.halama@vsb.cz

Abstract: The article describes the chosen results of low-cycle fatigue testing performed on AlSi10Mg printed with SLM technology. Proportional loading cases were realized in tension-compression and pure torsion. The nonproportional loading testing was realized in the form of 90-degree out of phase tests. Cyclic properties and lifetimes have been evaluated. Preheating of the building chamber to 170°C leads to a cyclically stable response of the material. The lifetimes differ for the three loading cases significantly. The highest values of the number of cycles to failure correspond to torsion and the smallest ones to the nonproportional loading case.

Keywords: AlSi10Mg, selective laser melting, cyclic plasticity, low-cycle fatigue, nonproportional loading

1. INTRODUCTION

Selective laser melting (SLM) is an additive manufacturing (AM) technology used to print functional parts from metallic powders using a high-energy laser beam. Compared to the static tensile properties of the parts produced, fatigue performance is less reported in recent research studies [1]. The fatigue properties of AM materials should be taken into account when evaluating materials for industrial use. The AlSi10Mg alloy is one of the most popular materials used in light structures produced by SLM and commonly used in the aviation and automotive industries due to its high resistance and fatigue properties [2].

This study shows a comparison of the low-cycle properties of AlSi10Mg for three loading cases: tension-compression, torsion and tension-compression/torsion (90 degrees out of phase test). Cyclic plasticity behaviour is also being studied, including uniaxial ratcheting of the aluminium alloy.

2. EXPERIMENTAL STUDY DESCRIPTION

All fatigue tests were done on vertically printed tubular specimens in as build state (using a recycled powder). Renishaw AM500E was used to manufacture the specimens. The laser power of 350W and the layer thickness of 30µm were applied. The resulting porosity was less than 0.3%. The LabControl 100kN/1000Nm hydraulic testing machine was used in conjunction with the Epsilon 3550 extensometer with a gauge length of 25 mm to control the axial and shear strain under uniaxial and multiaxial loadings. The experimental study is focused on the investigation of the properties of low-cycle fatigue (LCF) of AlSi10Mg [3].

The strain-controlled loading has been done keeping the same 0.5%/s strain rate. Experimental hysteresis loops were evaluated for each load path at the half of lifetimes. The cyclic stress-strain curves obtained under two proportional and one nonproportional loading paths are presented in Fig.1a, where the monotonic tensile curve is also shown.

The stress-controlled loading cases were done under uniaxial loading only considering different mean stress and stress amplitudes in the particular blocks of incremental loadings. The aim of the experiments was to obtain important data for evaluation of cyclic plasticity models developed with emphasis on ratcheting simulations using the finite element method (FEM).

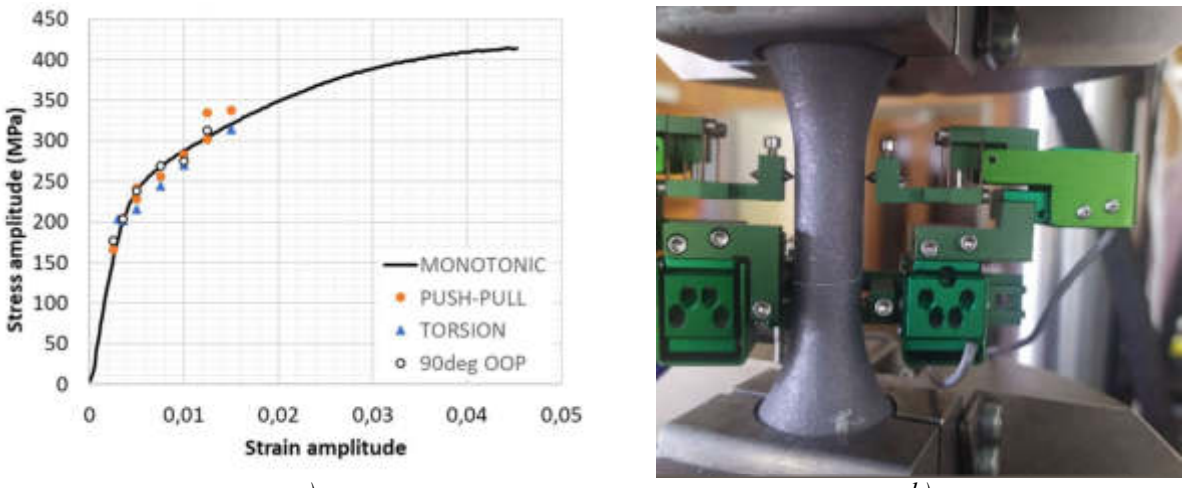

a) *b)*

Figure 1. LCF tests on AlSi10Mg: a) stress-strain curves, b) photo of a cracked specimen

3. DISCUSSION AND CONCLUSION

The stress-strain behaviour of AlSi10Mg prepared by SLM shows a good correlation of cyclic stress-strain curves corresponding to push-pull and out of phase loading (Fig.1a). Therefore, no additional hardening due to nonproportional loading was observed. The material also shows a slight cyclic softening below the strain amplitude of 1.25%. For higher amplitudes, a cyclic hardening is observed (verified under uniaxial loading only). The degree of nonproportionality of loading influences the fatigue life in its decrease, whereas this effect is more significant in high cycle fatigue than in LCF. The critical plane for axial loading (push-pull) is the cross-section of the specimen. The material cracks in a brittle mode. This is also the cause of the longer fatigue lifetimes for torsion than under tension-compression, because the preferred plane is the plane of maximum density of pores (usually the horizontal plane in the building space).

The experimental results in the form of stress-strain history will serve us for evaluation of various cyclic plasticity models. Chosen uniaxial strain-controlled tests and a ratcheting test were used elsewhere [4] to calibrate the Chaboche kinematic hardening model [5].

Acknowledgments: This work was supported by the Ministry of Education, Youth and Sports from the Specific Research Project (SP2022/26), and has been done in connection with the DMS project reg. no. CZ.02.1.01/0.0/17_049/0008407 financed by Structural Funds of Europe Union.

BIBLIOGRAPHY

1. E. Brandl, U. Heckenberger, V. Holzinger, Additive manufactured AlSi10Mg samples using Selective Laser Melting (SLM): Microstructure, high cycle fatigue, and fracture behavior, Materials & Design 34 (2012) 159-169.
2. A. Raja, S.R. Cheethirala, P. Gupta, J. V. Nilesh, R. Jayaganthan, A review on the fatigue behaviour of AlSi10Mg alloy fabricated using laser powder bed fusion technique, Journal of Materials Research and Technology 17 (2022) 1013-1029.
3. Renishaw, Magics Training: Material Profile Editing. RENISHAW: Apply Innovation, Renishaw, United Kingdom, 2016.
4. R. Halama, J. Šmach, B. Govindaraj, R. Čep, Implementation of the Chaboche model in numerical analysis of fatigue damage. Book chapter in: Cernescu et al. Fatigue Damage in Metals - Numerical Based Approaches and Applications, Elsevier, 2022 (in press).
5. J.-L. Chaboche, K. Van Dang, G. Cordier, Modelization of the strain memory effect on the cyclic hardening of 316 stainless steel, in: A. Jaeger, B.A. Boley (Eds.), Proceedings of 5th International Conference on Structural Mechanics in Reactor Technology, Division L11/3, Division L11/3, Berlin, 13–17 August 1979, Bundesanstalt für Materialprüfung, Berlin, 1979, pp. 1–10.

MTS CONFERENCE
MATERIAL TECHNOLOGIES IN SILESIA

12-15.06.2022
Crystal Mountain***** Hotel, Wisła, Poland

Simulation of the preparation laboratory for light microscopy in the form of a 3D educational game

R. Honysz

[a] Silesian University of Technology, Faculty of Mechanical Engineering, Department of Engineering Materials and Biomaterials
email: rafal.honysz@polsl.pl

Abstract: A virtual model of the laboratory of the Faculty of Mechanical Engineering of the Silesian University of Technology was developed, along with the equipment needed for the initial preparation of samples for further research. The proprietary application allows the user to familiarize himself with the basics of using preparation devices for light microscopy, such as a cutter, hot mounting press, sample grinder and light microscope

Keywords: virtual reality, simulation of research equipment, interactive game, preparation devices for light microscopy

1. INTRODUCTION

The process of creating simulators is no different from creating other software. Like all programs, they are written almost from scratch using one of the programming languages and the appropriate libraries already created for it. The language is selected depending on the requirements set for the simulator. C # is one of the most popular programming languages. This is due to its simplicity, efficiency and compatibility with Windows operating systems, which are most often used in enterprises. It is a high-level language developed mainly thanks to the support of Microsoft. A high-level language means a language whose syntax is to make the program code as easy as possible for humans to understand, thus distancing itself from the nuances present in low-level languages related to the hardware on which the programs are run.

When creating a machine simulator, the programmer's task is to reproduce the operation of the machine or simulated phenomena as accurately as possible. For this purpose, graphics engines are usually used, thanks to which, using specially created and animated models, the user will be able to interact with a virtual machine, enter data into it, observe the course of the simulated process and receive its result. Models can be created in any program that allows modelling, animation and 3D rendering.

2. PURPOSE AND SCOPE OF WORK

The aim of the work was to create a laboratory for the preparation of samples for light microscopy, equipped with devices at the disposal of the Department of Engineering and Biomedical Materials at the Faculty of Mechanical Engineering of the Silesian University of Technology. The scope of work was the creation of models of three-dimensional preparation machines for the purposes of light microscopy, the creation of the so-called stage, i.e. the environment in which these models were to be located and work in it. Another was to animate the movements of these machines so that they would reflect the actual operation of the presented devices as much as possible. The last step was to program the gameplay and start the animation at the right moment.

Machine models were created using Autodesk Inventor with the dimensions and colours as close as possible to realism. Animating the models was possible thanks to the use of the built-in game engine Unity3d and one of its tools called Mechanism. With its help, animations are created for individual model elements, e.g. by determining the position, rotation or its scale at a given time from the beginning of the sequence in three-dimensional space.

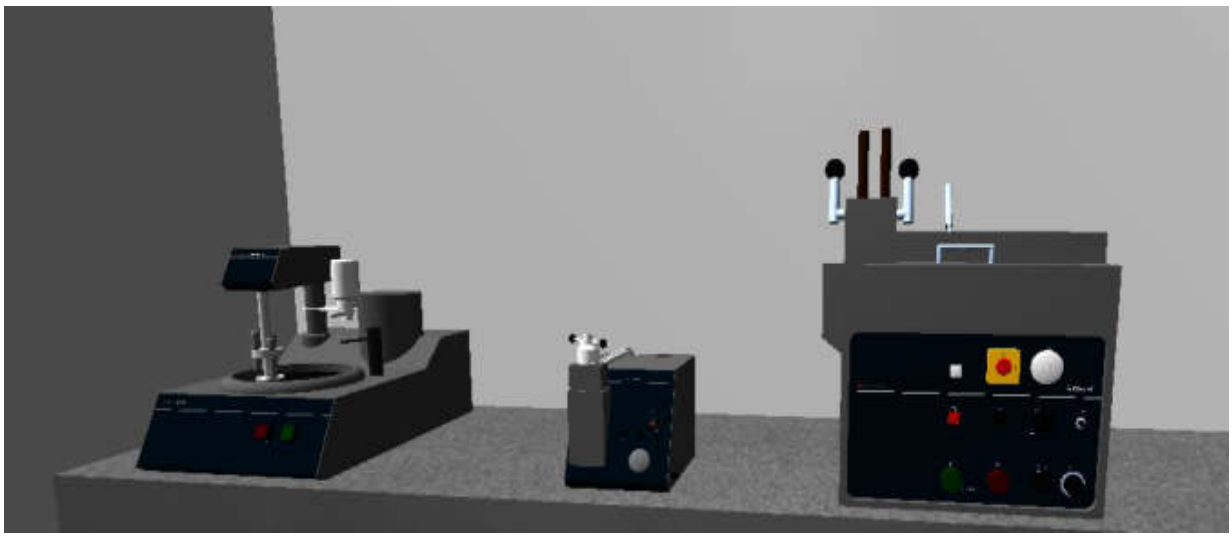

Figure 1. Simulated virtual laboratory, a) LaboPol-1 grinding and polishing machine, b) Predopress hot-mounting hydropneumatic press, c) Discotom-2 cutter, d) Olympus SZX9 microscope.

3. SUMMARY

The virtual materials science laboratory described in this article and implemented at the Department of Engineering Materials and Biomaterials met all training requirements in the field of materials science only in a virtual environment. Thanks to highly developed computer tools for three-dimensional modelling, it is now possible to recreate the appearance of all machines and devices, including laboratory devices. This allows them to present their work away from their real counterparts, making it possible to conduct training using even one computer with a projector. Computers, thanks to computer science armed with appropriate educational software, are one of the most interesting teaching aids, giving great opportunities to expand knowledge, skills and abilities.

BIBLIOGRAPHY

1. L.A. Dobrzański, Podstawy nauki o materiałach i metaloznawstwo, WNT, Warszawa, 2002
2. S. Prata, Szkoła programowania C++, Helion, Gliwice, 2006
3. W. Goldstone, Unity 3.x Game Development Essentials, Packt Publishing, 2011
4. M. Beer, C. Brom, F. Dignum, V.W. Soo, Agents for educational games and simulations: International Workshop, AEGS 2011, Taipei, Taiwan, 2012
5. L.A. Dobrzański, R. Honysz, The idea of material science virtual laboratory, Journal of Achievements in Materials and Manufacturing Engineering, 42/1-2, 2010, pp. 196-203.
6. L.A. Dobrzański, R. Honysz, On the implementation of virtual machines in computer aided education, Journal of materials Education, 31/1-2, 2009, pp. 131-140.
7. L.A. Dobrzański, R. Honysz, Informative technologies in the material products designing, Archives of Materials Science and Engineering 55/1, 2012, pp. 37-44
8. C. Gonzalez, Student Usability in Educational Software and Games: Improving Experiences: Improving Experiences, Hershey, 2012.
9. T.S. Mujber, T. Szecsi, M.S.J. Hashmi, Virtual reality applications in manufacturing process simulation, Journal of Materials Processing Technology, 155–156, 2004, pp. 1834-1838
10. https://www.struers.com/ - Metallographic products, knowledge and service | Struers.com
11. A. Barbacki (red.), Metody i techniki strukturalnych badań metali, Wydawnictwo Politechniki Poznańskiej, Poznań 1994
12. A.Werońskі (red.), Ćwiczenia laboratoryjne z inżynierii materiałowej, Politechnika Lubelska, Lublin, 2002.

MTS CONFERENCE
MATERIAL TECHNOLOGIES IN SILESIA

12-15.06.2022
Crystal Mountain***** Hotel, Wisła, Poland

Electrochemical Behaviour and Morphology of Selected Sintered Samples of $Mg_{65}Zn_{30}Ca_4Pr_1$ Alloy

B. Hrapkowicz[a], S. Lesz[a], M. Karolus[b], J. Popis[a], A. Gabryś[a]

[a] Silesian University of Technology, Faculty of Mechanical Engineering, Department of Engineering Materials and Biomaterials
[b] University of Silesia, Institute of Materials Engineering
E-mail: bartlomiej.hrapkowicz@polsl.pl

Abstract: In order to investigate the effect of the milling time on the corrosion resistance of the Mg65Zn30Ca4Pr1 alloy, powders of the alloy were milled for 13, 20, and 70 hours, respectively, were prepared. The samples were sintered using SPS technology at 350°C and pressure of 50 MPa. The samples were subjected to potentiodynamic immersion tests in Ringer's solution at 37°C. The obtained values of Ecorr were -1.36, -1.35, and -1.39 V, Polarization resistance 144.49, 188.89, and 101.11 Ω for samples milled for 13, 20, and 70h, respectively. The samples morphology showed cracks and pits, thus signaling pitting corrosion.

Keywords: magnesium, rare-earth elements, SPS, corrosion

1. INTRODUCTION

Materials used in modern medicine have the disadvantage of being permanent. After completing their task, such as bone stabilization, some elements must be removed. Symptoms such as infection or metal irritation are indications for immediate removal. Unfortunately, such an operation puts the patient at risk again, not to mention stress and potential complications. A reasonable solution seems to be the introduction of biodegradable materials, capable of self-decomposition. These materials, after the treatment period, and even partially during treatment, would be resorbed to supplement bone union and negate the need for reoperation.

Magnesium materials have long attracted the attention of scientists because of their specific characteristics. They are light and have mechanical properties like human bones. Moreover, they are biocompatible and biodegradable. Moreover, magnesium materials are susceptible to modifications that can significantly change and select their properties [1]. The methods of their production and the alloying additives are of particular importance here. Elements such as zinc and calcium have long been used to improve magnesium alloys, both in terms of mechanical and structural properties and, above all, corrosion resistance [2–4]. Rare earth elements drastically increase the mechanical properties of magnesium alloys, while many of them are toxic, which prevents their use for medical purposes. It is worth considering, however, some of them are characterized by low or negligible toxicity, which in a small amount can significantly improve the properties of the alloy [5,6].

The production of materials with such different melting points presents some technical problems that are difficult to overcome in the production of alloys by traditional methods, such as casting. Techniques such as mechanical synthesis gain an advantage here. Using the phenomenon of solid-state diffusion, they can obtain an alloy with a given chemical composition without the need to melt it [7, 8]. The powders obtained in this way can be relatively easily consolidated by incremental methods or by sintering. Thanks to such activities, it is possible to obtain specific materials and shapes, precisely personalized for a given patient.

With materials for medical applications, especially orthopedic or dental applications, it is very important to determine their behavior in corrosive conditions of the human body. Even more so with biodegradable material.

In this work, the Mg-Zn-Ca-Pr alloy prepared by the powder metallurgy method, namely with high-energy ball milling, was subjected to the spark-plasma sintering process. Subsequently, the samples prepared in this way were tested for their corrosion resistance. Potentiodynamic immersion tests were carried out to determine the corrosion current, corrosion potential, and using extrapolation of the Tafel anode and cathode slopes, polarization curves were determined from which corrosion resistance can be deduced.

2. MATERIAL PREPARATION AND METHODS

The research material was prepared by high-energy mechanical milling in a SPEX 8000D shaker ball mill. The powder mixture was prepared from pure Mg, Zn, Pr powders (99.99% wt.%) and pieces of Ca (99.99% wt.%). The powders were milled successively for 13, 20, and 70 h. The obtained powder was then sintered via Spark-Plasma Sintering HP D 25/3 device with 350°C sintering temperature and 50 MPa of compression strength, 5 min holding time, in a graphite die (Graphite type 2334). The heating rate was 50°C·min−1 up to 300°C and 25 °C·min−1 from 300°C to 350°C. The obtained specimens with 20 mm diameter were then cut and prepared for immersion tests. Corrosion testing was carried out in Ringer solution at 37°C, simulating the natural environment of the human body, on Autolab 302N potentiostat equipped with a cell containing the reference electrode (saturated calomel electrode) and the counter electrode (platinum rod). The samples were tested by 3600 s of open-circuit potential (EOCP) at a scan rate of 1 mV·s−1. The polarization curves with Tafel's extrapolation were

determined after stabilization time. To assess the corrosion effects surface images were collected by means of a Scanning Electron Microscope (SEM - Supra 35 Zeiss).

3. RESULTS

a) b)

Figure 1. a) Tafel plots for specimens subjected to immersion tests, b) surface morphology after electrochemical tests of the selected sample - SEM image of the surface affected by corrosion.

The sample after 13h had -1.36 V of the corrosion potential, the highest value of -1.35 V was obtained for the Mg65Zn30Ca4Pr1 sample milled for 20h, and the lowest of -1.39 V for the sample milled for 70h (Fig. 1a). The polarization resistance was 144.49 Ω, 188.89 Ω, and 101.11 Ω for samples after 13, 20, and 70h, respectively. The micrograph features the surface morphology after corrosion (Fig. 1b). The corrosion damage is clearly visible, and the corrosion products layers are dense and closely packed together. Small pits and cracks can be seen on the surface of the presented sample, and it is true for the rest of the samples as well. It can be concluded that the studied samples undergo pitting corrosion.

Table 1. Results of the potentiodynamic electrochemical tests for $Mg_{65}Zn_{30}Ca_4Pr_1$ alloy milled for 13, 20, and 70 h, respectively.

Sample	E_{corr} [V]	J_{corr} [μ A/cm^2]	i_{corr} [μA]	Corrosion rate [mm/year]	Polarization resistance [Ω]	OCP value
13 h	-1.36	87.00	87.00	1.01	144.49	-1.550
20 h	-1.35	57.25	57.25	0.67	188.89	-1.550
70 h	-1.39	201.17	201.17	2.34	101.11	-1.422

4. CONCLUSIONS

In our study, Mg65Zn30Ca4Pr1 samples were milled for 13, 20, and 70 h respectively, compressed with 50 MPa of force and sintered at 350°C by SPS method. Their corrosion behavior in Ringer's solution has been studied.

Based on the electrochemical test results, it can be stated the corrosion resistance is related to the milling time.

Samples milled for 13h (-1.36 V) and 20h (-1.35 V), have similar values of corrosion potential, although they considerably differ in polarization resistance with values of 144.49 Ω for 13h and 188.89 Ω for 20h. Those differences result in better corrosion resistance for the sample after 20h with 0.67 mm/year corrosion rate, as compared to 1.01 mm/year for 13h sample. The sample after 70h had the lowest values of -1.39 V, 101.11 Ω and 2.34 mm/year.

After immersion tests, the pitting corrosion was assessed via microscopic analysis of the samples' surface morphology. Small cracks and pits have been observed.

Acknowledgments: The financial support of the National Science Center, Poland, is gratefully acknowledged, grant no. 2017/27/B/ST8/02927.

BIBLIOGRAPHY

1. Witte, F. The History of Biodegradable Magnesium Implants: A Review. Acta Biomaterialia 2010, 6, 1680–1692, doi:10.1016/j.actbio.2010.02.028.
2. Byrne, J.H.; O'Cearbhaill, E.D.; Browne, D.J. Comparison of Crystalline and Amorphous Versions of a Magnesium-Based Alloy: Corrosion and Cell Response. European Cells and Materials 2015, 30, 75.
3. Kannan, M.B.; Raman, R.K.S. In Vitro Degradation and Mechanical Integrity of Calcium-Containing Magnesium Alloys in Modified-Simulated Body Fluid. Biomaterials 2008, 29, 2306–2314, doi:10.1016/j.biomaterials.2008.02.003.
4. Zberg, B.; Uggowitzer, P.J.; Löffler, J.F. MgZnCa Glasses without Clinically Observable Hydrogen Evolution for Biodegradable Implants. Nature Materials 2009, 8, 887–891, doi:10.1038/nmat2542.
5. Lesz, S.; Hrapkowicz, B.; Karolus, M.; Gołombek, K. Characteristics of the Mg-Zn-Ca-Gd Alloy after Mechanical Alloying. Materials 2021, 14, 1–14, doi:10.3390/ma14010226.
6. Lesz, S.; Hrapkowicz, B.; Gołombek, K.; Karolus, M.; Janiak, P. Synthesis of Mg-based Alloys with Rare-Earth Element Addition by Means of Mechanical Alloying. Bulletin of the Polish Academy of Sciences: Technical Sciences 2021, 69, doi:10.24425/BPASTS.2021.137586.
7. Amiya, K.; Inoue, A. Formation, Thermal Stability and Mechanical Properties of Ca-Based Bulk Glassy Alloys. MATERIALS TRANSACTIONS 2002, 43, 81–84, doi:10.2320/matertrans.43.81.
8. Polmear, I.; StJohn, D.; Nie, J.-F.; Qian, M. Novel Materials and Processing Methods; 2017; ISBN 9780080994314.

MTS CONFERENCE
MATERIAL TECHNOLOGIES IN SILESIA

12-15.06.2022
Crystal Mountain***** Hotel, Wisła, Poland

Upscaling of silvering copper particles

A. Hryniszyn[a], A. Wrona[a], K. Czechowska[a]

[a] Łukasiewicz Research Network — Institute of Non-Ferrous Metals
email: alicja.hryniszyn@imn.lukasiewicz.gov.pl

Abstract:
The article describes the idea of the silvering copper powder by chemical method. Also presented are the results of studies including particle size distribution, electron probe microanalysis and X-ray diffraction of prepared powder.

Keywords: silvering, copper powder, chemical method, electrical contacts

1. INTRODUCTION

Over the past few years, there has been a significant increase in energy consumption, especially in densely populated areas. This phenomenon is associated with the risk of overloading the power network, which results in the need to increase the efficiency of the high line voltage. However, the increase in the efficiency of electrical cables necessitates more stringent operating conditions for devices such as contacts that are involved in the transmission and distribution of electricity. Substation connectors are contacts that physically connect the transmission line, substation connectors, and the bus collective. They are mechanical type devices. This means that the coupling parts, i.e. the parts that transmit electrical energy, are mechanically connected with bolts using a special method of twisting to ensure the integrity of the connection and ensure adequate contact resistance. Contact resistance affects energy efficiency, stable voltage, long-term service life. If the resistance is high and unstable over time, it may contribute to the contact and its overheating shortened service life [Capelli and Gonzalez 2016]. It is therefore important to prevent an increase in contact resistance for this purpose the surface of the contacts made of copper and aluminum should be protected against the formation of an oxide passivation layer on them surface. Silver of all metals, it has the highest electrical and thermal conductivity, however, it has the high coefficient of friction it can lead to a relatively poor durability of the material. In addition, it easily forms a matted layer when treated sulphides and chlorides. The frosted layers are mainly covalently bonded semiconducting silver sulfides and /or silver chlorides, which are even less conductive. The resulting layers are soft at ambient temperature very easily worn semiconductors [Myers 2009]. Moreover, silver is a material characterized by significant plasticity, therefore, without alloying additives, it is not possible to obtain the correct protection against mechanical deformations and corrosion. When layer losses occur as a result of the action of mechanical forces then it begins the process of corrosion of the substrate, which contributes to the destruction of the contact, and as a consequence, the resistance is increased, which leads to an increase contact operating temperature. The improvement in the mechanical properties and the increase in the resistance to fogging can be brought about by addition of copper and addition of copper oxides [Slade et al. 1999, Kim et al. 2012]. The copper particles are unfortunately prone to oxidation. Jung et al. 2011 showed in their research that silver-coated copper particles (content silver was 20%) were stable even after 1 month of exposure to air.

1.1. Results of Electron Probe Microanalysis

The produced powder were analysed by Electron Probe Microanalysis. Sample images are shown below.

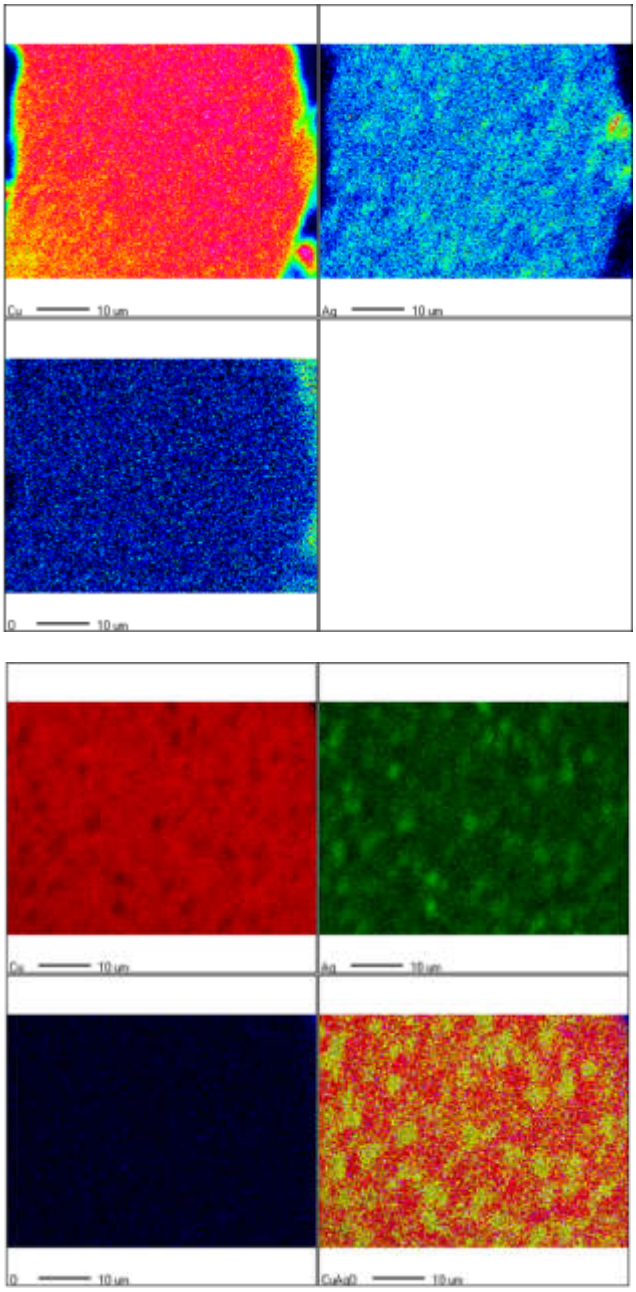

Figure 1. The image of silver coated copper powder section 2000x

Acknowledgments: The financial support of the National Centre for Research and Development Poland, is gratefully acknowledged, grant no. POIR.04.01.04-00-0093/18

BIBLIOGRAPHY

1. F. Capeli, J.R. Riba, D. Gonzalez. 2016. Thermal behavior of energy-efficient substation connectors. 10th International Conference on Compatibility, Power Electronics and Power Engineering (CPE-POWERENG).
2. M. Myers. 2009. The Performance Implications of Silver as a Contact Finish in Traditionally Gold Finished Contact Applications. the 55th IEEE HOLM 2009 Conference on Electrical Contacts.
3.P.G. Slade (ed.), Electrical Contacts Principles and Applications. : Marcel Dekker, Inc., New York, 2019
4. S.J.Kim, J.Y. Lee, M.J. Han, Y.C.Kim, H.D. Park, S.H. Sun, J.J. Lee, J.H. Cha, J.H. Jo, H. Jang. The Role of Copper on the Friction and Wear Performance of Automotive Brake Friction Materials, . SAE International Journal of Materials and Manufacturing 9-18 (2012).

MTS CONFERENCE
MATERIAL TECHNOLOGIES IN SILESIA

12-15.06.2022
Crystal Mountain***** Hotel, Wisła, Poland

Research of the dye-sensitized solar cells (DSSC) architecture based on hybrid nanostructures

P. Jarka*, A. Drygała, W. Matysiak, T. Tański

[a] Silesian University of Technology, Faculty of Mechanical Engineering, Department of Engineering Materials and Biomaterials
email: pawel.jarka@polsl.pl

Abstract: The authors focused on the investigation of dye sensitized solar cells (DSSC) with porous photoanodes containing of 1D ZnO and TiO2 nanostructures. The purpose of the work includes the photoanodes preparation from nanoparticles and nanowires blends, dye to obtaining high electron transport with low electron recombination. For the production of DSSC cells also were used comercial N719 - ruthenium complex dye (Di-tetrabutylammonium cis-bis(isothiocyanate)bis(2,2'-bipyridyl-4,4'-dicarboxylate)ruthenium(II)), EL-HSE high stability electrolyte, and platinum counter electrode produced by screen printing method. The results confirm the effectiveness of surface area expandsion with optical properties maintenance. Also obtained efficiencies comparable to receive in other scientific centers, it allows concluding that the combination of nanoparticles and nanowires is an interesting direction for the development of DSSC.

Keywords: dye-sensitized solar cells (DSSC), nanomaterials, one dimensional nanostructures ZnO, TiO_2

,

1. INTRODUCTION

Nowadays searching for alternative energy sources is one of the major challenges of the economy [1]. Ecological conditions and in particular the necessity of the emissions of SOx, COx, NOx minimalizing, cause inevitability explicit progress in the production of so-called clean energy [2, 3]. Solutions seeking to minimize the energy consumption of many industries are also sought and developed [4]. Also, alternative energy sources according to the latest requirements must have significant efficiency of energy conversion as well as a minimal impact on the environment in terms of practically zero emissions and impact on the landscape [5]. From this point of view, photovoltaic power plants are effective energy sources that do not have an environmental impact as in the case of hydropower plants and do not emit sound as in the case of wind farms. Besides, the costs of installing cells and the possibilities of expansion or modernization are relatively low. In recent years, continuous progress has been observed in the construction of photovoltaic devices [6-8]. Additionally, it was proven and DSSCs can operate with diffused sunlight (e.g. in case cloudy environment) what is unavailable in the case of thin-film solar devices [10]. However, the widespread use of DSSC technology in the photovoltaic market requires device refinement especially in terms of improving cell efficiency. Improving the operation of cells requires in particular optimization of the electrical properties of the optical elements of the cell through the days of materials, modification of their structure and surface morphology as well as geometric form. In particular, a lot of effort is currently being put into work on electrodes (photoanode and counter-electrode). Photoanode is responsible for light absorption and electrons transferring to the substrate in DSSC systems [11]. Thus, the high surface area created by the nanoporous TiO_2 layer decide about dye and hence light adsorption and facilitating the penetration of electrolyte within their pores. Also, the use of semiconductor nanowires due to the small dimensions indicates several interesting characteristics for DSSC applications like directed and high electron pathways [12,13] and obtaining higher light scattering capability but dye loading, in this case, is lower than in case 3D nanostructures [14-17]. Hence, composite one-dimensional (1D) with three-dimensional (3D) structure allows the use of their advantages while minimizing the disadvantages.
Considering the above, the Authors focus on manufacturing of DSSCs with nanowires/nanoparticle TiO_2/ZnO photoanode hybrid structure to increase the electron diffusion length in the photoanode while maintaining a large

surface area. The article introduces a method of high-efficiency DSSC manufacturing with the use of modern methods that provide high dimensional, structural repeatability of nanoparticles/nanowires photoelectrode

BIBLIOGRAPHY

[1] Abdul Karim N, Mehmood U, Fizza Zahid H, Asif T, 2019, Nanostructured photoanode and counter electrode materials for efficient, Dye-Sensitized Solar Cells (DSSCs), Sol. En. 185:165-188.
[2] Shahsavari A, Akbari M, 2018, Potential of solar energy in developing countries for reducing energy-related emissions. Renew. Sustain. Energy Rev. 90:275-291.
[3] Musztyfaga-Staszuk M, Dobrzanski L.A, Rusz S., Staszuk M, 2014, Application examples for the different measurement modes of electrical properties of the solar cells, Arch. Metal. Mat. 59:247-252.
[4] Tanski T, Dobrzanska-Danikiewicz A.D, Labisz K, Matysiak W, 2014, Long-term development perspectives of selected groups of engineering materials used in the automotive industry, Arch. Metal. Mat. 59:1717-1728
[5] Louwen A, van Sark W.G.J.H.M, Faaij A.P.C, Schropp R.E.I, 2016, Re-assessment of net energy production and greenhouse gas emissions avoidance after 40 years of photovoltaics development. Nat. Commun. 7:13728.
[6] Hammond A.L, 1972, Solar energy: the largest resource. Science 177:1088-1090.
[7] Green M.A, Emery K, Hishikawa Y, Warta W, E.D. Dunlop (2014) Solar cell efficiency tables (version 44), Prog. Photovolt. Res. Appl. 22:701–710,
[8] Bokalič M, Topič M, 2015, Spatially Resolved Characterization in Thin-Film Photovoltaics, Springer US, New York.
[9] Iwata S, Shibakawa S, Imawaka N, Yoshino K, 2018 Stability of the current characteristics of dye-sensitized solar cells in the second quadrant of the current–voltage characteristics. Energy Rep. 4:8-12.
[10] Suriani A.B, Muqoyyanah A, Mohamed A, Mamat M.H, Othman M.H.D. Ahmad M.K, Abdul Khalil H.P.S, Marwoto P, Birowosuto M.D ,2019, Titanium dioxide/agglomerated-free reduced graphene oxide hybrid photoanode film for dye-sensitized solar cells photovoltaic performance improvement, Nano-Structures & Nano-Objects 18:100314.
[11] Cao Y, Li Z, Wang Y, Zhang T, Li Y, Liu X, Li F, 2016, Influence of TiO2 nanorod arrays on the bilayered photoanode for dye-sensitized solar cells, J. Electron. Mater. 45:4989–4998.
[12] Qiu Q, Li S, Jiang J, Wang D, Lin Y, Xie T, 2017, Improved electron transfer between TiO2 and FTO interface by n-doped anatase TiO2 nanowires and its applications in quantum dot-sensitized solar cells, J. Phys. Chem. C ,121:21560-21570.
[13] Wu W.Q, Xu Y.F, Su C.Y, Kuang D.B, 2014, Ultra-long anatase TiO2 nanowire arrays with multi-layered configuration on FTO glass for high-efficiency dye-sensitized solar cells, Energy Environ. Sci. 7:644-649.
[14] Yang M, Neupane S, Wang X, He J, Li W, Pala N, 2013, Multiple step growth of single crystalline rutile nanorods with the assistance of self-assembled monolayer for dye sensitized solar cells, ACS Appl. Mater. Interfaces 5: 9809-9815.
[15] Luan X.N, Guan D.S, Wang Y, 2012, Facile synthesis and morphology control of bamboo-type TiO2 nanotube arrays for high-efficiency dye-sensitized solar cells, J. Phys. Chem. C, 116:14257-14263.
[16] Li Z.Q, Mo L.E, Chen W.C, Shi X.Q, Wang N, Hu L.H, Hayat T, Alsaedi A, Dai S.Y, 2017, Solvothermal synthesis of hierarchical TiO2 microstructures with high crystallinity and superior light scattering for high-performance dye-sensitized solar cells, ACS Appl. Mater. Interfaces 9:32026-32033.
[17] Umale S.V, Tambat S.N, Sudhakar V, Sontakke S.M, Krishnamoorthy K, 2017, Fabrication, characterization and comparison of DSSC using anatase TiO2 synthesized by various methods, Adv. Pow. Techn. 28:2859-2864.

MTS CONFERENCE
MATERIAL TECHNOLOGIES IN SILESIA

12-15.06.2022
Crystal Mountain***** Hotel, Wisła, Poland

Effect of spray distance on the microstructure and corrosion resistance of WC - based coatings sprayed by HVOF

E. Jonda[a], L. Łatka[b], A. Maciej[c], M. Godzierz[d], K. Gołombek[e], A. Radziszewski[f]

[a] Silesian University of Technology, Faculty of Mechanical Engineering, Department of Engineering Materials and Biomaterials, 18a Konarskiego St., 44100 Gliwice, Poland;
email: ewa.jonda@polsl.pl;
[b] Wroclaw University of Science and Technology, Faculty of Mechanical Engineering, Department of Metal Forming, Welding and Metrology, 5 Łukasiewicza St., 50371 Wroclaw, Poland;
email: leszek.latka@pwr.edu.pl;
[c] Silesian University of Technology, Faculty of Chemistry, Department of Inorganic and Analytical Chemistry and Electrochemistry, 6 B. Krzywoustego St., 44100 Gliwice, Poland;
email: artur.maciej@polsl.pl;
[d] Polish Academy of Sciences, Centre of Polymer and Carbon Materials, 34 M. Curie - Skłodowskiej St., 41819 Zabrze, Poland;
email: mgodzierz@cmpw-pan.edu.pl;
[e] Silesian University of Technology, Faculty of Mechanical Engineering, Materials Research Laboratory, 18a Konarskiego St., 44100 Gliwice, Poland;
email: Klaudiusz.golombek@polsl.pl;
[f] „RESURS" Company, A. Radziszewski, 12 Czarodzieja St., 03116 Warszawa, Poland;
email: resurs@resurs.pl;

Abstract: In this work, conventional WC-based powders (WC-Co and WC-Co-Cr) were sprayed with High Velocity Oxy Fuel (HVOF) onto AZ31 magnesium alloy with different spray distances (320 and 400 mm). The aim of the research was to investigate the effect of the spray distance on the microstructure of the coatings, phase composition, residual stress and electrochemical corrosion resistance. The manufactured coatings were analyzed by scanning electron microscopy (SEM), X-ray diffraction (XRD) and electrochemical corrosion tests such as potentiodynamic polarization. In order to characterize the sprayed coatings, statistical measurements of surface roughness and thickness of deposits were also performed.

Keywords: WC-based powders, High Velocity Oxy Fuel, AZ31 magnesium alloy, microstructure, corrosion resistance.

1. INTRODUCTION

Over the years, High Velocity Oxy Fuel (HVOF) technology has improved and now offers coatings with better densification and low chemical degradation, especially WC-based coatings. A big advantage of the HVOF process is the high velocity and associated low temperature achieved by the particles, with minimal potential damaging effects on the coating and substrate areas due to their potentially high erosion and corrosion resistance. The potential to extend component life is attractive in terms of reduced maintenance costs and reduced downtime. The increased demand and improvement in thermal spray coatings is also partly attributable to the third generation coatings produced by thermal spray technology with minimal porosity and high adhesion [1-3]. WC-Co thermal spray coating applied by HVOF method, considered feasible alternative to hard chrome plating due to excellent wear resistance durability and greener features. This the addition of metallic Cr to the Co binder matrix produces

noticeable results improved wear and oxidation resistance of WC-Co coatings that do not produce highly toxic substances by the spraying process chromium [4-6].

2. MATERIALS AND METHODS

Two powders WC-Co and WC-Co-Cr were sprayed onto AZ31 magnesium alloy with 320 and 400 mm spray distances. The delivery state for both powders was agglomerated and sintered. Moreover, the particle size range was - 45 + 15 µm for both feedstock. A spray system JP 5000 TAFA (Indianapolis, USA) from RESURS (Warsaw, Poland) was used to deposit the coatings. Before spraying, the sample surface was sandblasted with corundum and ultrasonically treated. The fuel media used for spraying were kerosene and oxygen, and the carrier gas was nitrogen.

3. RESULTS

Based on the investigations it was found that the coatings are characterized by a dense and relatively uniform structure, which consists of WC particles embedded in a Co or Co-Cr matrix, depending on the feedstock material. Phase composition of cermet coatings consists of hexagonal WC, hexagonal W_2C carbide, hexagonal Co, and cubic solid solution of tungsten in cobalt with composition $Co_{0.9}W_{0.1}$. Moreover, in WC-Co coating presence of cubic tungsten crystallites was detected. In the coatings sprayed with 400 mm distance, minor presence of WC_6O_6 was detected, most likely as an effect of higher spraying distance, leading to partially oxidation of WC at powder's particles boundaries. In all cermet coatings, linear stress exhibits compressive properties. In WC-Co, the shear stress is higher than that of WC-Co-Cr, most likely due to the presence of Cr in the cermet, which can partially absorb energy during the HVOF process. According to the corrosion tests results, it was found that all deposited coatings allow to improve corrosion resistance of AZ31 alloy, for which the polarization resistance is 241.3 Ω cm^2. The highest corrosion resistance was characteristic for WC-Co sprayed at a distance of 320 mm, the polarization resistance value of which was over seventeen times higher (Rp = 4180 Ω cm^2).

Acknowledgments: The financial support of the Ministry of Science and Higher Education of Poland, is gratefully acknowledged, grant no. DEC - 2019/03/X/ST5/00830.

BIBLIOGRAPHY

[1]. R. Akshay Govande, A. Chandak, B. Ratna Sunil, R. Dumpala, Carbide-based thermal spray coatings: A review on performance characteristics and post-treatment, International Journal of Refractory Metals and Hard Materials, 103 (2022), 105772, https://doi.org/10.1016/j.ijrmhm.2021.105772.

[2]. Taimin Gong, Pingping Yao, Xiaoting Zuo, Zhongyi Zhang, Yelong Xiao, Lin Zhao, Haibin Zhou, Minwen Deng, Qi Wang, Aiwen Zhong, Influence of WC carbide particle size on the microstructure and abrasive wear behavior of WC-10Co-4Cr coatings for aircraft landing gear, Wear 362-363 (2016) 135-145, http://dx.doi.org/10.1016/j.wear.2016.05.022.

[3]. Y. Y. Santana, La J. G. Barbera-Sosa, J. Caro, E. S. Puchi-Cabrera & M. H. Staia, Mechanical properties and microstructure of WC-10Co-4Cr and WC-12Co thermal spray coatings deposited by HVOF, Surface Engineering, (2008), 24:5, 374-382, DOI: 10.1179/174329408X326380.

[4]. A. Garfias Bulnes, V. Albaladejo Fuentes , I. Garcia Cano and S. Dosta, Understanding the Influence of High Velocity Thermal Spray Techniques on the Properties of Different Anti-Wear WC-Based Coatings, Coatings, (2020), 10, 1157; doi:10.3390/coatings10121157.

[5]. K.O. Méndez - Medrano, C.J. Martínez - González, F. Alvarado Hernández, O. Jiménez, V.H. Baltazar Hernández, and H. Ruiz - Luna, Microstructure and Properties Characterization of WC-Co-Cr Thermal Spray Coatings, Journal of Minerals and Materials Characterization and Engineering, (2018), 6, 482-497, https://doi.org/10.4236/jmmce.2018.64034.

[6]. W. Tillmann, C Schaak , L Hagen and M Dildrop, Investigation of HVOF-ID spraying with WC-CoCr - 15+5 µm feedstock powder Materials Science and Engineering, 480, (2019), 012008, IOP Publishing, doi:10.1088/1757-899X/480/1/012008.

MTS CONFERENCE
MATERIAL TECHNOLOGIES IN SILESIA

12-15.06.2022
Crystal Mountain***** Hotel, Wisła, Poland

Forming of structure and properties of metal surfacing welds made of CuAl7 and CuAl2 alloys subjected to the hot isostatic pressing process

J. Kalabis[a], J. Kulasa[a], A. Kowalski[a], D. Kołacz[a], S. Topolska[b]

[a] Łukasiewcz Research Network – Institute of Non-Ferrous Metals, Gliwice ul. Sowińskiego 5, POLAND.
[b] Silesian University of Technology, Faculty of Mechanical Engineering, Department of Welding, Gliwice ul. Konarskiego 18A, POLAND.

jaroslaw.kalabis@imn.lukasiewicz.gov.pl

Abstract: This paper presents the effect of hot isostatic pressing (HIP) process on the structure, mechanical properties, and corrosion resistance of aluminium bronze CuAl7 and CuAl2 surfacing welds made by the TIG method. The tested material CuAl7 is a widely available material on the welding wire market, while CuAl2 was produced as a prototype of a multiwire. The multiwire contains copper and aluminium fibre bundles in the form of tubes and rods. The individual fibres fuse together in an electric arc to form a CuAl2 alloy in a liquid weld pool. The welds were subjected to a Vickers hardness test, a neutral salt spray (NSS) corrosion test, an electrical conductivity test and a pin-on-disc tribological test. The structures were also observed using light microscopy. In addition, sections of the samples were subjected to an isostatic pressing process and all tests were repeated to compare the results obtained and to determine the effectiveness of the HIP process.

Keywords: material engineering, welding, multimetal materials

1. Introduction

Copper-aluminium alloys are the most commonly used materials in the marine industry for components operating in corrosive environments. CuAl alloys, due to their good mechanical properties and market availability, are the most commonly used materials for the production of ship propellers, steering systems, machine parts, shafts and aircraft engine parts. New technologies of manufacturing and modification of construction materials allow for longer service life of machines and a significant increase in their reliability. CuAl alloys are also characterised by high thermal conductivity and are susceptible to hot isostatic pressing (HIP), which leads to an increase in their strength due to the strain hardening effect [1, 2]. To improve the properties of CuAl alloys, the author of [3] notices the necessity of silicone addition, which causes uniform mixing of elements and slows down the local formation of intercrystalline phases. Additionally, silicon increases the mechanical properties, i.e., yield strength and hardness. Hot isostatic pressing is a technological process used to remove porosity from cast materials and objects manufactured using 3D printing techniques. The elimination of micro-porosity occurs by diffusion creep, leading to uniformity of mechanical properties throughout the material. The tensile strength and ductility of the material is comparable to heat-treated forged materials [2].

1.1 Materials and research methodology

The aim of this study was to determine the effect of the hot isostatic pressing (HIP) process on the surfacing welds produced by the TIG method. The CuAl7 welding wire is a commercially available material, while the wire with 2% aluminium addition is a new type of wire produced by drawing a bundle consisting of a copper tube inside which there is sheathed wire with an aluminium core and a copper tube. This solution has been named multiwire. Examples of fabricated multiwire are shown in Figure 1. Figure 1-a shows the wire bundle ($7^1 = 7$ aluminium fibers) that is used for the next stage. Figure 1-b illustrates the second stage of bundling ($7^2 = 49$ aluminium fibres), and Figure 1-c illustrates the final stage of bundling ($7^3 = 343$ aluminium fibres).

a) b) c)

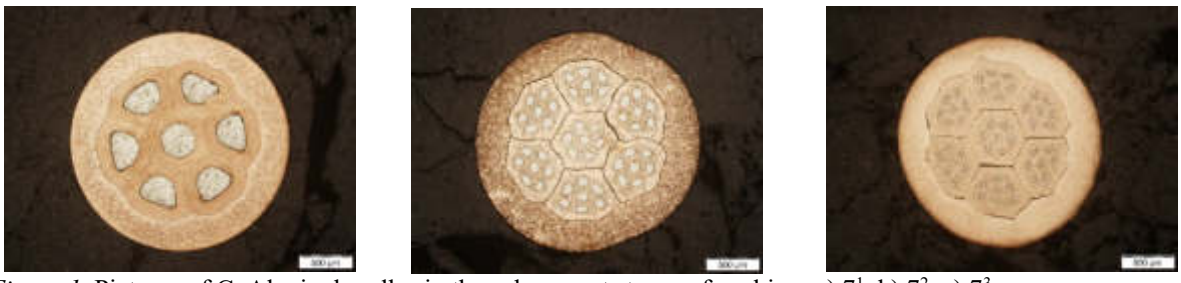

Figure 1. Pictures of CuAl wire bundles in the subsequent stages of packing: a) 7^1, b) 7^2, c) 7^3

In this work, welding tests were carried out using two types of material, CuAl2 (multiwire bundle 7^3) and CuAl7 available on the market. Welding tests were carried out using a Fronius TransTig 2200 welding machine. The produced surfacing welds were subjected to Vickers HV1 hardness tests (FutureTech FM700 hardness tester) and microscopic observations using light microscopy (Olympus GX71F microscope) to determine the grain size and the state of the surfacing weld (cavities, micro-shrinkage, gassing). In addition, tribological tests (Anton Paar THT tribometer) were performed using the 'pin on disc' method (load: 10N; sliding distance: 2000 m; counter sample material: 100Cr6 steel). Electrical conductivity tests were also performed using a Sigmatest Foerster 2.069 device. Additionally, the samples were subjected to corrosion tests in neutral salt spray. In the next step, the produced surfacing welds were subjected to the HIP process (AIP8-30H) at a temperature of 850°C and a pressure of 1500 bar. Comparative tests were carried out again in order to check the influence of the HIP process on the tested materials, from which the surfacing welds were made.

Acknowledgement
Work carried out as part of an Implementation Doctorate (Tittle: "Badania nad opracowaniem technologii wytwarzania multimetalowych drutów o strukturze multiwłóknistej do zastosowań w spawalnictwie i procesach przyrostowych") funded by the Ministry of Education and Science and a grant from the Łukasiewicz Research Network - Institute of Non-Ferrous Metals.

References

[1] A.Ravikumar, R.Sellamuthu, R. Saravanan *Effect of Cr Addition on Mechanical Properties and Wear Rate of Cast Al-Cu Alloy*, Indian Journal of Science and Technology, *Vol 9(34), DOI: 10.17485/ijst/2016/v9i34/100952, September 2016.*
[2] M.T. Kim, S.Y. Chang, J.B. Won, *Effect of HIP process on the micro-structural evolution of a nickel-based superalloy*, Materials Science and Engineering: A, Volume 441, Issues 1–2, 2006, Pages 126-134, ISSN 0921-5093.
[3] Y.Wang, X. Chen, S. Konovalov, C. Su, A. Siddiquee, N. Gangil, *In-situ wire-feed additive manufacturing of Cu-Al alloy by addition of silicone*, Applied Surface Science, Volume 487, 2019, Pages 1366-1375, ISSN 0169-4332.

MTS CONFERENCE
MATERIAL TECHNOLOGIES IN SILESIA

12-15.06.2022
Crystal Mountain***** Hotel, Wisła, Poland

Biomedical magnesium alloys with Gd addition

A. Kania [a]

[a] Silesian University of Technology, Faculty of Mechanical Engineering, Department of Engineering Materials and Biomaterials
email: aneta.kania@polsl.pl

Abstract: The article presents the results of structure and corrosion resistance investigations of MgCa2Zn1Gd3 alloy and the alloy with TiO_2 coating applied using dip coating, one of the sol-gel methods.

Keywords: MgCa2Zn1Gd3 alloy, TiO_2 coating, structure analysis, corrosion tests, corrosion resistance

1. INTRODUCTION

Magnesium alloys have many advantages in comparison with other biomaterials used today for bone implants. The density, modulus of elasticity, and tensile strength of Mg are similar to human bones. Moreover, the magnesium alloys have non-toxic, biocompatible and biodegradable nature [1]. Therefore, Mg alloys can be used as temporary implants. Magnesium, calcium and zinc are minerals which are vital to many bodily processes. In case of gadolinium, there are not so many works on its biocompatibility. But the addition of a low content of Gd (about 3 wt.%) to a Mg alloys is tolerated by the human body, what was confirmed by the cytotoxicity tests [2]. In addition, gadolinium improves mechanical properties of the Mg alloys. However, magnesium alloys are characterized by poor corrosion resistance in the physiological environment. The corrosion resistance of such the alloy implants can be improved by alloying additives (e.g. gadolinium) and protective coatings, such as TiO_2.

The work presents the results of structure and corrosion resistance investigations of MgCa2Zn1Gd3 and the alloy with TiO_2 coating (with a thickness of about 20 μm) applied using dip coating method.

2. RESULTS AND DISCUSSION

2.1. Structure and topography investigations

Observations of the samples' surface carried out in a scanning electron microscope (SEM) have shown, that MgCa2Zn1Gd3 alloy had a dendritic structure with interdendritic solute rich regions. Phases with gadolinium in a form of long precipitations along interdendritic regions appeared as bright areas [3]. It also was stated that the morphology of TiO_2 coating was homogeneous (Figure 1). It was characterized by grains of an elongated shape. Small discontinuities in the form of pores in the studied surface can be seen.

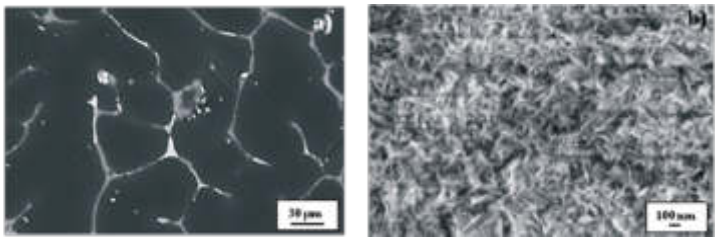

Figure 1. SEM images of: a) MgCa2Zn1Gd3 alloy, b) TiO_2 coating applied to MgCa2Zn1Gd3 alloy

Observations of surface topography in an atomic force microscope (AFM) of the alloy and TiO_2 coating applied lead to a conclusion that larger surface irregularities occurred for the TiO_2, and they were in the range

of -20 to +20 nm. Moreover, the surface extension for the TiO_2 deposited by dip coating was equal to 4.95%, and for the uncoated alloy was 0.4%. Surface roughness measurements have shown higher roughness values (roughness average, R_a, and root mean square, RMS) for the TiO_2 applied by dip coating (Table 1).

Table 1. Surface and roughness parameters of the TiO_2 coating applied, and MgCa2Zn1Gd3 alloy

Sample	Surface geometric area, μm^2	Surface area extension, μm^2	R_a, nm	RMS, nm
MgCa2Zn1Gd3	25	25.09	2.96	4.08
MgCa2Zn1Gd3 with TiO_2	25	26.09	11.9	15.1

2.2. Corrosion behavior of MgCa2Zn1Gd3 alloy with TiO_2 coating

Corrosion tests, both electrochemical and immersion were performed in Ringer solution at 37 ºC. Electrochemical results are presented in the form of potentiodynamic curves for the MgCa2Zn1Gd3 alloy and TiO_2 coating applied (Figure 2a). The corrosion potential (E_{corr}) of the TiO_2 coating was -1.55 V, while MgCa2Zn1Gd3 alloy has reached the E_{corr} value of -1.57 V. The lowest value of corrosion current density (i_{corr}), equal to 57 $\mu A \cdot cm^{-2}$, and the highest value for polarization resistance (R_p) (equal to 308 $\Omega \cdot cm^2$) were observed for the coating applied, which confirmed the improved corrosion resistance for the studied alloy with deposited TiO_2.

After electrochemical tests, the samples were immersed in the Ringer solution for 48 h, and the volume of hydrogen evolution was measured. The volume of released hydrogen after 48 h of immersion for the MgCa2Zn1Gd3 alloy was 45 $ml \cdot cm^{-2}$, and it was higher compared to the TiO_2 sample (which was equal to 11 $ml \cdot cm^{-2}$) (Figure 2b).

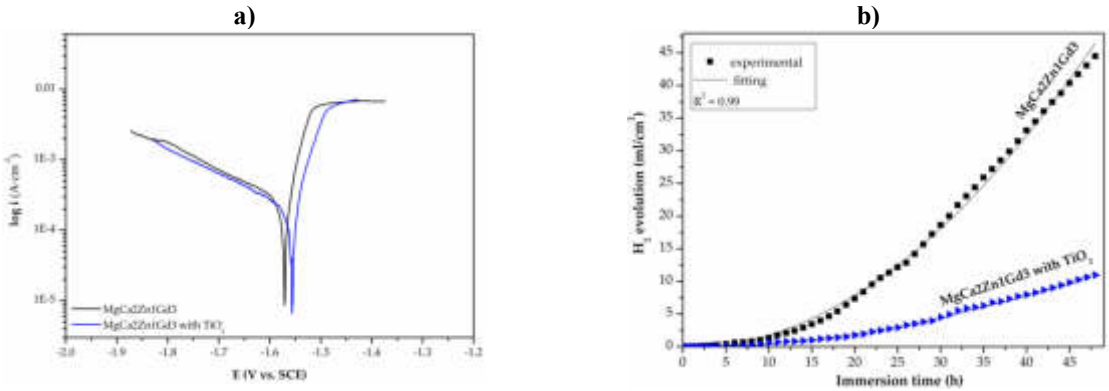

Figure 2. Polarization curves for MgCa2Zn1Gd3 alloy and TiO_2 coating applied in Ringer solution at 37 °C – a), and volume of hydrogen evolution as a function of immersion time in Ringer solution at 37 °C during 48 h for the studied alloy and the coating applied – b)

3. CONCLUSIONS

The results of the potentiodynamic and immersion corrosion tests have shown that the TiO_2 coating protects the MgCa2Zn1Gd3 alloy against corrosion. This indicates that such a combination of magnesium alloy with gadolinium addition and the TiO_2 coating is promising for possible application as implants in orthopedics.

BIBLIOGRAPHY

1. S. Agarwal, J. Curtin, B. Duffy, S. Jaiswal, Biodegradable magnesium alloys for orthopaedic applications: A review on corrosion, biocompatibility and surface modifications, Materials Science Engineering C 68 (2016) 948-963.
2. A. Kania, P. Nolbrzak, A. Radoń, A. Niemiec-Cyganek, R. Babilas, Effect of the thickness of TiO_2 films on the structure and corrosion behavior of Mg-based alloys, Materials 13/5 (2020) 1065.
3. A. Kania, R. Nowosielski, A. Gawlas-Mucha, R. Babilas, Mechanical and corrosion properties of Mg-based alloys with Gd addition, Materials 12/11 (2019) 1775.

MTS CONFERENCE
MATERIAL TECHNOLOGIES IN SILESIA

12-15.06.2022
Crystal Mountain***** Hotel, Wisła, Poland

Charakterystyka procesu produkcyjnego stali DP600

T. Kaźmierski[a,b],*, J. Krawczyk[c]

[a] ArcelorMittal Poland S.A. Oddział w Krakowie ul. Tadeusza Sendzimira 1, 31-752 Kraków,
[b] AGH Akademia Górniczo-Hutnicza, Szkoła Doktorska, al. A. Mickiewicza 30, 30-059 Kraków
[c] AGH Akademia Górniczo-Hutnicza, Wydział Inżynierii Metali i Informatyki Przemysłowej, al. A. Mickiewicza 30, 30-059 Kraków
*Autor do korespondencji: tomasz.kazmierski@arcelormittal.com

Abstrakt:
Stale dwufazowe o strukturze ferrytyczno-martenzytycznej znajdują szerokie zastosowanie w przemyśle motoryzacyjnym, głównie z uwagi na bardzo korzystne połączenie wysokiej wytrzymałości z podatnością na obróbkę plastyczną na zimno. Na nowoczesnych walcowniach posiadających odpowiednio do tego przystosowaną sekcję chłodzenia laminarnego możliwe jest uzyskanie blachy w kręgu o strukturze dwufazowej. Proces ich produkcji wymaga ścisłej kontroli parametrów procesu, począwszy od wygrzewania slabów w piecu pokrocznym poprzez walcowanie wstępne i wykańczające, na chłodzeniu laminarnym kończąc. Ze względu na specyficzne wymagania dotyczące własności mechanicznych gotowego wyrobu, szczególnego znaczenia nabiera konieczność dobrego poznania mechanizmów tworzenia się pożądanej struktury oraz określenie kluczowych parametrów procesu, za pomocą których można na tę strukturę wpływać.

Słowa kluczowe: stale dwufazowe, walcowanie na gorąco, chłodzenie laminarne, mikrostruktura, własności mechaniczne.

1. WPROWADZENIE

Z uwagi na łatwiejszą kontrolę finalnych własności, najpopularniejszą metodą produkcji blach DP o strukturze ferrytyczno-martenzytycznej jest proces polegający na wyżarzaniu blachy po walcowaniu na zimno, a następnie jej kontrolowanym chłodzeniu w celu uzyskania struktury dwufazowej. Alternatywną metodą, jest wytwarzanie blach DP bezpośrednio w procesie walcowania na gorąco dzięki zastosowaniu kontrolowanego walcowania i dwuetapowego chłodzenia. Zaletą tego drugiego procesu jest niższy koszt produkcji. Z uwagi na ograniczenia w możliwości prowadzenia badań w warunkach laboratoryjnych, w literaturze poświęcono dotychczas znacznie więcej uwagi procesowi wytwarzania blach DP na drodze wyżarzania. Niniejsze opracowanie stanowi próbę lepszego poznania zjawisk i mechanizmów zachodzących podczas produkcji stali DP na walcowni gorącej blach.

2. MATERIAŁ DO BADAŃ

Materiałem badawczym były próbki stali pobrane na trzech etapach procesu. Próbki ze slaba COS pobrano w celu analizy składu chemicznego, co pozwoliło na określenie stopnia mikro i makrosegregacji, mogących prowadzić do niepożądanej pasmowości mikrostruktury gotowego wyrobu. Analiza składu chemicznego oraz mikrostruktury podwalcowania pozwoliła na określenie stopnia homogenizacji składu chemicznego po procesie wygrzewania w piecu pokrocznym oraz dostarczyła informacji na temat morfologii austenitu bezpośrednio przed procesem walcowania wykańczającego. Badania mikrostrukturalne gotowej blachy pozwoliły na ocenę udziału objętościowego i morfologii fazy martenzytycznej i ferrytycznej. Wykonane próby rozciągania pozwoliły na określnie stopnia anizotropii własności blachy.

3. SKRÓT WYNIKÓW BADAŃ

Produkowana blacha ze stali DP charakteryzuje się małą anizotropią właściwości wytrzymałościowych porównując kierunek walcowania z kierunkiem poprzecznym (rys. 1a). Jeszcze mniejsze różnice występują dla materiału pobranego z początki i końca kręga walcowanego (rys. 1a). Ponieważ podczas walcowania występuje zmienna prędkość pasma stosowana jest zmienna intensywność chłodzenia. Jest to istotne ze względu na uzyskiwanie stabilnego w obszarze całego kręga udziału struktury ferrytycznej, który jest uzależniony od temperatury wytrzymywania w zakresie austenityczno-ferrytycznym oraz czasu tego wytrzymania (rys. 1b). Uzyskany materiał dwufazowy charakteryzuje się plastycznością, o której świadczą wyniki badań fraktograficznych zrywanych statycznie próbek. Przełom jest ciągliwy dołeczkowy (rys. 1c).

a) b) c)

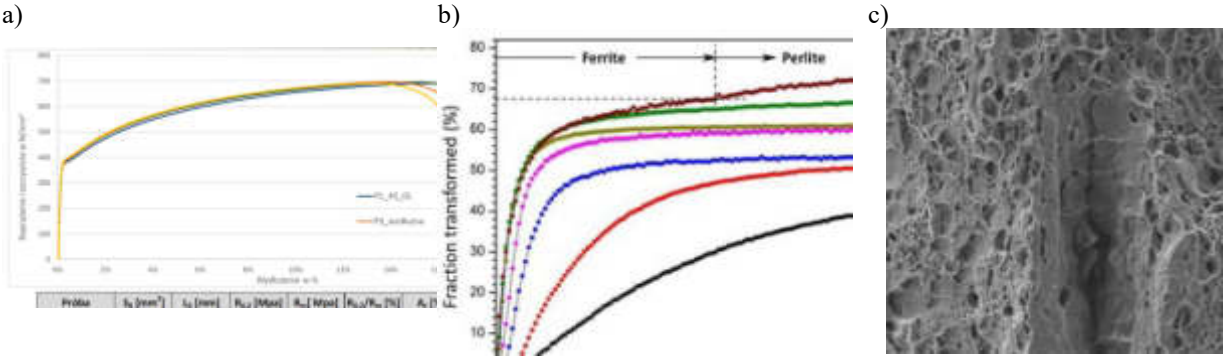

Rysunek 1. Przykładowe wyniki badań: a) wyniki próby rozciągania w trzech kierunkach b) stopień przemiany γ→α w zależności od czasu i temperatury wytrzymania w temperaturze międzykrytycznej [1], c) obraz przełomu po próbie rozciągania wykonany na elektronowym mikroskopie skaningowym.

4. SPOSTRZEŻENIA OGÓLNE

Wstępne badania procesu wytwarzania stali DP wskazują na małą anizotropię własności wytrzymałościowych. Jest to parametr istotny dla oceny podatności materiału na tłoczenie. Zdiagnozowano zakres możliwych czynników technologicznych wpływających na kształtowanie się mikrostruktury w blachach ze stali DP. Najbardziej istotnym wydaje się kontrola procesu w zakresie wytrzymania materiału w obszarze temperatur międzykrytycznych. Jest to obszar tzw. chłodzenia laminarnego, którego optymalizacja wydaje się jednym z najistotniejszych czynników kształtowania pożądanych własności blachy ze stali DP pod kątem podatności na procesy tłoczenia.

Podziękowania: Praca finansowana przez Ministerstwo Edukacji i Nauki w ramach V edycji doktoratów wdrożeniowych.

LITERATURA

1. Kairo de Barros Guimarães, Túlio Magno Füzessy de Melo, Dagoberto Brandão Santos, *Effect of cooling conditions after hot rolling on the microstructure and mechanical properties of a dual phase steel of 800 MPa strength*, “11th International Rolling Conference” 2019, vol. 11, 774-784.

MTS CONFERENCE
MATERIAL TECHNOLOGIES IN SILESIA

12-15.06.2022
Crystal Mountain***** Hotel, Wisła, Poland

Digital Image Correlation- method development, scope and principle of functioning, future goals

M. Kempny[a]

[a] Łukasiewicz Research Network Institute for Ferrous Mettalurgy, Silesian University of Technology, Faculty of Mechanical Engineering, Laboratory of Nanotechnology and Materials Science and Technology
email: mkempny@imz.pl , mkempny@polsl.pl

Abstract: This paper presents the basics of the Digital Image Correlation System, presents the algorithm of operation, method of data recording, and the method of implementation. In addition, the paper characterizes in detail the standard bench instrumentation necessary for the implementation of this type of measurement. The paper also describes the procedure of sample preparation and classifies the main methods of applying the marker to the surface of the sample. The paper highlights the main advantages of the system, the main difficulties associated with its operation and indicates the important parameters affecting the quality of the measurement. The paper shows the wide range of applications of Digital Image Correlation (DIC) and the possibilities of cooperation with other measurement systems as well as extended versions of the system such as Digital Volumetric Correlation. The paper also outlines further directions for the development of the DIC research methodology including, among others, extending the temperature range in which the method can be applied as well as increasing the speed of camera image registration. Such modifications will allow the image correlation method to be used for research where it has not been possible to apply DIC to date.

Keywords: Digital Image Correlation, Digital Volume Correlation, non-destructive tests, research methodology

BIBLIOGRAPHY

[1] W. Zielecki, A. Kubit, Ł. Święch Wydział Budowy Maszyn Lotnictwa, and P. Rzeszowska, "Analiza doświadczalna odkształcenia elementów klejonych w próbie statycznego oddzierania," 2013.

[2] D. Rama Seshu, C. Manjula, T. D. G. Rao, and C. B. K. Rao, "A new way of using welded wire mesh [wwm] for enhancing the shear strength in reinforced concrete beams," *Cem. Wapno, Bet.*, vol. 2020, no. 3, pp. 188–197, 2020, doi: 10.32047/CWB.2020.25.3.3.

[3] H. Gao, G. Agarwal, M. Amirthalingam, M. J. M. Hermans, and I. M. Richardson, "Investigation on hot cracking during laser welding by means of experimental and numerical methods," *Weld. World*, vol. 62, no. 1, pp. 71–78, 2018, doi: 10.1007/s40194-017-0524-z.

[4] W. Wang *et al.*, "A new method combining finite element analysis and digital image correlation to assess macroscopic mechanical properties of dentin," *Materials (Basel).*, vol. 8, no. 2, pp. 535–550, 2015, doi: 10.3390/ma8020535.

[5] M. van Rooyen, T. Becker, J. Westraadt, and G. Marx, "Creep damage assessment of ex-service 12% Cr power plant steel using digital image correlation and quantitative microstructural evaluation," *Materials (Basel).*, vol. 12, no. 19, 2019, doi: 10.3390/ma12193106.

[6] P. Qi, G. Wang, Z. Gao, X. Liu, and W. Liu, "Measurements of temperature distribution for high temperature steel plates based on digital image correlation," *Materials (Basel).*, vol. 12, no. 20, 2019, doi: 10.3390/ma12203322.

[7] G. Tozzi, M. P. Fernández, S. Davis, A. Karali, A. P. Kao, and G. Blunn, "Full-field strain uncertainties and residuals at the cartilage-bone interface in unstained tissues using propagation-based phase-contrast XCT and digital volume correlation," *Materials (Basel).*, vol. 13, no. 11, pp. 1–15, 2020, doi: 10.3390/ma13112579.

[8] S. Tavana, J. N. Clark, N. Newell, J. D. Calder, and U. Hansen, "In vivo deformation and strain measurements in human bone using digital volume correlation (Dvc) and 3t clinical mri," *Materials (Basel).*, vol. 13, no. 23, pp. 1–15, 2020, doi: 10.3390/ma13235354.

[9] Y. Wang, K. Ueda, R. Nagao, and S. Tsutsumi, "Measurements Using DIC and XRD," *Materials (Basel).*, vol. 14, no. 19, pp. 1–11, 2021.

[10] G. Li, J. Gu, Z. Ren, F. Zhao, and Y. Zhang, "Damage evaluation of concrete under uniaxial compression based on the stress dependence of ae elastic wave velocity combined with DIC technology," *Materials (Basel).*, vol. 14, no. 20, 2021, doi: 10.3390/ma14206161.

[11] W. Song and J. E. Houston, "Local deformation and Mn-C short-range ordering in a high-Mn Fe-18Mn-0.6C steel," *Metals (Basel).*, vol. 8, no. 5, 2018, doi: 10.3390/met8050292.

[12] S. Chakraborty, J. Indeck, P. Steinmetz, J. Friess, K. Hazeli, and A. L. Genau, "Localized strain analysis of ce-and mg-treated cast iron under uniaxial compression," *Metals (Basel).*, vol. 10, no. 12, pp. 1–10, 2020, doi: 10.3390/met10121638.

[13] V. V. Skripnyak and V. A. Skripnyak, "Localization of plastic deformation in ti-6al-4v alloy," *Metals (Basel).*, vol. 11, no. 11, 2021, doi: 10.3390/met11111745.

[14] G. Borstnar, F. Gillard, M. N. Mavrogordato, I. Sinclair, and S. M. Spearing, "Three-dimensional deformation mapping of Mode i interlaminar crack extension in particle-toughened interlayers," *Acta Mater.*, vol. 103, pp. 63–70, 2016, doi: 10.1016/j.actamat.2015.09.059.

[15] K. Genovese, L. Casaletto, J. D. Humphrey, and J. Lu, "Digital image correlation-based point-wise inverse characterization of heterogeneous material properties of gallbladder in vitro," *Proc. R. Soc. A Math. Phys. Eng. Sci.*, vol. 470, no. 2167, 2014, doi: 10.1098/rspa.2014.0152.

[16] S. N. Grama, S. J. Subramanian, and F. Pierron, "On the identifiability of anand visco-plastic model parameters using the virtual fields method," *Acta Mater.*, vol. 86, pp. 118–136, 2015, doi: 10.1016/j.actamat.2014.11.052.

[17] K. A. Kasvayee, E. Ghassemali, K. Salomonsson, S. Sujakhu, S. Castagne, and A. E. W. Jarfors, "Strain localization and crack formation effects on stress-strain response of ductile iron," *Mater. Sci. Eng. A*, vol. 702, no. Dic, pp. 265–271, 2017, doi: 10.1016/j.msea.2017.07.018.

[18] K. Karolewska, B. Ligaj, and D. Boroński, "Strain analysis of Ti6Al4V titanium alloy samples using digital image correlation," *Materials (Basel).*, vol. 13, no. 15, pp. 1–19, 2020, doi: 10.3390/ma13153398.

[19] D. Marcinczak Wzmacnianie konstrukcji betonowych za pomocą materiałów kompozytowych. Nauka i Budownictwo nr.66 luty 2019

MTS CONFERENCE
MATERIAL TECHNOLOGIES IN SILESIA

12-15.06.2022
Crystal Mountain***** Hotel, Wisła, Poland

A Short Survey on 3D Printed Auxetic Materials

A. Kloc-Ptaszna[a]

[a] Silesian University of Technology, Faculty of Mechanical Engineering, Department of Engineering Materials and Biomaterials
email: anna.kloc@polsl.pl

Abstract: The purpose of this article is to provide the reader with basic information on auxetic materials produced by 3D printing technology. Most materials have a positive Poisson's ratio, meaning that they get thinner when stretched and fatter when compressed. Auxetic materials are characterized by a Poisson's ratio less than zero, meaning that they get fatter when stretched and thinner when compressed. Because of their unusual properties, auxetic materials are a very attractive research subject. The article begins by giving definitions of auxetic materials. Then, Then, shows the basic auxetic structures produced using 3D printing. Finally, applications and research perspectives of the materials considered are discussed.

Keywords: Auxetic materials, Additive Manufacturing (AM), 3D printing, Negative Poisson's Ratio (NPR)

1. INTRODUCTION

Additive manufacturing (AM), also known as 3D printing or additive technology, has seen incredible popularity in recent years. In the most general terms, AM can be defined as the printing of components layer by layer to create an object. The simplicity and accessibility of this type of technology have made additive manufacturing more important and popular than ever. Because the range of applications for this reliable technique is unlimited, AM can be used by anyone with imagination and access to the necessary equipment. With additive manufacturing, materials' specific mechanical or physical properties can be obtained that would be difficult or impossible to achieve with traditional manufacturing methods. Therefore, the potential of this technique to produce new materials with unusual properties has been recognized. Because in recent years there has been an interest among researchers in printing auxetic materials, the most important information on these types of materials will be presented below [3].

1.1. Auxetic Materials

Auxetic materials are rational man-made structures characterized by a Negative Poisson's Ratio (NPR). When subjected to axial tension, specimens made from such materials behave differently from most materials that have a positive Poisson ratio. When a specimen is axially stretched, its cross-sectional dimension should decrease because the Poisson's ratio, interpreted as the negative ratio of the relative change in the body's cross-sectional dimensions to its relative elongation. However, in the case of auxetic materials, the opposite is true. That is, in at least one direction, the cross-sectional dimension of a sample made of an auxetic material increases in tension, while it decreases in compression [4].

Properties are highly dependent on microstructural geometry. Auxetic materials are usually modeled using the Finite Element Method (FEM). However, only for selected microstructures, comparisons were made between analytical results and experimental results. To fully compare the mechanical properties of each of them, more experimental studies need to be performed. Once actual data are collected, it will be possible to fabricate new auxetic materials, which have not yet been investigated [8].

Manufacturing auxetic materials is not easy because of their complex microstructure and structural geometries. Specialized manufacturing processes are required to produce such complex structures. Such processes should enable the required dimensional accuracy of the product to be achieved, reduce material losses, and speed up production. Therefore, it is extremely beneficial to manufacture auxetic structures using incremental manufacturing (AM) techniques. Using AM techniques, a structure can be built with extreme precision and

accuracy according to the designed geometry. On the basis of the literature review, it can be seen that the development of AM techniques in the fabrication of auxetic structures has been gradual. Both two- and three-dimensional auxetic structures have been fabricated using AM Techniques. In article [3], valuable information is provided on the applications, limitations, and prospects of AM for auxetic materials. Figure 1 shows the basic auxetic structures produced by 3D printing [6].

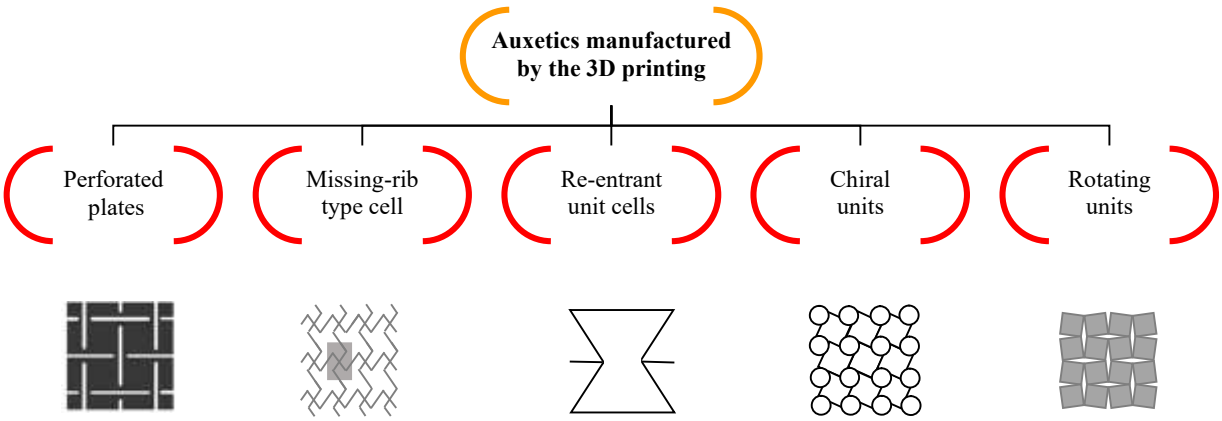

Figure 1. Classification of auxetic structure manufactured by 3D printing [6]

In recent years, the remarkable properties of auxetic materials and their wide range of potential applications have begun to be recognized. An example is Nike, which in 2016 launched a running shoe with a sole made of auxetics material. The solution was found to allow the athletes to move more naturally. The auxetic material sole is said to allow better control of the foot than of the shoe. The use of auxetic materials in sport is thought to be more about shock absorption than grip and friction. These materials can be used in a wide range of sports, from tennis racket grips to pads, gloves, helmets, and even mats [2]. In addition to sports applications, auxetic materials can also be used in medical industries, such as prosthetics, orthotics, ergonomic appliances, performance enhancement devices, in vitro medical devices to interact with cells, and advanced medicinal clinical products, especially tissue engineering scaffolds with living cells [1,3-7]. Because of their unusual properties, auxetic materials are a very attractive research subject.

BIBLIOGRAPHY

1. Y.J. Choo, M. Boudier-Revéret, M.C. Chang, 3D printing technology applied to orthosis manufacturing: narrative review, Ann Palliat Med. 2020 Nov;9(6):4262-4270. doi: 10.21037/apm-20-1185.
2. O. Duncan, T. Shepherd, C. Moroney, L. Foster, P.D. Venkatraman, K. Winwood, T. Allen, A. Alderson, Review of auxetic materials for sports applications: expanding options in comfort and protection, Appl. Sci.-Basel, 8 (6) (2018), doi.org/10.3390/app8060941.
3. A. Joseph, V. Mahesh, D. Harursampath, On the application of additive manufacturing methods for auxetic structures: a review. Adv Manuf. 2021;9(3):342-368. doi: 10.1007/s40436-021-00357-y.
4. T. C. Lim, Auxetic materials and structures (Vol. 2779). Singapore: Springer 2015.
5. V.A. Lvov, F.S. Senatov, A.A. Veveris, V.A. Skrybykina, A. Díaz Lantada, Auxetic Metamaterials for Biomedical Devices: Current Situation, Main Challenges, and Research Trends. Materials (Basel). 2022 Feb 15;15(4):1439. doi: 10.3390/ma15041439.
6. A. V. Mazaev, O. Ajeneza, M V Shitikova, Auxetics materials: classification, mechanical properties and applications, IOP Conf. Series: Materials Science and Engineering 747 (2020) doi:10.1088/1757-899X/747/1/012008.
7. W. Wang, Y. Xiong, R. Zhao, X. Li, W. Jia, A novel hierarchical biofunctionalized 3D-printed porous Ti6Al4V scaffold with enhanced osteoporotic osseointegration through osteoimmunomodulation, J Nanobiotechnology. 2022 Feb 5;20(1):68. doi: 10.1186/s12951-022-01277-0.
8. J. Zhang, G. Lu, Z. You, Large deformation and energy absorption of additively manufactured auxetic materials and structures: A review. Composites Part B: Engineering 201 (2020). doi.org/10.1016/j.compositesb.2020.108340.

MTS CONFERENCE
MATERIAL TECHNOLOGIES IN SILESIA

12-15.06.2022
Crystal Mountain***** Hotel, Wisła, Poland

Properties and microstructure of low-carbon steel processed by the novel hybrid SPD method

K. Kowalczyk[a], M.B. Jabłońska, I. Bednarczyk, M. Tkocz[a], S. Rusz[b]

[a] Silesian University of Technology, Faculty of Materials Engineering, Department of Material Technologies
email: karolina.kowalczyk@polsl.pl
[b] Technical University of Ostrava VSB, Faculty of Mechanical Engineering

Abstract: This paper presents results the influence of severe plastic deformation on the evolution of structure and mechanical properties of low-carbon steel. The commercial DC01 steel was deformed at a room temperature with unconventional SPD process - dual rolls equal channel extrusion (DRECE). Mechanical properties and structure of ferritic steel in initial state and after selected steps of deformation were investigated.

Keywords: SPD process, steel, microstructure, mechanical properties

1. INTRODUCTION

Dual Rolls Equal Channel Extrusion (DRECE) is an unconventional severe plastic deformation (SPD) process that can effectively produce the ultrafine-grained microstructure in metals and alloys. The material in the form of a sheet or strip is introduced into the working space by means of the main roll and the supporting rolls and then pressed through the shaping tool with the given α angle. The upper support and the upper fitting ensure the correct movement of the strip between the rollers during the process. The shaping process is based on the extrusion technology with zero reduction of strip's thickness while achieving a high degree of deformation in the material being formed. Multiple plastic deformations carried out this way determine the change of the structure and mechanical properties in relation to the initial material.

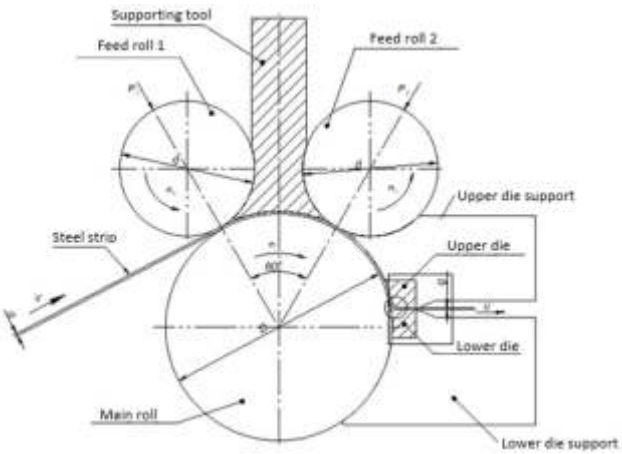

Figure 1. Schematic representation of the DRECE device

The strength of the DRECE-processed low-carbon ferritic steel strips increased with an increase in the number of passes. The most distinct material strengthening was obtained after the first pass. In the further passes, it was less intensive. After 7 DRECE passes the yield strength of 475 MPa and the ultimate tensile strength of 483 MPa were reached, which are significantly higher than the corresponding strength values characterizing the material at the initial state (180 MPa and 316 MPa, respectively).

Processing DC01 steel by DRECE causes distortion of the grain boundary lines and the formation of faults in comparison to the boundary lines observed in the material in the initial state. Such a phenomenon may be a consequence of the development of shear bands. The intensification of micro-shear bands development and their mutual intersection as a result of severe plastic deformation and high shear deformation leads to the fragmentation of the grain into smaller volumes and, consequently, to the formation of an ultra-fine grain structure.

Table 1. Mechanical properties of the investigated steel in the initial state and after the DRECE process

Condition	UTS, MPa	YS, MPa	El, %	UE, %
Initial state	316 ± 6	180 ± 5	47 ± 4	21 ± 2
After 1 DRECE pass	393 ± 10	387 ± 8	14 ± 4	1.2 ± 0.1
After 4 DRECE passes	430 ± 6	411 ± 8	9 ± 3	1,1 ± 0,1
After 7 DRECE passes	483 ± 3	475 ± 9	9 ± 5	1,1 ± 0,2

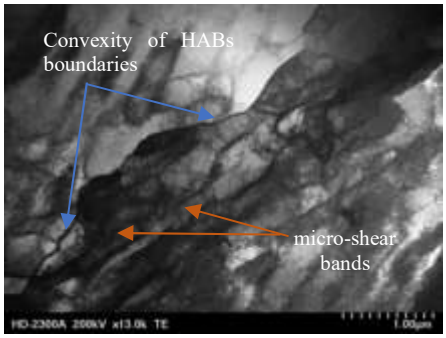

Figure 1. STEM photographs of the DC01 steel microstructure after 4 DRECE passes

Acknowledgments: The financial support of the National Science Center, Poland, is gratefully acknowledged, grant no. 2018/31/N/ST8/03134.

BIBLIOGRAPHY

1. S. Rusz, A. Kłyszewski, M. Salajka, O. Hilser, L. Cizek, M. Klos M, Possibilities of application methods DRECE in forming of non – ferrous metals. Arch. Metall. Mater. 60: 3011–3016; 2015
2. S. Rusz S, L. Cizek, V Michenka, J. Dutkiewicz J, M. Salajka, O. Hilsner, S. Tylsar, J. Kedron, M. Klos, New type of device for achievement of grain refinement in metal strip. Adv. Mater. Res. 1127: 91-97; 2015
3. M.B. Jabłońska, K. Kowalczyk, M. Tkocz, T. Bulzak, Dual rolls equal channel extrusion as unconventional SPD process of the ultralow-carbon steel: finite element simulation, experimental investigations and microstructure analysis. Arch. Civ. Mech. Eng. 2021
4. R. Preistner, A.K. Ibraheem, Processing of steel ultrafine ferrite grain structures. J. Mater. Sci. Tech. 16: 1267–1278; 2000
5. O. Saray, G. Purcek, I. Karaman, T. Neidorf, H.J Maier, Equal channel angular sheet extrusion of interstitial-free: microstructural evolution and mechanical properties. Mater. Sci. Eng. A.528: 6573-6583; 2011

MTS CONFERENCE
MATERIAL TECHNOLOGIES IN SILESIA

12-15.06.2022
Crystal Mountain***** Hotel, Wisła, Poland

Wpływ obniżonych oraz podwyższonych temperatur odkształcenia na intensywność efektu TWIP w stali wysokomanganowej

A. Kozłowska[a], A. Grajcar[a], P. Stawarczyk[b], K. Radwański[b]

[a] Politechnika Śląska, Wydział Mechaniczny Technologiczny, Katedra Materiałów Inżynierskich i Biomedycznych
email: aleksandra.kozlowska@polsl.pl; adam.grajcar@polsl.pl
[b] Sieć Badawcza Łukasiewicz – Instytut Metalurgii Żelaza w Gliwicach
email: piotr.stawarczyk@imz.pl; krzysztof.radwanski@imz.pl

Streszczenie: Stale wysokomanganowe wykazujące efekt TWIP (Twinning Induced Plasticity) zawierające 18-30% wag. Mn charakteryzują się szczególnie korzystnym połączeniem wytrzymałości i plastyczności, co umożliwia projektowanie lżejszych i zarazem bardziej bezpiecznych konstrukcji samochodów i innych środków transportu. Intensywność efektów strukturalnych determinujących własności mechaniczne tego typu stali jest zależna od temperatury odkształcenia. Czynnik temperaturowy występuje podczas kształtowania technologicznego blach oraz jest generowany podczas ich odkształcenia w trakcie ewentualnej kolizji drogowej z dużą szybkością. Celem pracy jest określenie wpływu temperatur odkształcenia w zakresie od -40°C do 200°C na intensywność efektu TWIP w stali wysokomanganowej typu X4MnSiAlNbTi27-4-2. Szczegółowych obserwacji mikrostruktury próbek w stanie wyjściowym oraz odkształconych w statycznej próbie rozciągania w zróżnicowanych temperaturach dokonano przy zastosowaniu skaningowego mikroskopu elektronowego (SEM) oraz metody dyfrakcji elektronów wstecznie rozproszonych EBSD. Zaobserwowano, że stal w stanie wyjściowym charakteryzuje się jednorodną strukturą austenityczną z ziarnami wydłużonymi zgodnie z kierunkiem walcowania. Odnotowano także występowanie bliźniaków wyżarzania. Próbki odkształcone w temperaturach z zakresu -40°C-200°C charakteryzowały się występowaniem bliźniaków odkształcenia oraz pasm poślizgu o intensywności zależnej od temperatury odkształcenia. Dokonano ilościowej analizy wkładu bliźniakowania mechanicznego w całkowite umocnienie stali.

Słowa kluczowe: stal wysokomanganowa, temperatura odkształcenia, bliźniakowanie mechaniczne, stal dla motoryzacji

1. WPROWADZENIE

Stale wysokomanganowe wykazują wysoki potencjał aplikacyjny w przemyśle motoryzacyjnym. Stale tego typu charakteryzują się wysokimi własnościami wytrzymałościowymi (R_m = 900-1200 MPa) przy zachowaniu dobrej plastyczności (A = 40-60%), co predysponuje ich zastosowanie na konstrukcje energochłonne samochodów osobowych [1, 2]. Własności mechaniczne stali wysokomanganowych są ściśle zależne od dominującego mechanizmu umocnienia występującego podczas odkształcenia plastycznego. W stalach typu TWIP (Twinning Induced Plasticity) tworzą się bliźniaki mechaniczne, które stanowią przeszkody dla ruchu dyslokacji. W literaturze [3, 4] zjawisko to nazywane jest dynamicznym efektem Halla-Petcha, który skutkuje zwiększeniem szybkości umocnienia odkształceniowego stali, prowadząc do uzyskania korzystnych własności mechanicznych. W stalach wysokomanganowych może występować również efekt TRIP (Transformation Induced Plasticity), który jest związany z przemianą austenitu w martenzyt ε lub α' podczas odkształcenia plastycznego [5].

Na dominujący mechanizm umocnienia występujący w stalach wysokomanganowych silnie wpływa wartość EBU, która jest zależna od składu chemicznego stali oraz temperatury odkształcenia [6, 7]. Efekt TRIP jest dominujący dla EBU <25 mJ/m^2. Dla EBU w zakresie od 25 do 60 mJ/m^2, dominującym mechanizmem umocnienia jest efekt TWIP. W przypadku gdy wartość EBU jest większa niż 60 mJ/m^2, dominuje poślizg dyslokacji. Wzrost temperatury odkształcenia powoduje, że dominujący mechanizm umocnienia zmienia się

z efektu TRIP na efekt TWIP [8]. Dla wysokich temperatur odkształcenia intensywność efektów TWIP oraz TRIP może być w znacznym stopniu zredukowana lub mogą one zostać całkowicie zastąpione przez poślizg dyslokacji, co prowadzi do zmniejszenia własności mechanicznych stali. Shterner i in. [9] odnotowali, że wzrost temperatury odkształcenia stali typu Fe-0.6C-18Mn-1Al wykazującej efekt TWIP istotnie wpłynął na ewolucję mikrostruktury badanej stali. Konsekwencją realizacji odkształcenia plastycznego w podwyższonych temperaturach było znaczne obniżenie własności mechanicznych. Najbardziej korzystny zespół własności mechanicznych uzyskano dla próbek odkształconych w temperaturze pokojowej. Asghari i in. [10] dokonali klasyfikacji mechanizmów odkształcenia w stali typu Fe-0.07C-18Mn-2Si-2Al w zależności od temperatury odkształcenia. Efekt TRIP stanowił główny mechanizm umocnienia odkształceniowego stali w zakresie temperatury 25°C-200°C. W przypadku temperatur 200°C-300°C dominowało bliźniakowanie mechaniczne. Powyżej 700°C zaobserwowano występowanie efektów aktywowanych cieplnie takich jak zdrowienie dynamiczne oraz rekrystalizacja. Salas-Reyes i in. [11] zaobserwowali, że realizacja odkształcenia plastycznego w podwyższonych temperaturach może prowadzić do lokalnych zmian składu chemicznego na skutek powstawania wydzieleń, co istotnie wpływa na wartość EBU.

Skład chemiczny stali wysokomanganowych typu TWIP powinien być zaprojektowany w taki sposób, aby w zakresie temperaturowym ich eksploatacji uzyskać maksymalną intensywność bliźniakowania mechanicznego. Do tej pory badania stali wysokomanganowych dotyczyły głównie odkształcenia plastycznego w temperaturze pokojowej. Nadal niewiele jest kompleksowych doniesień dotyczących wpływu temperatur obniżonych oraz podwyższonych na ewolucję mikrostruktury stali wysokomanganowych. Biorąc pod uwagę powyższe, celem pracy było określenie wpływu temperatury odkształcenia w zakresie -40°C-200°C na intensywność bliźniakowania mechanicznego w stali typu X4MnSiAlNbTi27-4-2. Dokonano szczegółowych obserwacji mikrostruktury przy zastosowaniu skaningowego mikroskopu elektronowego (SEM) oraz przeprowadzono analizę ilościową intensywności bliźniakowania w poszczególnych temperaturach odkształcenia przy zastosowaniu metody dyfrakcji elektronów wstecznie rozproszonych (EBSD).

Podziękowania: Praca wykonana i finansowana w ramach grantu Narodowego Centrum Nauki, nr 2017/27/B/ST8/02864.

BIBLIOGRAFIA

1. J.K. Kim, M.H. Kwon, B.C. De Cooman, On the deformation twinning mechanisms in twinning-induced plasticity steel, Acta Materialia 141 (2017) 444–455.
2. M.B Jabłońska, K. Kowalczyk, Microstructural aspects of energy absorption of high manganese steels. Procedia Manufacturing 27 (2019) 91–97.
3. O. Bouaziz, S. Allain, C. Scott, Effect of grain and twin boundaries on the hardening mechanisms of twinning-induced plasticity steels, Scripta Materialia 58 (2008) 484–487.
4. M. Opiela, G. Fojt-Dymara, A. Grajcar, W. Borek, Effect of grain size on the microstructure and strain hardening behavior of solution heat-treated low-C high-Mn steel, Materials 13 (2020) 1489.
5. Q. Xie, Z. Pei, J. Liang, D. Yu, Z. Zhao, P. Yang, R. Li, M. Eisenbach, K. An, Transition from the twinning induced plasticity to the γ–ε transformation induced plasticity in a high manganese steel, Acta Materialia 161 (2018) 273–284.
6. J. Kowalska, J. Ryś, G. Cios, W. Bednarczyk, The effect of reduced temperatures on microstructure development in tensile tested high-manganese steel, Materials Science and Engineering A 767 (2019) 138406.
7. X. Li, L. Chen, Y. Zhao, R.D.K. Misra, Influence of manganese content on ε-/α′-martensitic transformation and tensile properties of low-C high-Mn TRIP steels, Materials and Design 142 (2018) 190–202.
8. S. Curtze, V.T. Kuokkala, Dependence of tensile deformation behavior of TWIP steels on stacking fault energy, temperature and strain rate, Acta Materialia 58 (2010) 5129–5141.
9. V. Shterner, I.B. Timokhina, H. Beladi, On the workhardening behaviour of a high manganese TWIP steel at different deformation temperatures, Materials Science and Engineering A 669 (2016) 437–446.
10. A. Asghari, A. Zarei-Hanzaki, M. Eskandari, Temperature dependence of plastic deformation mechanisms in a modiGed transformation-twinning induced plasticity steel, Materials Science and Engineering A 579 (2013) 150–156.
11. A.E. Salas-Reyes, I. Mejia, A. Bedolla-Jacuinde, A. Boulaajaj, J. Calvo, J.M. Cabrera, Hot ductility behavior of highMn austenitic Fe–22Mn–1.5Al–1.5Si–0.45C TWIP steels microalloyed with Ti and V, Materials Science and Engineering A 611 (2014) 77–89.

MTS CONFERENCE
MATERIAL TECHNOLOGIES IN SILESIA

12-15.06.2022
Crystal Mountain***** Hotel, Wisła, Poland

Kształtowanie mikrostruktury i właściwości fazy β stopu tytanu

J. Krawczyk[a,*], J. Ryś[a], M. Madej[a], J. Augustyn-Nadzieja[a], M. Goły[a], J. Kowalska[a], M. Witkowska[a], Ł. Frocisz[a], P. Matusiewicz[a], A. Radziszewska[a], W. Borek[b]

[a] AGH Akademia Górniczo-Hutnicza, Wydział Inżynierii Metali i Informatyki Przemysłowej, al. A. Mickiewicza 30, 30-059 Kraków,
[b] Politechnika Śląska, Wydział Mechaniczny Technologiczny, ul. Konarskiego 18A, 44-100 Gliwice
email: jkrawcz@agh.edu.pl

Abstrakt:
Przedstawiono zmiany mikrostruktury w stopie tytanu β. Badania prowadzono dla warunków odkształcenia w zakresie których w mikrostrukturze stopu występowała tylko faza β o strukturze krystalograficznej RPC. W przypadku odkształcenia na zimno stosowano materiał w stanie przesyconym, natomiast w przypadku odkształcania na gorąco stosowano przesycanie po odkształceniu aby zapobiec wydzielaniu się fazy α. Pozwoliło to określić procesy odkształcenia, zdrowienia oraz rekrystalizacji dynamicznej i statycznej w strukturze RPC stopu tytanu. Określono niejednorodność odkształcenia oraz przebieg procesów zdrowienia i rekrystalizacji oraz odnieść te procesy do zmiany twardości jak i umocnienia materiału podczas odkształcenia. Zastosowano różne sposoby odkształcania: spęczanie, rozciąganie oraz walcowanie pielgrzymowe.

Słowa kluczowe: stop tytanu β, niejednorodność odkształcenia plastycznego, zdrowienie, rekrystalizacja, umocnienie

1. WPROWADZENIE

Stopy tytanu β lub bliskie β są istotne jako materiał konstrukcyjny. Z tego względu istotnym jest poznanie procesów kształtowania ich mikrostruktury celem kształtowania własności mechanicznych. Prowadzone są więc nadal badania naukowe [1], które mogą stanowić podstawę dla projektowania procesów technologicznych w sposób pozwalający uzyskać pożądane właściwości mechaniczne. Dodatkowo poznanie procesów kształtowania się mikrostruktury oraz umocnienia materiału pozwala na wskazanie tzw. okien procesowych pozwalających na prowadzenie odkształcenia plastycznego materiału w zakresie jego stabilności płynięcia [2]. Należy to wiązać z zagadnieniem tzw. dyssypacji energii [2].

2. MATERIAŁ DO BADAŃ

Materiałem badawczym był stop tytanu bliski β Ti3Al8V6Cr4Zr4Mo. Do badań dla materiału w stanie dostawy (zestarzonego), który był nagrzewany do zakresu występowania fazy β, celem uzyskania jednorodnej struktury β, materiał wyżarzano w temperaturze 950°C przez 1 godzinę. Następnie materiał intensywnie chłodzono w wodzie aby uzyskać przesycenie, w wyniku którego w materiale występowało jedynie równoosiowe ziarno fazy β.

3. SKRÓT WYNIKÓW BADAŃ

Odkształcenie plastyczne na zimno skutkuje powstawaniem niejednorodności w postaci pasm ścinania oraz podziałem na podziarna (rys. 1a). Rozwój mikrostruktury odkształcenia rozwija się w kolejności ze zwiększeniem jego stopnia poprzez: pojedyncze systemy poślizgu, liczniejsze systemy poślizgu, uwidocznienie podziarn, zanikanie granic ziarn, pasma odkształcenia, pasma ścinania (rys. 1b). Procesy zdrowienia a zwłaszcza

rekrystalizacji dynamicznej skutkują sekwencyjnym umacnianiem i osłabianiem się materiału (rys. 1c). Rekrystalizacja inicjuje się w obszarach niejednorodności odkształcenia (rys. 1d). Próbka podczas odkształcenia ulega niejednorodnemu umocnieniu w jej obszarze a na ten proces wpływa selektywna rekrystalizacja dynamiczna (rys. 1e). Rekrystalizacja statyczna po odkształceniu jest uzależniona od stopnia odkształcenia oraz warunków wyżarzania, natomiast stopy tytanu podatne są na stabilizujące fazę α oddziaływanie tlenu z powietrza (rys. 1f).

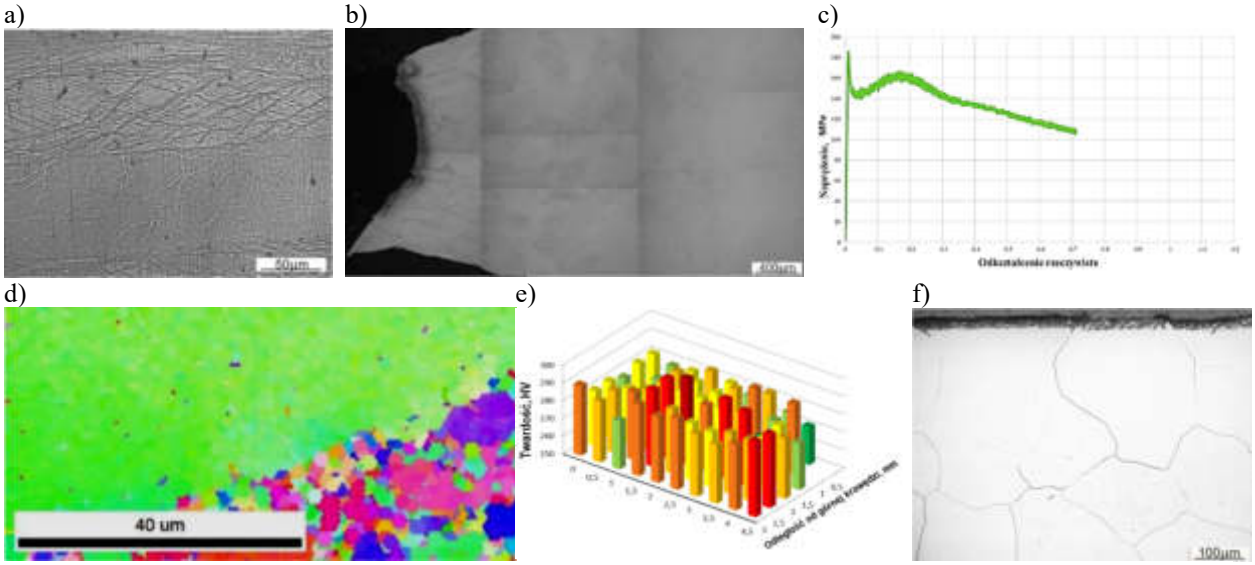

Rysunek 1. Przykładowe wyniki badań: a) mikrostruktura odkształcenia po walcowaniu pielgrzymowym na zimno (62% odkształcenia), b) mikrostruktura w obszarze szyjki po statycznej próbie rozciągania w temperaturze pokojowej, c) krzywa umocnienia podczas spęczania próbki na gorąco, d) badania EBSD procesu rekrystalizacji podczas spęczania próbki ze stopu tytanu bliskiego B w temperaturze 900°C, e) rozkład twardości na w reprezentatywnej ćwierci próbki po spęczaniu na gorąco, f) mikrostruktura po rekrystalizacji próbki po rozciąganiu z widocznym efektem powstawania fazy α przy powierzchni w efekcie działania utleniającego powietrza.

4. SPOSTRZEŻENIA OGÓLNE

Odkształcenie plastyczne detali wykonanych ze stopu tytanu nie pozwala na uzyskanie jednorodnego zakresu umocnienia w całej objętości. Dostęp powietrza podczas kształtowania plastycznego na gorąco jak i wyżarzania rekrystalizującego skutkuje powstawaniem w warstwie wierzchniej fazy α. Dyssypacja energii odkształcenia na procesy zdrowienia i rekrystalizacji dynamicznej skutkuje sekwencyjną zmianą umocnienia materiału. Zakres zachodzenia procesu rekrystalizacji dynamicznej jest różny w objętości materiału i zachodzi w różnym czasie w zależności od obszaru w odkształcanej próbce.

Podziękowania: Praca została zrealizowana dzięki funduszom z grantu wewnętrznego Wydziału Inżynierii Metali i Informatyki Przemysłowej 16.16.110.663 zadanie nr 18.

LITERATURA

1. Sander B., Raabe D., Texture inhomogeneity in a Ti–Nb-based β-titanium alloy after warm rolling and recrystallization, Materials Science & Engineering A479, 1-2 (2008) 236-247
2. Lypchanskyi O., Śleboda T., Wojtaszek M., Muszka K., Łukaszek-Sołek A., Stanik R., Gude M.: The analysis of flow behavior of Ti-6Al-2Sn-4Zr-6Mo alloy based on the processing maps, International Journal of Material Forming10.1007/s12289-019-01533-z (2000)

MTS CONFERENCE
MATERIAL TECHNOLOGIES IN SILESIA

12-15.06.2022
Crystal Mountain***** Hotel, Wisła, Poland

Microstructure and properties of ultralight and ultrafine grained Mg-Li-Al alloy

M. Król

Silesian University of Technology, Faculty of Mechanical Engineering, Department of Engineering Materials and Biomaterials
email: mariusz.krol@polsl.pl

Abstract: In this work, the effect of TiB and Sr modifiers on the changes in the crystallization process, structure and mechanical properties of Mg-12Li-1.5Al cast alloys has been presented. Such properties as phase nucleation temperature, solidus temperature, amount of heat of crystallization, hardness and compressive strength have been analyzed. The influence of modifiers on grain size was also studied.
Keywords: Mg-Li alloy, grain modification, microstructure, mechanical properties

1. INTRODUCTION

Magnesium alloys are an interesting new generation engineering material, even though they have been known since the II World War. In recent years, there has been a growing interest in magnesium alloys, which are considered to be innovative engineering plastics.

Magnesium alloys are increasingly used in lightweight structures, especially in the aerospace industry. Weight reduction in means of transport brings savings in operating costs (mainly decrease in fuel consumption). Magnesium alloys have a low density of about ρ=1.8g/cm^3, high specific strength and low manufacturing costs. In addition, an important feature of magnesium and its alloys is a low coefficient of friction (μ=0.1). Modern magnesium alloys also have a good corrosion resistance, which can be further improved by applying appropriate coating treatment [1].

Interest in magnesium alloys for structural components for the aerospace industry dates back to the 1940s. Already during the II World War, when magnesium and its alloys were used mainly for military purposes, the world production of magnesium increased ninefold [2].

The alloys of the group Mg-Li are interesting due to their low lithium density. The density of alloys of this group, at a concentration of 14-16 wt.% Li reaches 1.35-1.45 g/cm^3. The reason why Mg-Li alloys are interesting structural materials is their low density while maintaining high strength. In addition to their high stiffness and low density, Mg-Li alloys also exhibit good machinability. One disadvantage of these materials is that they are much more chemically active than other Mg alloys [3].

a)

b)

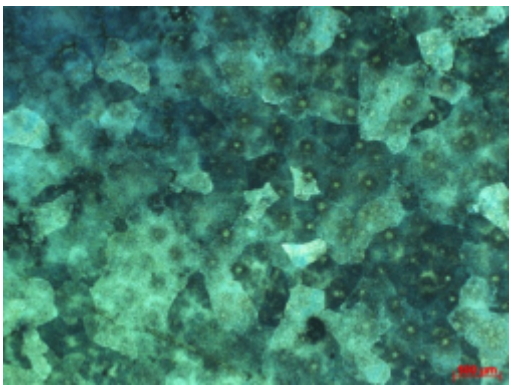

c) d)

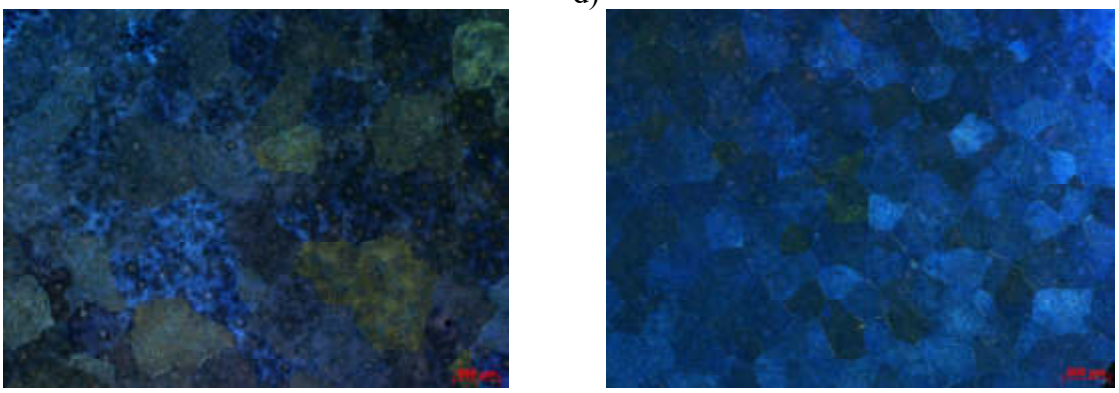

Figure 1. Microstructure of analysed alloys: a) Mg-12Li-1.5Al, b) Mg-12Li-1.5Al+0.2TiB, c) Mg-12Li-1.5Al+0.2Sr, d) Mg-12Li-1.5Al+0.2TiB+0.2Sr

a) b)

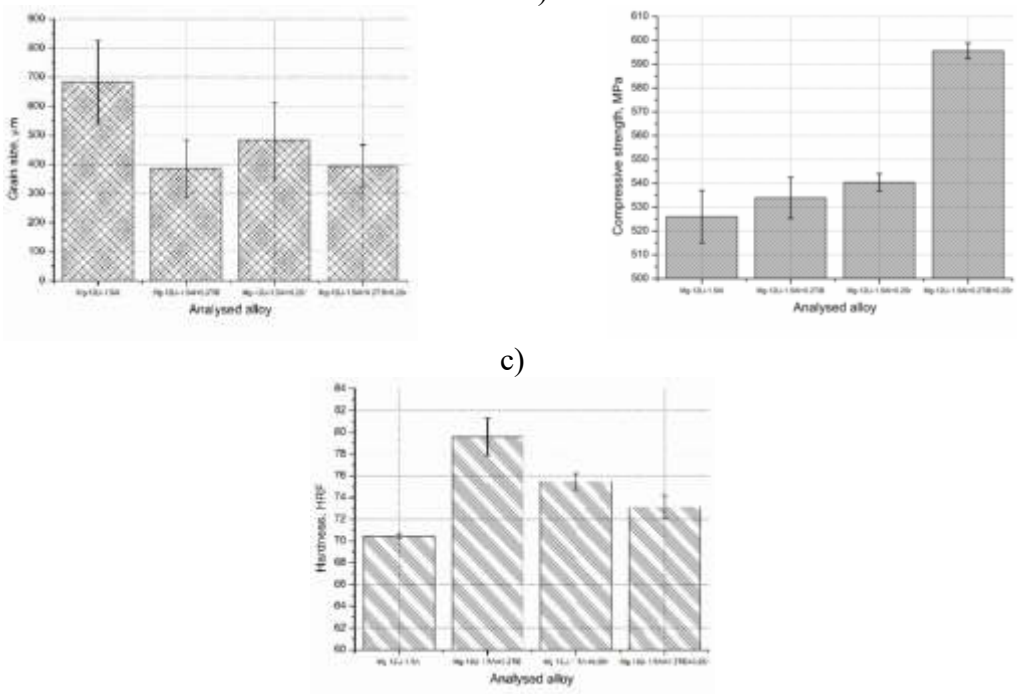

c)

Figure 2. Influence of TiB and Sr grain modifiers on Mg-Li alloys on a) grain size, b) compressive strength, and c) hardness

BIBLIOGRAPHY

1. M. Staszuk, Ł. Reimann, A. Ściślak, J. Jaworska, M. Pawlyta, T. Mikuszewski, D. Kuc, T. Tański, i A. Kriz, Investigations of TiO2, Ti/TiO2, and Ti/TiO2/Ti/TiO2coatings produced by ALD and PVD methods on Mg-(Li)-Al-RE alloys substrates, Bulletin of the Polish Academy of Sciences, Technical Sciences, 69/5 (2021) 1-10.
2. M. Gupta, N.M.L. Sharon, Magnesium Alloys and Magnesium Composites, John Wiley & Sons, New Jersy 2011.
3. M. Król, Magnesium-lithium alloys with TiB and Sr additions, Journal of Thermal Analysis and Calorimetry, 138/6 (2019) 4237-4245.

MTS CONFERENCE
MATERIAL TECHNOLOGIES IN SILESIA

12-15.06.2022
Crystal Mountain***** Hotel, Wisła, Poland

Thermal analysis of the drive nozzle cooling system using CAD software

Ł. Krzemiński[a], G. Matula[b]

a Silesian University of Technology, Faculty of Mechanical Engineering, Scientific and Didactic Laboratory of Nanotechnology and Material Technologies
email: lukasz.krzeminski@polsl.pl
b Silesian University of Technology, Faculty of Mechanical Engineering, Scientific and Didactic Laboratory of Nanotechnology and Material Technologies
email: grzegorz.matula@polsl.pl

Abstract: The operating conditions of the spraying or driving nozzles depend on the properties of the construction and material they are made of. The material properties of the nozzle structure determine the working temperature of the nozzle, the pressure in the combustion chamber and the geometry of the exhaust flame stream. Numerical analysis of thermal conditions in the nozzle with the use of protective coatings, active and passive cooling system allows for the construction and material design of the nozzle and optimization of the use of the driving medium. The use of cooling systems as well as thermal barriers can significantly affect the thermodynamic conditions of operation of the exhaust gas nozzle. The use of additive manufacturing technology can meet the challenges of producing the construction of nozzles with complex shapes determined by computer simulation of temperature conditions.

Keywords: materials, analysis, symulation, nozzle, thermal

1. INTRODUCTION

The material used in combustion engine drives requires materials resistant to aggressive chemical and thermall conditions. The corrosion of the material can be limited by changing the chemical composition or the use of special protective coatings. However, if the temperature of the part of the internal combustion nozzle exceeds the permitted values, the cooling of the constructional material should be increased. Cooling can be provided by removing heat from the nozzle material by heat conduction in the materials or the heat radiation emissions to the surrounding center. Depending on the possibility of expanding the structure of the internal combustion nozzle and the size of the cooling system, more extensive cooling systems can be used.

However, a change in combustion parameters in the drive nozzle or spraying can reduce the efficiency of the nozzle. The required pressure and temperature in the combustion chamber of the nozzle must be maintained to ensure adequate outlet speed of the operating gases.

Figure 1. Example of a propeller nozzle design. The view from the working gas supply side.

One method of decrease the temperature of the exhaust nozzle material is to use a cooling system. The heat emission from the nozzle material can be realized by transferring the heat to the enviroment or flowing coolant.

These two solutions of heat emission can be realized by the flow of the cooling medium through the structure of the nozzle or by enhacement the radiation surface on the outer surface of the nozzle. However, the formation of a geometrically complicated construction of the cooling channels in the body material is difficult to implement through conventionally methods e.g machining or casting. Complicated geometry of the cooling system can be produced by additive manufacturing method including SIntering Laser Meliting (SLM).

Creating cooling channels through which the coolant will flow is one of the solutions reducing the temperature of the nozzle material. The shape of the flow channels can be significantly expanded, thus increasing the contact surface of the cooling medium with the cooled material. The system of cooling channels can be straight or twisted several times, which allows to increase the amount of cooling agent flowing through the nozzle structure, as shown in the example below:

Figure 2. A cross-section of the model of the drive nozzle with cooling channels, produced by the SLM printing method (left) and the arrangement of the cooling channels in the model of the drive nozzle cooled by the coolant (right)

Dreceasing the nozzle material temperature can also be realized by the emission of heat in the form of radiation from the external surface. In order to intensify the emissivity and the amount of emitted energy, it should be create a radation structure thanks to the additive manufacturing technology.

Figure 3. The improvement of the nozzle surface cooling system by expanding the radiation surface with wavy or straight plates.

The developed models of cooling systems can be simulated in CAD software. The simulation was performed taking into account high temperature, pressure and flammable gas flow. As a result of analytical calculations, the efficiency of individual cooling system solutions was described. The temperature reduction of the inner surface of the nozzle material has been determined.

MTS CONFERENCE
MATERIAL TECHNOLOGIES IN SILESIA

12-15.06.2022
Crystal Mountain***** Hotel, Wisła, Poland

Marine propeller printed using the 3D Metal Printing technology (3DMP®) based on CuAl-based material

J. Kulasa[a], A. Kowalski[a], M. Krystowska[a], A. Brudny[a], M. Maleta[a], W. Burian[a], S. Neubert[b], M. Scafè[c], G. Magnani[c], E. Leoni[c], A. Tatì[d]

[a] Łukasiewicz Research Network – Institute of Non-Ferrous Metals, Centre of Advanced Materials Technologies
email: joanna.kulasa@imn.lukasiewicz.gov.pl
[b] GEFERTEC GmbH, Berlin, Germany
email: sebastian.neubert@gefertec.de
[c] Italian National Agency for New Technologies, Energy and Sustainable Economic Development (ENEA), Department for Sustainability, Division Sustainable Materials, Laboratory Material Technologies Faenza, Faenza Italy
email: matteo.scafe@enea.it
[d] Italian National Agency for New Technologies, Energy and Sustainable Economic Development (ENEA), Department for Sustainability, Division Sustainable Materials, Laboratory Chemical and Physical Technologies, Rome Italy
email: angelo.tati@enea.it

Abstract: The printing technology of prototype of propellers using Cu-based materials is presented. The WAAM printing of the prototype of propellers was performed with the complex machine systems from GEFERTEC GmbH. The CAD/CAM modelling was carried out with the in-house advanced multi-axis-deposition tool based on the Siemens-NX-platform. The prototypes of a marine propeller were printed at GEFERTEC GmbH by means of the 3DMP® technology. The printed elements were subjected to quality checks and tests including the X-Ray and Ultrasonic techniques which were used to investigate the defects and porosities in the objects.

Keywords: 3D printing technology, copper alloys, WAAM, NDT, marine equipment

1. INTRODUCTION

The main aim of the project was developing Cu-based wires as feedstock materials for the use in additive manufacturing and also developing printing technology of elements such as propellers. The components were manufactured by means of the 3D Metal Printing (3DMP®) process which belongs to the Wire Arc Additive Manufacturing (WAAM). The 3DMP® process is considered as alternative, competitive, and more environmentally friendly to presently used conventional metal processing technologies. The principle of the 3DMP® process is to make the final product layer-by-layer from the wire as a feedstock material. The result of the project is ready to implement 3DMP® technology for manufacturing corrosion resistant components, in particular marine propellers. Moreover, the developed materials and production technology can be used to manufacture other products in many branches of the industry

The main advantages of WAAM technology are lower investment costs, as well as shortening the production time by reducing the number of stages. In addition, the significant advantages of this technology include high deposition rate of successive layers of material (high efficiency of the 3DMP® process), possible reduction of the weight of elements, low material losses, and the possibility of reusing post-production waste (1-4).

The project proved that it is possible and viable to replace traditional manufacturing technologies with additive manufacturing successfully. The full-size five-blades prototype of the propeller was successfully printed and machined (Fig. 1.).

Figure 1. Printed and machined prototype of a propeller

The 3D printing technology (WAAM) is therefore an excellent alternative to the production of this type of elements in relation to the currently used casting technology and can be successfully used in the shipbuilding industry.

Acknowledgments: The research presented in this paper was conducted within the project (18072): *3DMPWire. Material-efficient Cu wire-based 3D printing technology* (2019-2021) and co-funded by EIT RawMaterials.

BIBLIOGRAPHY

1. S.W. Williams, F. Martina, A.C. Addison, J. Ding, G. Pardal, P. Colegrove, Wire + Arc Additive Manufacturing, Materials Science and Technology, Vol. 32, Iss.7, 641-647, 2016.
2. C. Dharmendra, B.S. Amirkhiz, A. Lloyd, G.D. Janaki Ram, M. Mohammadi, Wire-arc additive manufactured nickel aluminum bronze with enhanced mechanical properties using heat treatments cycles, Additive Manufacturing 36, 101510, 2020.
3. Laukik P. Raut, Ravindra V. Taiwade, Wire Arc Additive Manufacturing: A Comprehensive Review and Research Directions, Journal of Materials Engineering and Performance, 4768, Volume 30 (7), 2021.
4. Project 3DMPWIRE. Material-efficient Cu wire-based 3D printing technology, EIT RawMaterials, 2019-2021 (http://3dmpwire.com).

MTS CONFERENCE
MATERIAL TECHNOLOGIES IN SILESIA

12-15.06.2022
Crystal Mountain***** Hotel, Wisła, Poland

Microstructure and corrosion behaviour of Zn-Al-Mg alloy with addition of Sn

M. Kusý[a], Z. Gabalcová[a], H. Suchánek[a], P. Gogola[a]

[a] Slovak University of Technology, Faculty of Materials Science and Technology, Institute of Materials Science
email: martin.kusy@stuba.sk

Abstract: In this study, the addition of Sn in the range from 0.5 to 3 wt. % on the Zn 1.6 wt.% Al 1.6 wt.% Mg (Magizinc - MZ) alloy was studied. MZ alloy is mainly used as hot-dip coatings. Phase transformation temperatures and phase composition was investigated via differential scanning calorimetry (DSC), scanning electron microscopy (SEM) and x-ray diffraction (XRD) techniques. The main phases identified in the studied alloys were η(Zn) and α(Al) solid solutions as well as Mg_2Zn_{11}, $MgZn_2$ and Mg_2Sn intermetallic phases. The corrosion behaviour of these samples in salt spray testing was investigated. Samples with 0.5 wt.% of Sn showed overall the best corrosion properties outperforming even the pure MZ alloy. Use of MZ + 3.0Sn alloys could be considered only with an annealing treatment applied.

Keywords: materials, laser treatment, polimers

1. INTRODUCTION

Due to potential applications with increased temperature exposure (>300 °C), as-cast and annealed states of MZ alloys with addition of Sn in the range from 0.5, 1, 2 and 3 wt.% were investigated [1]. In line with results of related research data [2–4], phases expected to be formed are η(Zn) and α(Al) solid solutions as well as Mg_2Zn_{11}, $MgZn_2$ and Mg_2Sn intermetallic phases Additionally, the corrosion behaviour of these samples in salt spray testing was investigated [5]. The potential to form intergranular (IG) corrosion in Zn-Al-Mg coatings was indicated by various literature sources [6,7] and therefore inspected for an entire range of alloys.

2. RESULTS

The microstructures of as-cast samples can be observed in Figure 1. Annealing did not change the phase composition in a significant way compared to as-cast samples. On the other side, microstructure appearance of annealed samples changes with increasing Sn content, which allowed gradually a more effective spheroidization and agglomeration of individual phase particles (Figure 2). IG corrosion was observed for all alloys in both as-cast and annealed states. However, due to microstructure spheroidisation in the annealed samples, potential IG corrosion paths are significantly reduced. The MZ + 3.0Sn alloy is the best example as it showed very poor corrosion performance in the as-cast state. 3 wt.% of Sn enabled very “effective” propagation of IG corrosion through the microstructure. After annealing, as mentioned, potential paths for IG corrosion propagation are significantly reduced.

3. CONCLUSIONS

Samples with 0.5 wt.% of Sn showed overall the best corrosion properties outperforming even the pure MZ alloy. Use of MZ + 3.0Sn alloys could be considered only with an annealing treatment applied.
Finally, the corrosion products formed during salt spray testing were investigated by XRD. The main ones identified for all samples were simonkolleite and hydrozincite. Occasionally, ZnO and AlO were identified in limited amounts. Other sources show comparable qualitative and even semi-quantitative results [6–8].

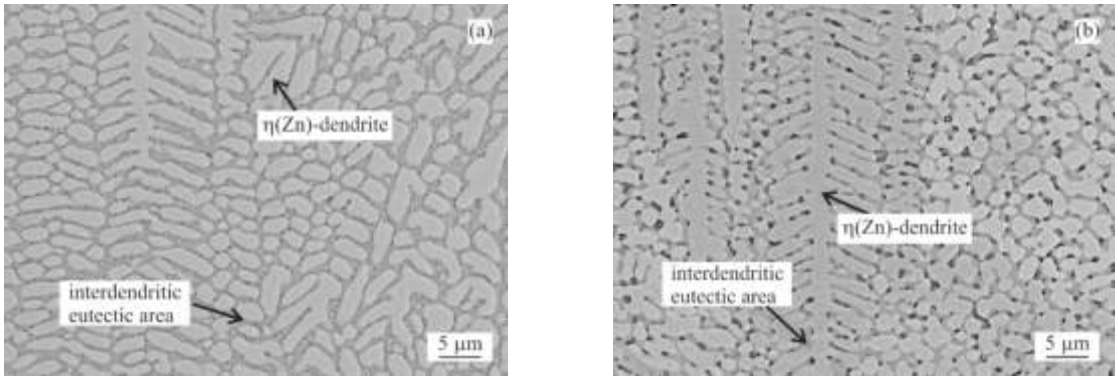

Figure 1 Microstructure of as-cast samples; a) MZ + 0.0 wt.% Sn, b) MZ + 0.5 wt.% Sn

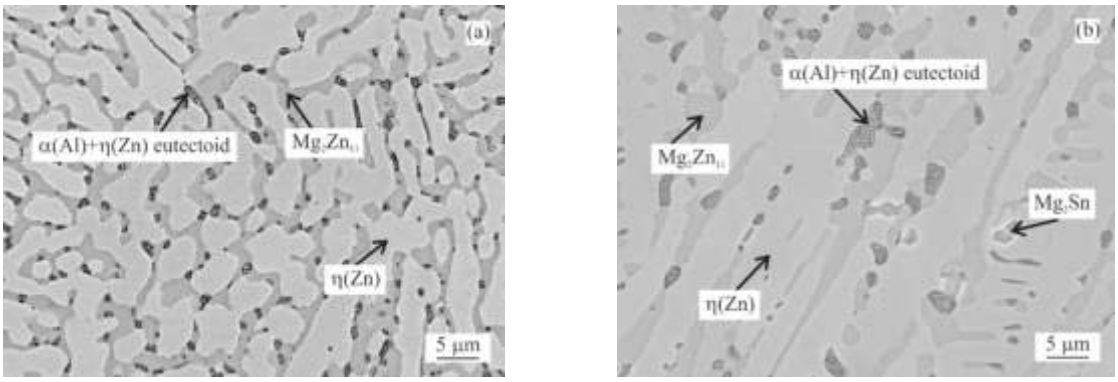

Figure 2 Microstructure of annealed samples; a) MZ + 0.0 wt.% Sn, b) MZ + 0.5 wt.% Sn, c) MZ + 3.0 wt.% Sn

Acknowledgments: The financial support of the VEGA Scientific Grant Agency under grant no. 1/0531/22 is gratefully acknowledged.

BIBLIOGRAPHY

1. Coffin, C.; Depamelaere, H.; King, D.; Van Raemdonck, W. Evaluation of High Temperature Behavior of Zn and ZnAl Coatings on Core Wires and Strands for ACSR, ACSS and alike Overhead power conductors, WJI 2010, Monterrey ITC Preview, pp. 68–75.
2. Tanaka, S.; Honda, K.; Takahashi, A.; Morimoto, Y.; Kurosaki, M.; Shindo, H.; Nishimura, K.; Sugiyama, M. The performance of a Zn-Al-Mg-Si hot-dip galvanized steel sheet. In Proceedings of the 5th International Conference on Zinc and Zinc Alloy Coated Steel Sheet (GALVATECH 2001), p. 153, ISBN 3-514-00673-3.
3. Nishimura, K.; Shindo, H.; Kato, K.; Morimoto, Y.; Funaki, S.O. Microstructure and corrosion behaviour of Zn–Mg–Al hot-dip galvanized steel sheet. In Proceedings of the 4th International Conference on Zinc and Zinc Alloy Coated Steel Sheet (GALVATECH '98), 1998; pp. 437–442.
4. Tsujimura, T.; Komatsu, A.; Andoh, A. Influence of Mg content in coating layer and coating structure on corrosion resistance of hot-dip Zn–Al–Mg–Si alloy coated steel shee. In Proceedings of the 5th International Conference on Zinc and Zinc Alloy Coated Steel Sheet (GALVATECH 2001), pp. 145–152, ISBN 3-514-00673-3.
5. Corrosion tests in artificial atmospheres-Salt spray tests; ISO 9227:2017; International Organization for Standardization: Geneva, Switzerland, 2017.
6. Thierry, D.; Persson, D.; Luckeneder, G.; Stellnberger, K.-H. Atmospheric corrosion of ZnAlMg coated steel during long term atmospheric weathering at different worldwide exposure sites. *Corros. Sci.* **2019**, *148*, 338–354
7. Azevedo, M.S.; Allély, C.; Ogle, K.; Volovitch, P. Corrosion mechanisms of Zn(Mg, Al) coated steel in accelerated tests and natural exposure 1. The role of electrolyte composition in the nature of corrosion products and relative corrosion rate. *Corros. Sci.* **2015**, *90*, 472–481.
8. Prosek, T.; Persson, D.; Stoulil, J.; Thierry, D. Composition of corrosion products formed on Zn–Mg, Zn–Al and Zn–Al–Mg coatings in model atmospheric conditions. *Corros. Sci.* **2014**, *86*, 231–238.

MTS CONFERENCE
MATERIAL TECHNOLOGIES IN SILESIA

12-15.06.2022
Crystal Mountain***** Hotel, Wisła, Poland

Experiences in joining cell packs used in the automotive industry

K. Kwiecinski[a], K. Lota[b], M. Kiełbasiński[c], J. Pikuła[a], P. Śliwiński[a], K. Kubik[a], S. Stano[a], Sz. Kowieski, E. Janowska[b], R. Manczak[b]

[a] Łukasiewicz Research Network – Institute of Welding, Research Group for Materials Weldability and Welded Structures
email: krzysztof.kwiecinski@is.lukasiewicz.gov.pl,
[b] Łukasiewicz Research Network – Institute of Non-Ferrouse Metals Division in Poznań, Research Group of New Technologies of Energy Storage,
email: katarzyna.lota@claio.poznan.pl,
[c] Łukasiewicz Research Network - Tele & Radio Research Institute, Research Group of Ultrasound Technologies

Abstract: The subject of work will be selection and development of joining technology of battery cells and accumulators for modern electric cars. During the works there were carried out tests of joining cells using such methods as: ultrasonic and resistance welding, laser beam welding, electron beam welding , microplasma and TIG welding. The developed technologies will allow to optimise the manufacturing process of Polish batteries. The presentation discusses the results obtained so far.

Keywords: battery cells, accumulators, joining technologies, laser treatment, ultrasonic and resistance welding, laser beam welding, electron beam welding , microplasma, TIG welding, electric cars

1. INTRODUCTION

The aim of reducing carbon dioxide emissions into the atmosphere is forcing car manufacturers to develop emission-free means of transport. The significant increase in the production and sales of plug-in hybrid and all-electric cars in recent years has made it necessary for manufacturers to increase production capacity and continuously improve the performance, reliability and durability of vehicles, which depend significantly on the quality of the electrical connections of the individual cells.

The cell joining process has a significant impact on the efficiency, safety and durability of batteries and accumulators. Therefore, it is important to choose the right joining technology taking into account the specific requirements of battery production and an efficient joining process.

Currently typical joining techniques, such as spot welding, can generate too much heat, which can harm the sensitive cells. For this reason, it is crucial to develop joining technologies that provide design freedom and maximum safety while maintaining a high level of productivity [1].

2. ŁUKASIEWICZ RESEARCH NETWORK PROJECT

The subject of the project carried out under the Łukasiewicz Research Network Targeted Grants is to select technologies for joining battery cells and accumulators for modern electric cars. The proposed technologies such as ultrasonic and resistance welding, laser beam, electron beam, microplasma and TIG welding will allow to optimise the production process of Polish batteries. The process of ultrasonic welding was performed on Łukasiewicz-ITR Sonic Welder series ultrasonic welder using ultrasonic systems (Sonic Blaster series generators, Sonic Converter ultrasonic converters, Sonic Booster boosters and dedicated ultrasonic sonotrodes). The project will develop five dedicated tools for welding packages with different weld outline shapes. FEM simulations of the mechanical wave distribution in the welded parts will be performed. The laser welding process was carried out on a workstation equipped with a TruPulse 103 pulsed laser, allowing the performance of classical pulsed laser welding and [using a workstation for single-mode laser welding with a fusion depth measurement system. The

electron welding process was performed on an electron device model XW150:30/756 designed for welding and surface modification. The plasma welding process will be carried out on a station equipped with an MSP 51 and an Eu Tronic Gap 3001, while TIG welding will be carried out with an ARISTOTIG IG 160 DC (Kemppi).
The optimisation of techniques for joining materials intended for fasteners of battery packs will also require the development of numerical models of welding and seam processes for selected configurations of joined elements and their verification. SysWeld and Sorpas environment will be used to build numerical (thermal) models allowing modelling of temperature fields. The final result of the task will be complete numerical (thermal) models allowing determination of temperatures of joined elements depending on the technological conditions of welding and welding processes characteristic for a given process. The obtained models will enable the development of final joining technologies for selected fasteners in terms of geometric dimensions and applied materials.

2. RESULTS

At the current stage of the project, FEM numerical models of the battery terminal welding process were developed using SYSWELD software. The aim of the calculations was to define the influence of welding parameters and technological solutions on the temperature field and weld dimensions, as well as deformations and welding stresses. The modelling involved the preparation of models in which various technological solutions for the execution of cell element joints were taken into account. The task involved the application of technological solutions and their modifications, including welding paths, the time between successive welds and the method of restraining the element. The effects of the welding path, the time between successive welds and the method of restraining the element on the temperature field and dimensions of the weld as well as deformations and weld stresses were defined. In addition, numerical models of tools intended for ultrasonic welding were also developed [Fig. 1]. A series of trial welded joints using a laser and electron beam were also performed (Fig. 2).

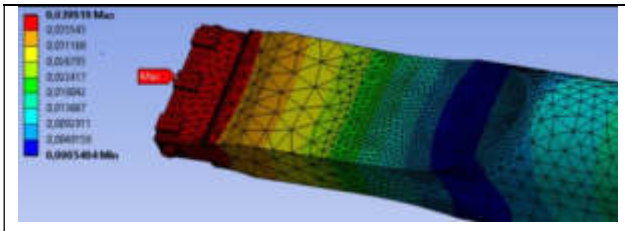	
Figure 1. Sample of the tool for ultrasonic welding	*Figure 1. Sample of joined elements*

3. FURTHER ACTION

As part of the following work, the joints with the most suitable parameters will be selected. Based on the results obtained, target joints will be made.

Acknowledgments: The financial support of the Łukasiewicz Research Network, Poland, is gratefully acknowledged, Research project carried out under the specific grant from the President of the Łukasiewicz Centre - (PB)CellWeld. 01.07.2021 - 30.06.2023.

BIBLIOGRAPHY

1. S. Shawn Lee, H. Tae, Kim and S. Jack Hu, Joining Technologies for Automotive Lithium-ION Battery Manufacturing. Proceedings of the ASME 2010 International Manufacturing Science and Engineering Conference, MSEC2010, San Diego, 2002.
2. M.F.R. Zwicker, M. Moghadam, W. Zhang, C.V. Nielsen, Automotive battery pack manufacturing – a review of battery to tab joining, Journal of Advanced Joining Processes, 1, 2020.

MTS CONFERENCE
MATERIAL TECHNOLOGIES IN SILESIA

12-15.06.2022
Crystal Mountain***** Hotel, Wisła, Poland

New powders based on aluminium alloys for additive manufacturing technologies

M. Lis[a], A. Wrona[a], A. Kukofka[b], K. Pęcak[a], J. Mazur[a], A. Janoszka[a], M. Osadnik[a], D. Ślizak[b]

[a] Łukasiewicz Research Network – Institute of Non-Ferrous Metals, Centre of Powder and Composite Materials
email: marcin.lis@imn.lukasiewicz.gov.pl
[b] Progresja New Materials Sp. z o.o.

Abstract:
The paper presents a method for the production of surface-modified powders based on aluminium alloys of 7xxx group, with appropriate physical and technological properties that enable their use in additive manufacturing technologies.

Keywords: spherical powders, powder metallurgy, additive manufacturing, aluminium alloys

1. INTRODUCTION

With the rapid development of new materials and technologies, demand for materials of good mechanical properties that can be used in special applications is increasing. Such materials include aluminium alloys, which are extensively used in many industries, especially in the aerospace, automotive and petrochemical industries. They are characterized by such properties as low density, high specific strength, good thermal and electrical conductivity as well as high wear and corrosion resistance [1].

Aluminium alloys have been divided into series, taking into account the content of alloying additives which significantly define their strength parameters and properties. The most commonly used alloying elements are: copper, silicon, magnesium, manganese, nickel and zinc. The alloying additives increase primarily strength, and corrosion resistance and improve machinability.

Currently, research works on new materials, including those based on aluminium alloys with significantly better properties than traditional casting alloys or alloys for plastic working, are being carried out. This area includes also powder materials dedicated to additive manufacturing processes. The recent data indicate materials reinforced with ceramic particles that are becoming widely used in the aerospace and automotive industries [2]. Ceramic particles dispersed in a metal matrix increase strength due to the interactions with dislocations and through dispersed reinforcement. Additionally, ceramic particles increase the hardness and resistance to deformation [3]. Such ceramic particles as Al_2O_3, SiC, TiC, B_4C, Si_3N_4, TiB_2 are the most commonly used as an additive to the aluminium alloys. Among the methods for introduction of the particles, the following may be mentioned: method with application of mechanical mixing of the liquid matrix, infiltration, spraying, powder metallurgy, the molten salt method [1, 4, 5].

The first composite powders based on aluminium alloys dedicated to additive printing have recently appeared on the market. This may be a result of very high requirements that are placed on powders used for additive manufacturing methods, e.g. SLM or SLS. Such powders have to be characterized by high purity, narrow particle size range (15 – 45μm), the spheroidal shape of particles, strictly defined chemical composition and composition stability. The literature data show that aluminium based composite powders modified with metallic or ceramic particles are characterized by significantly higher strength (also at high temperatures) than the AlSi10 i AlSi12 alloys currently used in SLM technology.

1.1 Preparation of powders for the plasma spheroidization process

Surface modified powders were prepared for the plasma spheroidization process. There were used a base aluminium alloy powder AA 7075 from Valimet with a grain size of 20-55µm and powders: TiB_2 (Alfa Aesar) and rhenium (Metraco). Figure 1 presents the morphology of the starting powders for the modification process.

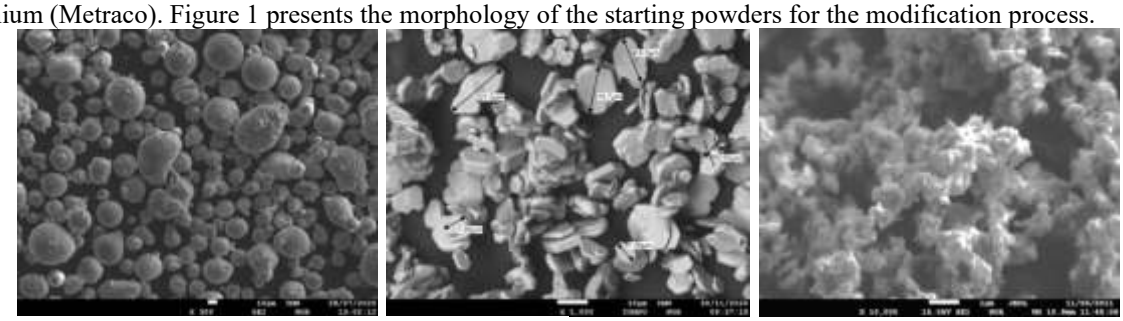

Figure 1. Morphology of AA 7075, TiB2 and Re powders.

In order to produce AA 7075 powder with the addition of rhenium, the process of thermo-reduction of the base powder with the application of ammonium perrhenate was used. There was produced a powder with 3wt.% of rhenium intended for the spheroidization process. The powder AA 7075-3wt.%TiB_2 was produced by mixing the powders in a ball mill.

The process of spheroidization of the produced powders was carried out with the application of a prototype installation, which consists of a vertical reaction chamber equipped with the AP-50 plasma system by FST and a torch with an internal feeding of powder into the plasma flame.

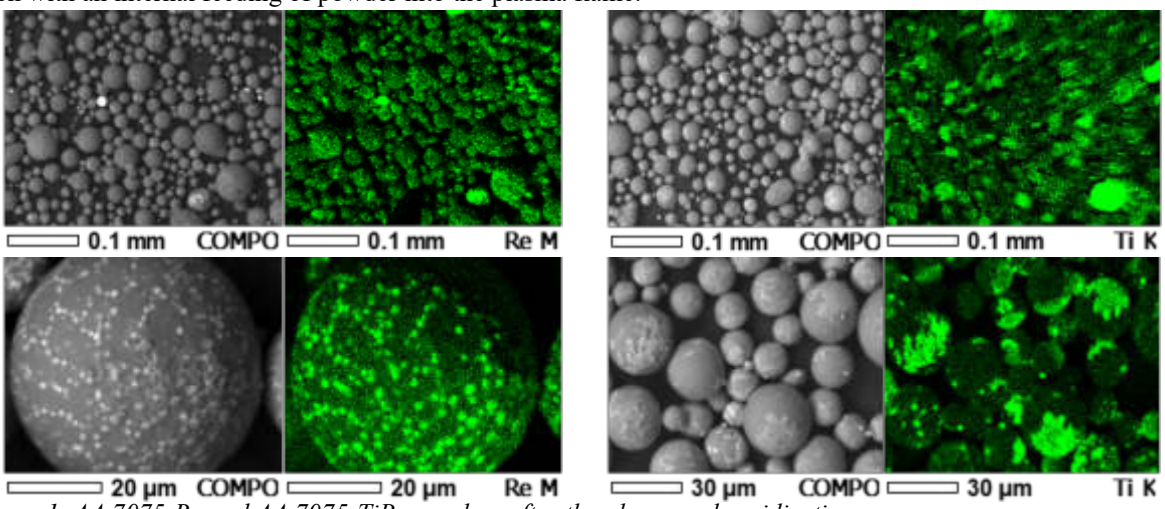

Figure 1. AA 7075-Re and AA 7075-TiB_2 powders after the plasma spheroidization process.

The plasma spraying process enables the production of spherical alloy powders of AA 7075 type with a surface modified with rhenium and TiB_2 ceramics.

Acknowledgements: The financial support - „Szybka Ścieżka_2020", project no. POIR.01.01.01-00-0289/20, „Modified powders from light metal alloys as a new raw material for additive manufacturing technologies".

BIBLIOGRAPHY

1. Bi Jiang, Lei Zhenglong, Chen Xi, Li Peng, Lu Nannan, Chen Yanbin, Microstructure and mechanical properties of TiB2-reinforced 7075 aluminium matrix composites fabricated by laser melting deposition, Ceramics International 45 (2019) 5680–5692
2. L.X. Zhang, B.Y. Li, H. Wu, W. Wang, S.C. Zhai, J. Xu, Z.Z. Niu, Y. Wang, Microstructure and property characterization of Al-based composites reinforced with CuZrAl particles fabricated by mechanical alloying and spark plasma sintering, Adv. Powder Technol. 29 (7) (2018) 1695–1702
3. S.C. Tjong, Novel nanoparticle-reinforced metal matrix composites with enhanced mechanical properties, Adv. Eng. Mater. 9 (2007) 639-652
4. M. Huang, X. Li, H. Yi, N. Ma, H. Wang, Effect of in situ TiB2 particle reinforcement on the creep resistance of hypoeutectic Al-12Si alloy, J. Alloy. Comp. 389 (2005) 275-280.
5. M.F. Najafabadi, M. A. Golozar, A. Saidi, H. Edris, Wear behaviour of aluminium matrix TiB_2 composite prepared by in situ processing, Mater. Sci. Technol. 19 (2003) 1531-1532

MTS CONFERENCE
MATERIAL TECHNOLOGIES IN SILESIA

12-15.06.2022
Crystal Mountain***** Hotel, Wisła, Poland

Modern methods of surface modification of new generation titanium alloys

J. Lisoń[a], A. Taratuta, M. Antonowicz, Z. Paszenda, M. Basiaga

[a] Silesian University of Technology, Faculty of Biomedical Engineering, Department of Biomaterials and Medical Devices Engineering
email: julia.lison@polsl.pl

Abstract:.
The article describes the idea of the atomic layer deposition method and its possible applications on new generation titanium alloy for biomedical applications. Also presented are the exemplary test results of tin oxide (SnO_2) thin layers deposited by the ALD method using in skeletal system. The aim of this study was to evaluate the physicochemical properties of a Ti13Nb13Zr alloy used for elements of the skeletal system. As the temperature and the number of cycles vary, the results show that the surface area of the samples changes. The uncoated Ti13Nb13Zr alloy exhibits hydrophilic properties, however, all coated specimens improve in this respect and provide improved clinical results. It has contributed the risk mineralization of postoperative complications. As a result it has increased effectiveness, decreased the indicator of complications and improved life of the patients.

Keywords: titanium alloy, atomic layer deposition, surface modification, skeletal system, antibacterial layers

1. INTRODUCTION

Bone implants generally consist of light metals or alloys such as titanium and titanium alloys. With the economic and technological growth, the number of elderly people seeking unsuccessful replacement of organs and their replacement with products is growing rapidly. It is estimated that 70-80% of biomedical devices are made of metallic material. Metal implants are extremely effective in rebuilding damaged hard tissue. As an individual's lifespan increases, the demand for biomaterials will surely grow on a huge scale. Due to their remarkable properties such as corrosion resistance, non-toxicity and cytocompatibility, titanium alloys are now widely used. However, the most famous titanium alloys Ti6Al4V and Ti6Al7Nb are replaced due to the content of aluminum or cytotoxic vanadium causing allergies, so the authors refuse to use them in the human body. The existence of the elements Nb and Zr is more biocompatible and cannot cause side effects, including cytotoxicity and neurological diseases, caused by the elements vanadium and aluminum, respectively. Nevertheless, Ti-based alloys seem to have relatively low abrasion resistance [1]. Currently, more biocompatible materials are used [2]. New generation materials have a similar value to the Young's modulus of bone in the case of alloys with the addition of Zr, Fe, Ta. Biomaterials used for bone implants are characterized by good corrosion resistance, appropriate mechanical and electrical properties, high metallurgical quality, surface homogeneity, biocompatibility, abrasion resistance and relatively low production costs. The aim of the study was to assess the impact of the physicochemical and mechanical properties of the modified Ti13Nb13Zr alloy, considered to be a material with a high level of biocompatibility and Young's modulus similar to the value of bone tissue, which is particularly important in the context of the treatment of the skeletal system and the process of osseointegration.

In order to maintain optimal mechanical stability during implantation and to improve the physicochemical properties, various surface modification methodologies are used [3]. Nowadays application of nano-layers is one of the most popular surface modifications. Nanoparticles can be deposited on the surface of implants to change their surface chemistry. For example, Ag nanoparticles were initially used to coat orthopedic pins to prevent bacterial colonization, and dispersed silver nanoparticles can be used in polymethyl methacrylate (PMMA) as bone cement. In addition, nanoscale titanium sol-gel layers with deposited Ag, Zn, Hg, Cu, Co and Al metal salts deposited on titanium surfaces were used. Bone implants with modified titanium and zirconium oxide nanocrystalline coatings were tested for osseointegration and antibacterial activity [4]. Atomic layer deposition (ALD) method provides coating of materials in atomic-scale precision. This surface modification is about self-limiting chemical reactions on surfaces, therefore yielding atomic-level control over the film thickness and composition without the need for line-of-site access to the precursor source, for example Al_2O_3, TiO_2, ZnO or application SnO_2 [5].

2. MATERIALS AND METHODS

The layer of zinc oxide was applied using the Atomic Layer Deposition method, obtaining further variants using different cycles number and temperature. In order the assess suitability of the surface modification method proposed in this way, the authors proposed a series of tests. As part of the assessment of the physicochemical properties of the surface layers formed, pitting corrosion resistance tests were carried out and tests using electrochemical impedance spectroscopy (EIS). These tests provided information concerning the structural characteristics of the layers, possible defects, lack of sealing, substrate reactivity and the presence of barrier properties involving the electrolyte. In the research surface wettability tests, scratch test and tribological tests with imaging were also completed, which showed the differences resulting from temperature changes and the number of cycles and their impact on individual parameters tested.

2. RESULTS

The obtained data showed different physicochemical properties of antibacterial films generated under different parameters in case of temperature and number of cycles in the ALD process. These results directly assist the optimization of the SnO_2 layer creation process using ALD-based methods on surfaces of Ti13Nb13Zr alloy implants intended for skeletal system, thus improving their functional properties. The results have obtained can be used as a base to develop more detailed criteria of final quality of medical devices which will ensure the required biocompatibility of implants. It has contributed the risk mineralization of postoperative complications. As a result it has increased effectiveness, decreased the indicator of complications and improved life of the patients.

Acknowledgments: Research funded by statutory activities of Department of Biomaterials and Medical Devices Engineering, Faculty of Biomedical Engineering, Silesian University of Technology, no. 07/020/BK_22/0073

BIBLIOGRAPHY

1. Quinn, J.; McFadden, R.; Chan, C.W.; Carson, L. Titanium for Orthopedic Applications: An Overview of Surface Modification to Improve Biocompatibility and Prevent Bacterial Biofilm Formation. *iScience* **2020**, *23*, 101745, doi:10.1016/j.isci.2020.101745.
2. Bansal, P.; Singh, G.; Sidhu, H.S. Improvement of surface properties and corrosion resistance of Ti13Nb13Zr titanium alloy by plasma-sprayed HA/ZnO coatings for biomedical applications. *Mater. Chem. Phys.* **2021**, *257*, doi:10.1016/j.matchemphys.2020.123738.
3. Bansal, P.; Singh, G.; Sidhu, H.S. Plasma-Sprayed Hydroxyapatite-Strontium Coating for Improved Corrosion Resistance and Surface Properties of Biodegradable AZ31 Mg Alloy for Biomedical Applications. *J. Mater. Eng. Perform.* **2021**, *30*, 1768–1779, doi:10.1007/s11665-021-05490-0.
4. Bhalshankar, S. EasyChair Preprint Application of Nano Technology in Biomedical Engineering APPLICATION OF NANO TECHNOLOGY IN BIOMEDICAL ENGINEERING . **2021**.
5. Aravindan, V.; Jinesh, K.B.; Prabhakar, R.R.; Kale, V.S.; Madhavi, S. Atomic layer deposited (ALD) SnO2 anodes with exceptional cycleability for Li-ion batteries. *Nano Energy* **2013**, *2*, 720–725, doi:10.1016/j.nanoen.2012.12.007.

MTS CONFERENCE
MATERIAL TECHNOLOGIES IN SILESIA

12-15.06.2022
Crystal Mountain***** Hotel, Wisła, Poland

Strain hardening of titanium after KOBO extrusion in 350°C and cold rolling

M. Łagoda[a], W. Bochniak[b], P. Ostachowski[b]

[a] Łukasiewicz Research Network – Institute of Non-Ferrous Metals, Centre of Advanced Materials Technologies
email: marek.lagoda@imn.lukasiewicz.gov.pl
[b] AGH – University of Science and Technology, Faculty of Non-Ferrous Metals

Abstract: The work focuses on the problem of deformability of titanium subjected to low-temperature extrusion by the KOBO method with a high extrusion ratio and the possibility of its further plastic forming after this process. Based on experimental studies, it was found that KOBO extruded bars of titanium are characterized by a good surface condition, homogeneous structure and high mechanical properties. Moreover, their additional cold rolling can be carried out without the need of any heat treatment, and then they acquire much higher mechanical properties than in the case of commercial bars.
Keywords: KOBO extrusion; Titanium; Mechanical properties; Structure

1. INTRODUCTION

Within the project described in this paper, attempts at producing rods with a diameter of ø8mm out of pure titanium (Grade 2) using innovative cold KOBO deformation [1,2] were undertaken. The KOBO method includes a range of unconventional deformation [3,4] procedures (extrusion, rolling, casting and drawing) of metals and alloys, the main idea of which is applying additional, cyclically changing deformation with an alternative direction to the plastic flow during the main deformation procedure [5].

Most research on the KOBO method to date has been performed on the process of direct extrusion [6]. The procedure involves a reversibly rotating die, which forces an additional twisting of the extruded material. Hence, as compared to conventional extrusion, KOBO therefore has five, not three, degrees of freedom. The additional parameters, apart from the conventional rate, temperature and extrusion ratio λ, are the frequency and angle of reverse rotating die, which enable us to control not only the process itself [6], but also the structure [7] and mechanical properties [8] of the final product in a way that is impossible to obtain in conventional manufacturing procedures [9]. In paper [10] it has been concluded that the specific structure and mechanical properties of KOBO extruded materials result from the generation of highly over-equilibrial concentrations of point defects, particularly self-interstitial atoms, which initiate viscous flow of the extruded metal, resembling liquid viscous flow and form strengthening nano-sized clusters (collections of self-interstitial atoms) in the final product.

2. EXPERIMENT

The experimental research was conducted on commercial titanium (Grade 2). The material (in the form of ø40×40 mm rods) was direct extruded by the KOBO method at a temperature of 350 °C (0.32 Tm) into rods with a diameter of 8mm (extrusion ratio λ = 25) at the rate (punch speed) of 0,2 mm/s with simultaneous cyclic twisting at an angle of ±8° and frequency of 5 Hz on an experimental horizontal hydraulic 1 MN press with the KOBO system and then subjected to rolling.

3. RESULTS

Example mechanical characteristics of titanium Grade 2 in commercial state and extruded via the KOBO method are presented in Fig. 1.

The KOBO extruded titanium's ultimate tensile strength is 540 MPa, around 10% higher than of the commercial one's (492 MPa). Similarly, its plasticity is also higher after the extrusion, particularly in terms of elongation, which is roughly 30% higher than in commercial titanium.

Structural observations confirm that both titanium in commercial state (used as billet material) and KOBO extruded have equiaxial grains of an average size of around 40μm (Fig. 2).

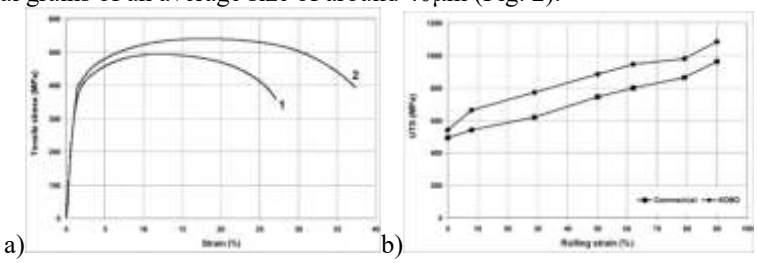

Figure 1. a) example tensile curves of titanium in commercial (1) and extruded by the KOBO method (2) b) strain rate during tensile test ε̇ = 8 × 10–3 s–1; b) comparison of the impact of rolling strain on the ultimate tensile strength of titanium (Grade 2) extruded by the KOBO method and in commercial state.

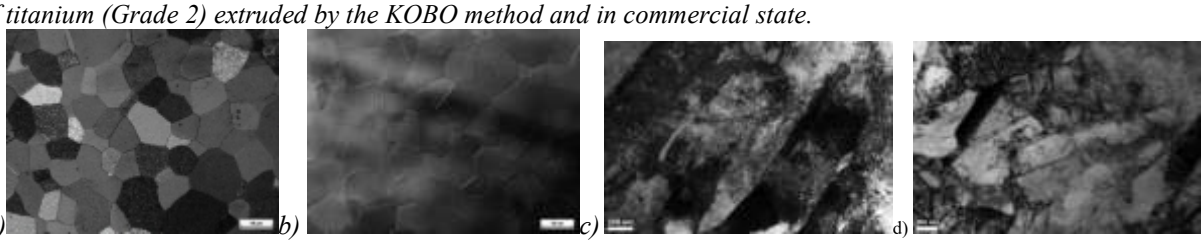

Figure 2. Optical microscopy structure of longitudinal cross-sections of a) commercial titanium Grade 2 and (b) titanium Grade 2 after KOBO extrusion; and TEM microstructure of titanium Grade 2 c) commercial state, d) extruded by the KOBO method.

Detailed TEM microstructural observations revealed high dislocation density in the commercial material (Fig. 2c), which decreases after KOBO extrusion (Fig. 2d). The recovery effects visible in the structure of the extruded titanium seem contradictory to its higher strength properties. Such results can be interpreted using the Korbel concept [10,11] that the KOBO method reorganizes the structure of products on a nanometric scale. It is influenced by the generated strongly over-equilibrium concentration of interstitial atoms and their reorganization in the form of nanometric (below 2 nm) clusters which is strengthening deformed material.

BIBLIOGRAPHY

1. A. Korbel, W. Bochniak. Method of plastic forming of materials. U.S. Patent No 5,737,959 (1998).
2. W. Bochniak, A. Korbel. Plastic flow of aluminium extruded under complex conditions. Mater. Sci. and Techn. 16 (2000) 664.
3. Y. Estrin, A. Vinogradov. Extreme grain refinement by severe plastic deformation: A wealth of challenging science. Acta Mater 61 (2013) 782.
4. R.Z. Valiev, R.K. Islamgaliev, I.V. Alexandrov. Bulk nanostructured materials from severe plastic deformation. Prog Mater Sci 45 (2000) 103.
5. A. Korbel, W. Bochniak. Refinement and control of the metal structure elements by plastic deformation. Scripta Mater 51 (2004) 755.
6. A. Korbel, W. Bochniak, P. Ostachowski, L. Błaż. Visco–plastic flow of metal in dynamic conditions of complex strain scheme. Metallurgical Materials Transactions A 42 (2011) 2881.
7. A. Korbel, K. Piela, P. Ostachowski, M. Łagoda, L. Błaż, W. Bochniak, M. Pawlyta. Structural phenomena induced in the course of and post low – temperature KOBO extrusion of AA6013 aluminum alloy. Materials Science and Engineering A 710 (2018) 349.
8. A. Korbel, W. Bochniak. Lüders deformation and superplastic flow of metals extruded by KOBO method. Philos Mag 93 (2013) 1883.
9. A. Korbel, W. Bochniak, J. Borowski, L. Błaż, P. Ostachowski, M. Łagoda. Anomalies in precipitation hardening process of 7075 aluminum alloy extruded by KOBO method. Journal of Materials Processing and Technology 216 (2015) 160.
10. A. Korbel, W. Bochniak. Stratified plastic flow in metals. International Journal of Mechanical Sciences 128–129 (2017) 269.
11. W. Bochniak, A. Korbel, P. Ostachowski, M. Łagoda, Plastic flow of metals under cyclic change of deformation path conditions. Archives of Civil and Mechanical Engineering 18 (2018) 679.

MTS CONFERENCE
MATERIAL TECHNOLOGIES IN SILESIA

12-15.06.2022
Crystal Mountain***** Hotel, Wisła, Poland

Structure and properties of CuCrTiAl alloy after plastic deformation

M. Łagoda[a], W. Głuchowski[a], M. Maleta[a], J. Domagała-Dubiel[a], R. Drajewicz[a]

[a] Łukasiewicz Research Network - Institute of Non-Ferrous Metals, Centre of Advanced Material Technologies
email: rafal.drajewicz@imn.lukasiewicz.gov.pl

Abstract: The development of the automotive industry leads to a search for newer and newer tool materials used in the production process. The most commonly used joint in the production of cars is the resistance weld, which uses electrode caps made of a well-known alloy (CuCrZr). Therefore, newer alloys and technologies for their production are sought to extend service life and thus reduce production costs.
Precipitation hardening CuCrTiAl alloy was analysed in this article. After casting, CuCrTiAl alloy was subjected to cold and hot deformation and then tested for its usability. The obtained results confirmed the potential of this alloy to make electrodes for resistance welding.

Keywords: CuCrTiAl alloy, plastic deformation, precipitation hardening, microstructure

1. INTRODUCTION

There are studies on modifications to the technology of producing welding caps [1], which are aimed at improving their operational parameters, and thus reducing operating costs [2]. This topic is so interesting that there were even attempts to use modern severe plastic deformation technologies in order to improve the properties of the CuCrZr alloy [3]. Bearing in mind the above, it was found that it is important to use the knowledge of phenomena in the field of not only the selection of alloys for specific applications, but also the impact of plastic forming and heat treatment technology in the search for better usability of materials for welding caps. Only the combination of all three issues gives hope for improving the properties of resistance welding electrodes. To achieve the assumed goals, knowledge from articles [4,5] and the team members` experience were used to develop the CuCrTiAl alloy and its heat and plastic treatment technology.

2. EXPERIMENT

After testing many CuCrTiAl alloys, an alloy with the composition CuCr0.81Ti0.24Al0.064 was selected for further research, which was produced according to the block diagram in Figure 1.

3. RESULTS

The cast bars were characterized by the conductivity of 25,4 MS/m and the hardness of 97 HV. Due to the small diameter of the bars and the intensive cooling during casting, aging was carried out without prior supersaturation, the purpose of which was to check the quality of supersaturation during casting. The results of this experiment are shown in Figures 2 and 3. The experiment showed no significant effect of supersaturation on the effects of aging. However, in order to maintain the purity of the measurement, it was decided to use the supersaturation treatment for all tested variants. Next, cold and hot deformation tests were carried out (Figures 4 and 5). Results show that in the case of hot deformation in the tested alloy, although higher deformation temperatures improve the hardness, they worsen the conductivity, and the intermediate temperatures (800 and 850 °C) have the tested parameters at the level of the commercial CuCrZr alloy, the conductivity of which is 44-48 MS/m, and the hardness of 140-166 HV after plastic working and heat treatment. The most interesting result, however, is the sample aged after cold deformation, which after 90 minutes of aging achieved the hardness of 166 HV, i.e., in the upper limit of the conventional alloy, and the conductivity of 44,5 MS/m. The hot-deformed and aged sample had a homogeneous structure (Figure 6). The grain size in the material after cold deformation and aging, was similar to that in the material after hot deformation (850 °C) and aging (Figure 7).

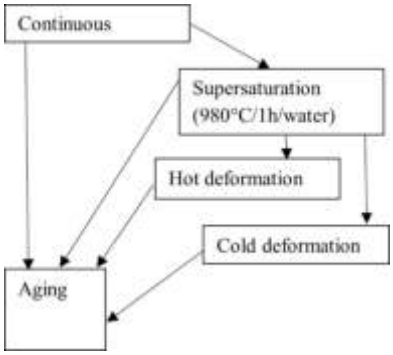

Figure 1. Scheme of the experiment.

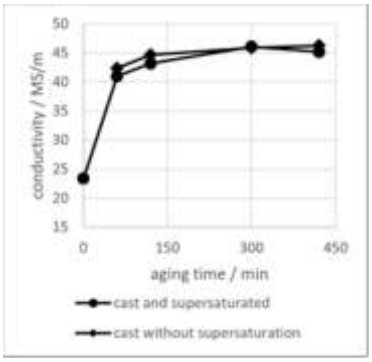

Figure 2. The influence of aging time on the conductivity of cast CuCrTiAl alloy.

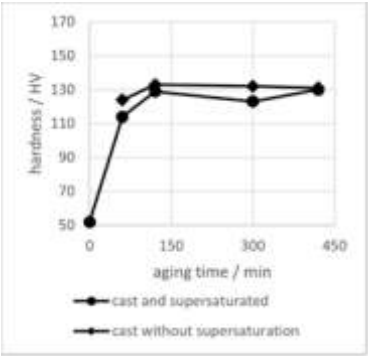

Figure 3. The influence of aging time on the hardness of cast CuCrTiAl alloy.

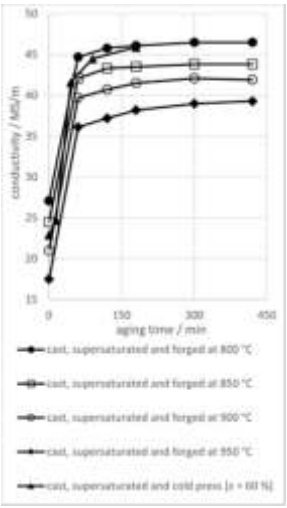

Figure 4. The influence of aging time on the conductivity of pressed CuCrTiAl alloy

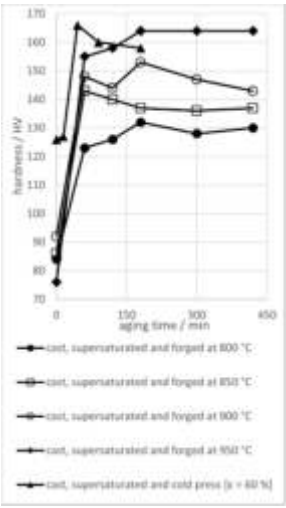

Figure 5. The influence of aging time on the hardness of pressed CuCrTiAl alloy.

Figure 6. Microstructure of the CuCrTiAl alloy after hot deformation and aging at 480 °C for 2 hours.

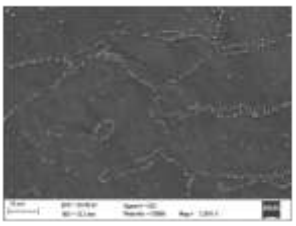

Figure 7. Microstructure of the CuCrTiAl alloy after cold deformation and aging at 480 °C for 90 minutes.

Acknowledgments: The authors are pleased to acknowledge the help of Professor Z. Rdzawski in the discussion. The work received funding from the project: TECHMATSTRATEG1 / 347960/6 / NCBR /.

BIBLIOGRAPHY

1. K. Franczak, P. Kwasniewski, G. Kiesiewicz, M. Zasadzinska, B. Jurkiewicz, P. Strzepek, Z. Rdzawski, Research of mechanical and electrical properties of Cu-Sc and Cu-Zr alloys. Archives of Civil and Mechanical Engineering 20 (2020) 1, Article Number: 28.
2. M. Wagner, S. Kolb, Efficiency improvements for high frequency resistance spot welding. 15th European Conference on Power Electronics and Applications 10.1109/ EPE.2013.6634720 2-6 Sept. 2013 Lille, France.
3. P. Ostachowski, W. Bochniak, M. Łagoda, S. Ziółkiewicz, Strength properties and structure and structure of CuCrZr alloy subjected to low-temperature KOBO extrusion and heat treatment. The International Journal of Advanced Manufactoring Technology 105 (2019) 12, 5023-5044.
4. Z. Rdzawski, W. Gluchowski, J. Stobrawa, W. Kempinski, B. Andrzejewski, Microstructure and properties of Cu-Nb and Cu-Ag nanofiber composites. Archives of Civil and Mechanical Engineering, 15 (2015) 3, 689-697.
5. J. P. Stobrawa, Z. M. Rdzawski, W. J. Gluchowski, Dispersion and Precipitation Strengthened Nanocrystalline and Ultra Fine Grained Copper. Journal of Nanoscience and Technology, 12 (2012) 12, 9102-9111.

MTS CONFERENCE
MATERIAL TECHNOLOGIES IN SILESIA

12-15.06.2022
Crystal Mountain***** Hotel, Wisła, Poland

The analysis of the properties of bimetallic wires CoNi using in energy production

D. Łukowiec [a, *], T. Wasiak[b], D. Janas[b], E. Drzymała[c], J. Depciuch[c], T. Tarnawski[c], J. Kubacki[d,e,], S. Wacławek[f], A. Radoń[a,g]

[a] Materials Research Laboratory, Faculty of Mechanical Engineering, Silesian University of Technology, Konarskiego 18 a, 44-100 Gliwice, Poland,
[b] Faculty of Chemistry, Silesian University of Technology, B. Krzywoustego 4, 44-100 Gliwice, Poland
[c] Institute of Nuclear Physics Polish Academy of Sciences, Radzikowskiego 152, 31-342 Kraków, Poland
[d] A. Chelkowski Institute of Physics, University of Silesia, 75 Pułku Piechoty 1A, 41-500 Chorzów, Poland
[e] Silesian Center for Education and Interdisciplinary Research, 75 Pułku Piechoty 1, 41-500 Chorzów, Poland
[f] Institute for Nanomaterials, Advanced Technologies and Innovation, Technical University of Liberec, Studentská 1402/2, 461 17 Liberec 1, Czech Republic
[g] Łukasiewicz Research Network - Institute of Non-Ferrous Metals, Sowińskiego 5 St., 44-100 Gliwice, Poland

email: dariusz.lukowiec@polsl.pl

Abstract: This work presents newly developed catalyst supports in the form of bimetallic wires (CoNi) for electrooxidation of ethanol in an alkaline medium. Electrocatalysts composed of CoNi wires decorated with Pd particles (Pd NPs) were made at varying metal ratios and their chemical composition and structure was investigated in detail. The synthesis involved a wet chemical reduction assisted by a magnetic field, which led to the generation of wires, followed by the deposition of spherical Pd on their surface. The best catalytic activity was obtained for the catalyst support of Co_3-Ni_7 decorated with Pd, which exhibited more than 8000 mA/mg_{Pd} (EOR) for 0.86 wt% of Pd loading. The results can be explained by the synergistic effect between the morphology of the bimetallic support and the favorable interaction of oxophilic Co, Ni with catalytic Pd.
Keywords: bimetallic wires CoNi, catalyst support, ethanol oxidation reaction, direct ethanol fuel cells

1. INTRODUCTION

Because of the great social and economic importance of the energy deficit problem, scientists are conducting a broad and very intensive search for new catalysts that are being evaluated for their performance [1]. The commonly used alcohol oxidation catalysts working in direct alcohol fuel cells include nanostructured systems based on Pt, Pd and Ru [2]. Current work is focused on the preparation of efficient and stable catalysts for the oxidation of alcohols but requiring the use of smaller amounts of noble metals. On the other hand, apart from the chemical composition, the morphology of the catalyst as well as the structure of the support on which it is deposited play an important role in catalytic performance. The use of metallic support in the form of wires (1D) can contribute to faster diffusion through liquid alcohol, reduction of surface energy (better control over agglomeration and solubility), and consequently improve electron transport and optimize the use of the noble metal catalyst. The second thing worth noting is the oxophilic nature of Ni or Co which increases the tolerance to poisoning of the noble metal by CO and thus increases its catalytic efficiency. Therefore, an interesting issue seems to be the synthesis of bimetallic wires as supports which could further enhance the catalytic properties of the deposited catalyst due to the synergistic effect.

2. EXPERIMENTAL STUDY

Different supports in the form of cobalt-nickel wires with changing ratio of metals (5:5, 3:7, 1:9, 7:3, 9:1) decorated by palladium particles were synthesized. Herein, the structure and morfology of obtained composites

was studied in detail. The synthesis of bimetallic CoNi wires was based on the wet chemical reduction assisted with the magnetic field. The crystal and electronic structure, morphology and chemical composition of obtained nanocomposites were determined by transmission electron microscopy (TEM), X-ray photoelectron spectroscopy (XPS), X-ray diffraction (XRD), electron diffraction (ED), Energy-dispersive X-ray spectroscopy (EDS) and Inductively Coupled Plasma Optical Emission Spectrometry (ICP-OES). The cyclic voltammeter measurements were used to determine the electrochemical behaviour and verify the catalytic properties of the obtained supports.

3. RESULTS AND DISCUSSION

Fig. 1 presents the morphology of synthesized wires. The influence of type and mass fraction of used metal (Ni, Co, Pt) on catalytic properties of obtained composites was determined. Cyclic voltammetry tests demonstrate that the material in the form of cobalt-nickel wires is a promising support catalyst towards ethanol oxidation reactions. The catalyst support of Co_3-Ni_7 decorated with Pd (0.75 mM) achieved the best EOR activity, which can be attributed to the presence of two different crystalline phases: metallic Ni(Co) cubic phase and highly disordered $Co_{0.75}Ni_{0.25}$ phase and additionally can be easily oxidized to the cobalt and nickel oxides. We postulate that the balance between oxidized, disordered and crystalline phases of Co-Ni support is the key.

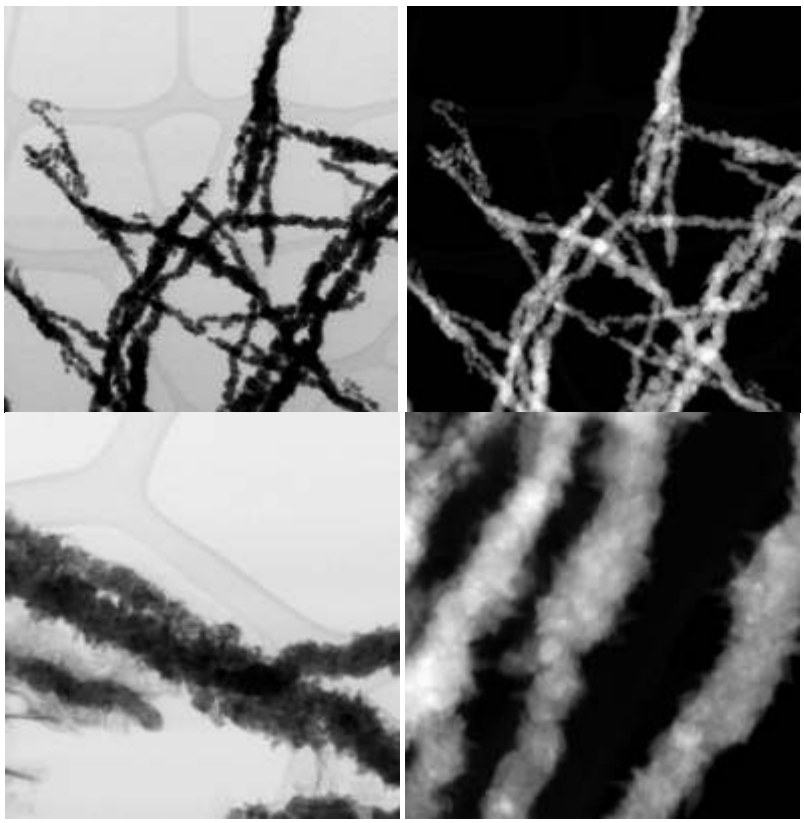

Figure 1. Cobalt-nickel wires as a efficient catalyst support.

BIBLIOGRAPHY

1. Y. Zhao et al., Methanol electro-oxidation on Ni@Pd core-shell nanoparticles supported on multi-walled carbon nanotubes in alkaline media. *Int. J. Hydrogen Energy 35*, 3249–3257 (2010)
2. Z. Qi et al., Novel nanocrystalline PdNi alloy catalyst for methanol and ethanol electro-oxidation in alkaline media. *J. Power Sources 196*, 5823–5828 (2011)

MTS CONFERENCE
MATERIAL TECHNOLOGIES IN SILESIA

12-15.06.2022
Crystal Mountain***** Hotel, Wisła, Poland

Badania mikrostruktury i własności mechanicznych brązów aluminiowych o zmiennej zawartości Fe, Ni i Al

M. Maleta[a], J. Kulasa[a], P. Kwaśniewski[b]

[a] Sieć Badawcza Łukasiewicz – Instytut Metali Nieżelaznych, Centrum Zaawansowanych Technologii Materiałowych, ul. Generała Józefa Sowińskiego 5, 44-121 Gliwice
email: marcin.maleta@imn.lukasiewicz.gov.pl,
[b] Akademia Górniczo-Hutnicza im. Stanisława Staszica, Wydział Metali Nieżelaznych, al. A. Mickiewicza 30, 30-059 Kraków

Streszczenie:
W pracy przedstawiono wpływ zmiennej zawartości Fe, Ni i Al na mikrostrukturę i własności mechaniczne brązów aluminiowych w stanie po odlaniu, a także wyniki prób odkształcania na zimno tych stopów w procesie walcowania. Wykazano, że niewielki dodatek żelaza (0,8%mas.) wpłynął na zmianę mikrostruktury oraz na podniesienie własności wytrzymałościowych brązów aluminiowych.

Abstract:
The paper presents the influence of the variable content of Fe, Ni and Al on the microstructure and mechanical properties of aluminium bronzes after casting, as well as the results of cold deformation tests of these alloys in the rolling process. It was shown that a small addition of iron (0.8% by weight) changed the microstructure and increased the strength properties of aluminium bronze.

Słowa kluczowe: brąz aluminiowy, mikrostruktura, SEM, przeróbka plastyczna

1. WPROWADZENIE

Brązy aluminiowe to stopy miedzi o dużej wytrzymałości i odporności na zmienne obciążenia i warunki korozyjne. Głównym składnikiem stopowym jest aluminium, które zwiększa wytrzymałość i twardość. Oprócz aluminium ważnymi dodatkami są żelazo, mangan i nikiel. Żelazo ma działanie modyfikujące, zapewniając drobnoziarnistą mikrostrukturę, co pozytywnie wpływa na wzrost wytrzymałości, twardości i odporności na ścieranie. Dodatek manganu poprawia właściwości mechaniczne, a także zwiększa odporność na korozję. Zwiększając wytrzymałość stopu, nikiel zwiększa również przewodność cieplną i elektryczną oraz temperaturę pracy. Brązy aluminiowe o zawartości do 9% masy aluminium wykazują jednofazową mikrostrukturę α w warunkach równowagi. W warunkach chłodzenia nierównowagowego ulegają one przemianie martenzytycznej β w wysokich temperaturach. Faza β ulega rozkładowi eutektoidalnemu w niższych temperaturach do α + γ2. Powstawanie γ2 jest niepożądane, ponieważ obniża ciągliwość stopu i zwiększa podatność na korozję. Tworzenie niepożądanego γ2 jest hamowane przez dodanie niklu i żelaza, które zwiększają granicę rozpuszczalności glinu do 11% i wpływają na wytrącanie się bardziej pożądanych faz κ. Zjawisko to wykorzystywane jest do ulepszania cieplnego brązu aluminiowego w celu podwyższenia właściwości wytrzymałościowych [1 - 3]. W wielu pracach badawczych analizowano wpływ szybkości wyżarzania, przeróbki plastycznej na gorąco i chłodzenia na mikrostrukturę i właściwości mechaniczne brązów niklowo-aluminiowych [4 - 6]. Brązy aluminiowe zwykle poddaje się obróbce na gorąco ze względu na ograniczoną obrabialność na zimno, niską ciągliwość i szybkie utwardzanie.

2. MATERIAŁ I METODYKA

Materiał do badan stanowiły próbki pobrane z wlewków brązu aluminiowego o zmiennej zawartości Al, Fe, Ni i stałej zawartości Mn. Wlewki wytworzono na drodze topienia w otwartym piecu indukcyjnym i odlewania statycznego do wlewnicy żeliwnej. Skład chemiczny badanych materiałów przedstawiono w tabeli 1.

Tabela 1. Skład chemiczny wytworzonych stopów, % mas.
Table 1. Chemical composition of produced alloys, % wt.

Stop	Al	Fe	Ni	Mn	Cu
1	8,60	1,63	1,50	1,58	reszta
2	9,03	4,31	3,95	1,50	
3	8,95	3,45	4,00	1,55	

Próbki w stanie po odlaniu poddano badaniom mikrostruktury przy użyciu mikroskopii świetlnej oraz skaningowej mikroskopii elektronowej. Wielkość krystalitów analizowano za pomocą oprogramowania mikroskopu. Wykonano 70 pomiarów dla losowo wybranych dendrytów fazy α w badanym obszarze próbki. Własności wytrzymałościowe wyznaczono w pomiarach twardości metodą Vickersa (HV10) oraz w statycznej próbie rozciągania. Podatność do przeróbki plastycznej badano w procesie walcowania. Proces prowadzono z jednostkowym gniotem około 20%. Próbki walcowano do maksymalnego stanu utwardzenia i pękania materiału.

3. WYNIKI BADAŃ I PODSUMOWANIE

Zwiększenie zawartości Al o 0,43 % mas., Fe o 2,68 % mas, Ni o 2,45 % mas. w stopie 2 w stosunku do stopu 1, wpłynęło na zmniejszenie średniej wielkości krystalitów odlewu brązu aluminiowego z około 256 µm do 50 µm (rys. 1), a także na zwiększenie wytrzymałości na rozciąganie o 34% i twardości o 36%. Wprowadzenie dodatkowej ilości żelaza na poziomie 0,8% mas. do brązu aluminiowego o stałej i zbliżonej zawartości Al, Ni, Mn (wyższa zawartość Fe w stopie 2 w porównaniu do stopu 3) wpłynęło na rozdrobnienie krystalitów od około 89 µm do 50 µm, zwiększyło wytrzymałość na rozciąganie o około 17% i twardość o 11%. Dla zastosowanych parametrów procesu walcowania (gniot jednostkowy około 20%) stopy o wyższej zawartości Fe osiągnęły graniczną odkształcalność po przekroczeniu odkształcenia rzeczywistego 0,36. Stop o niższej zawartości Al, Fe i Ni charakteryzuje się lepszą podatnością do przeróbki plastycznej. Podobne właściwości mechaniczne uzyskano po zastosowaniu odkształcenia rzeczywistego na poziomie 0,61.

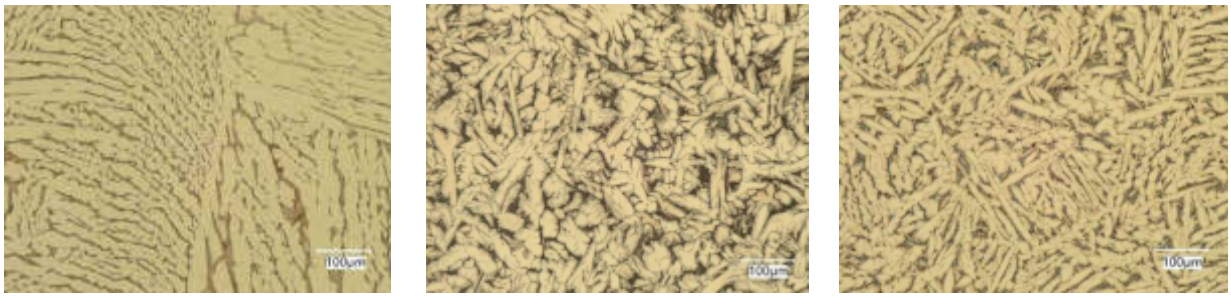

Stop 1 Stop 2 Stop 3

Rys. 1. Mikrostruktura wytworzonych stopów w stanie po odlaniu, mikroskopia świetlna, powiększenie 400x
Fig. 1. Microstructure of produced alloys after casting process, light microscopy, magnification 400x

Podziękowania: Badania przeprowadzono w ramach realizacji programu Doktorat Wdrożeniowy w Sieć Badawcza Łukasiewicz – Instytucie Metali Nieżelaznych w Gliwicach

LITERATURA

1. Copper Development Association, Aluminium Bronze Alloys for Industry, CDA Publication (1986) 83.
2. I. Richardson, C. Powell, Guide to Nickel Aluminium Bronze for Engineers, Copper Development Association, 222 (2016).
3. E. A. Culpan, G. Rose, Microstructural characterization of nickel aluminium bronze cast, Journal of materials science, 13 (1978), 1647 – 1657.
4. J. Anantapong, V. Uthaisangsuk, S. Suranuntchai, A. Manonukul, Effect of hot working on microstructure evolution of as-cast Nickel Aluminium Bronze alloy, Materials & Design, 60 (2014), 233 – 243.
5. L. Yuting, W. Liqiang , H. Yuanfei, X. Xiaoyan, L. Weijie, Investigation of microstructure and mechanical properties of hot worked NiAl bronze alloy with different deformation degree, Materials Science and Engineering A, 643 (2015), 17 – 24.
6. Y. Liu, Z. Ye, X. Wang, B. Liang, Y. Zhang, Microstructure and mechanical behavior of Cu–9Al–4Ni-3.5Fe-0.5Mn alloy fabricated by laser melting deposition, Materials Science &Engineering A (2021),

MTS CONFERENCE
MATERIAL TECHNOLOGIES IN SILESIA

12-15.06.2022
Crystal Mountain***** Hotel, Wisła, Poland

Practical applications of nanobainitic steels

S. Marciniak[a], A. Gołaszewski[a], E. Skołek[b], K. Wasiak[b], W. A. Świątnicki[b], A. N. Wieczorek[c]

[a] NanoStal Sp. z o.o.
[b] Warsaw University of Technology, Faculty of Materials Science and Engineering
[c] Silesian University of Technology, Department of Mining Mechanization and Robotisation
email: szymon.marciniak@nanostal.com

Abstract: This article discusses the possibility of creating a nanobainitic structure in massive items made of readily available steels of normalized grades. The possibility of combining the technology of producing a nanobainitic structure utilizing phase transformations with surface engineering techniques: carburization and nitriding, is also presented. The results of mechanical and functional properties' tests which served as the basis for selecting suitable steel grades and variants of nanobainitization treatment for practical applications, are shown. Prototype products made in nanobainitic steel technology, such as cold-work punches, screws, gears, inserts for dies for plastics, are demonstrated. The results of real-condition tests carried out on prototype items are presented and compared with the results obtained for steel items subjected to conventional martensitic hardening heat treatment.

Keywords: nanobainite, nanostructure, nanostructured steels

1. INTRODUCTION

Steels of a certain chemical composition, with the the Si and/or Al content at about 1.5% as the key characteristic, allow to obtain a specific type of bainite, called carbide-free bainite during isothermal quenching. Such a structure consists of bainitic ferrite plates separated by films of stable austenite without cementite content. When a sufficiently low temperature of isothermal transformation is used, ferrite plates and austenite films are fragmented down to nanometric sizes. Therefore, steel subjected to such treatment becomes a nanostructured material, often called nanobainite. Nanobainite, compared with steel after a conventional quenching and tempering treatment for similar hardness, has: better fatigue strength, lower quenching deformations, higher brittle fracture resistance, and better compromise between its strength and plasticity. Another advantage of nanobainitic steels is the possibility of modifying their properties in a much wider range than in conventional steels, which allows improvements to products already available on the market, e.g. by increasing their durability, as well as introduction of new products with unique features. However, in spite of these advantages, the practical use of such steels has been minimal so far. This article describes various potential applications of nanobainitic steels that have been tested on prototype items under real operating conditions.

1.1. Prototype items

Prototype items made of nanobainitic steels for a wide variety of applications are shown in Figure 1. They include new 14.6 HV class bolts for tensioned connections, which are characterized by high strength compared with their yield stress, self-tapping concrete screws for multiple assembly in top-class concretes, gears with increased fatigue strength for high-power transmissions, cold-work punches with a nitride layer for chromium VI elimination, as well as die inserts for plastics with low quenching distortion.

Figure 1. Prototype items made of nanobainitic steels

Acknowledgments:

The results presented in this paper have been obtained within projects: „An Innovative technology combining steel nanostructurization process with methods of surface engineering" (POIR.01.01.01-00-0513/20), „Development of an innovative technology for the manufacture of toothed components with hybrid surface layers with nanostructure base for drive units of conveyors designed to be used in extreme operating conditions" (POIR.04.01.04-00-0064/15), "Production of nanocrystalline steels using phase transformations" (POIG 01.01.02-14-100/09) and thanks to the "Nanostal" team carrying out tasks at NanoStal Sp. z o.o. and at the Faculty of Materials Science and Engineering of the Warsaw University of Technology.

BIBLIOGRAPHY

1. W.A. Świątnicki, K. Pobiedzińska, E. Skołek, A. Gołaszewski, S. Marciniak, Ł. Nadolny, J. Szawłowski: „Nanocrystalline structure formation in steels using bainitic transformation". Inżynieria Materiałowa, rok XXXIII, nr 6, 524-529 (2012)
2. E. Skołek, K. Wasiak, W.A. Świątnicki: Structure and properties of the carburised surface layer on 35CrSiMn5-5-4 steel after nanostructurization treatment, Materials and Technology (Materiali in Tehnologije) 49 (2015) 6, 933–939
3. E. Skołek, S. Marciniak, W.A. Świątnicki, Thermal Stability of Nanocrystalline Structure in X37CrMoV5-l Steel, Archives of Metallurgy and Materials, vol. 60, No. 1 (2015) pp. 511-516
4. A. Gołaszewski, J. Szawłowski, W.A. Świątnicki: Multiphase steel microstructure and properties optimisation through a new heat treatment process, Materials Science and Technology (2021), Vol. 37, No. 13, 1083-1089

MTS CONFERENCE
MATERIAL TECHNOLOGIES IN SILESIA

12-15.06.2022
Crystal Mountain***** Hotel, Wisła, Poland

Optymalizacja parametrów obróbki cieplnej wyrobów ze stali maraging wytwarzanych z zastosowaniem technologii przyrostowych

J. Marcisz[1], A. Żak[1], W. Burian[2], M. Karpiński[2], A. Radoń[2], A. Kowalski[2], M. Polański[3], J. Kluczyński[3], J. Sienkiewicz[3]

1) Łukasiewicz-Instytut Metalurgii Żelaza
2) Łukasiewicz-Instytut Metali Nieżelaznych
3) Wojskowa Akademia Techniczna
email: jaroslaw.marcisz@imz.lukasiewicz.gov.pl

Streszczenie
Technologie przyrostowe (druk 3D) znajdują się wciąż w fazie rozwoju, szczególnie w zakresie projektowania nowych materiałów. W procesie doboru składu chemicznego stopu dla technologii druku 3D należy uwzględnić specyficzne cechy wytwarzania na etapie krzepnięcia. Duża szybkość odprowadzania ciepła w trakcie krzepnięcia i bezpośrednio po zakrzepnięciu z jednej strony ogranicza stopień segregacji a z drugiej strony wywołuje powstanie naprężeń. Z kolei optymalizacja parametrów technologii przyrostowych jest niezbędna dla uzyskania wysokiej jakości wewnętrznej, w tym jak najniższej porowatości. W artykule przedstawiono wyniki badań dwóch gatunków stali maraging: MS300 i eksperymentalnej MS400. Stale maraging charakteryzuje struktura martenzytu listwowego umacnianego wydzieleniowo w procesie starzenia oraz ultrawysoka wytrzymałość wyższa od 2000 MPa. Materiał badań wytworzono z zastosowaniem technologii przyrostowych (druk 3D) w odmianach SLM-Selective Laser Melting (MS300) i LENS-Laser Engineered Net Shaping (MS400). Zakres badań w pierwszym etapie obejmował charakterystykę makro i mikrostruktury w stanie po drukowaniu. Następnie przeprowadzono eksperymenty obróbki cieplnej przesycania i starzenia, w tym krótkotrwałego, w celu doboru parametrów tych zabiegów cieplnych dla uzyskania optymalnego zestawu właściwości mechanicznych, w szczególności wytrzymałości i ciągliwości. Właściwości mechaniczne wyznaczono w statycznych testach rozciągania i ściskania. Uzyskane wyniki badań odniesiono do materiału wytwarzanego z zastosowaniem standardowej technologii odlewania i przeróbki plastycznej.

Słowa kluczowe: technologie przyrostowe, stal maraging, obróbka cieplna, mikrostruktura, właściwości mechaniczne

Abstract
Additive manufacturing technologies (3D printing) are still in the development stage, especially for the design of new materials. In the process of designing the chemical composition of an alloy for 3D printing technology, the specific features of manufacturing at the solidification stage must be taken into account. The high rate of cooling during solidification and immediately after solidification reduces the degree of segregation on the one hand, and induces stresses on the other. At the same time, optimisation of parameters of the additive technology is necessary to achieve high internal quality, including the lowest possible porosity. This paper presents the results of examinations two maraging steel grades: MS300 and experimental MS400. The maraging steels are characterised by a lath martensite structure strengthened by ageing and an ultra-high strength higher than 2000 MPa. The experimental material was produced using the following additive technologies: SLM-Selective Laser Melting (MS300) and LENS-Laser Engineered Net Shaping (MS400). The first stage of the research included the characterisation of the macro and microstructure in the as-printed state. This was followed by solution heat treatment and aging experiments, including short-term aging, in order to select the parameters of these processes to obtain an optimal combination of mechanical properties, particularly strength and toughness ratio. Mechanical properties were determined in static tensile and compression tests. The results obtained were compared to a material manufactured using standard casting and hot working technology.

Key words: additive manufacturing, maraging steel, heat treatment, microstructure, mechanical properties

MTS CONFERENCE
MATERIAL TECHNOLOGIES IN SILESIA

12-15.06.2022
Crystal Mountain***** Hotel, Wisła, Poland

Structure and properties of $Al_{65}Cr_{20}Fe_{15}$ and $Al_{65}Zr_{20}Fe_{15}$ alloys manufactured by different cooling rates

K. Młynarek-Żak [a], P. Gębara[b], R. Babilas[a]

[a] Silesian University of Technology, Faculty of Mechanical Engineering, Department of Engineering Materials and Biomaterials
[b] Częstochowa University of Technology, Faculty of Production Engineering and Materials Technology, Department of Physics

email: katarzyna.mlynarek-zak@polsl.pl

Abstract: The purpose of the work was to investigate the influence of the structure of $Al_{65}Cr_{20}Fe_{15}$ and $Al_{65}Zr_{20}Fe_{15}$ alloys produced by different cooling rates from the liquid state on the corrosion, mechanical and magnetic properties. The highest corrosion resistance was found in alloys with the addition of zirconium, while a higher hardness was noticed for alloys with the addition of chromium. The alloys were characterized by low magnetization, while an increase in ferromagnetic properties was observed for the $Al_{65}Cr_{20}Fe_{15}$ alloy.

Keywords: aluminum alloys, complex metallic alloys, quasicrystalline structure, corrosion resistance, hardness, magnetic properties

1. INTRODUCTION

The development of various industrial sectors creates a demand for advanced aluminum alloys [1]. Rapid solidification (RS) technologies, together with the chemical composition design of aluminum alloys, make it possible to obtain unique structures and properties. The most common RS technologies include high-pressure casting into a copper mold and melt spinning. Through these manufacturing methods, it is possible to produce aluminum-based alloys with amorphous, nanocrystalline, or quasicrystalline structures, as well as their combinations [2]. Special attention is paid to aluminum alloys with additions of transition metals (TM) such as chromium, zirconium, and iron because of many favorable properties, such as improved corrosion resistance and higher strength. In the latest work [3] for Al-Cr-Fe alloys, it was possible to obtain a crystalline structure in the presence of a complex metallic alloy (CMA) phase. The CMA-type structures are intermetallic crystalline compounds. They are characterized by large unit cells that can be made up of thousands of atoms. The CMA type alloys offer many interesting properties and innovative applications, such as low-temperature thermal insulation, hydrogen storage, thermoelectricity, increased catalytic efficiency at lower costs, reduced friction, optimization of composite materials, nanostructured metallic aggregates or thin films, development of innovative coating processes adapted to complex surface shapes, etc. [4,5]. Corrosion, mechanical, and magnetic studies are necessary to determine further directions of development of Al-TM alloys; therefore, the aim of this work was to determine the influence of the structure, Cr, and Zr additions as well as manufacturing technology on properties.

2. MATERIALS AND METHODS

The samples were produced by induction melting of chemical elements (99.99%) and then slowly cooling, and high-pressure casting into a water-cooled copper mold. Structural studies were performed using X-ray diffraction and Mössbauer spectroscopy. The corrosion behavior was analyzed on the basis of electrochemical measurements carried out by the potentiodynamic method and electrochemical impedance spectroscopy (EIS) at a 3.5% NaCl aqueous solution. The hardness was measured using the Vickers method with a load value of 100 gf.

The magnetization behavior of the investigated Al-based alloys was measured using a vibrating sample magnetometer (VSM) method.

3. RESULTS

The $Al_{65}Cr_{20}Fe_{15}$ alloy produced at two different cooling rates showed a crystalline structure with the presence of the $Al_{65}Cr_{27}Fe_{8}$ phase that is CMA (complex metallic alloy) type. The alloys with the addition of zircon were characterized by a multiphase, crystalline structure. The best corrosion resistance was demonstrated by alloys with the addition of zirconium [3]. The polarization curves of studied chemical compositions are presented in Fig.1a. The Niquist diagrams of the most resistant ingots are visible in Fig.1b. The alloys with Zr addition indicated the lowest hardness values. In the case of alloys with Cr addition, the effect of rapid solidification on higher hardness values was clear. The results of magnetic measurements using the VSM technique showed that none of the hysteresis loops shows the saturation effect and their magnetization is low. The increase in ferromagnetic properties took place for the $Al_{65}Cr_{20}Fe_{15}$ alloy (ingot).

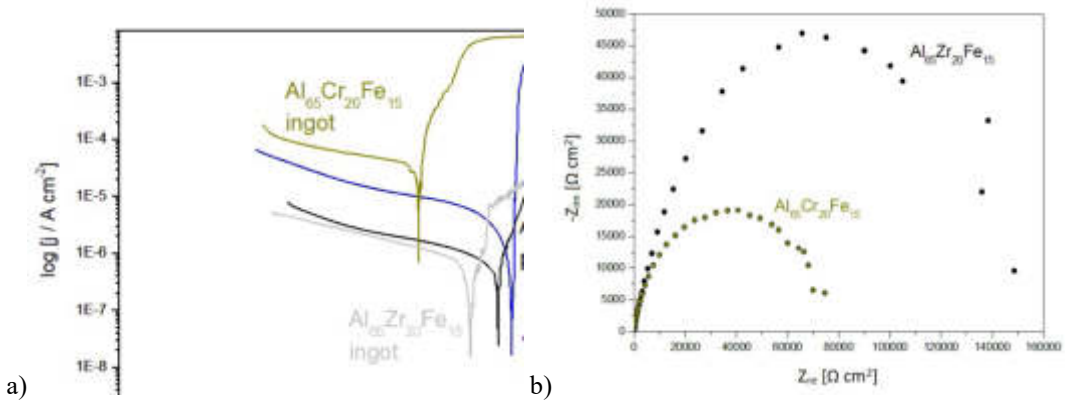

Figure 1. Polarization curves for the studied alloys (a), Niquist diagrams of the most corrosion resistant alloys in the form of ingots (b).

Acknowledgments: The work was supported by the National Science Centre of Poland under research project no. 2018/29/B/ST8/02264.

BIBLIOGRAPHY

1. A.K. Mieczysław Kaczorowski, Konstrukcyjne materiały metalowe, ceramiczne i kompozytowe, Oficyna Wydawnicza Politechnika Warszawska, Warszawa, 2008.
2. A. Inoue, H. Kimura, Fabrications and mechanical properties of bulk amorphous, nanocrystalline, nanoquasicrystalline alloys in aluminum-based system, J. Light Met. 1 (2001) 31–41.
3. K. Młynarek-Żak, A. Wierzbicka-Miernik, M. Kądziołka-Gaweł, T. Czeppe, A. Radoń, R. Babilas, Electrochemical characterization of rapidly solidified Al-(Cr,Cu,Ni,Y,Zr)-Fe alloys, Electrochim. Acta. 409 (2022) 139836.
4. J.M. Dubois, E. Belin-Ferré, Complex Metallic Alloys: Fundamentals and Applications, Wiley-VCH Verlag GmbH & Co. KGaA, Weinheim 2010.
5. E. Ura-Binczyk, A. Beni, M. Lewandowska, P. Schmutz, Passive oxide film characterisation on Al-Cr-Fe and Al-Cu-Fe-Cr complex metallic alloys in neutral to alkaline electrolytes by photo- and electrochemical methods, Electrochim. Acta. 139 (2014) 289–301.

MTS CONFERENCE
MATERIAL TECHNOLOGIES IN SILESIA

12-15.06.2022
Crystal Mountain***** Hotel, Wisła, Poland

Strength analysis of vacuum soldering connection of conventional tool steels and printed powder steels with the use of BNi-2 Nickel solders

J. Mytnik[a], J Mazurkiewicz[b], M. Król[b]

[a] Listemann Polska Sp.z o.o., Biskupińska str. 23, Kraków, Poland
[b] Silesian University of Technology, Faculty of Mechanical Engineering, Department of Engineering Materials and Biomaterials
email: janusz.mazurkiewicz@polsl.pl

Abstract:
The paper presents the results of vacuum brazing with B-Ni2 nickel solder of tool steels used in the polymer processing industry. Currently, many technological problems arise during the brazing of conventionally produced steels and steels obtained from powders using the SLM technique (so-called printed steels). The paper presents the results of strength properties of brazed joints of Bohler's commercial M789 steel produced conventionally and laser-sintered from powders in various configurations. The article also presents the results of structural tests of the analyzed brazed joints. It was found that the highest strength properties of the brazed joints were obtained for the pair consisting of conventional steels only. A lower strength of the soldered joint by about 32% was obtained for a pair only composed of printed steels. The worst results were obtained for a brazed joint of conventional steel-printed steel. For the best-brazed joint, a tensile strength level of 53% of the strength of brazed conventional steel was achieved. The key to obtaining good strength in a brazed joint is to prepare the steel for the brazing process properly.

Keywords: vacuum brazing, nickel solders, tool steels, strength of brazed joints, structure of brazed joints, etching of tool steels, SLM technology

1. INTRODUCTION

High-temperature vacuum brazing is an advanced process that allows the joining of parts made of various engineering materials, resulting in a solid metallic bond providing high strength properties, especially where there is no possibility of using welded joints. The process of joining with this technology, among other things, tool steels, eliminates many barriers in engineering design, and production efficiency and allows strongly diversified materials to be joined together. Massive progress in manufacturing technology is also being made in incremental methods, where the laser powder melting (SLM) method is one of the key techniques. The SLM technique gives great freedom in design, no restrictions in terms of part geometry, waste reduction, simplified production, and shorter delivery times. In the processing of polymeric materials, steels obtained using the SLM technique and conventional steels are joined, however, this raises technological problems related to the limited wettability of steel with solder. The issues are related to the chemical composition of the solder and steel, the surface preparation method, and the soldering process parameters.

The scientific objective of this work is to study the mechanisms influencing the wettability of nickel-based brazed surfaces of structural tool steels obtained with the innovative technology of laser powder melting (SLM-Selective laser melting), and steels of the same grade got conventionally.

2. TESTING METHODOLOGY AND TEST MATERIAL

The structural steel grades to be tested were selected based on market availability and the application possibilities of industrial partners. Four steels, both conventional and SLM, were chosen for testing. The steels

selected are W302-1.2344, W722 - 1.2709 and W360 AMPO; and M789-AMPO. This paper presents test results for Bohler's M789 AMPO steel (tab. 1). The first stage of the research is the preparation of specimens for strength and structural testing, as well as the design and manufacture of the necessary instrumentation to carry out brazing in industrial vacuum furnaces. A series of samples were made using SLM technology from M789 steel powder and from conventional steel. The test pieces were prepared by turning and grinding. Test specimens with a diameter of 8 mm in the brazed part were joined using BNi2 foil (50 µm, tab. 1) at 1050 °C for 45 min (fig.1). The brazed samples were then heat treated by quenching and tempering. Samples in SLM/SLM, conventional/SLM, convention-nal/conventional pairs were subjected to different surface preparation processes related to etching and machining. Brazing was performed in a vacuum furnace using designed fixtures. The soldered samples in different sets were subjected to strength tests at ambient temperature on a wedge-jaw testing machine. Impact strength, hardness, microhardness and fatigue tests at elevated temperatures were also performed. Similarly, for the same sets of soldered materials structural investigations using light microscopy, high-resolution scanning electron microscopy with EDS and EBSD, high-resolution transmission electron microscopy, structural X-ray diffraction, corrosion and tomography investigations were performed.

Figure 1. View of a set of samples printed with the SLM technique prepared for soldering with conventional steel

Table 1. Chemical composition of M789 AMPO Bohler steel and chemical composition of BNi2 solder

Content of alloying elements in steel by weight [%]						Content of alloying elements in the solder by weight [%]				
C	Cr	Mo	Ni	Ti	Al	Ni	Cr	Fe	Si	B
<0,02	12,2	1,0	10,0	1,0	0,6	up to 100%	7	3	4,1	3

3. SUMMARY OF RESEARCH RESULTS

It was found that the heat-treated conventional steel tested achieved a tensile strength of 1812 MPa, while the SLM-printed steel only achieved 1470 MPa. The highest strength values of the brazed joint after heat treatment, analogous to those of conventional steel and SLM-printed steel, were obtained for the brazed conventional steel whose surfaces were etched with hydrofluoric acid. The average tensile strength of the brazed joint for this pair of materials is 955 MPa, i.e. about 53% of the strength of the steel. On the contrary, the lowest average strength of the brazed joint was found for the SLM-produced material pair at 654 MPa. Such significant differences in joint strength for pairs made of steel obtained using different technologies are related to the different levels of steel surface wettability and the chemical composition of the surface after the pickling process. Analyzing the obtained breakthroughs of brazed joints, it was found that they have a strongly differentiated surface morphology, and several characteristic zones can be distinguished, as presented in fig. 2. The analysis of the chemical composition in the area of the solder joint breakthroughs with the use of the EDS technique has revealed places of insufficient adhesion of the solder to steel. These spots were subjected to metallographic analysis on cross-sections.

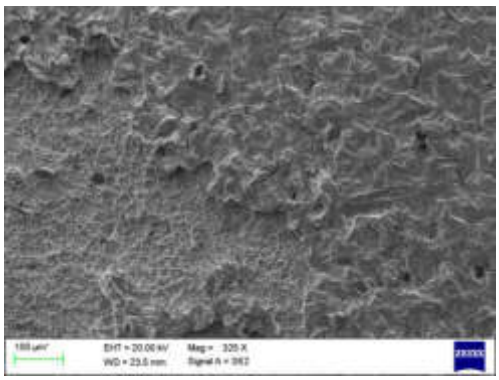

Figure 2. Structure of BNi2 solder joint of M789 AMPO steel obtained from laser powder sintering.

Acknowledgments: The research presented in the paper is part of an implementation doctorate financed by MEiN.

BIBLIOGRAPHY

1. X.L. Gu, C. J. Yang, Z. J. Chen, C. D. Wu, L. L. Feng, Effect of temperature on microstructure and mechanical poroperties of 316L stainless steel brazed joints, Advanced Materials Research Vol. 418-420, 2021, p. 1494-1497;
2. Y. Han, Y. Wu, G. Li, F.S. Pan, R. Fan, X. Liu, Elements Diffusion and Mechanical Properties of 15-5PH Stainless Steel Joint Brazed with BNi-2 Filler Metal, Materials Science Forum Vol. 850, 2016, p. 700-705;

MTS CONFERENCE
MATERIAL TECHNOLOGIES IN SILESIA

12-15.06.2022
Crystal Mountain***** Hotel, Wisła, Poland

Metalurgia wodorowa – wytwarzanie stali bezpośrednio z rudy żelaza

M. Niesler[a]

[a] Sieć Badawcza Łukasiewicz – Instytut Metalurgii Żelaza im. Stanisława Staszica, Grupa Badawcza: Procesy Surowcowe
email: marian.niesler@imz.lukasiewicz.gov.pl

Streszczenie: W artykule opisano nowy sposób wytwarzania stali wg patentu Łuksiewicz-IMŻ/Mróz J. nr 236288, który charakteryzuje się tym, że stal jest wytwarzana bezpośrednio z rudy żelaza w jednym agregacie metalurgicznym, oraz zastosowaniem wodoru jako reduktora. W zależności od udziału wodoru w fazie gazowej, w procesie tym możliwe jest zmniejszenie o ok. 70% lub całkowite wyeliminowanie emisji CO_2 do atmosfery w stosunku do obecnej technologii wielki piec-konwertor tlenowy. Redukcja tlenków żelaza przebiega w fazie ciekłej, co pozwala zwielokrotnić wydajność produkcyjną w stosunku do tradycyjnej technologii wytwarzania stali.

Słowa kluczowe: wodór, ruda żelaza, redukcja bezpośrednia

1. WPROWADZENIE

W tradycyjnej metalurgii żelaza i stali zasadniczymi procesami są: redukcja, utlenianie i rafinacja, a w nich najważniejszą rolę odgrywają węgiel i tlen. W nowych intensywnie rozwijanych metodach otrzymywania żelaza, stali i innych metali coraz większe znaczenia ma wodór jako podstawowy reduktor tlenków. Wszystkie te procesy, w których celowo stosuje się wodór nazywa się metalurgią wodorową. Wodór jest doskonałym reduktorem tlenków metali. W kontakcie z tlenkami nawet tak trwałymi jak Al_2O_3, MgO, CaO i SiO_2 wodór wykazuje zdecydowanie silniejsze właściwości redukujące niż inne reduktory. Produktami reakcji redukcji jest woda, w odróżnieniu od reduktorów węglowych (C i CO) dających emisje CO_2.

W tablicy 1 przedstawiono możliwość wykorzystania wodoru jako podstawowego reduktora w procesach metalurgii żelaza.

Tablica 1. Stan metod produkcji żelaza i perspektywy rozwoju zastosowań wodoru jako zasadniczego reduktora
Table 1. State of iron production methods and prospects for using hydrogen as the essential reducer

Metoda, proces otrzymywania żelaza	Główny reduktor	Horyzont czasowy wdrożenia na skalę przemysłową redukcji wodorem w %, lata
Wielkopiecowy	Koks + wodór	20–40%, przygotowywana, 2030– 2050
Bezpośrednia redukcja (typu Midrex i tp)	Koks, gaz ziemny + wodór	50–60 %, rozwijana, 2020–2030
Bezpośrednia redukcja (typu Smelting Reduction)	Węgiel, gaz redukcyjny, wodór	50–80 %, rozwijana, 2020 –2030
Mini wielkie piece	Węgiel drzewny, Wodór	20–30 %, próby, 2040 –2050
Corex,Finex, Hismelt Tecnored i inne	Gaz, węgiel, koks, wodór, plazma wodorowa	40–90%, intensywnie rozwijane i wdrażane, 2015–2030

Istotnym zmianom ulegnie technologia otrzymywania żelaza, ponieważ coraz szersze stosowanie wodoru jako reagenta pozwala na: dużą sprawność i wysoką szybkość redukcji tlenków już w stosunkowo niskich temperaturach, wprowadzanie wodoru nie tylko do wielkiego pieca, ale i wielu urządzeń bezpośredniej redukcji rud (tzw. DRI, SM), eliminuje częściowo lub całkowicie koks metalurgiczny, wyraźnie ograniczyć emisję gazów cieplarnianych, przerabiać rudy o zmiennym bogactwie. Największy udział wodoru jako reduktora będzie miał

miejsce w metodach redukcji bezpośredniej rud w latach 2020–2030. Znacznie później wodór zastępować będzie koks i gaz ziemny[1].

Łukasiewicz – Instytut Metalurgii Żelaza również prowadzi szereg badań nad technologią otrzymywania żelaza z wykorzystaniem wodoru.

1.1. Wytwarzanie stali bezpośrednio z rudy żelaza

Nowy sposób wytwarzania stali opatentowany przez Łuksiewicz-IMŻ/Mróz J. nr 236288, charakteryzuje się tym, że stal jest wytwarzana bezpośrednio z rudy żelaza w jednym agregacie metalurgicznym, oraz zastosowaniem wodoru jako reduktora. W zależności od udziału wodoru w fazie gazowej, w procesie tym możliwe jest zmniejszenie o ok. 70% lub całkowite wyeliminowanie emisji CO_2 do atmosfery w stosunku do obecnej technologii wielki piec-konwertor tlenowy. Redukcja tlenków żelaza przebiega w fazie ciekłej, co pozwala zwielokrotnić wydajność produkcyjną w stosunku do tradycyjnej technologii wytwarzania stali.

Sposób wytwarzania stali bezpośrednio z rudy żelaza w jednym reaktorze metalurgicznym, charakteryzuje się tym, że do reaktora wprowadza się przez wdmuchiwanie, miałkie rudy żelaza, topniki w ilości zapewniającej wymaganą zasadowość żużli, oraz reduktor gazowy w postaci wodoru albo mieszaniny wodoru i tlenku węgla, i prowadzi się redukcję tlenków żelaza w temperaturze nie niższej niż 1300°C, przy czym pożądaną, końcową zawartość węgla w stali reguluje się poprzez wprowadzenie takiej ilości gazowego reduktora węglowego w atmosferze redukcyjnej, albo wprowadzenie takiej ilości węgla bezpośrednio do kąpieli metalowej, która zapewnia osiągnięcie założonego poziomu nawęglenia stali. Na rys 1. przedstawiono schemat obecnie stosowanej dwuetapowej technologii wytwarzania stali wielki piec – konwertor tlenowy w porównaniu do sposobu otrzymywania stali bezpośrednio z rudy żelaza [2].

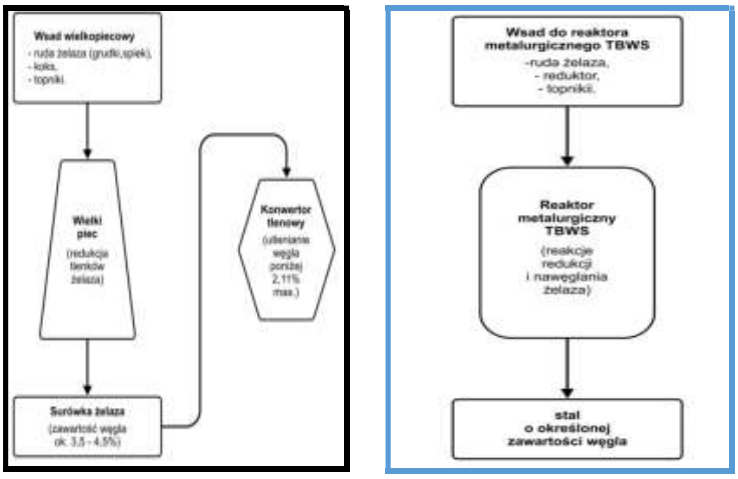

Rys.1. Schemat obecnie stosowanej dwuetapowej technologii wytwarzania stali wielki piec – konwertor tlenowy w porównaniu do sposobu otrzymywania stali bezpośrednio z rudy żelaza

Figure 1. The currently used two-stage steelmaking technology – blast furnace – oxygen converter in integrated steel plants.and obtaining steel directly from iron ore.

Celem wynalazku jest istotne obniżenie nakładów inwestycyjnych w przeliczeniu na jednostkę wyprodukowanej stali, ze względu na wyeliminowanie kosztów inwestycyjnych związanych z budową wydziałów koksowni, spiekalni rud i wielkich pieców, obniżenie kosztów reduktora tlenków żelaza poprzez zastąpienie koksu metalurgicznego gazem ziemnym i wodorem oraz znaczące obniżenie emisji CO_2 do atmosfery w porównaniu z linią technologiczną wielki piec – konwertor tlenowy.

BIBLIOGRAPHY

1. K. Mamro, Metalurgia wodorowa – składowa cywilizacji wodorowej, Prace IMŻ 4 (2009)
2. J.Mróz, M. Niesler, J.Stecko PL Patent 236288, Sposób wytwarzania stali bezpośrednio z rudy żelaza, 2020.

MTS CONFERENCE
MATERIAL TECHNOLOGIES IN SILESIA

12-15.06.2022
Crystal Mountain***** Hotel, Wisła, Poland

Biodegradable wood-polymer composites (WPCs) intended for food contact

A.J. Nowak[a]; P. Drynda[b]

[a] Silesian University of Technology, Faculty of Mechanical Engineering, Scientific and Didactic Laboratory of Nanotechnology and Materials Technologies, Gliwice, Poland.
email: agnieszka.j.nowak@polsl.pl
[b] Member of Student Scientific Circle of Plastics and Composites Processing "HEAD TO HEAD", Faculty of Mechanical Engineering, Silesian University of Technology.

Abstract: The work presents basic issues concerning Wood Plastic Composites (WPCs), specifically composites based on a biodegradable matrix and their ecological significance as well as possible applications. The composites were formed by combining a thermoplastic polymer BIOPLAST GS 2189 and wood particles used as a filler. Microscopic observations of selected components structure of the composite material, as well as the interface between the matrix and reinforcing phase, were carried out. The composite material exhibited excellent adhesion between the polymer matrix and reinforcement particles.

Keywords: biodegradable polymers, wood-plastic composites, SEM.

1. INTRODUCTION

One of the most commonly used engineering materials for the production of packaging and disposable items in the food industry are polymer materials because of their high durability, sterility, and relatively low production costs. In 2018, as much as 61% of plastic waste in the EU came from the disposable packaging sector [1]. In recent years, the problem of "plastic" pollution of the oceans, rivers, and groundwater has also been raised, increasing frequently [2]. This is a serious threat to these ecosystems that are essential to us. Annually, it is estimated that 4.8 to 12.7 million tonnes of plastic are released to the seas and oceans. An alternative to synthetic materials are biopolymers such as cellulose, starch, chitosan, and various types of biocomposites [3]. These plant-based materials reduce the role of fossil fuels. For their production, products or wastes of plant or animal origin can be used. Moreover, most importantly, they are characterized by high biodegradability. Wood-polymer composites (WPCs) are a group of composites with a thermoplastic or thermosetting matrix and a wood filler used as reinforcement. They are mainly formed by injection moulding or extrusion technology. The advantages of WPCs are good mechanical properties, including high stiffness, as well as low weight and cost. Wood-polymer composites are used in the automotive industry, as extruded profiles for windows, doors, railings, platforms, floor panels, and stairs, as well as for everyday items such as flower pots, toys, or packaging [4].

The aim of the work was to develop a fully biodegradable material substitute for packaging and disposable products intended for contact with food. The composite was formed by combining a thermoplastic polymer BIOPLAST GS 2189 and wood particles used as filler. Matrix polymer produced by BIOTEC GmbH & Co. is a completely biodegradable material in an industrial composting environment. Moreover, it contains 75% of renewable raw material. As the reinforcing phase, the sawdust from deciduous trees (oak, ash) with a size of 160-500 mm was used. This study considered initial research of raw polymer and different percentage content of wood filler i.e. 5%, 10%, 15%, 20% - initial research.

1.1. Materials and initial research

The created composite is based on the material under the trade name BIOPLAST GS 2189, produced by german company BIOTEC GmbH & Co. The manufacturer provides that it is completely biodegradable in an industrial composting environment. Moreover, it contains 75% of renewable raw material. This thermoplastic material is suitable for injection moulding, thermoforming and blown film extrusion (MFR 35 g/10min in 190ºC, 2.16 kg). The density stands at 1.35 g/cm^3. As the reinforcing phase, the sawdust from the deciduous tree (oak, ash) was used. A local sawmill provided the raw wood byproduct. The sawdust was screened with a sieve shaker HAVER EML 200 digital plus having screens with opening cells of 160 and 500 µm. The obtained wood fraction with a size of 160-500 mm was subjected to density tests on a gas pycnometer Micromeritics AccuPyc II 1340. The sawdust has a density of 1,5 g/cm^3. Before the production process, the filler was dried in a laboratory drying oven at 100˚C for 4 h. The sawdust structure was presented on picture 1. The wood flour has a fibrous structure and a rectangular shape. ZWISS Supra 25 (SEM) microscope were used to realize the images on raw material samples. During observation of the BIOPLAST GS 2189, the presence of particles up to nanometric size up to 10 µm was revealed. These particles have multi-walled geometry and are evenly distributed throughout the entire

volume of material. To identify them, EDS point analysis was performed (Fig. 1c), which showed a high percentage of calcium in the matrix material. This may indicate a calcium carbonate content in the matrix.

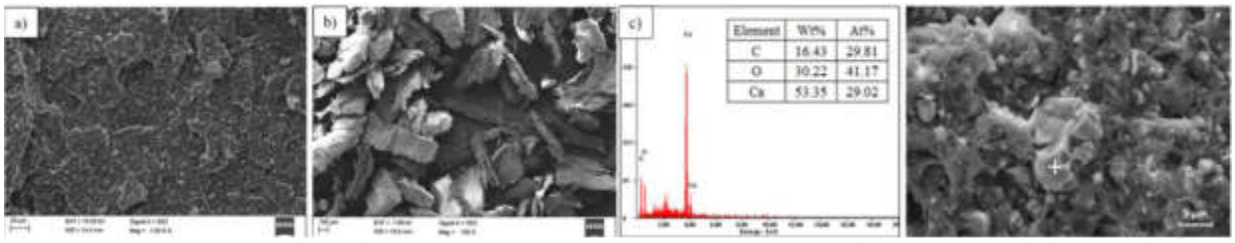

Figure 1. SEM-micrograph of the structure a) of raw BIOPLAST GS 2189; b) of raw wood flour; and c) EDS analysis of the raw BIPLAST GS 2189. The atomic % of C, O and Ca was done on the table and an SEM picture of the tested area.

Microscopic observations using a stereoscopic microscope showed an even distribution of wood particles in the matrix. Agglomerates and polymers without the reinforcing phase were not detected. All samples, both raw polymers and composites, show the brittle fracture. The boundary between the matrix and wood particles was investigated by SEM microscope. There was no discontinuity, and all particles have been distinguished by good adhesion with matrix material (Fig. 2). It was also observed that the fracture of the composite also runs through the volume of wood partials, not only in the matrix. The composites structure showed discontinuities, i.e. pores, with average values of 100 μm located in the entire breakthrough surface.

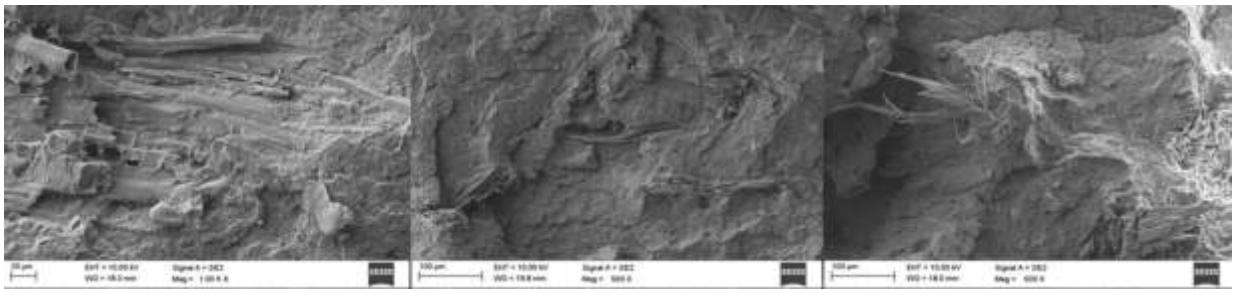

Figure 2. The exemplary SEM-micrograph of the structure of created composite material.

1.2. Summary

The WPCs were elaborated by mixing biopolymer BIOPLAST GS 2189, and wood particles with various filler amount: 5%, 10%, 15%, 20%. This combination allowed the production of an eco-friendly material that is fully degradable. Microscopic observations showed an even distribution and good adhesion of wood particles in the matrix. Discontinuities in the composite structure in the form of pores were also detected, which may affect the reduction of the samples mechanical properties. The next step of research will be conducted to increase the share of fillers to reduce production costs and increase the speed of controlled biodegradation. The materials produced at a later stage of the research should still have good strength results, slightly different from those obtained for composites with a 50 and 30% share of selected fillers. The effects of reinforcement volume fraction on mechanical properties developed composites and water absorption of the composite were investigated and will be published soon.

BIBLIOGRAPHY

1. U. Qasim, A.I. Osman, A.H. Al-Muhtaseb, et al. Renewable cellulosic nanocomposites for food packaging to avoid fossil fuel plastic pollution: a review. Environ Chem Lett, Vol 19, 613–641 (2021).
2. H.V. Ford, N. H. Jones, A. J. Davies, B. J. Godley, J. R. Jambeck, I. E. Napper, C. C. Suckling, G. J. Williams, L. C. Woodall, H. J. Koldewey, The fundamental links between climate change and marine Science of The Total Environment, Vol. 806, Part 1 (2022).
3. H. A. Khalil et al. Seaweed-based sustainable films and composites for food and pharmaceutical applications: A review. Renew Sustain Energy Rev 77:353–362 (2017).
4. M. Z. R. Khan, S. K. Srivastava, M. K. Gupta, A state-of-the-art review on particulate wood polymer composites: Processing, properties and applications, Polymer Testing, Vol. 89, (2020).

The project carried out as part of the Student Scientific Circle of Plastics and Composites Processing "HEAD TO HEAD"

MTS CONFERENCE
MATERIAL TECHNOLOGIES IN SILESIA

12-15.06.2022
Crystal Mountain***** Hotel, Wisła, Poland

Określenie stabilności mechanicznej austenitu szczątkowego w ściskanych dynamicznie wielofazowych stalach średniomanganowych

W. Pakieła[a,*], W. Borek[a], M. Morawiec[b], P. Nuckowski[b], A. Skowronek[a], A. Grajcar[a]

[a] Politechnika Śląska, Wydział Mechaniczny Technologiczny, Katedra Materiałów Inżynierskich i Biomedycznych
[b] Politechnika Śląska, Wydział Mechaniczny Technologiczny, Laboratorium Badania Materiałów
email: *wojciech.pakiela@polsl.pl

Streszczenie: W pracy wytworzono próbki osiowosymetryczne ze stali 3Mn-1.5Al oraz 5Mn-1.5Al o mikrostrukturze składającej się z osnowy bainitycznej oraz udziale austenitu szczątkowego od 15 do 20%. Kontrolę przemian fazowych podczas obróbki cieplnej dokonano metodą dylatometryczną. Następnie przeprowadzono testy ściskania w symulatorze termomechanicznym Gleeble w zakresie szybkości odkształcenia od 0,01 do 50s^{-1}. Próby prowadzono w zakresie temperatury odkształcenia od 20 do 300°C. Określono stopień przemiany austenitu w martenzyt odkształceniowy w zależności od zawartości manganu oraz szybkości i temperatury odkształcenia. Dokonano szczegółowej analizy mikrostruktury stali ze szczególnym uwzględnieniem udziału austenitu szczątkowego w stanie wyjściowym oraz po próbach dynamicznego ściskania. Własności mechaniczne wyznaczono na podstawie pomiarów twardości metodą Vickersa.

Słowa kluczowe: austenit szczątkowy, stabilność mechaniczna, ściskanie dynamiczne, mikrostruktura wielofazowa

1. WPROWADZENIE

Poznanie charakterystyk dynamicznych stali karoseryjnych jest kluczowe dla przewidywania ich zachowania podczas obciążeń kontrolowanych bądź niekontrolowanych zachodzących z dużą szybkością. Charakterystyki takie wyznacza się zazwyczaj w dynamicznych próbach rozciągania lub ściskania. W przypadku wielofazowych stali karoseryjnych kluczowe jest poznanie stabilności mechanicznej austenitu szczątkowego, będącego jedną z kluczowych faz decydujących o końcowych własnościach materiałowych, a także o zdolności elementów konstrukcyjnych do pochłaniania energii zderzenia. Austenit szczątkowy podczas przetwarzania blach na zimno (formowanie wytłoczek) lub w przypadku niekontrolowanych obciążeń dynamicznych (np. w wyniku kolizji, zderzenia, itd.) ulega przemianie martenzytycznej i wnosi wkład w jednoczesne umocnienie i zwiększenie plastyczności dzięki efektowi TRIP (TRansformation Induced Plasticity).

W trakcie odkształcenia plastycznego duża część energii mechanicznej zostaje przemieniona w ciepło. Gronostajski i in. [1] stwierdzili, że w trakcie odkształcenia dynamicznego stali wielofazowych, globalna temperatura materiału może wzrosnąć o 100°C, a w miejscu przewężenia osiągnąć nawet 500°C. Jest to bardzo istotne, gdyż temperatura ma kluczowy wpływ na stabilność austenitu szczątkowego. Kozłowska i in. [2] podają, że stabilność austenitu istotnie wzrasta, gdy temperatura odkształcenia wynosi ≥ 100°C. Jest to związane ze wzrostem energii błędu ułożenia (EBU) austenitu wraz ze wzrostem temperatury. Innym ważnym aspektem odkształcenia z dużymi szybkościami jest powstawanie adiabatycznych pasm ścinania [3]. Pasma te powstają w związku ze zmianą pracy odkształcenia plastycznego w ciepło w czasie odkształcenia. Przy odkształceniach z dużą szybkością powstałe ciepło nie może rozproszyć się do otoczenia ze względu na intensywny przebieg odkształcenia. Lokalny, gwałtowny wzrost tempratury powoduje „mięknięcie" materiału. Gdy jest ono większe niż umocnienie odkształceniowe powoduje niestabilny przebieg odkształcenia plastycznego, co w rezultacie prowadzi do powstawania pasm ścinania [4]. Pasma te są zazwyczaj efektem nieporządanym, gdyż prowadzą do powstawania pęknięć i niszczenia materiału. Marcisz i Janiszewski [5] zaobserwowali występowanie

adiabatycznych pasm ścinania w stali nanobainitycznej poddanej odkształceniu dynamicznemu. Stwierdzili oni, że dwoma istotnymi aspektami związanymi z tworzeniem się pasm jest szybkość odkształcenia oraz poziom odkształcenia. Stwierdzili oni również, że twardość pasm znacznie przewyższa twardość osnowy.

Kluczowe znaczenie z punktu widzenia stabilności austenitu szczątkowego ma rówież sposób odkształcenia plastycznego. Stabilność austenitu jest różna przy ściskaniu i rozciąganiu. Kim i in. [6] poddali analizie stabilność mechaniczną austenitu w funkcji temperatury oraz sposobu odkształcenia. Stwierdzili oni, że efekt TRIP zachodzi najłatwiej w przypadku rozciągania, i najsłabiej przy ściskaniu. Jest to związane ze wzrostem objętości spowodowanej przemianą austenitu w martenzyt. W przypadku rozciągania, naprężenia rozciągające zapewniają „miejsce" dla powstania nowego martenzytu, natomiast przy ściskaniu naprężenia ściskające ograniczają powstawanie martenzytu.

Podziękowania: Praca wykonana i finansowana w ramach grantu Narodowego Centrum Nauki, nr 2017/27/B/ST8/02864.

BIBLIOGRAFIA

1. Z. Gronostajski, A. Niechajowicz, R. Kuziak, J. Krawczyk, S. Polak, The effect of the strain rate on the stress-strain curve and microstructure of AHSS, Journal of Materials Processing Technology 242 (2017) doi:10.1016/j.jmatprotec.2016.11.023.
2. A. Kozłowska, A. Grajcar, A. Janik, K. Radwański, U. Krupp, K. Matus, M. Morawiec, Mechanical and thermal stability of retained austenite in plastically deformed bainite-based TRIP-aided medium-Mn steels, Archives of Civil and Mechanical Engineering 21 (2021) doi:10.1007/s43452-021-00284-6.
3. P. Landau, S. Osovski, A. Venkert, V. Gartnerova, D. Rittel, The genesis of adiabatic shear bands, Scientific Reports 6 (2016) doi:10.1038/srep37226.
4. J. Pelleg, Chapter nine – fracture in AM and traditional manufactured components, Additive and Traditionally Manufactured Components. A Comparative Analysis of Mechanical Properties, 2020, s. 563.
5. J. Marcisz, J. Janiszewski, Mechanical behavior of nanostructured bainitic steel under high strain rate shear and compression loading. Archives of Metallurgy and Materials 64 (2019) doi:10.24425/amm.2019.129508.
6. H. Kim, J. Lee, F. Barlat, D. Kim, M.G. Lee, Experiment and modeling to investigate the effect of stress state, strain and temperature on martensite phase transformation in TRIP-assisted steel, Acta Materialia 95 (2015) doi:10.1016/j.actamat.2015.06.023.

MTS CONFERENCE
MATERIAL TECHNOLOGIES IN SILESIA

12-15.06.2022
Crystal Mountain***** Hotel, Wisła, Poland

Researches of hybrid anti-wear layers obtained on tool materials

D. Pakuła[a], M. Staszuk[a], A. Kříž[b], P. Kožmín[c], A. Čermák[c]

[a] Silesian University of Technology, Faculty of Mechanical Engineering, Department of Engineering Materials and Biomaterials, Konarskiego 18A, 44-100 Gliwice, Poland
email: daniel.pakula@polsl.pl
[b] Jan Evangelista Purkyně University in Ústí nad Labem, Faculty of Mechanical Engineering, Institute of Technology and Materials, Pasteurova 1, 400 01 Ústí nad Labem, Czech Republic
[c] HOFMEISTER s.r.o, Daimlerova 9, 301 00 Pilsen, Czech Republic

Abstract: The aim of this study is to determine the effect of synergistic interaction of hybrid surface treatment of tool materials using PVD physical vapour phase coating deposition and laser texturing methods on the structure and properties of newly developed surface layers on sintered tool material substrates. Extensive studies using scanning electron microscopy (SEM), morphology studies using atomic force microscopy (AFM) and confocal microscopy, and chemical composition studies of the developed materials using an X-ray diffraction spectrometer (EDS) are presented. In addition, performance properties were investigated, including adhesion of PVD coatings to the substrate by scratch test, abrasion resistance by a pin on the disc, and hardness and roughness. It was found that laser texturing of the PVD surface provides an adequate modification of the structure by developing the surface on the micro-and nanoscale, thereby improving the tribological properties of the materials studied.

Keywords: tool materials, PVD, laser texturing, LIPSS

1. INTRODUCTION

Current PVD methods make it possible to produce coatings with extreme tribological properties. However, there is no universal coating suitable for various applications. Therefore, looking for new solutions in this field, the authors of this paper have performed a hybrid surface treatment of tool materials consisting of a PVD process and laser texturing. It has been shown in many scientific papers in recent years that the use of laser texturing on the surface of various engineering materials contributes to the improvement of the properties of these materials. Laser surface texturing, which consists of a local and short-lived thermal or photochemical action of a focused appropriately profiled laser beam, results in the formation of so-called LIPSS - Laser-Induced Periodical Surface Structures. The advantage of this technology, which makes it very interesting for many applications, is the ability to create a nanostructured surface (on a scale below 500 nm) and a microstructured surface in a single process step. LIPSS nanoripples significantly improve the properties of surface layers of engineering materials. They have found wide applications in photonics, biomedicine, thermal conductivity, wettability, tribology, and other areas [1-6].

2. METHODOLOGY

A Zeiss Supra 35 scanning electron microscope was used to observe both the structure and morphology of the obtained surface layers as well as damage to the surface resulting from examination of scratch test and tribological tests. A chemical composition analysis in micro-areas was made with the Energy Dispersive Spectrometry (EDS) method. The LIPSS nanostructure research was carried out using the Park Systems XE-100 AFM atomic force microscope in a non-contact mode. Surface roughness and abrasion profiles were measured with a Surftec 3+ profilometer by RankTaylor Hobson. The adhesion of the coating to the substrate was evaluated with a scratch test method with Revetest equipment by CSEM. Tribological tests were carried out on the CSEM „pin-on-disc" tester.

3. RESULTS

Scanning electron microscopy (SEM) studies have confirmed the formation of a honeycomb-like microstructure and the occurrence of numerous lubricating surfaces (Fig. 1a). Moreover, detailed investigations allow for the conclusion that selective laser texturing of the surface layer of the investigated PVD tool materials causes fragmentation of the microstructure within the laser beam interaction. This characteristic surface development is referred to as laser-induced periodic surface structures (LIPSS), referred to briefly as nanoripples. The visible nanocrystalline texture is characterized by the uniform shape and similar width of the resulting LIPSS nanoripples (Fig. 1b).

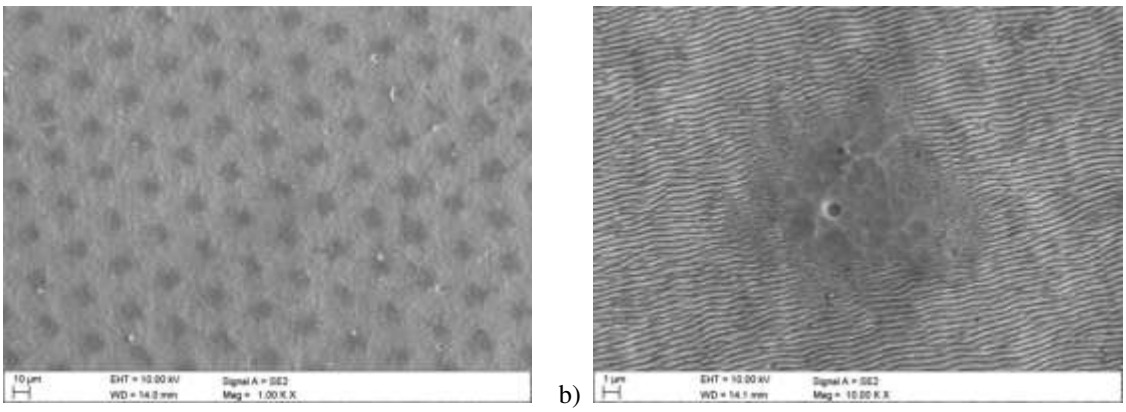

Figure 1. The surface of PVD coating after laser texturing a) visible lubricant reservoirs, b) visible LIPSS nanoripples

Pin-on-disc abrasion resistance tests of the tested PVD-coated tool materials show that laser texturing improves the tribological properties. The abrasion on the surfaces of the tested materials after laser texturing is more uniform along the edges of the tribological trace. It is also observed that the resulting microstructure/nanostructure reduces the contact area with the counter sample material, thus contributing to a reduction in the depth of abrasion. The confirmation that the LIPSS nanoripples improve tribological properties is also provided by the fact that they act as a barrier to damage propagation in the coating when the critical load is exceeded during the scratch test.

Acknowledgments: The investigations are co-financed by the International Visegrad Fund through the Visegrad Scholarship Program.

BIBLIOGRAPHY

1. D. Pakuła, M. Staszuk, M. Dziekońska, P. Kožmín, A. Čermák, Laser Micro-Texturing of Sintered Tool Materials Surface, Materials (2019), 12/19, 3152.
2. D. Pakuła, M. Staszuk, M. Dziekońska, P. Kožmín, A. Čermák, Structure and properties of coating obtained by Chemical Vapour Deposition with the laser microstructuring, Vacuum, 154 (2018) 272–284.
3. D. Pakuła, M. Staszuk, M. Wawrzyczek, P. Kožmín, A. Čermák, Influence of laser texturing on tribological properties of tool materials, Proceedings of the 28th International Conference on Metallurgy and Materials – Metal 2019, 1121–1126.
4. D. Neves, A.E. Diniz, M.S.F. Lima, Microstructural analyses and wear behavior of the cemented carbides tools after laser surface treatment and PVD coating, Applied Surface Science, 282 (2013) 680–688.
5. P. Gregorcic, M. Sedlacek, B. Podgornik, J. Reif, Formation of laser-induced periodic surface structures (LIPSS) on tool steel by multiple picosecond laser pulses of different polarizations, Applied Surface Science, 387 (2016) 698–706.
6. S.K. Mishra, S. Ghosh, S. Aravindan, 3D finite element investigations on textured tools with different geometrical shapes for dry machining of titanium alloys, International Journal of Mechanical Sciences, 141 (2018) 424–449.

MTS CONFERENCE
MATERIAL TECHNOLOGIES IN SILESIA

12-15.06.2022
Crystal Mountain***** Hotel, Wisła, Poland

Thermal diffusivity measurements of foam glass using active infrared thermography

S. Pawlak[a], M.T. Lis[b], P. Sakiewicz[b], K. Gołombek[c]

[a] Silesian University of Technology, Faculty of Mechanical Engineering, Scientific and Didactic Laboratory of Nanotechnology and Materials Technologies
email: sebastian.pawlak@polsl.pl
[b] Silesian University of Technology, Faculty of Mechanical Engineering, Department of Engineering Materials and Biomaterials
[c] Silesian University of Technology, Faculty of Mechanical Engineering, Materials Research Laboratory

Abstract: In this work, the authors applied a simple active infrared thermography technique for the determination of thermal diffusivity of foam glass insulation material. The tests were carried out under the condition of one-dimensional unsteady heat flow, in accordance with ASTM E1461 standard. Three different specimen thicknesses were prepared to analyse the effect of specimen thickness on the measured thermal diffusivity values. The experimental results showed that the thermal diffusivity values increase with increasing specimen thickness; these values varied from 5.63×10^{-7} to 6.97×10^{-7} m^2/s, for 4.9 and 10.5 mm thick specimens, respectively.

Keywords: apparent thermal diffusivity, infrared thermography, unsteady state heat transfer, foam glass

1. INTRODUCTION

Since the last decade, a significant increase of studies concernig the use of active infrared (IR) thermography for the non-destructive testing (NDT) of engineering materials has been observed. Typicaly, this method is applied in both in-service diagnostic and post-production quality control procedures. The active IR thermography has become a widely accepted alternative to traditional testing methods since it can produce a fully quantitative results; for example, by performing the experiment in conditions, which enable to extract the thermal diffusivity values from recorded sequences of thermal images. The testing procedure applied in this paper belongs to a group of transient (heat-pulse) methods for the thermal diffusivity determination, which is based on the *flash method*, firstly introduced by Parker et al. in 1961 [1]. The principle is to heat the front surface of the specimen under investigation (with uniform heat pulse of relatively short duration) and recording the resulting temperature rise on the back surface by IR detector. Due to the simplicity of measurement procedure and low sensitivity to boundary conditions, this method has become the most popular method for the thermal diffusivity determination. However, it has been found from experiments that the thermal diffusivity values determined by means of a pulse method is strongly dependent on the specimen size (thickness), which can be attributed to, e.g., increasing heat losses (during the heat flow) with increasing thickness of the specimen [2]. In this paper, the authors investigated the effect of specimen thicknesses on the measured thermal diffusivity values of foam glass.

2. EXPERIMENTAL PROCEDURE

The in-house test apparatus (scheme shown in Fig. 1) was applied for recording the sequences of thermal images on the back surface of the foam glass specimens (40 x 40 mm^2), in accordance with ASTM E1461 standard [3]. The $t_{0.5}$ values (half-time) taken from normalized temperature-time plot (exemplary shown in Fig. 2) together with specimen thickness (L) were used to calculate the thermal diffusivity (α), based on the equation $\alpha = 1.38L^2/\pi^2 t_{0.5}$ [1,3]. The $t_{0.5}$ values together with calculated thermal diffusivity values are shown in Table 1.

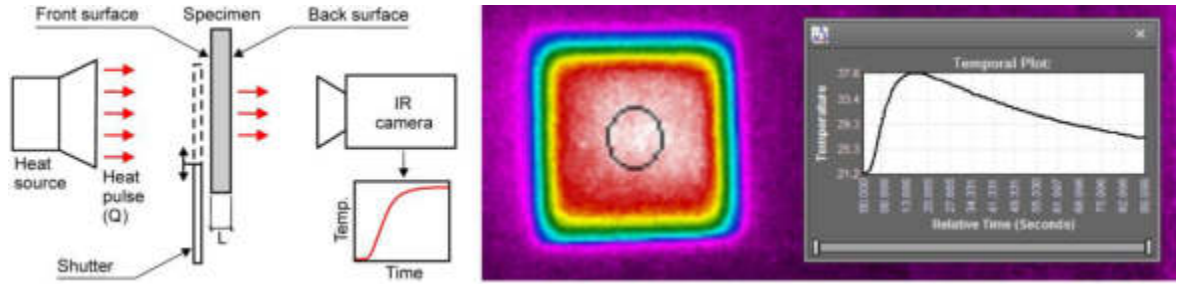

Figure 1. Scheme for the thermal diffusivity measurements and exemplary thermal image of 4.93 mm specimen

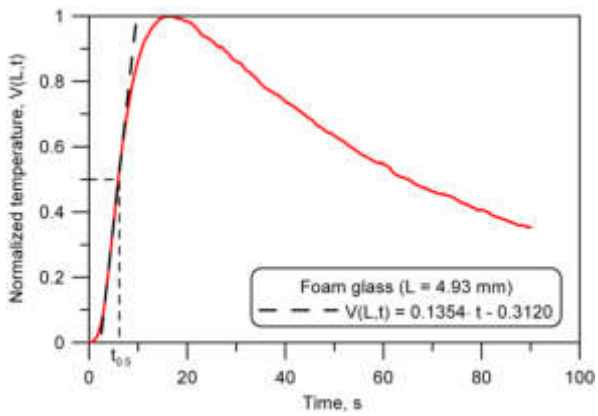

Figure 2. Normalized temperature increase on a back surface of 4.93 mm specimen

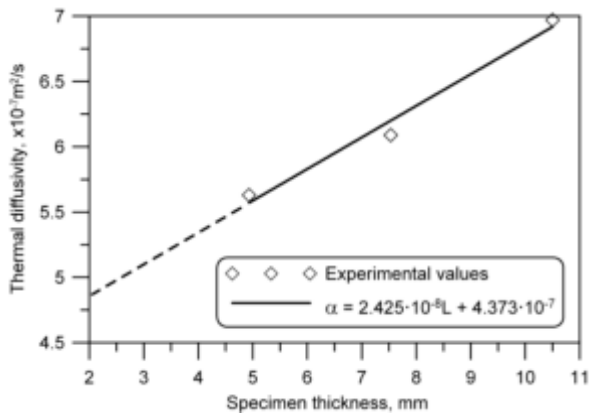

Figure 3. Effect of specimen thickness on measured values for the thermal diffusivity of foam glass

Table 1. Specifications and experimental thermal diffusivity values for tested specimens

Specimen no.	Thickness [mm]	Density [g/cm^3]	Time $t_{0.5}$ [s]	Thermal diffusivity [m^2/s]
1	4.93	0.35	6.00	5.626 x10^{-07}
2	7.53	0.30	12.92	6.089 x10^{-07}
3	10.50	0.28	21.96	6.970 x10^{-07}

3. CONCLUSIONS

In this study, the effect of specimen thickness on the thermal diffusivity values of a low thermal conductivity foam glass specimens was investigated by using a simple IR thermography technique. The obtained experimental results showed that the thermal diffusivity values increase with increasing specimen thickness, which is attributed to greater heat losses during the measurement for specimens of higher thickness. The tests were carried out on the specimens of relatively high thicknesses, hence the value of thermal diffusivity, which will be closer to the real value, can be obtained by extrapolating the experimental line (Fig. 3) to lower thickness values.

Acknowledgments: The research was carried out as part of the project "Process optimisation and valorisation of combustion by-products in the transition to a circular economy (UPS-Plus)", grant number POIR.04.04.00-00-31B4/17-00, financed by the TEAM-TECH Core Facility by Foundation for Polish Science.

BIBLIOGRAPHY

1. W.J. Parker, R.J. Jenkins, C.P. Butter, G.L. Abbot, Flash method of determining thermal diffusivity, heat capacity and thermal conductivity, Journal of Applied Physics 32 (1961) 1679-1684.
2. D.P.H. Hasselman, K.Y. Donaldson, Effects of detector nonlinearity and specimen size on the apparent thermal diffusivity of NIST 8425 graphite, International Journal of Thermophysics 11 (1990) 573–585.
3. ASTM E1461-07 Standard test method for thermal diffusivity by the flash method.

MTS CONFERENCE
MATERIAL TECHNOLOGIES IN SILESIA

12-15.06.2022
Crystal Mountain***** Hotel, Wisła, Poland

Spark plasma sintering of irregular and plasma spheroidized $AlCoCrFeNiTi_x$ powders

K. Pęcak[a], A. Janoszka[a], M. Osadnik[a], K. Bilewska[a], A. Wrona[a], P. Tomczyk[a], M. Lis[a], K. Pepłowska[a], A. Duda[a]

[a] Łukasiewicz Research Network – Institute of Non-Ferrous Metals, Centre of Powder and Composite Materials
email: krzysztof.pecak@imn.lukasiewicz.gov.pl

Abstract: Mechanical alloying of AlCoCrFeNiTix powders has been carried out with the use of a planetary ball mill. Alloy powders were plasma spheroidized to improve flowability. Irregular and spherical powders were sintered with the use of Spark Plasma Sintering System HP D-5 by FCT.

Keywords: High Entropy Alloys (HEA), Complex Conentrated Alloys (CCA), metal powder, mechanical alloying, plasma spheroidization, spark plasma sintering

1. INTRODUCTION

Most of the currently used metal alloys are based on one primary element, that is then alloyed with various other elements to change and improve the properties of the alloy. In recent years, a new concept has been gaining increased interest – High Entropy Alloys - HEAs (more recently, Complex Concentrated Alloys - CCAs, Multi-Principal Element Alloys – MPEAs, or "baseless" alloys). These alloys are made of many (typically 5 or more) elements that are present in concentrations between 5 and 35 percent [1]. Concurrent idea that is gaining traction in the research community is to describe these materials as alloys, that are located in the central regions of multi-component phase diagrams [2]. Regardless of specific definitions, this new approach resulted in multitude of new phases and properties originating from the vast number of compositions opened for study. Contrary to previous beliefs, such alloys often exhibit much simpler phase structures, than implied by Gibbs phase rule. In fact, even single-phase alloys can be obtained in this group.
Some HEAs, particularly consisting of aluminium and 3d transition metals can exhibit very high tensile strength, while also maintaining relatively low density [3]. In this work, $AlCoCrFeNiTi_x$ alloys were selected as materials that can achieve high specific strength and still posses relatively high elastic modulus with a value close to steel (~180GPa) [4]. Alloys were synthesized by mechanical alloying in planetary mill, using tungsten carbide vials with tungsten carbide balls. Different parameter combinations were explored, including process control agent (PCA) type and amount, synthesis time, ball-to-powder ratio (BPR), rotations per minute (RPM) and milling schemes. Powder was then spheroidized with the use of a proprietary plasma spheroidization system. Obtained irregular and spherical powders were Spark Plasma Sintered to obtain solid samples.

1.1. Mechanical alloying parameter range

Table 1. Parameter range used for synthesis investigations.

Atmosphere	PCA	Rotation speed	BPR	Time	Powder load
-	% wt.	RPM	-	h	g
Air, argon	Acetone, ethanol 1-5, stearic acid 1-6, none	150-300	5:1, 10:1	5-30	50, 100

1.2. Phase composition

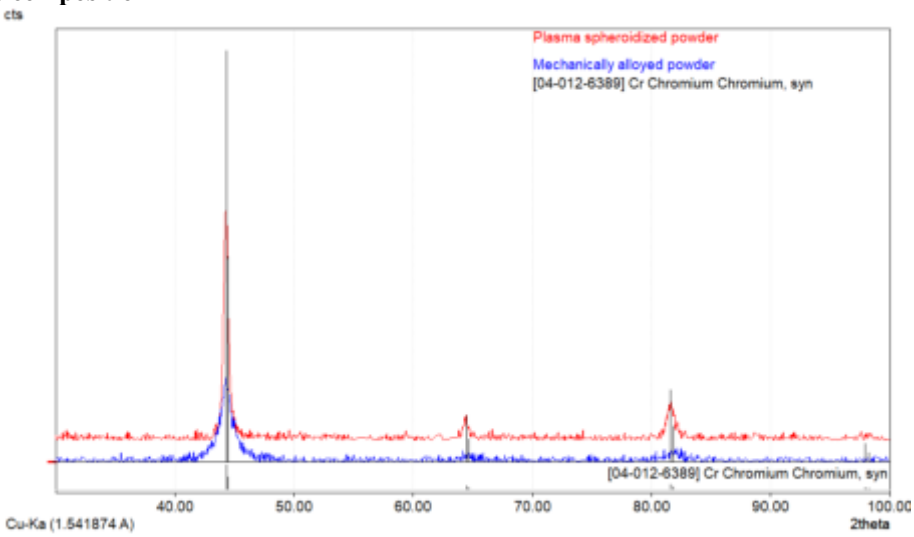

Figure 1. XRD patterns of synthesised powder and plasma spheroidized powder.

1.3. Powder morphology

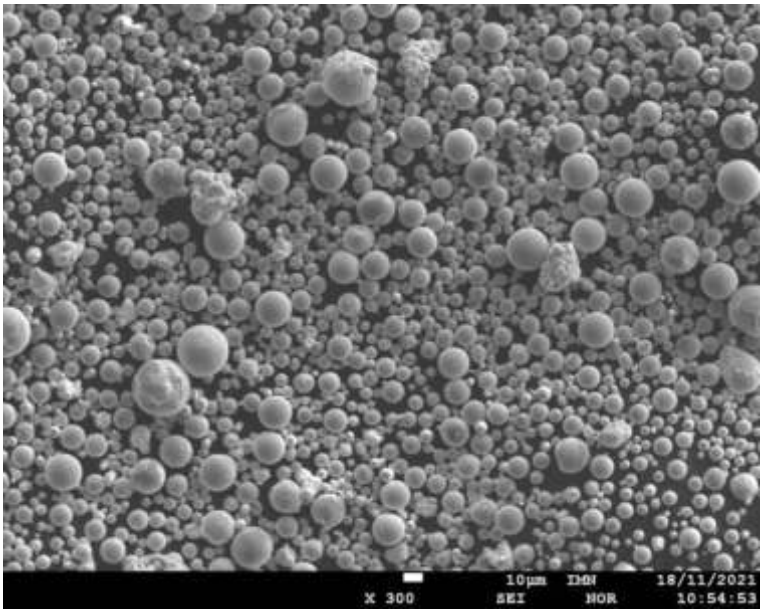

Figure 2. Spheroidized powder morphology, topological contrast, magnification 300x.

Acknowledgments: This research has been carried out as part of Ministry of Science and Education subventions, reports number 8072/20 "Nowe proszki ze stopów o wysokiej entropii dedykowane do wytworzenia elementów spiekanych" and 8186/21 "Synteza mechaniczna stopów o wysokiej entropii przeznaczonych do technologii przyrostowych".

BIBLIOGRAPHY

1. B.S. Murth, J. Yeh, S.S. Ranganathan, P.P.Bhattacharjee, High-Entropy Alloys 2nd edition, Elsevier, 2019.
2. S. Gorsse, J-P. Couzinié, D.B.Miracle, From high-entropy alloys to complex concentrated alloys, Comptes Rendus Physique 19 8 (2018) 721-736.
3. S. Gorsse, M.H. Nguyen, O.N. Senkov, D.B. Miracle, Database on the mechanical properties of high entropy alloys and complex concentrated alloys, Data in Brief 21 (2018) 2664-2678.
4. Y.J. Zhou, Y. Zhang, Y.L. Wang, G.L. Chen, Solid solution alloys of AlCoCrFeNiTix with excellent room-temperature mechanical properties, Applied Physics Letters 90 181904 (2007).

MTS CONFERENCE
MATERIAL TECHNOLOGIES IN SILESIA

12-15.06.2022
Crystal Mountain***** Hotel, Wisła, Poland

Optimization of welding of structures with respect to welding distortion using the finite element method

J. Pikuła[a], M. Węglowski[a], K. Kubik[a], K. Kwieciński[a], R. Czech[b], M. Spólnik[b]

[a] Łukasiewicz Research Network – Institute of Welding, Bł. Czesława 16-18 44-100 Gliwice
email: janusz.pikula@is.lukasiewicz.gov.pl
[b] Naftoremont-Naftobudowa Sp. z o.o., ul. Sikorskiego 17, 38-460 Jedlicze

Abstract: The article describes the optimization of welding of structures with respect to welding distortion. The research was conducted using finite element method (FEM). The influence of different type of welding clamps on welding distortion has been investigated.

Keywords: welding, welding distortion, FEM, welding clamps

1. INTRODUCTION

The prevention of welding distortion is one of the most important and, at the same time, most difficult issues in welding engineering. Welding distortion often could even lead to the disqualification of the final product failing to satisfy related standard requirements concerning maximum distortion values. Welding distortion occurs along with stresses generated in the welded joint area as well as in areas located farther from the joint (fig. 1).

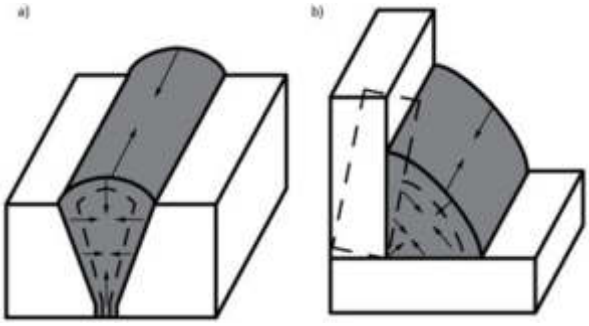

Figure 1. Direction of volume changes in butt (a) and fillet (b) welds during cooling down after the welding process

The possibility of forecasting the probable structure imperfections during assembly and the prevention of such imperfections as early as at the design stage and when scheduling assembly make it possible to reduce costs and delays resulting from the removal of distortion. The use of appropriate methods can reduce welding distortion yet it does not ensure their entire elimination. For this reason, the forecasting of distortion-triggered consequences is of great importance. Knowledge about possible structure defects when designing the process of assembling and that of welding can be utilised to prevent the occurrence of unwanted results through, among other things, providing allowances in elements being welded. Engineering practice relies on analytical methods involving calculations of total distortion presents in elements of welded structures. Knowledge concerning possible welding distortion can also be obtained by performing FEM-based numerical analyses concerned with the welding of structures [1-11].

2. SCOPE OF RESEARCH

The purpose of the analyzes was to forecast welding distortion of the furnace wall. Various configurations of the element clamping during welding (fig. 2a) were calculated (fig. 2b). The modelling process included the preparation of geometry, finite element mesh and the determination of boundary conditions, i.a. the clamping of the element during welding. FEM mesh was made of shell elements with defined thickness material properties. Modelling of welding was performed using the "shrinkage method". In the area of welded joints it was induced the shrinkage, which value was defined by the coefficient of thermal expansion of the material.

a) b)

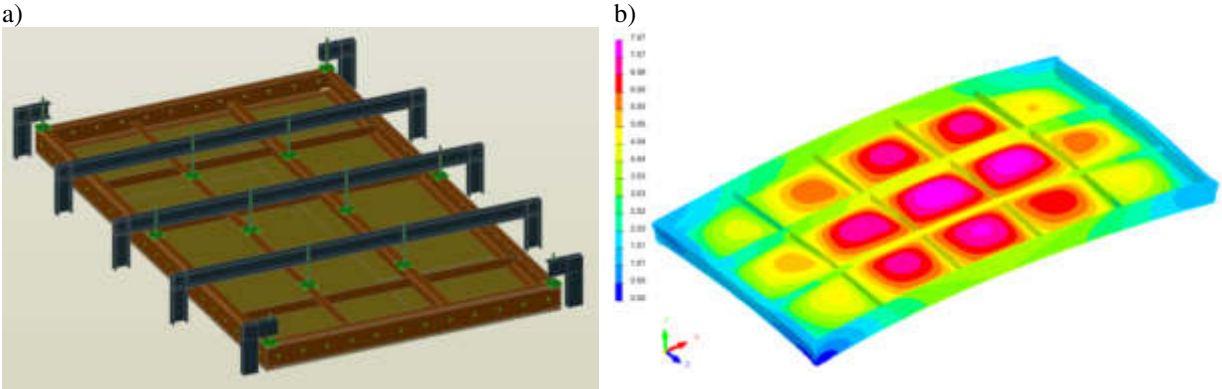

Fig 2. a) The analysed welded structure and clamping method, b) total displacements after welding clamping release

3. CONCLUSIONS

Dimensionally significant displacements occurred in the direction perpendicular to the furnace wall surface. The largest displacements were noticed in the central region of the modelled structure in all analyzed clamping configurations. The structure after clamping release was characterized by local bulging of the plate between the ribs. It was also observed general bulging of the entire structure. Comparing all analysed clamping configurations, the difference of maximum displacement in the perpendicular direction of the analyzed structures was up to 4%. The difference of average displacement at selected points was up to 11%.

Acknowledgments: The project was carried out within the framework of "Regional Operational Programme" (ROP) for the 2014-2020 period for Podkarpackie Voivodship contract No RPPK.01.02.00-IZ.00-18-012/19.

BIBLIOGRAPHY

1. Kowalski D.: Wpływ imperfekcji wykonawczych na stan naprężeń w płaszczu stalowego zbiornika walcowego o osi pionowej. Praca doktorska, Politechnika Gdańska, Wydział Inżynierii Lądowej, Katedra Konstrukcji Metalowych, 2004.
2. Ziółko J.: Imprefekcje stalowych zbiorników walcowych, przyczyny ich powstawania, metody ograniczania. Konferencja "Problemy Eksploatacyjne Baz Magazynowych Produktór Naftowych", Poznań, 11-12 May 1999.
3. Kelly S.M., Martukanitz R.P.: Minimizing buckling distortion in welding by hybrid laser-arc welding. Minimization of Welding Distortion and Buckling. Modelling and Implementation, 2011, pp. 241–273.
4. Wang J., Yuan H., Ma N., Murakawa H.: Recent research on welding distortion prediction in thin plate fabrication by means of elastic FE computation. Marine Structures, 47, 2016, pp. 42–59.
5. Hübner A., Teng J.G., Saal H.: Buckling behaviour of large steel cylinders with patterned welds. International Journal of Pressure Vessels and Piping, 2006, 1, 83, pp. 13–26.
6. Li Y., Wang K., Jin Y., Xu M., Lu H.: Prediction of welding deformation in stiffened structure by introducing thermo-mechanical interface element. Journal of Materials Processing Technology, 216, 2015, pp. 440–446.
7. Barsoum Z., Bhatti A.A., Balawi S.: Computational weld mechanics – towards a simplified and cost effective approach for large welded structures. Procedia Engineering, 114, 2015, pp. 62–69.
8. Fu G., Lourenço M.I., Duan M., Estefen S.F.: Influence of the welding sequence on residual stress and distortion of fillet welded structures. Marine Structures, 46, 2016, pp. 30–55.
9. Zhou Q., Wang Y., Choi S-K., Cao L., Gao Z.: Robust optimization for reducing welding-induced angular distortion in fiber laser keyhole welding under process parameter uncertainty. Applied Thermal Engineering, 129, 2018, pp. 893–906.
10. Park J., An G.. Prediction of the welding distortion of large steel structure with mechanical restraint using equivalent load methods. International Journal of Naval Architecture and Ocean Engineering, 3, 9, 2017, pp. 315–325.

MTS CONFERENCE
MATERIAL TECHNOLOGIES IN SILESIA

12-15.06.2022
Crystal Mountain***** Hotel, Wisła, Poland

Development of technologies and equipment for recycling polyethylene terephthalate waste into consumables and finished product

A. Polishchuk [a], M. T. Tański [b]

[a] Khmelnytskyi National University, Faculty of Mechanical Engineering, Transport and Architecture, Department of Machines and Apparatuses, Electromechanical and Power Systems
email: opolishchuk71@gmail.com
[b] Silesian University of Technology, Faculty of Mechanical Engineering, Department of Engineering Materials and Biomaterials
email: tomasz.tanski@polsl.pl

Abstract: The article describes the technologies and equipment for recycling polyethylene terephthalate waste into consumables and finished product

Keywords: 3D-printers, extruder, shredder, polymer material, polyethylene terephthalate

The problem of recycling PET waste is relevant for the whole world community, so it must be solved by joint efforts based on research and advanced technologies.
One way to recycle plastics is to use recycled polyethylene terephthalate waste, in particular PET bottles and light industry textile waste, into consumables for 3D-printers. The use of additive technologies is one of the most striking examples of how new developments and equipment can significantly improve traditional production [1].

The problem of processing hollow thin-walled containers and the rational use of crushed polymers can be solved by creating new efficient equipment for grinding and technologies for further processing.

It was proposed to use a rotary knife crusher to grind such products [2]. In such equipment the concentrated cutting of waste by knives which are located both in a rotor and in a stator is carried out.

The shredder consists of the housing, hopper, tray, rotor with fixed knives, fixed knives mounted on the housing, removable calibrated grid, the size of the holes which determines the required dispersion of crushed materials. The transmission of torque from the shaft of the motor to the rotor is carried out by a belt drive consisting of a pulley, a flywheel with a pulley and V-belts.

The process of grinding the material begins with its loading into the window, where it falls on the rotor and its knives. The material is crushed in interaction with the rotor blades and fixed stator blades. After that, the material is sifted through a sieve and enters the hopper of the finished product.

When grinding waste polymeric materials, the rotary crusher has a fairly high productivity and uniformity of work. The main criterion of these indicators is the correct loading of waste into the working chamber, which is carried out by the operator manually.

However, when grinding used bottles of polyethylene terephthalate was a significant disadvantage of the process of loading them into the crusher. Containers, getting into the working chamber, come into contact with the movable blades of the rotor, chaotically reflected from them and the process of grinding them is accompanied by delays. The reason is the proportionality of the space between the knives and the size of the containers.

Preliminary experiments were performed, during which the time of grinding bottles with a capacity of 2 liters with successive continuous loading was determined. Experiments have shown that when loading bottles that are cut lengthwise into three parts, the productivity of grinding is 5… 6 times higher than when loading the whole container.

As a result of the experiment, it was concluded that it is expedient to equip the crusher with a roller device for deformation and pre-cutting of used bottles, which should be installed at the entrance to the working chamber.

Based on the analytical dependences that link the design and technological parameters of rolling devices with energy costs, productivity of these devices and the quality of recycled polymer waste, equipment for processing polymer waste from the garment and footwear industries was developed, namely polyester. The quality of the processed material is determined by the degree of orientation of the structure of the obtained polymer fragments and their shape. To destroy the structure of the polymeric material, a device with toothed rolls and a device with rolls of the Relo profile are used. After the weakening process, the polymeric material comes under the action of the needle cutter, where it is finally defocused.

The resulting crushed material can be used as a raw material for a 3D printer in the manufacture of finished products and materials [3].

When processing polyethylene terephthalate products into raw materials for a 3D printer, the following operations are performed sequentially: sorting of waste by color and removal of plastic impurities of the second type; grinding of the selected waste with the use of a rotary crusher and obtaining a flex of a given dispersion; washing flakes with clean water; drying of flakes by a stream of hot air in the drying device.

The obtained results confirmed the possibility of using PET-flex as a raw material for a 3D printer for the manufacture of finished products and parts.

The installation for the manufacture of products and parts of industrial engineering and light industry and experimental research will be developed on the basis of an 3D printer Anycubic Mega S with FMD printing technology from the Chinese company Anycubic.

The filament feed mechanism in this model has been improved. A short Titan-type extruder is used, which allows you to increase torque, organize accurate filament feed and print parts.

In the first case, a strip of PET bottle is used as a raw material for this 3D printer. The strip of the set width is preliminary cut by the specially developed device.

In the second case, the raw material is crushed polymer. Therefore, in this installation, the filament print head will be dismantled and an extruder will be installed to process the polymer masses entering it in the form of crushed polymers, such as PET flex.

The 3D model of the designed extruder in the SolidWorks software environment is shown in Fig.1.

Figure 1 - Extruder model in SolidWorks software environment

Pre-conducted experimental studies on the developed extruder using crushed PET-flex as raw materials confirmed its performance. In the future, it will be installed a developed device on Anycubic Mega S and setting up optimal operating modes for the manufacture of finished products and details.

Acknowledgments: Andrii Polishchuk is a holder of Scholarship of International Visegrad Fund, granted for the period between September 2021 and June 2022.

BIBLIOGRAPHY

1. P.F. Zozulya, O.S. Polishchuk, A.O. Polishchuk Prospects for the use of 3D printing in light industry / Bulletin of the Khmelnytsky National University.- 2017. - №4. - P.102-104.
2. M.E. Skiba, O.V. Misiats, A.O. Polishchuk, V.P. Misiats, M.M. Rubanka. System of adaptive frequency control of rotation speed of asynchronous three-phase electric motor of rotor crusher drive Visnyk of Khmelnytsky National University. Technical sciences, 2021. – №2. – P.139-146.
3. Oleh Polishchuk, Petro Zozulia, Andrii Polishchuk, Pavlo Maidan, Mykola Skyba. Development and research of equipment for processing of granulated polymeric materials via 3d printing for the needs of light industry. Fibres and Textiles. 2020. №4. P.75-80.

MTS CONFERENCE
MATERIAL TECHNOLOGIES IN SILESIA

12-15.06.2022
Crystal Mountain***** Hotel, Wisła, Poland

The manufacturing products of branch mechanical engineering by 3D-printing method from composite filaments with high metal content

O. Polishchuk[a], M. Bonek[b]

[a] Khmelnytskyi National University, Faculty of Mechanical Engineering, Transport and Architecture, Department of Machines and Apparatuses, Electromechanical and Power Systems
email: opolishchuk71@gmail.com
[b] Silesian University of Technology, Faculty of Mechanical Engineering, Department of Engineering Materials and Biomaterials
email: miroslaw.bonek@polsl.pl

Abstract: The article describes the technological process and equipment for manufacturing products of branch mechanical engineering by 3D-printing method from composite filaments with high metal content

Keywords: 3D-printing, extrusion machine, stainless steel metal powder, polymer material

The yield, in some industries, is not more than 30% of the material used. 3D metal printing consumes less energy and reduces waste to a minimum. In addition, the finished 3D-printed product can be up to 60% lighter, compared to the milled or cast part. The strength and lightness of parts are required in the production of certain products in various industries. This, in turn, also leads to a reduction in the cost of products [1].

The proposed technology of manufacturing products using filament with a high content of metal powders based on stainless steel with the use of 3D-printers with a closed construction chamber in a wide range of printing parameters, working on the technology of layer-by-layer surfacing of polymer thread (FDM) [2, 3].

The scheme of technological process of manufacturing products of branch mechanical engineering by the method of 3D-printing from composite filaments with high content of the metal is presented in Fig. 1. This technology consists of five stages: mixing of fine metal powder and binder polymer material; making filament for 3D-printing from a mixture; printing on a 3D-printer «green» part; removal of the polymeric binder to obtain a "brown" part; sintering in the oven and obtaining the finished product. The raw material for this technology is a mixture of fine metal powder and a polymeric binder.

Stainless steel metal powder from a Chinese manufacturer was used to make the filament. Stainless steel metal powder particles were examined by energy-dispersive X-ray spectroscopy (EDS) to assess their chemical composition. The chemical composition of stainless steel particles includes: iron (Fe), chromium (Cr), nickel (Ni), molybdenum (Mo), silicon (Si). The main elements of this steel are Fe (approximately 65%), Cr (17%) and Ni (9%). As a result of research, it was found that the composition meets the standard characteristics of stainless steel AISI 316L.

At the first stage of the described technology (Fig. 1) using a mixer there is a mixing of two components for obtaining raw materials. In the second stage, an extrusion machine is used to receive a filament for 3D-printing. The proposed extrusion machine consists of the following parts: the housing with the heating system to the required melting point of the polymer; the loading unit through which a pre-prepared mixture of polymer and metal particles of stainless steel enters the cavity of the housing; cavities of the casing with a screw to move raw materials from the loading node to the molding nozzle; screw; extrusion head, which sets the diameter of the manufactured thread; cooling and winding systems for filament; control and management systems that supports the required technological mode.

Due to the fact that a metal powder is included in the composition of the filament, the design of a screw for feeding material was developed and manufactured. The form of an extrusion head that sets the diameter of the manufactured thread was developed.

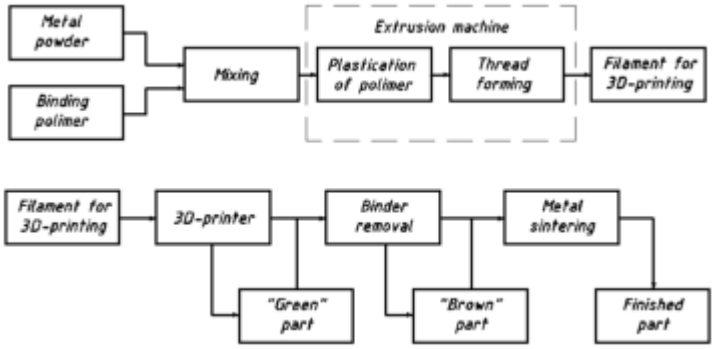

Figure 1. Scheme of technological process of manufacturing products of branch mechanical engineering by 3D-printing method from composite filaments with high metal content

Experimental studies of wearing extrusion head of the extruder were conducted in contact with abrasive philistine. For this purpose, extrusion heads are made of various materials. As a result of the experiment, it is found that the smallest of the head is made of steel. Therefore, for the full operation of the extruder, it was proposed to use in the extruder forming head of tempered steel E3D with a diameter of 1,75 mm. The manufacture of a filament when using the forming brass nozzle resulted in a rapid wear of brass. The wear of the material leads to an increase in the diameter of the filament, which should be precisely 1,75 mm.

Filament consisting of 85% stainless steel powder and 15% binding polymer is made by extruding the raw material on the proposed equipment at a heating temperature of 130 C and extrusion velocity of 50 mm / min. The extruded thread with a diameter of 1,75 is fed through a coercive cooling system and is uniformly wound on a coil. For printing, a 3D-printer 4max Pro of the Chinese firm AnyCubic has been selected.

One of the factors in choosing was that this 3D-printer has a fully closed design. This will allow to maintain the temperature required for printing from the use of a filament filled with stainless steel powder.

Due to the fact that threads with metal fillers (especially with stainless steel powder) are very abrasive and require a printer with another load mechanism, as well as another design of the printing head, an extruder improvement was performed.

Improvement was concluded in the development of a new mechanism for transporting a filament with abrasive material.

Also, experimental studies of wearing the nozzle of the extruder were carried out in contact with abrasive filament. Similarly, as well as the molding head of an extrusion machine. For a complete operation of the printer, it was proposed to use an extruder with a tempered steel E3D with a diameter of 5 mm.

Thus, on the basis of the obtained polymer thread at certain optimal parameters on an advanced 3D-printer was printed "green" part (Fig. 1). Subsequently, the connector was removed from the obtained part and its metal particles were sintered in the furnace. Experimental studies of the finished product using optical and scanning electron microscopy have shown that it has low porosity and reduced volume (shrinkage) due to polymer loss. This factor must be taken into account at the design stage of the product. The resulting part has electrically conductive properties as a metal. It can then be subjected to technological operations of grinding and polishing.

Acknowledgments: Oleh Polishchuk is a holder of Scholarship of International Visegrad Fund, granted for the period between September 2021 and June 2022.

BIBLIOGRAPHY

1. O. Polishchuk, M. Bonek, M. Skyba, A. Polishchuk, S. Lisevich Prospects of using composite filaments with high metal content for manufacture of industrial machine building products method of 3d printing. IX Ukrainian-Polish Scientific Dialogues: Conference Proceedings. International Scientific Conference, 20-23 October 2021, Khmelnytskyi (Ukraine). – Khmelnytskyi National University, 2021. – P.390-396.
2. Marius A. Wagner, Amir Hadian, Tutu Sebastian, Frank Clemens, Thomas Schweizer, Mikel Rodriguez-Arbaizar, Efrain Carre˜no-Morelli, Ralph Spolenak. Fused filament fabrication of stainless steel structures - from binder development to sintered properties. Additive Manufacturing. Volume 49, January 2022, 102472.
3. Fábio Cerejo, Daniel Gatões, M.T. Vieira. Optimization of metallic powder filaments for additive manufacturing extrusion (MEX). The International Journal of Advanced Manufacturing Technology (2021) 115:2449–2464.

MTS CONFERENCE
MATERIAL TECHNOLOGIES IN SILESIA

12-15.06.2022
Crystal Mountain***** Hotel, Wisła, Poland

Polymer composites with carbon fillers

M. Polok-Rubiniec[a], A. Włodarczyk-Fligier

[a] Silesian University of Technology, Faculty of Mechanical Engineering, Department of Engineering Materials and Biomaterials
email: magdalena.polok-rubiniec@polsl.pl

Abstract: The article described properties of the polymer composites with a charcoal and anthracite fillers. The tested polymer composites in the form of granules were produced by extrusion, and then standardised test profiles were made by injection moulding. Results of surface and volume resistivity of the tested PP composite - charcoal and PP composite – anthracite are presented.

Keywords: Polymers composites, carbon fillers, resistivity,

1. INTRODUCTION

Carbon fillers, which include various types of carbon black and graphite, as well as hard coal, shungite, anthracite, are very popular, they are an alternative to expensive fillers made of carbon nanotubes. Carbon fillers enhance the resistance of polymers to heat, environmental factors and UV radiation. Depending on the type of carbon filler, it is possible to achieve the desired volume and surface resistivity and magnetostrictive properties of polymers, preponderantly for polyolefin-matrix composites. In addition to improving electrical properties, carbon fillers are expected to improve mechanical properties, in particular abrasive wear resistance and hardness. It was found that the use of carbon black evenly distributed in the polypropylene matrix significantly increases the value of the longitudinal stiffness modulus and causes a slight increase in the mechanical strength of the material. The addition of shungite and anthracite in polypropylene matrices increased the hardness and stiffness of the tested composites [1-6].

2. EXPERIMENTAL

The investigations were carried out on the samples of the polypropylene (PP) matrix composite with addition of 10%, 20%, 30%, 40%, 50% of anthracite dust and charcoal powder. The anthracite dust and charcoal powder was dried for several hours at 100°C and mixed with polypropylene granules. The blends PP/anthracite dust and PP/charcoal powder were homogenised using a Göetffert counter-rotating twin-screw extruder, with an L/D25 ratio, equipped with a bar extrusion head with an exit diameter of ø 3 mm. The extrusion parameters were used: 1st zone temp. 200°C; 2nd zone temp. 220°C; 3rd zone temp. 230°C; head temp. 240°C; turnover: 6-8 rpm. As a result of extrusion, a granulate was obtained from which test pieces were prepared (in the form of 1Awg type "paddles" as per PN-EN ISO 527-2:2012 standard) by injection moulding using the Battenfeld Plus 35/75 injection moulding machine with a Unilog B2 control system, with a ratio of L/D 17.

The surface and volume resistivity of the PP/anthracite and PP/charcoal composites tested were determined using a test voltage of 300 V. The tests were carried out in accordance with the research methodology according to ASTM D257-14 and IEC 60093:1980 and were determined using the Keithley Instruments Inc. model 8009 electrometer.

3. RESULTS

The volume and surface resistivity of the produced PP/anthracite and PP / charcoal composites were tested, due to the filler used in the form of anthracite dust and charcoal powder, which is to improve the electrical

properties of the polymer composite. It was found out that the surface and volume resistivity has declined by introducing anthracite dust and charcoal powder into the polymer material (Tab.1). Surface and volume resistivity values for PP are, respectively, 1.17E+17Ω and 1.12E+17Ωcm. The presence of anthracite with 50% content reduces the surface and volume resistivity to 1.77E+15Ω and 4.62E+15Ω. The values examined for the samples are indeed 10 to 100 times lower than those for an unmodified material, but they are still relatively high and do not allow to classify the obtained materials as semiconductors (conventional limit value of 10^7Ωm). The produced PP/antracite and PP/charcoal composites can be used wherever an increase in anti-electrostatic properties is needed – e.g. in electronics or components working in potentially explosive areas. It is worth noting that the tests showed a much greater impact of the charcoal filler introduction on the volume resistance value than on the surface resistance. This is probably due to the formation of percolation paths deep inside the material, which allowed the flow of electric charges. However, the effects associated with the flow of a plasticised composite during the formation of samples prevented the formation of this type of electrical connections on the surface of the samples.

Table 1. Effects of anthracite and charcoal content on surface and volume resistance

Marking of the samples	Surface resistance (ASTM D257/IEC 60093) U=300V [Ω]	Volume resistance (ASTM D257/IEC 60093) U=300V[Ωcm]
PP	1.17E+17	1.12E+15
PP/10% anthracite	4.84E+15	7.67E+13
PP/20% anthracite	1.86E+15	2.64E+13
PP/30% anthracite	9.28E+14	1.00E+13
PP/40% anthracite	6.15E+14	2.44E+12
PP/50% anthracite	1.77E+15	4.62E+13
PP/10% charcoal	6.64E+14	4.06E+15
PP/20% charcoal	6.41E+14	1.89E+08
PP/30% charcoal	1.01E+15	5.00E+07
PP/40% charcoal	1.61E+15	5.12E+07
PP/50% charcoal	1.69E+15	3.77E+08

4. SUMMARY

The introduction of anthracite dust and charcoal powder into the polypropylene matrix increased the electrostatic properties, but worsened the electrical insulating properties. The resistivity of the material was managed to be lowered only slightly by introducing anthracite into the polypropylene matrix.

BIBLIOGRAPHY

1. A. Boczkowska, J. Kapuściński, Z. Lindermann, Composites, OWPW, Warsaw, 2003, in polish
2. J. Stabik, M. Chomiak, Ł. Suchoń, A. Dybowska, K. Mrowiec: Chosen manufactured methods of polymeric graded materials with electrical and magnetic properties gradation, Archives of Materials Science and Engineering 54/2 (2012) 218-226
3. J. Korol, A. Hejna, D. Burchart-Korol, B. Chmielnicki, K. Wypiór: Water Footprint Assessment of Selected Polymers, Polymer Blends, Composites, and Biocomposites for Industrial Application, Polymers 11/11 (2019) 1791
4. H. Nazarpour-Farrad, K. Rad-Moghadam, F. Shirini, M.H. Beheshty, G.H. Asghari: Reinforcement of epoxy resin/carbon fiber composites by carboxylated carbon nanotubes: a dynamic mechanical study, Polymers 63/4 (2018) 253-263
5. H. Liu, D. Bai, H. Bai, Q. Zhang, Q. Fu: Manipulating the filler network structure and properties of Polylactide/carbon black nanocomposites with the aid of stereocomplex crystallites, The Journal of Physical Chemistry C *122/*8 (2018) 4232-4240
6. M. Polok-Rubiniec, A. Włodarczyk-Fligier, B. Chmielnicki: The properties of a polypropylene matrix composite with anthracite filler, Archives of Metallurgy and Materials 66/1 (2021) 305-3011

MTS CONFERENCE
MATERIAL TECHNOLOGIES IN SILESIA

12-15.06.2022
Crystal Mountain***** Hotel, Wisła, Poland

Wpływ długotrwałej pracy w warunkach pełzania na właściwości użytkowe stopu 800HT

H. Purzyńska[a]

[a] Sieć Badawcza Łukasiewicz – Instytut Metalurgii Żelaza im. St. Staszica, 44-100 Gliwice, ul. K. Miarki 12-14 email: hanna.purzynska@imz.lukasiewicz.gov.pl

Abstract: W pracy przedstawiono wyniki badań stopu 800HT w stanie wyjściowym oraz po długotrwałej eksploatacji w warunkach pełzania. Przeprowadzono badnia właściwości mechanicznych w temperaturze pokojowej oraz próby pełzania. Wykonano obserwację mikrostruktury badanego materiału pod kątem opisu zmian struktury i rozwoju procesów wydzieleniowych.

Abstract: The paper presents the results of tests of the 800HT alloy in its initial state and after long-term creep service. The study of mechanical properties at room temperature and creep tests were carried out. Observation of the microstructure of the tested material was perfomed in terms of description of structure changes and development precipitation processes.

Keywords: microstructure, 800HT alloy, mechanical properties, creep tests

1. WSTĘP

Długotrwała praca w warunkach pełzania urządzenia powoduje znaczne zmiany w materiale, powodując utratę trwałości eksploatacyjnej. Definiuje się nią jako zdolność do zachowania wymaganych właściwości użytkowych do chwili osiągnięcia umownego stanu granicznego, powyżej którego eksploatacja jest niewskazana.

Badania mikrostruktury stopów na bazie niklu po długotrwałym oddziaływaniu temperatury i naprężenia umożliwiają ocenę dynamiki zmian mikrostruktury oraz zachodzącego intensywnego procesu wydzieleniowego, co pozwala na obiektywna interpretację degradacji stopów wskutek długotrwałej eksploatacji w warunkach pełzania. Materiał do badań stanowił stop Inconel 800HT w stanie wyjściowym oraz po eksploatacji, przeznaczony na rury katalityczne reformerów metanu.

W ostatnich latach nastąpił gwałtowny wzrost zapotrzebowania przemysłu na wodór. Jest on wykorzystywany w branży rafineryjnej, hutniczej, przemyśle stalowniczym, przemyśle chemicznym oraz planuje się także odnaleźć mu miejsce w energetyce. Przeprowadzone studium literaturowe wykazało, że dotychczas nie są jednoznacznie określone przyczyny degradacji materiału rur katalitycznych w czasie eksploatacji, w związku z tym, przeprowadzona została analiza zmian, jakie zachodzą w strukturze stopu Incoloy 800 HT w trakcie eksploatacji reformera metanu i jaki ma on wpływ na właściwości użytkowe tego stopu.

Mikrostrukturę obserwowano przy użyciu mikroskopu świetlnego (LM) przy powiększeniach do 1000x oraz przy użyciu skaningowego mikroskopu elektronowego (SEM) przy powiększeniach do 10 000x. Identyfikacja wydzieleń została przeprowadzona przy użyciu transmisyjnego mikroskopu elektronowego (TEM) firmy TITAN.

1.1. Wyniki badań

Obserwację mikrostruktury badanego stopu Inconel 800 HT wykonano na zgładach metalograficznych dla stanu wyjściowego oraz po eksploatacji h w warunkach pełzania.

Przykładowe obrazy mikrostruktury badanego materiału w stanie wyjściowym oraz po eksploatacji w warunkach pełzania pokazano na rys. 1. Na rys. 2 pokazano wydzielenia zidentyfikowane w stopie Inconel 700 HT w stanie wyjściowym.

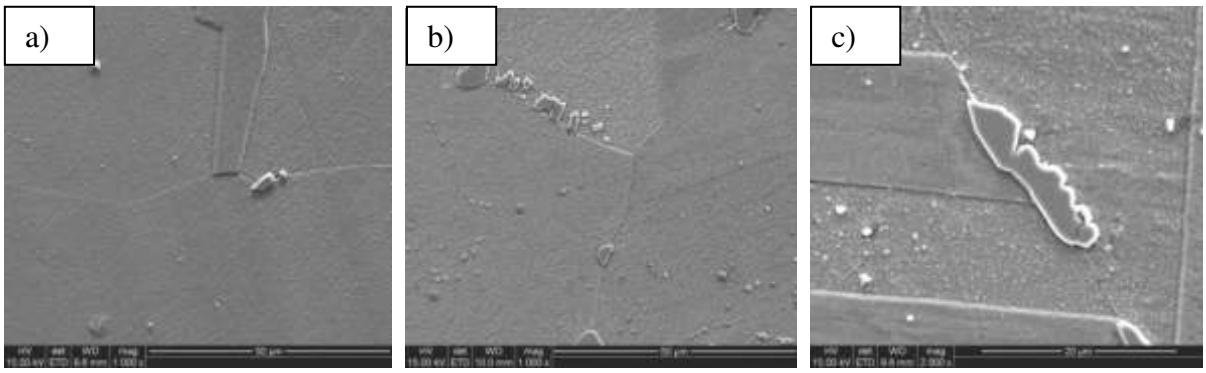

Rys.1. Mikrostruktura stopu Incoloy 800HT a) stan dostawy (SEM), b) po eksploatacji

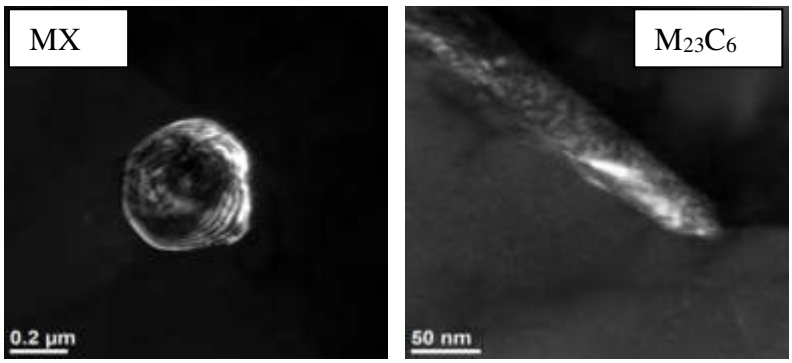

Rys.2. Obrazy elementów struktury cienkiej folii z materiału wycinka rury kompensacyjnej w stanie wyjściowym ze stopu Inconel 800HT (X8NiCrAlTi32-21). Obrazy zarejestrowane w trybie transmisyjnym w polu ciemnym

Wyniki badań wytrzymałościowych materiału rur kompensacyjnych reformera ze stopu Inconel 800HT w stanie wyjściowym oraz po eksploatacji w odniesieniu do normy ASTM B407. pokazano w tablicy nr.1.

Table 1. Wyniki badań właściwości wytrzymałościowych stopu Inconel 800HT

Inconel 800 HT	Właściwości wytrzymałościowe		
	R_m [MPa]	R_{et} [MPa]	A_5 [%]
Stan wyjściowy	521	240	66,0
Po 70 000 h eksploatacji	536	240	51,0
WYMAGANIA WG ASTM B407	min. 450	min. 170	min. 30

BIBLIOGRAPHY

1. Zieliński A. Monografia**,** Trwałość eksploatacyjna żarowytrzymałych stall o osnowie austenitycznej, 2021
2. Dobrzański J. Monografia, Materiałoznawcza interpretacja trwałości stali dla energetyki, Wydawnictwo Open Access Library, 3, 2011, ISBN 978-83-63553-43-2
3. Łabanowski J. Monografia, Ocena procesów niszczenia rur katalitycznych w eksploatacji reformerów metanu, 2003
4. Purzyńska H., Golański G., Zieliński A., Dobrzański J., Sroka M. Precipitation study in Ti-stabilised austenitic stainless steel after 207,000 h of service, Materials at High Temperatures, 36, 4, 296-303, 2019
5. H Purzyńska, J Dobrzański, Ewolucja mikrostruktury i właściwości użytkowych austenitycznej stali X8CrNiTi18-10 (T321H) podczas długotrwałej eksploatacji w warunkach pełzania, Prace Instytutu Metalurgii Żelaza 69, 2017

MTS CONFERENCE
MATERIAL TECHNOLOGIES IN SILESIA

12-15.06.2022
Crystal Mountain***** Hotel, Wisła, Poland

Procedura uzyskania uprawnień renomowanego wytwórcy odkuwek dla energetyki do pracy w warunkach pełzania na przykładzie stali X10CrWMoVNb9-2 (P92)

H. Purzyńska [a], J. Dobrzański [a]

[a] Sieć Badawcza Łukasiewicz – Instytut Metalurgii Żelaza im. Stanisława Staszica (Łukasiewicz Research Network – Institute for Ferrous Metallurgy), Research Group: Materials Research for Power Engineering
email: hanna.purzynska@imz.pl

Abstract:
Opracowano procedurę oraz zdefiniowano zakres badań i kryteria dla uzyskania uprawnień renomowanego wytwórcy odkuwek przeznaczonych na elementy urządzeń energetycznych pracujących w warunkach pełzania uzgodnionych z dozorem technicznym. Jej realizację pokazano na przykładzie wyników badań odkuwek swobodnie kutych wykonanych w warunkach przemysłowych ze stali X10CrWMoVNb9-2 (P92) dla dwóch zakresów ich grubości. Wykonano badania struktury i podstawowych właściwości wytrzymałościowych w temperaturze pokojowej i podwyższonej oraz badania udarności z wyznaczeniem progu kruchości. Ponadto wykonano badania sprawdzające wytrzymałości na pełzanie oraz długotrwałe wyżarzanie w temperaturze odpowiadającej zakresowi temperatury pracy z wyznaczeniem podstawowych właściwości mechanicznych. Uzyskane wyniki badań odniesiono do zdefiniowanych w wymaganiach właściwości i struktury.

Słowa kluczowe: procedura uprawnień renomowanego wytwórcy, odkuwki, stal P92 dla energetyki, struktura, właściwości mechaniczne, pełzanie, długotrwałe wyżarzanie

Keywords: authorization procedure from a reputable manufacturer, forgings, P92 steel for power plants, microstructure, mechanical properties, creep test, long-term annealing

1. WPROWADZENIE

Wyroby hutnicze znajdujące zastosowanie na elementy części ciśnieniowej bloków energetycznych muszą spełniać wymagania w zakresie jakości zdefiniowane i potwierdzone poprzez służby dozoru technicznego. Wymagania te szczególnie dotyczą uzyskiwania zdefiniowanego poziomu właściwości mechanicznych i struktury. Ponadto dla znajdujących zastosowanie w wytwarzaniu elementów pracujących w warunkach pełzania muszą być spełnione wymagania dotyczące poziomu czasowej wytrzymałości na pełzanie potwierdzone w przeprowadzonych próbach pełzania. Opracowany i zastosowany sposób podejścia pokazano na przykładzie odkuwek swobodnie kutych wykonanych ze stali X10CrWMoVNb9-2 (P92) [1-3].

2. PROCEDURA BADAWCZA

Poniżej na rys. 1 przedstawiono istotne elementy procedury dla spełnienia wymagań materiału odkuwek w zakresie czasowej wytrzymałości na pełzanie. Na rys. 1a pokazano sposób tworzenia parametrycznej krzywej Larsona-Millera czasowej wytrzymałości na pełzanie w postaci zależności wytrzymałości na pełzanie od parametru L-M [log $R_{z/t/T}(\sigma) = f(L\text{-}M)$], na rys. 1b sposób wyznaczenia wymaganego poziomu naprężenia badania σ_b dla wymaganej temperatury badania T_b oraz oczekiwanego czasu do zerwania t_r, a na rys. 1c sposób wyznaczenia minimalnej wymaganej wartości czasu do zerwania $t_{r\ min}$ dla zadanych parametrów temperatury badania T_b i naprężenia badania σ_b z parametrycznej krzywej Larsona-Millera (L-M) czasowej wytrzymałości na pełzanie wyznaczającej dolne dopuszczalne pasmo rozrzutu uzyskiwanych wyników prób pełzania.

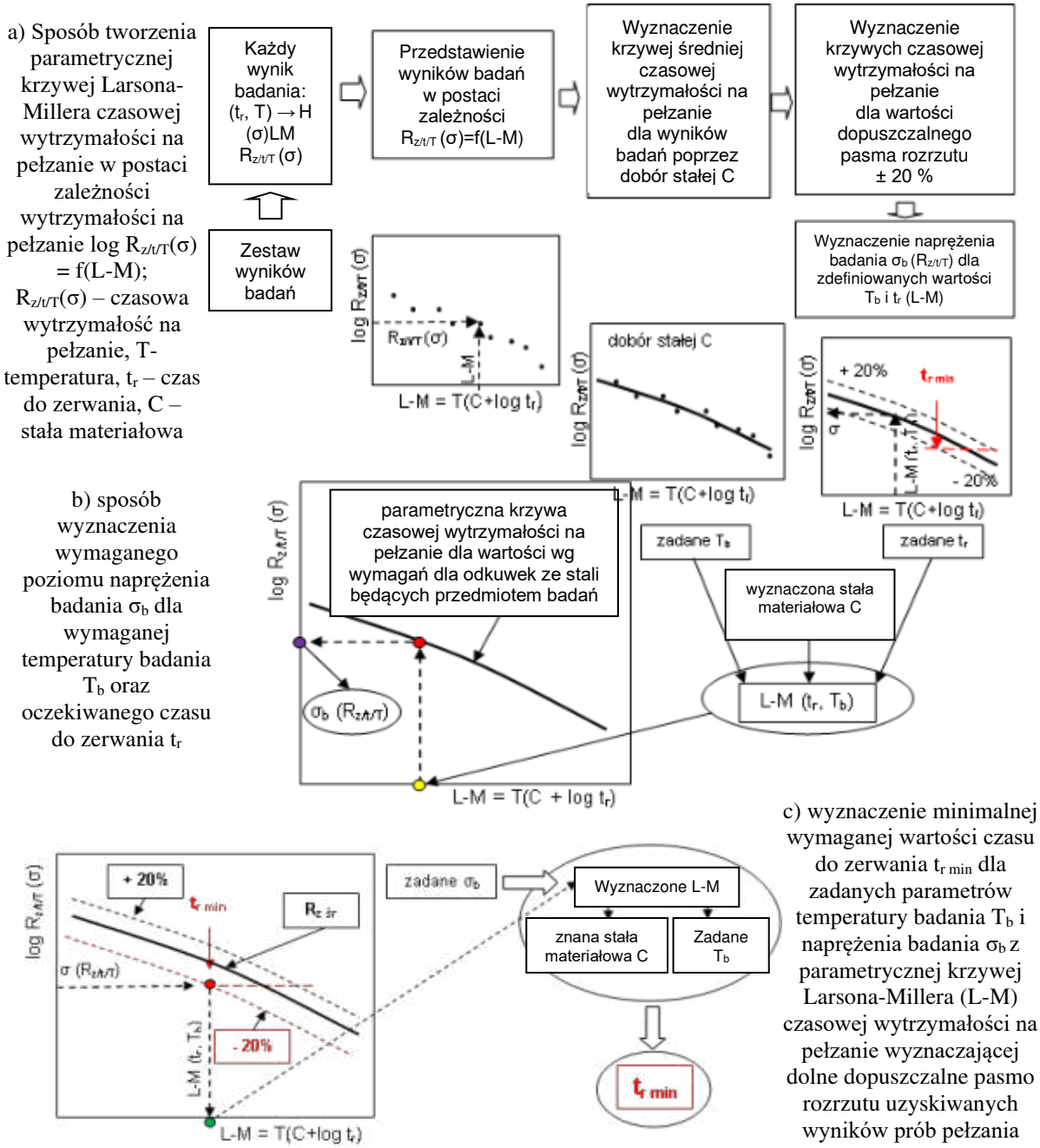

Rys. 1. Procedura dla spełnienia wymagań materiału odkuwek w zakresie czasowej wytrzymałości na pełzanie celem otrzymania uprawnień renomowanego wytwórcy wyrobów hutniczych dla wytwarzania elementów ciśnieniowych bloków energetycznych

LITERATURA

1. J. Dobrzański, H. Purzyńska, A. Zieliński, Sprawozdanie IMŻ nr B0-1618, Badania pełzania do zerwania materiałów dla energetyki stali:15NiCuNb5-6-4 (1.6368), X10CrMoVNb9-1 (1.4903), X10CrWMoVNb9-2 (1.4901) oraz długotrwałego wyżarzania stali X10CrWMoVNb9-2 dla uzyskania uznania Vd TUV/UDT na produkcję odkuwek swobodnie kutych cz.1-3 Gliwice 2018-2020 (nie publikowane)
2. J. Dobrzański, Trwałość elementów ciśnieniowych bloków energetycznych, Monografia, Wydawnictwo Instytutu Metalurgii Żelaza, Gliwice 2019
3. A. Hernas, J. Dobrzański, J. Pasternak, St. Fudali, Charakterystyki nowej generacji materiałów dla energetyki Monografia , Wydawnictwo Politechniki Śląskiej, Gliwice 2015
4. A. Hernas, J. Dobrzański, Trwałość i niszczenie elementów kotłów i turbin parowych, Wydawnictwo Politechniki Śląskiej, Gliwice 2003
Badania pełzania do zerwania materiałów dla energetyki stali:15NiCuNb5-6-4 (1.6368), X10CrMoVNb9-1 (1.4903), X10CrWMoVNb9-2 (1.4901) oraz długotrwałego wyżarzania stali X10CrWMoVNb9-2 dla uzyskania uznania Vd TUV/UDT na produkcję odkuwek swobodnie kutych

MTS CONFERENCE
MATERIAL TECHNOLOGIES IN SILESIA

12-15.06.2022
Crystal Mountain***** Hotel, Wisła, Poland

Zmiany w mikrostrukturze w jednoimiennym złączu spawanym stali Super 304H po 1000 godzin starzenia w temperaturze 700 i 750°C

T. Puszczało [a,c], H. Purzyńska [b], K. Sówka [a,c], M. Sroka [a], A. Zieliński [b]

[a] Silesian University of Technology, Faculty of Mechanical Engineering, Department of Engineering Materials and Biomaterials
[b] Łukasiewicz Research Network – Institute For Ferrous Metallurgy
[c] Zakłady Remontowe Energetyki Katowice S.A.
email: tomasz.puszczalo@polsl.pl

Streszczenie: W pracy przedstawiono wyniki badań mikrostruktury oraz twardości jednoimiennego złącza spawanego ze stali Super 304H po 1000 h starzenia w temperaturze 650°C oraz 700°C. Stal Super 304H jest powszechnie stosowana na elementy wysokociśnieniowe w nowoczesnych blokach energetycznych na nadkrytyczne parametry pary. W artykule skupiono się na porównaniu twardości w odniesieniu do obrazów mikrostruktury w stanie wyjściowym oraz po starzeniu. Badania mikrostruktury wykonano w oparciu o mikroskopię skaningową, natomiast badania twardości wykonano na twardościomierzu stacjonarnym w skali HV10.
Abstract: This study presents the results of microstructure and hardness tests of a homonymous welded joint made of Super 304H steel after 1000 h of aging at the temperature of 650°C and 700°C. Super 304H steel is commonly used for high-pressure elements of modern power units for supercritical steam parameters. The article focuses on the comparison of hardness in relation to the microstructure images in the initial state and after aging. The microstructure tests were carried out on the basis of scanning microscopy, while the hardness tests were carried out on a stationary hardness tester in the HV10 scale.

Keywords: steel S304H, microstructure, creep, annealing,

1. WSTĘP

Aktualny i perspektywiczny stan polskiej energetyki jest i będzie oparty na tak zwanym miksie energetycznym, na który w chwili obecnej składa się głównie udział produkcji energii wytwarzanej z wykorzystaniem paliw kopalnych, oraz udział produkcji ze źródeł energii odnawialnej [1].

Ciągły wzrost zapotrzebowania na energię w Polsce wymaga dalszego rozwoju energetyki z wykorzystaniem konwencjonalnych źródeł energii ze względu na bezpieczeństwo energetyczne kraju, pomimo wzrostu udziału energii ze źródeł odnawialnych [2]. Podstawowy kierunek rozwoju jest związany z sukcesywnym zwiększaniem sprawności wytwarzania energii poprzez podnoszenie parametrów roboczych pary. Uzyskiwanie parametrów nadkrytycznych w blokach energetycznych wymaga zastosowania materiałów nowej generacji o wyższej od stali o osnowie ferrytycznej wytrzymałości na pełzanie i żaroodporności oraz mogącej pracować w temperaturze dochodzącej do 700°C [2]. Należą do nich między innymi nowe stale o osnowie austenitycznej [1] w tym stal Super304H (X10CrNiCuNb18-9-3), która powstała w wyniku modyfikacji składu chemicznego klasycznej stali typu 18/8. W tabeli 1 przedstawiono nominalny skład chemiczny stali Super 304H [3].

Tablica 1. Nominalny skład chemiczny stali Super 304H (% masy)

Skład chemiczny stali Super 304H (% masy)											
C	Si	Mn	P	S	Cu	Cr	Ni	Nb	B	N	Al
0,7 0,13	max. 0,3	max. 1,00	max. 0,040	max. 0,010	2,5 3,5	17,0 19,0	7,5 1,5	0,3 0,6	0,001 0,010	0,05 0,12	0,003 0,030

Spośród wszystkich właściwości mechanicznych najbardziej istotne i decydujące o przydatności do eksploatacji w warunkach pełzania są właściwości wyznaczane w próbie pełzania. Wytrzymałość na pełzanie, będąca podstawą do obliczeń projektowych, decyduje o zdolności do przenoszenia obciążeń eksploatacyjnych elementów wykonanych z badanej stali. Długotrwała eksploatacja powoduje obniżanie czasowej wytrzymałości na pełzanie. Niezbędną jest zatem znajomość, dla różnych stanów materiału po różnym czasie eksploatacji, wartości tej wytrzymałości na pełzanie, definiowanej jako trwałość resztkowa lub resztkowa wytrzymałość na pełzanie [1].

2. PRZYGOTOWANIE PRÓBEK DO BADAŃ

Próbki do badań laboratoryjnych pobrane zostały z rur ϕ48,4x6,3 wykonanych ze stali Super 304H. Odcinki rur zostały połączone parami za pomocą spoin obwodowych. Spoiny przebadano w kierunku wykrycia niezgodności spawalniczych za pomocą zestawu badań nieniszczących objętościowych i powierzchniowych. Pozytywna weryfikacja spoin pozwoliła na wycięcie próbek zarówno do badań w stanie dostawy, jak i poddanych procesowi starzenia w czasie 1000 godzin w temperaturze 700°C i 750°C. Po starzeniu z próbek pobrano wycinki w charakterystycznych przekrojach złącza spawanego uwzględniając: materiał rodzimy 1 i 2, strefy wpływu ciepła 1 i 2 oraz spoinę. Z wycinków wykonano zgłady metalograficzne

3. WYNIKI BADAŃ

Badania mikrostruktury przeprowadzono przy użyciu skaningowego mikroskopu elektronowego (SEM) Inspect F na zgładach trawionych elektrolitycznie

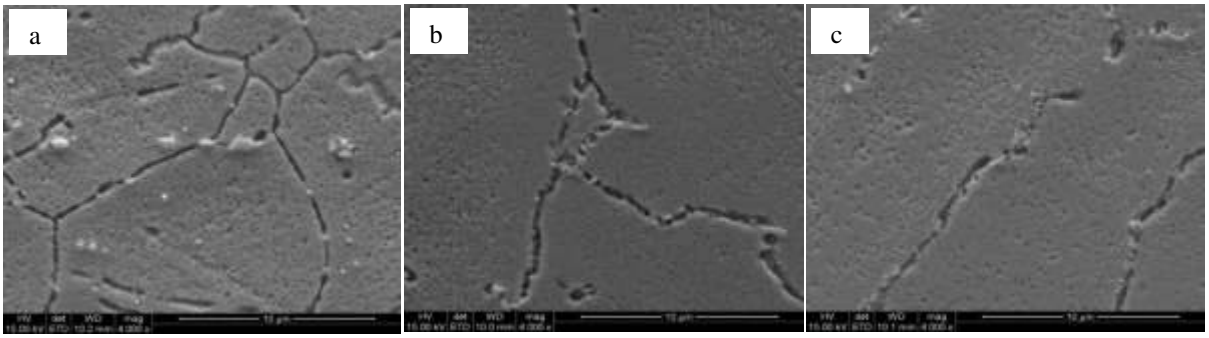

Rys. 1. Mikrostruktura stali Super 304H po 1000 godzin starzenia w temperaturze 750°C
a) – Materiał rodzimy 1, b) - Spoina, c) – Strefa wpływu ciepła 1

W stanie dostawy badana stal charakteryzuje się drobnoziarnistą austenityczną strukturą o wielkości ziarna o numerze 7-9 według wzorców ASTM, oraz widocznymi bliźniakami wyżarzania o granicach koherentnych jak i niekoherentnych i pojedynczymi pierwotnymi wydzieleniami NbCN (MX) zróżnicowanej wielkości, rozmieszczonymi wewnątrz ziaren. Drobnoziarnista struktura zapewnia stali dobre właściwości ciągliwe wyrażane udarnością, a także wytrzymałościowe i plastyczne. Ponadto pozytywnie wpływa na odporność na utlenianie w porównaniu do stali gruboziarnistych.

W badanej stali po 1000 godzinach starzenia na granicach ziaren występują wtórne wydzielenia $M_{23}C_6$ oraz pierwotne wydzielenia MX wewnątrz ziaren. Charakterystycznym elementem są nieciągłe układy cząstek węglika $M_{23}C_6$ po granicach ziaren. W porównaniu do wnętrza ziaren, granice ziaren jako defekty powierzchniowe o nieuporządkowanej budowie krystalicznej, umożliwiają szybszą dyfuzję pierwiastków stopowych.

LITERATURA

1. Zieliński, A. (2021) Trwałość eksploatacyjna żarowytrzymałych stali o osnowie austenitycznej. Instytut Metalurgii Żelaza im. Stanisława Staszica: s. 6, 16.
2. Sroka, M. (2019) Analiza procesów wydzieleniowych zachodzących w mikrostrukturze stali Samicro 25 w temperaturze podwyższonej. Instytut Metalurgii Żelaza im. Stanisława Staszica: s. 11, 20.
3. VdTÜV-Werkstoffblatt 550 - Warmfester Walz- und Schmiedestahl X10CrNiCuNb18-9-3 (1.4907), 2012.

MTS CONFERENCE
MATERIAL TECHNOLOGIES IN SILESIA

12-15.06.2022
Crystal Mountain***** Hotel, Wisła, Poland

Analiza wielkości ziarna z wykorzystaniem dyfrakcji elektronów wstecznie rozproszonych

K. Radwański[a]

[a]Sieć Badawcza Łukasiewicz – Instytut Metalurgii Żelaza im. Stanisława Staszica
email: krzysztof.radwanski@imz.pl

Abstract: W pracy opisano wykorzystanie metody dyfrakcji elektronów wstecznie rozproszonych (EBSD) w badaniach wielkości ziarna, na przykładzie próbki o strukturze ferrytycznej po częściowej rekrystalizacji statycznej. Przedstawiono wyniki średniej średnicy równoważnej ziarna dla przykładowych różnych zadanych kryteriów przynależności punktów analizy do ziarna. Stwierdzono, że wyznaczona średnia średnica równoważna ziarna przy zadanych parametrach analizy EBSD jest zależna od przyjętej kątowej tolerancję ziarna oraz minimalnej ilości punktów analizy składających się na ziarno.

Keywords: wielkość ziarna, EBSD, struktura

1. INTRODUCTION

Wielkość ziarna jest ściśle powiązana z właściwościami mechanicznymi materiałów metalicznych. Stąd też bardzo często zachodzi konieczność jej wyznaczenia. Powszechnie stosowaną metodą jest badanie struktury z wykorzystaniem mikroskopii świetlnej i następnie porównanie uzyskanej wielkości ziarna do ustandaryzowanych wzorców. Dokładniejszym sposobem jest zastosowanie ilościowej analizy obrazu, co wymaga natomiast stosunkowo dużego nakładu pracy [1, 2]. Metody te charakteryzują się pewnymi ograniczeniami związanymi, np. z rozdzielczością mikroskopu świetlnego czy brakiem możliwości rozróżnienia ziarn od podziarn, szczególnie w przypadku analizy materiałów po częściowej rekrystalizacji. W takim przypadku dla wyznaczenia wielkości ziarna celowe wydaje się zastosowanie metody EBSD, charakteryzującej się lepszą rozdzielczością oraz umożliwiającą analizę kątów dezorientacji.

2. MATERIAŁ i METODYKA BADAŃ

Materiałem do badań była stal o strukturze ferrytycznej po walcowaniu na zimno i następnie poddana procesowi nagrzewania z wykorzystaniem dylatometru do temperatury 690°C z szybkością 3°C/s. Próbkę po nagrzaniu schłodzono helem celem zamrożenia struktury, tak aby otrzymać materiał częściowo zrekrystalizowany.

Badania struktury przeprowadzono z wykorzystaniem elektronowego mikroskopu skaningowego INSPECT F z wykorzystaniem metody EBSD. Badania wykonano w obszarze 180x70µm z krokiem analizy 0.5µm. Obróbkę uzyskanych wyników badań przeprowadzono z wykorzystaniem oprogramowania TSL OIM Analysis firmy TSL. Wyznaczono wielkość ziarna dla różnych zdefiniowanych kryteriów przynależności punktów analizy do ziarna. Kątową tolerancję ziarna zmieniano w zakresie od 2 do 15°, natomiast minimalną ilość punktów analizy składających się na ziarno różnicowano w zakresie od 2 do 8 punktów.

3. WYNIKI BADAŃ

Mapy rozkładu ziarn dla różnych wartości kątowej tolerancji ziarna przy założonej minimalnej ilości punktów analizy wynoszącej 2 przedstawiono na rysunku 1. Zwiększenie wartości kątowej tolerancji ziarna w zakresie 2-15° istotnie wpływa na średnią średnicę ziarna, która rośnie w tym zakresie od 1,21 do 3,13 µm.

Zwiększenie minimalnej wartości punktów analizy definiujących ziarno z 2 do 8, dla przyjętej wartości kątowej tolerancji ziarna wynoszącej 5°, powoduje zwiększenie średniej średnicy równoważnej w zakresie od 1,78 do 3,26 µm. Im wyższa założona wartość minimalnej ilości punktów składających się na ziarno, tym w strukturze uzyskiwany jest wyższy udział niezidentyfikowanych punktów analizy, będących efektem braku spełnienia przyjętych kryteriów przynależności do ziarna.

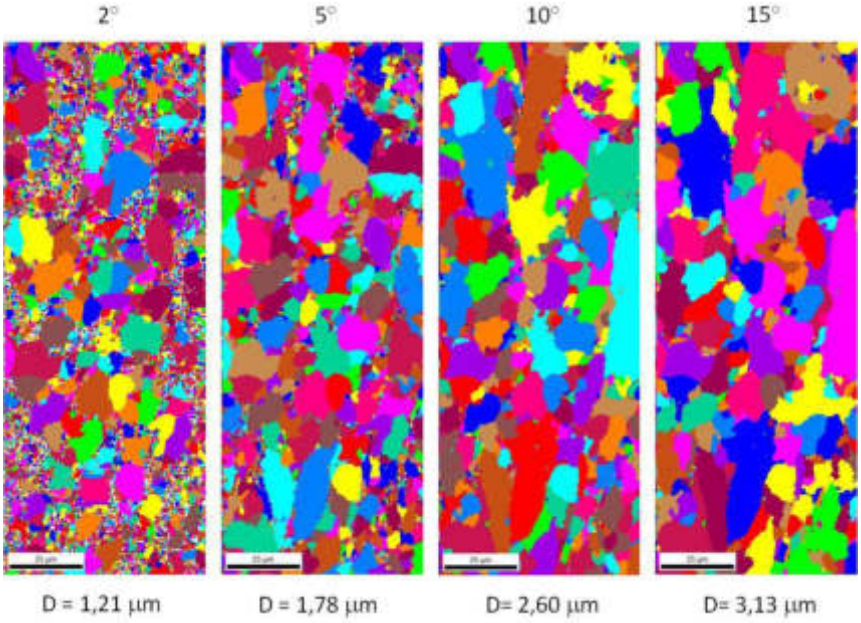

Rysunek 1. Mapy rozkładu ziarn w zależności od przyjętej wartości kątowej tolerancji ziarna wyznaczone dla minimalnej ilości punktów analizy definiujących ziarno wynoszącej 2 [3].
Figure 1. Grain distribution maps depending on the grain tolerance angle determined for the minimum grain size of 2 pixels defining a grain.

Wyniki badań pokazują, że metoda EBSD jest właściwym narzędziem w badaniach wielkości ziarna, jednak niezbędne jest właściwe zdefiniowanie kryteriów przynależności punktów analizy do ziarna. Przy doborze kryteriów przynależności punktów analizy do ziarna należy brać pod uwagę m. in. występujące składniki struktury, stopień rozdrobnienia ziarn czy też stan materiału.

4. PODSUMOWANIE

W ramach pracy wykazano, że:
- wielkość ziarna wyznaczana metodą EBSD jest zależna od przyjętych kryteriów przynależności punktów analizy do ziarna,
- zwiększenie kątowej tolerancji ziarna przy stałej określonej wartości minimalnej ilości punktów analizy tworzących ziarno powoduje zwiększanie średniej średnicy równoważnej ziarna,
- zwiększenie minimalnej wartości ilości punktów analizy dla zadanej wartości kątowej tolerancji ziarna wpływa na wzrost średniej średnicy równoważnej ziarna,
- prezentacja wyników analizy wielkości ziarna w oparciu o metodę EBSD wymaga każdorazowo podania kryteriów przynależności punktów analizy do ziarna,
- przy doborze kryteriów przynależności punktów analizy należy brać pod uwagę m. in. występujące składniki strukturalne, stopień rozdrobnienia, jak również stan materiału.

BIBLIOGRAFIA

1. P.L. Orsetti-Rossi, C.M. Sellars, Quantitative metallography of recrystallization. Acta Materialia, 45 (1997), 137-148.
2. E.E. Underwood, Quantitative Stereology. Addison-Wesley, Reading, Massachusetts, 1970
3. K. Radwański, Zastosowanie mikroskopii skaningowej i dyfrakcji elektronów wstecznie rozproszonych w badaniach struktury blach ze stali wielofazowych na różnych etapach procesu ciągłego wyżarzania, Monografia nr 8, Instytut Metalurgii Żelaza im. Stanisława Staszica, Gliwice , 2016.

MTS CONFERENCE
MATERIAL TECHNOLOGIES IN SILESIA

12-15.06.2022
Crystal Mountain***** Hotel, Wisła, Poland

Quality requirements for the heat treatment process

M.T. Roszak [a]

[a] Silesian University of Technology, Faculty of Mechanical Engineering, Department of Engineering Materials and Biomaterials
email: marek.roszak@polsl.pl

Abstract:
The article presents an analysis of the requirements for the quality assurance system for heat treatment processes, indicating the most important activities that the organization should take on by the methodology of the Deming Circle.

Keywords: heat treatment, quality assurance, Deming Circle.

1. INTRODUCTION

The quality requirements of customers towards products are increasing. Producers have to act to satisfy them. With the emergence of new customer requirements, manufacturers are forced to improve the quality of their production processes and offered products. The new requirements relating to the quality of products and implemented processes, as well as their supervision and improvement. In particular, this issue applies to material manufacturing processes for the automotive, aviation and rail industries.

A special type of process is heat treatment processes included in the so-called special processes. Special processes are those processes, the results of which cannot be verified by subsequent inspections and tests or those in which defects arising in the production process may appear only during the use of the product by the customer. Due to the limited possibilities of their verification, supervision over such processes is subject to special restrictions. These processes are required to be constantly monitored. It is recommended that special processes be managed using the applied quality management tools and methods [1-3].

The implemented, maintained and improved quality management systems in manufacturing companies are a tool supporting the fulfilment of quality requirements.

2. HIERARCHY OF QUALITY REQUIREMENTS

The basic standard defining the requirements for organizations in quality management is ISO 9001 (2015) Quality management systems. The nature of the requirements specified in the ISO 9001 standard is general and addressed to every organization, regardless of the scope of its activity. There is a need to develop standards targeted at individual industry areas, for example, the automotive industry - an example is the IATF (International Automotive Task Force) 16949 (2016) Quality management system requirements for automotive production and relevant service parts organizations. There was also a need to define a quality standard for specific activities of the company, including special processes. For these processes, it is recommended that enterprises adopt and implement the requirements specified in the CQI (Continuous Quality Improvement) 9 Special Process: Heat Treat System Assessment specification, developed by the AIAG Automotive Industry Action Group [1-3].

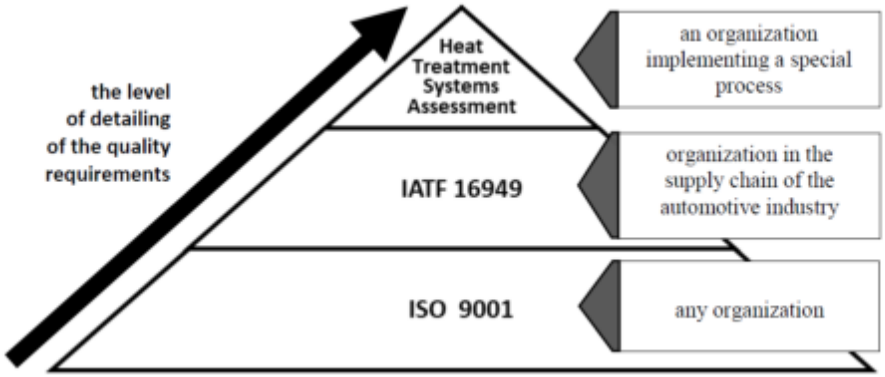

Figure 1. Hierarchy of requirements in quality management - an example of automotive and heat treatment (own elaboration)

3. CONCLUSION

Quality management is based on the fundamental principle of improvement. The basic idea behind it concerns the so-called Deming Circle (Plan, Do, Check, Act). The use of the Deming Circle enables the organization to provide adequate resources for its processes and appropriate management and identify and consider opportunities for improvement. This also applies to heat treatment processes. The scope of the individual stages of the Deming Circle about heat treatment processes within the requirements of the CQI-9 specification is defined below:

- Plan: detailed analysis of the requirements for the product and process - including by APQP and PPAP, including meeting the requirements of the quality management system, developing a quality plan, developing a quality control plan - including the requirements contained in the Process Tables attached to the CQI-9 specification and HTSA detailed requirements, P-FMEA risk analysis development, feasibility analysis, technology development - including operational documents in accordance with the management system, SAT - System Accuracy Test, TUS - Temperature Uniformity Survey test, evaluation of the quenching properties, device calibration.

- Do: implementation of the process, application of the requirements contained in the documents used in the enterprise, implementation of the process by the developed technology and the functioning quality management system, meeting the requirements contained in the HTSA - including the requirements of the Process Tables, monitoring of product entrapment sites.

- Check: analysis of the obtained product properties, including microstructure, analysis of the fulfilment of quality requirements resulting from the adopted assumptions for the implementation of the technological process and the functioning quality management system, analysis of inconsistencies in the process, analysis of reprocessing, analysis of quality indicators, analysis of process implementation parameters (time, temperature, atmosphere, Quench Delay Time, Temper Delay Time) - by the Process Tables, analysis of downtime reports, execution of a Job Audit.

- Act: defining actions to improve the product/process, modification of the management mechanisms of the quality management system functioning so far, along with the change of technological documentation, employee training, and development of a continuous improvement plan.

Meeting the requirements of the CQI-9 standard by an organization allows demonstrating its ability to continuously deliver a product that meets the requirements of customers and the requirements of applicable legal and other regulations, as well as striving to increase customer satisfaction through the effective use of the system, including processes for continuous improvement of the system.

BIBLIOGRAPHY

1. M. Roszak, Ł. Krzemiński, Quality management in heat treatment process, Archives of Material Science and Engineering 61/1 (2013) 30-37
2. CQI 9 Special Process: Heat Treat System Assessment, Automotive Industry Action Group, 2020
3. S. Rašková, Quality Management System Requirements from Heat Treatment Processes, Journal of Heat Treatment and Materials, Volume 71, issue 6, (2016) 272–277

MTS CONFERENCE
MATERIAL TECHNOLOGIES IN SILESIA

12-15.06.2022
Crystal Mountain***** Hotel, Wisła, Poland

Product quality planning in the production part approval process

Ł. Rudolf [a], M. Roszak [b]

[a] School of Doctors, Silesian University of Technology, Faculty of Mechanical Engineering, Department of Engineering Materials and Biomaterials
email: lukasz.rudolf@polsl.pl
[b] Silesian University of Technology, Faculty of Mechanical Engineering, Department of Engineering Materials and Biomaterials
email: marek.roszak@polsl.pl

Abstract:
The article concerns the analysis of the applicable normative requirements in the field of product quality planning in the process of approving parts for production. The analysis in particular concerns the correlation of the use of appropriate methods and quality management tools in the quality planning process.

Keywords: quality planning, production process, quality management methods and tools

1. INTRODUCTION

In industries that are characterized by large-scale production with a simultaneous global dispersion of suppliers in the supply chain, it is extremely difficult to maintain universal quality standards for all partners in the production chain. The automotive industry is an example of this, because the final product, which is a car, is made of parts and components whose suppliers are located all over the world, and the quality of individual components directly affects the quality of the final product, which is currently one of the indicators of the company's evaluation (next to financial, marketing and environmental criteria). By proactively engaging the company in activities related to quality planning, the quality of manufactured products is improved, which allows the company to increase its revenues, market share, build customer loyalty and its image [1-3].

The answer to the above needs was the development by the American automotive association AIAG (Automotive Industry Action Group) of five main quality planning tools, which have been described and published as “Reference Manuals”, initially only for the automotive market and now also for use in other industrial sectors. The following quality manuals are used in the automotive industry: APQP and CP (Advanced Product Quality Planning and Control Plan), PPAP (Production Parts Approval Process), MSA (Measurement Systems Analysis),- SPC (Statistical Process Control), FMEA (Potential Failure Modes and Effects Analysis) [4].

2. QUALITY PLANNING TOOLS IN THE PPAP PROCESS

The PPAP process includes 18 quality evidence necessary to submit to the customer, which is to prove that the organizations fully understand the design assumptions and the possibility of launching serial production of parts in accordance with the customer's requirements. The amount and method of submitting is defined and imposed on the supplier by the customer, who takes into account: the impact of the part on the safety and relevance of the part / subassembly in the final product, legal requirements, supplier experience and opinion, having certification for compliance with IATF 16949 or ISO 9001 [5].

3. CONCLUSION

Correct use of quality planning tools in the product and process development is a determinant of the effectiveness of the implementation of individual phases of APQP. Figure 1 shows in a simplified way the relationship between the APQP phases and the quality tools / evidence developed in the PPAP process (according to PPAP level 3).

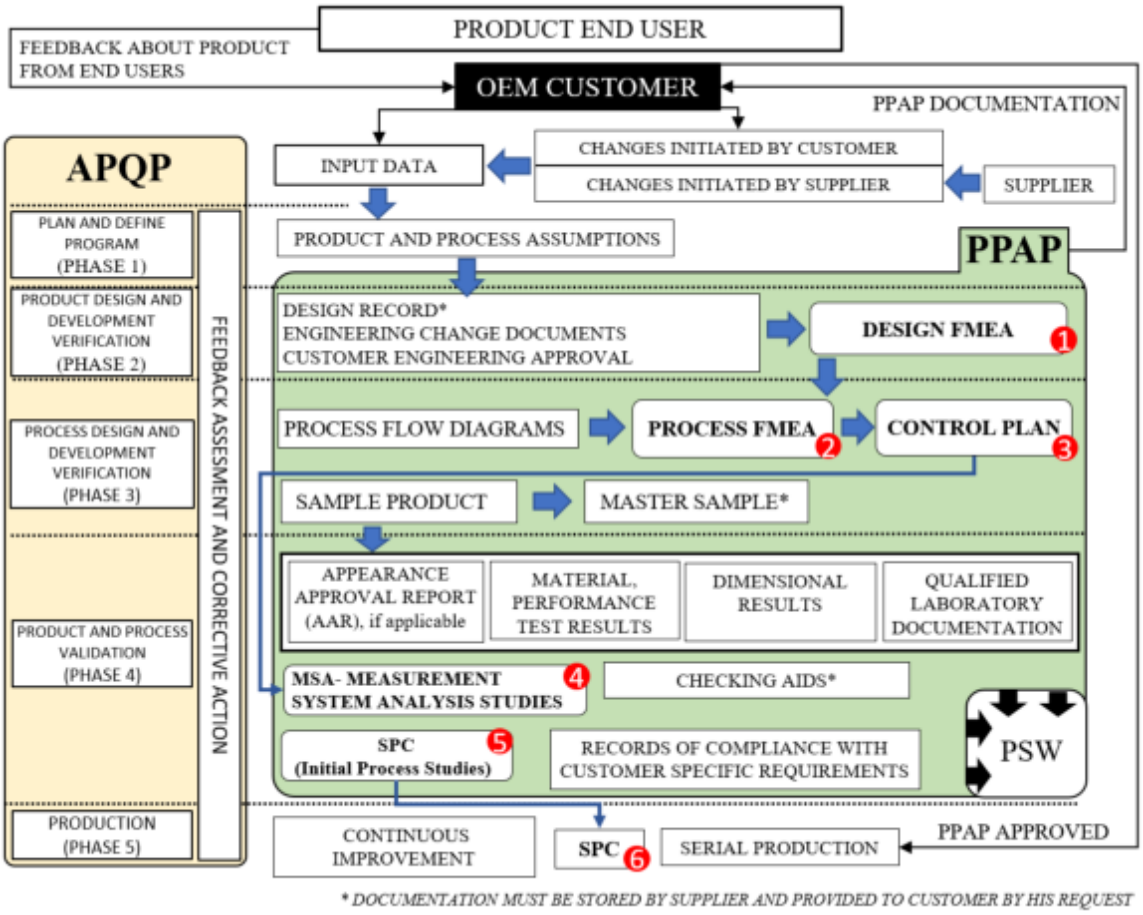

Figure 1. Diagram of dependencies of particular quality planning tools (own study based on [4])

The individual quality tools are related to each other, but only their correct use can protect the project against errors or misunderstandings between the supplier and the customer.

Acknowledgments: The study was created as part of the doctoral studies at the Joint Doctoral School covered by the program of the Ministry of Science and Higher Education "Implementation doctorate".

BIBLIOGRAPHY

1. A. Rydström, J. Viström, Production part approval process evaluation. Chalmers University of Technology, Gothenburg, Sweden, 2020.
2. M. Folta, J. Bradáč, Production part approval process in the metallurgical sector for automotive industry, Conference: Metal 2015, Brno, http://konsystest.tanger.cz/files/proceedings/21/papers/4156.pdf
3. J. A. Doshi, D.A. Desai, Role of production part approval process in continuous quality improvement and customer satisfaction, [in:] International Journal of Engineering Research in Africa, Vol. 22, pp. 174-183), 2016.
4. Advanced Product Quality Planing and Control Plan (APQP), Reference Manual. 2nd Edition. AIAG 2008.
5. IATF 16949:2016: Automotive Quality Management System Standard, Quality management system requirements for automotive production and relevant service parts organization, Edition 1, 2016.

MTS CONFERENCE
MATERIAL TECHNOLOGIES IN SILESIA

12-15.06.2022
Crystal Mountain***** Hotel, Wisła, Poland

Innovative Forming Technology

S. Rusz[a], O. Hilšer[a], J. Švec[a], R. Zabystrzan[b], P. Szkandera[a], M. Pastrňák[a], M. Vindyš[a], W. Borek[c], J. Vontorová[a]

[a] Silesian University of Technology, Faculty of Mechanical Engineering, Department of Engineering Materials and Biomaterials
[a] VSB - Technical University of Ostrava, Ostrava, Czech Republic, EU; s.rusz@vsb.cz
[b]SteelTec.cz, s. r.o. Třinec, Czech Republic, EU, rostislav.zabystrzan@steeltec.cz
[c]Silesian University of Technology, Department of Engineering Materials and Biomaterials, 18a Konarskiego Street, Gliwice, Poland, wojciech.borek@polsl.pl

Abstract:
On the newly developed forming device, unlike the rolling technology, the material is significantly strengthening after the forming process, while maintaining the initial strip sheet dimensions. We want to achieve a significant increase in mechanical properties in as few passages as possible by the forming device, in particular increasing the yield strength Re and the ultimate tensile strength Rm, while maintaining good formability. The above-described forming method was used to extrude of low carbon steel. Overall, the effect of the individual passages on the increasing of mechanical properties of low carbon steel as tested in a total number of 1 to 7 passes through forming device.

Keywords: low carbon steel, severe plastic deformation, mechanical properties, structural analyzes

1. INTRODUCTION

New technologies, which use the high deformation for obtaining the fine-grained structures, are intensively studied by many authors [1,2]. This research concerned the whole production of ultrafine-grained (UFG) materials using Severe Plastic Deformation (SPD). Several types of the SPD technologies serving for production of the UFG metals were developed already at the beginning of the nineties as the following ones: ECAP (Equal Channel Angular Pressing) , DCAP (Dissimilar Channel Angular Pressing), CONFORM (Continual Extrusion Forming), HPT (High Pressure Torsion), CCDC, (Cyclic Channel Die Compression) ARB (Accumulative Roll Bonding), Twist Extrusion (TE), CEC (Cyclic Extrusion Forming), RCS (Repetitive Corrugation and Strengthening, HE (Hydrostatic Extrusion), CGP (Constrain Groove Pressing) and MAXStrain with Gleeble System [3-4].

1.1. Materials and Methods

One type of low carbon steels suitable for cold forming were verified experimentally- steel DC01. Chemical composition of tested steel have been shown at Table 1.

Table 1. Chemical composition of tested steel

C [%]	Mn [%]	Si [%]	P [%]	S [%]	Cr [%]	Ni [%]	Mo [%]	Cu [%]
0.050	0.203	0.020	0.014	0.008	0.053	0.056	0.005	0.075

The tests were performed on the upgraded forming equipment using the principle of cold severe plastic deformation (method DRECE). Device "DRECE - Dual Rolls Equal Channel Extrusion" (Dual Rolls Pressure Combined with Equal Channel Extrusion) is used for production of metallic materials with very fine grain size. During the actual forming process, the principle of severe plastic deformation is used. The device is composed of the following main parts: “Nord” type gearbox, electric motor with frequency speed converter, multi-plate clutch, feed roller and pressure rollers with regulation of thrust, and of the forming tool itself – made of Dievar steel type.

Metallic strip with dimensions 58 x 2 x (1000 – 2000) mm (width x thickness x length) is inserted into the device. During the forming process the main cylinder in synergy with the pressure roller extrude the material through the forming tool without any change of cross section of the strip. In this way, a significant refinement of grain is achieved by severe plastic deformation. This method is used for various types of metallic materials, non-ferrous metals and their alloys.

Figure 1. Forming equipment

1.2 Analysis of SPD process influence on mechanical properties

Experimentally was carried out 7 passes through the forming device. After each pass, the mechanical properties obtained were evaluated. On the basis of the results obtained from the tensile tests, it can be stated with respect to the initial state, that after the 1st passes the yield strength $R_{p0,2}$ is increased by 51.7 % and the ultimate tensile strength R_m by 10 %. At the same time, there will be a slight decrease in the ductility by 25 %. After the 5th passes through the forming tool, the yield strength $R_{p0,2}$ increased by 87 % and the ultimate tensile strength Rm increased by 42 % relative to the initial state. As it is seen from results showed at Figure 2 the yield strength (Fig. 2a) and ultimate tensile strength (Fig. 2b) after SPD processing are increased while the elongation A_{80} (Fig. 2c) is decreased. The ductility value A_{80} = 44 % is sufficient after the five passes through forming tool.

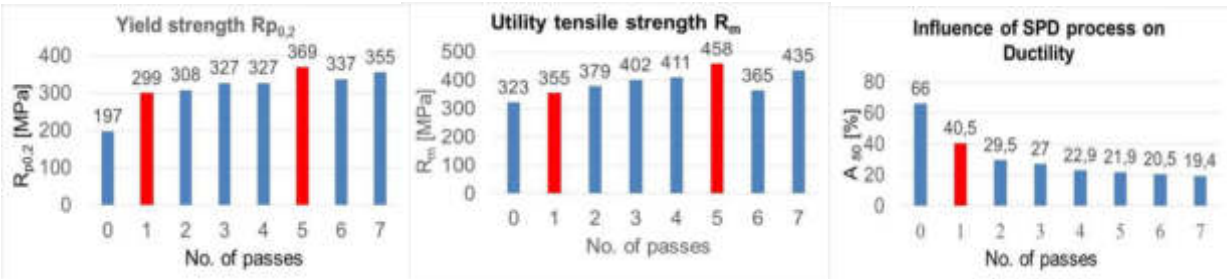

Figure 2. Influence of SPD process on a) Yield strength, b) Utility tensile strength, c) Ductility.

Acknowledgments: This paper was created within the projects Epsilon of Technology Agency of the Czech Republic, Development of a new technology for increasing the quality of steel strips, No. TH04010416 and project Innovative and additive manufacturing technology - new technological solutions for 3D printing of metals and composite materials, reg. no. CZ.02.1.01/0.0/0.0/17_049/0008407 financed by Structural and Investment Founds of Europe Union.

BIBLIOGRAPHY

1. Gutkin, M.Y.; Ovidko, I.A.; Pande, C.S. Theoretical models of plastic deformation processes in nanocrystalline materials. Rev. Adv. Mater. Sci. 2001, Volume 2, 80–102.
2. Valiev R.Z. Recent developments of severe plastic deformations techniques for processing bulk nanostructured materials. Mater. Sci. Forum, 2008, Volume 579, 1–14, doi.org/10.4028/www.scientific.net/MSF.579.1.
3. Tanski, T.; Snopinski, P.; Borek, W. Strength and structure of AlMg3 alloy after ECAP and post-ECAP processing. Mater Manuf Process. 2017, *Volume*: 32/12, 1368-1374, DOI: 10.1080/10426914.2016.1257131.
4. Tański, T.; Snopiński, P.; Pakieła, W.; Borek, W.; Prusik, K.; Rusz, S. Structure and properties of AlMg alloy after combination of ECAP and post-ECAP ageing. *Arch. Civil Mech. Eng*. 2016, Volume 16, 325–334, DOI: 10.1016/j.acme.2015.12.004.

MTS CONFERENCE
MATERIAL TECHNOLOGIES IN SILESIA

12-15.06.2022
Crystal Mountain***** Hotel, Wisła, Poland

Creep properties of some as-cast magnesium alloys and their composites

T. Rzychoń

[a] Silesian University of Technology, Faculty of Materials Engineering, Department of Material Technologies
email: tomasz.rzychon@polsl.pl

Abstract: In this paper the creep properties and microstructure of as-cast Mg-Al-Ca, Mg-Y-RE, Mg-Y-Zn, Mg-Zn-RE-Zr, Mg-Sn-Si and WE43 matrix composite reinforced with SiC particles are reported. The microstructure was characterized using light microscopy, scanning and transmission electron microscopy. Phase identification was made by SAED and XRD analysis. Creep tests were carried out in the temperature range from 180°C to 200°C at applied stress of 60 MPa. The microstructure of non heat-treated magnesium alloys (Mg-Al-Ca, Mg-Zn-RE) consists of α-Mg solid solution and intermetallic phases in the interdendritic areas. In heat-treated magnesium alloys, the fine precipitates appear inside the α-Mg grains. It promotes better creep resistance compared to untreated magnesium alloys. Homogeneously distributed SiC particles in WE43 composite and contribute to increasing hardness. At the interface, additional products deplete the matrix of alloying elements. This contributes to the deterioration of the mechanical properties at ambient temperature and the creep resistance.

Keywords: magnesium alloys, creep resistance, microstructure

1. INTRODUCTION

Magnesium alloys are among the lightest materials used in construction. Their relatively low density in combination with satisfactory mechanical and casting properties cause them to be widely used in the automotive and aviation industries [1,2]. In the case of the common Mg-Al alloys, the mechanical properties are dramatically reduced above 120°C [3]. Thus, it becomes necessary to develop magnesium alloys which could operate at elevated temperatures. To increase the creep resistance of Mg-Al alloys, alloying elements are introduced, such as silicon [4], strontium [5,6], calcium [5-7] and rare earth metals [8,9]. In the last decade, a Al-free magnesium-alloy grades with high creep resistance have been developed, which can be used for components working at a temperature of up to 300°C. This group comprises the following alloys: Mg-Zn-RE [10], Mg-Y-Nd-Zr and Mg-Nd-Gd-Zr [11-13]. These alloys have a very good thermal stability of the main strengthening phase at up to 250°C. However, the Mg-Y-Nd-Zr alloys have high associated cost due to the high cost of yttrium and the difficulties in casting. Therefore there is a need for an alternative alloy (Mg-Nd-Gd-Zr) which has similar properties to Mg-Y alloys, but with foundry handling and associated costs like non-yttrium containing alloys [11-14].
Among these alloys, EZ33 magnesium alloy exhibits good creep properties up to 200ºC. This alloy containing zinc, rare earth metals (mischmetal mixture) and zirconium. Zinc is usually used in combination with aluminum, zirconium or rare earths to produce precipitation-hardenable magnesium alloys having good strength. Addition of the rare earth metals increase the strength at elevated temperatures. Zirconium has a powerful grain-refining effect on magnesium alloys. The EZ33 alloy exhibits excellent casting characteristics with components being both pressure tight and weldable. The tendency to hot cracking in difficult castings is low [15-17].
A good alternative for Mg-Zn-RE alloys is available in the newest Mg-Al-Ca alloys. After gravity casting and suitable modification of the molten metal the mechanical properties of these alloys are comparable to those of expensive Mg–RE–Zn–Zr (ZRE1) alloys (tensile strength about 140 MPa and yield strength about 90 MPa) [18]. Calcium exerts a positive effect on the creep resistance of Mg-Al alloys. Moreover, the calcium boasts the low density and cost [2]. The creep resistance of Mg-Al-Ca alloys may also be heightened by the addition of strontium due to solid solution strengthening [18].

One possible way to increase the high-temperature mechanical properties of cast magnesium alloys at low manufacturing costs is the addition of silicon because the Mg_2Si phase exhibits a high melting temperature (1085°C), high hardness, low thermal coefficient and high elastic modulus [19]. Mg-Si alloys can be divided into two groups: hypoeutectic (below 1.45 at.% Si) and hypereutectic (above 1.45 at.% Si). Unfortunately, the as-cast hypereutectic alloys have a low mechanical properties due to the presence of primary Mg_2Si compound which forms the large particles in the matrix [19].

Acknowledgments: The present work was supported by the National Science Centre under the project UMO-2011/03/D/ST8/03869 and partially supported by the Polish Ministry of Science and Higher Education under the project No. POIG.01.01.02-00-015/09.

BIBLIOGRAPHY

1. J. Bai, Y. Sun, S. Xun, F. Xue, T. Zhu, Microstructure and tensile creep behavior of Mg–4Al based magnesium alloys with alkaline-earth elements Sr and Ca additions. Mater. Sci. Eng. A419 (2006) 181–188.
2. E. Aghion, B. Bronfin, F. Von Buch, H. Friedrich, S. Schumann, Newly Developed Magnesium Alloys for Powertrain Applications, JOM 55(11) (2003) 30-33.
3. K. U. Kainer, Magnesium - Alloys and Technologies, Wiley-VCH, 2003.
4. A.A. Luo, Recent magnesium alloy development for elevated temperature applications, Int. Mater. Reviews 49(1) (2003)13-30.
5. H. Friedrich, B.L. Mordike, Magnesium Technology, Metallurgy, Design Data, Applications, Springer-Verlag Berlin Heidelberg 2006.
6. T. Rzychoń., B. Adamczk-Cieślak, A. Kiełbus, J. Mizera, The influence of hot-chamber die casting parameters on the microstructure and mechanical properties of magnesium-aluminum alloys containing alkaline elements, Materialwiss. Werkstofftech. 43(5) (2012) 421-426.
7. T. Rzychoń, J. Szala, T. Kukiełka, Detection of intermetallic compounds in a Mg-5Al-3Ca-0.7Sr-0.2Mn magnesium alloy, Solid State Phenom. 197 (2013) 137-142.
8. T. Rzychoń, A. Kiełbus, L. Lityńska-Dobrzyńska, Microstructure, microstructural stability and mechanical properties of sand-cast Mg-4Al-4RE alloy, Mater. Charact. 83 (2013) 21-34.
9. T. Rzychoń, A. Kiełbus, Microstructure and tensile properties of sand cast and die cast AE44 Magnesium Alloy, Arch. Metall. Mater. 53 (2008) 901-907.
10. M. Gupta, N.M.L. Sharon, Magnesium, magnesium alloys and magnesium composites, John Wiley & Sons, Inc., Hoboken, New Jersey, 2011.
11. A. Kiełbus, T. Rzychoń, L. Lityńska-Dobrzyńska, G. Dercz, Characterization of β and $Mg_{41}Nd_5$ equilibrium phases in Elektron 21 magnesium alloy after long-term annealing, Solid State Phenom. 163 (2010) 106-109.
12. T. Rzychoń, A. Kiełbus, M. Serba, The influence of pouring temperature on the microstructure and fluidity of Elektron 21 and WE54 magnesium alloys, Arch. Metall. Mater. 55 (2010) 7-13.
13. B. Dybowski, A. Kiełbus, R. Jarosz, Effect of mould components on the cooling rate, microstructure, and quality of WE43 magnesium casting alloy, Arch. Metall. Mater. 29 (2014) 1527-15322.
14. A. Kiełbus, T. Rzychoń, The intermetallic phases in sand casting magnesium alloys for elevated temperature, Mater. Sci. Forum 690 (2011) 214-217.
15. www.magnesium-elektron.com (DS455.pdf).
16. M. Podosek, G.W. Lorimer, The influence of intergranular microstructure of Mg-Zn-RE alloys on properties at elevated temperatures, Arch. Metall. 45(1) (2000) 47-55.
17. I.P. Moreno, T.K. Nandy, J.W. Jones, J.E. Allison, T.M. Pollock, Microstructural stability and creep pf rare-earth containing magnesium alloys, Scripta Mater. 48 (2003) 1029-1034.
18. T. Rzychoń, Microstructure of MgAl5Ca3Sr alloy after creep deformation and high-temperature heat treatment, Materialwiss. Werkstofftech. 5 (2014) 1-10.
19. A. Suzuki, N.D. Saddock, L. Riester, E. Lara-Curzio, J.W. Jones, T.M. Pollock, Effect of Sr additions on the microstructure and strength of a Mg-Al-Ca ternary alloy, Metallurgical and Materials Transactions A 38A (2007) 420-427.
20. N. Zheng, H.Y. Wang, Z.H. Gu, W. Wang, Q.C. Jiang, Development of an effective modifier for hypereutectic Mg–Si alloys, J. Alloys Compd. 463 (2008) L1-L4.

MTS CONFERENCE
MATERIAL TECHNOLOGIES IN SILESIA

12-15.06.2022
Crystal Mountain***** Hotel, Wisła, Poland

Zmiany składu chemicznego kąpieli metalowej w procesie stalowniczym w produkcji stali wysokokrzemowych

K. Ścibisz[ab*], J. Krawczyk[c]

[a] ArcelorMittal Poland S.A. Oddział w Krakowie ul. Tadeusza Sendzimira 1, 31-752 Kraków,
[b] AGH Akademia Górniczo-Hutnicza, Szkoła Doktorska, al. A. Mickiewicza 30, 30-059 Kraków
[c] AGH Akademia Górniczo-Hutnicza, Wydział Inżynierii Metali i Informatyki Przemysłowej, al. A. Mickiewicza 30, 30-059 Kraków
*Autor do korespondencji: kamila.scibisz@arcelormittal.com

Abstrakt: Przedstawiono analizę zmian składu chemicznego podczas procesu stalowniczego stali wysokokrzemowych, docelowo przeznaczonych do produkcji blach transformatorowych. W analizie uwzględniono zmienność C, Mn, Si, S, Al i N. Omówiono role poszczególnych procesów stalowniczych na zmianę składu chemicznego. Odniesiono te zmiany do konkretnych stanowisk i stosowanych zabiegów. Zaproponowano sposób określania udziału poszczególnych rodzajów endogenicznych wtrąceń niemetalicznych oraz składu chemicznego osnowy metalicznej. Uzyskane wyniki zostały odniesione do wymagań i klasyfikacji stali wysokokrzemowych pod kątem ich zastosowania. Analizę procesu przeprowadzono dla wytopów uzyskanych w różnych sekwencjach wytopowych. Zmiany odniesiono do temperatury kąpieli metalowej. Przedstawiono również kinetykę zmiany składu chemicznego. Odniesiono tą zmienność do czynników surowcowych (np. klas złomu). Oceniono zawartość AlN w zależności od temperatury.

Słowa kluczowe: stale wysokokrzemowe, proces stalowniczy, skład chemiczny, endogeniczne wtrącenia niemetaliczne

1. WPROWADZENIE

Stale wysokokrzemowe wymagają spełnienia ścisłych wymagań odnośnie składu chemicznego. Dodatkowo kontrola wysokiej zawartości krzemu wpływa na wyjątkowość procesu stalowniczego. Proces stalowniczy musi więc być wyjątkowo ściśle kontrolowany ze względu na konieczność uzyskania zawartości pierwiastków w ściśle określonych przedziałach. Istotnym w tym zakresie jest np. stosunek Al/N. Końcowy skład chemiczny stali w zakresie zawartości Al, N, S i O oraz Ti, Nb i V, będzie pozwalał na szacowanie zawartości endogenicznych wtrąceń niemetalicznych w stali takich jak siarczki, tlenki i azotki. Oszacowanie zawartości takich wtrąceń jest istotna dla oceny ich wpływu na finalne właściwości magnetyczne stali transformatorowych.

2. MATERIAŁ DO BADAŃ

Analizie poddano 6 wytopów stali wysokokrzemowej uzyskanych w dwóch sekwencjach. Stal odlewano w zakładzie produkcyjnym firmy ArcelorMittal zgodnie z obowiązującymi standardami. Skład chemiczny analizowano na poszczególnych etapach procesu, za punkt początkowy przyjęto odsiarczanie surówki na stacji odsiarczania, etapem końcowym analizy było ciągłe odlewanie stali na maszynie COS3. Materiałem badawczym były wyniki analiz chemicznych uzyskane z prób przy standardowej produkcji.

3. SKRÓT WYNIKÓW BADAŃ

Złożoność procesu produkcyjnego i określona ścieżka produkcyjna determinują zmienną zawartość wybranych pierwiastków na poszczególnych etapach procesu produkcyjnego. Jako pierwszy analizie poddano węgiel. Zaobserwowano ubytek węgla po procesie konwertorowym średnio o 0,0038. Najniższy zanotowany spadek wynosił 0,0002 natomiast najwyższy 0,0086. Ostatecznie dla wszystkich wytopów uzyskano zbliżoną zawartość C w zakresie 0,0323% – 0,035%. Kolejnym pierwiastkiem poddanym analizie był Si, końcowa uzyskana zawartość Si mieściła się w zakresie 3,069%-3,2047% (rys. 1). Szczególną uwagę zwróconą na udział Al i N, dla których uzyskano odpowiednio wyniki: Al od 0,015% do 0,016%; N od 0,0078% do 0,0085%. Wyniki badań przedstawiono na wykresach.

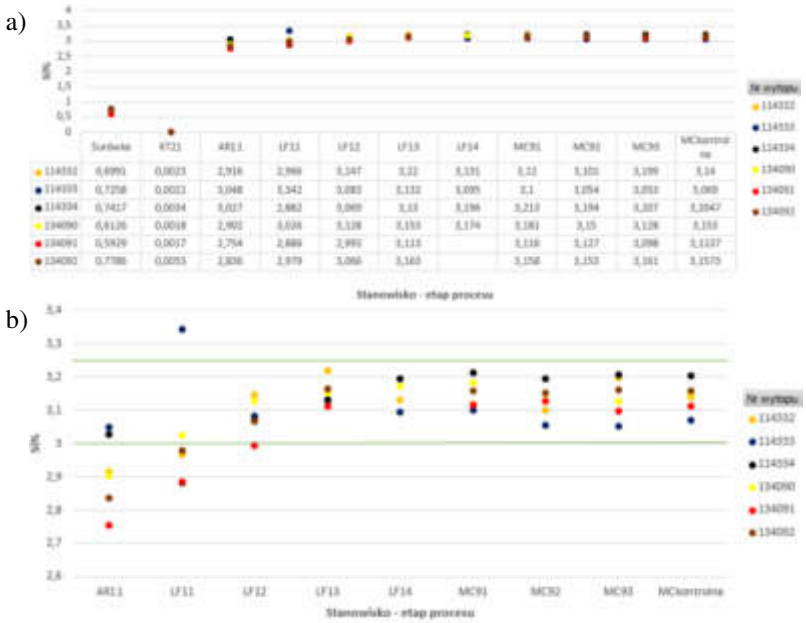

Rysunek 1. Przykładowe wyniki badań: a) *zawartość %Si na poszczególnych etapach procesu stalowniczego, b) zawartość %Si na wybranych etapach procesu stalowniczego (z pominięciem początkowych procesów stalowniczych).*

4. SPOSTRZEŻENIA OGÓLNE

W procesie stalowniczym analizowano zmiany składu chemicznego pierwiastków związanych z wtrąceniami niemetalicznymi endogenicznymi. Każdy analizowany pierwiastek powinien być kontrolowany w zdefiniowanym, założonym zakresie. Istotnym czynnikiem jest kontrola stosunku aluminium do azotu. Drobne wydzielenia AlN są inhibitorami pożądanej tekstury dla wyrobów końcowych - blach transformatorowych [1]. Ich ilość i wielkość różni się w zależności od struktury. W strukturze ferrytycznej azotki utrzymują się dłużej natomiast w zakresie austenitycznym azotki są całkowicie rozpuszczalne. W związku z tym w założonej temp walcowania jeśli występuje austenit to azotków nie będzie w strukturze. Jednym z istotniejszych zagadnień jest określenie azotków AlN głównie podczas walcowania na gorąco stali wysokokrzemowych. W tym celu użyto symulacji komputerowej programu Carb_Nit [2], przykładowe wyniki przedstawiono na rysunku 2.

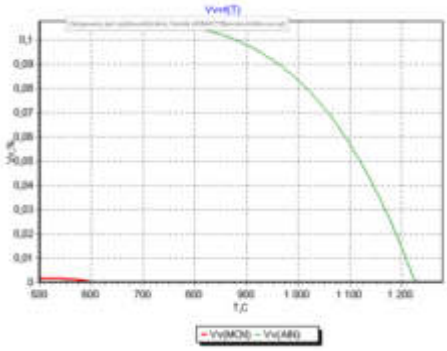

Rysunek 2. Przykładowe wyniki badań: Procentowy udział AlN w zależności od temperatury występujący w strukturze ferrytycznej stali wysokokrzemowej

Podziękowania: Praca finansowana przez Ministerstwo Edukacji i Nauki w ramach V edycji doktoratów wdrożeniowych.

LITERATURA

1. Różański P., Radwański K., Niesler M., Zdonek B., Mazur A., Pidvysots'kyy V., Kuziak R., Innowacyjna stal wysokokrzemowa z regulowaną zawartością zanieczyszczeń I wtrąceń niemetalicznych o kontrolowanej morfologii oraz odpowiednim poziomie inhibitora AlN z przeznaczeniem na wysokojakościowe blachy transformatorowe, Journal of Metallic Materials 72 (2) (2020) 63-82
2. Carb_Nit – program komputerowy autorstwa Adrian H.

MTS CONFERENCE
MATERIAL TECHNOLOGIES IN SILESIA

12-15.06.2022
Crystal Mountain***** Hotel, Wisła, Poland

The isothermal treatment of an intercritically annealed 38CrAlMo7-10 steel for gear application

E. Skołek [a], A. Gołaszewski [a], M. Węsierska-Hinca [a], Sz. Marciniak [a], J.R. Sobiecki [a]

[a] Warsaw University of Technology, Faculty of Materials Science and Engineering
email: emilia.skolek@pw.edu.pl

Abstract: The aim of this work is to design heat treatment consisting of bainitic isothermal holding preceded by intercritical annealing that leads to formation of multiphase submicron-sized microstructure based on bainite and stabilized retained austenite in 38CrAlMo7-10 steel in terms of gear application. During the first stage of the proposed treatment steel is heated up and held within the two-phased region (ferrite + austenite), between the A1 and A3 temperatures, then subsequently quenched to an isothermal stop with cooling rate higher than critical. Isothermal holding at temperature above Ms lead to the austenite decomposition into bainite. The schematic of the TRIP-assisted steel heat treatment is shown in Fig. 1. The accurate selection of time and temperature of individual stages of the heat treatment enables formation of a microstructure containing 50-60% ferrite, 25-40% bainite and 5-15% austenite.
Parameters of the proposed heat treatment of 38CrAlMo7-10 steel were established using computer simulations, dilatometric studies and hardness measurements accompanied by microscopic observations (LM) of the heat treated samples. The conducted research allowed to determine the influence of time and temperature of the intercritical annealing on Ms temperature, based on which the isothermal holding was designed.

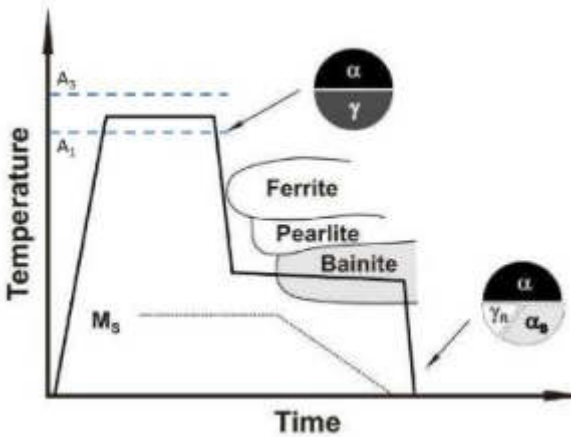

Figure 1. Schematic of the heat treatment in TRIP-assisted steels [1]. α – ferrite, γ_R – retained austenite, α_B – bainite.

Keywords: TRIP effect, bainite, austenite, austempering, intercritical annealing

1. INTRODUCTION

The isothermal treatment of the intercritically annealed steels has been successfully adapted in automotive industry. This type of heat treatment is especially dedicated to steels containing approx.. 3.5% wt. of alloying elements, including 0.12–0.55 wt.% C, 0.2–2.5 wt.% Mn and 0.4–1.8 wt.% Si or Al. It allows to obtain ferrite-bainite-martensite triple phase microstructure that exhibits a wide range of mechanical properties controlled by the volume fraction of particular phase constituents. The characteristic features of the intercritically annealed steels are the absence of a sharp yield point, very low $R_{0,2}$/Rm coefficient and high formability index (A x Rm).

Moreover, the stabilized retained austenite present in the microstructure is able to absorb energy through martensitic transformation during deformation (TRIP effect), which is crucial in case of collision in automotive application. However, the relatively low hardness in TRIP-assisted steels can limit its application in various industries. On the other hand, low hardness enables heat treatment of the semi-finished products, from which the finished elements eventually will be made. This solution allows elimination of the last stage of production – grinding and avoids the need of material allowances, frequently associated with heat deformation, surface defects resulting from the treatment, etc. Therefore, the TRIP-assisted steels can be implemented, among others, in production of gears for various applications, including gear transmission systems in mining machines. The high toughness, high bending fatigue resistance of gear teeth and enhanced surface hardness are required for the manufacture of heavy-duty gears. The first two parameters can be achieved applying isothermal treatment to an intercritically annealed steel, whereas the last criterion can be attained for finished elements using surface engineering processes. 38CrAlMo7-10 steel meets the above requirements.

The main aim of this research is the evaluation of the possibility of applying an isothermal heat treatment to the intercritically annealed 38CrAlMo7-10 steel and selection of the optimal parameters leading to formation of multiphase submicron-sized microstructure based on bainite and stabilized retained austenite with potential use in the manufacturing of gears.

2. RESULTS

First part of this research involved determination of critical transformation temperatures, such as Ac1 and Ac3 equal to 770°C and 885°C, respectively. Consequently, on the basis of obtained results supported by simulations of phase composition with varying intercritical annealing temperature (ferrite and austenite fraction, carbon concentration in austenite, carbide: $M_{23}C_6$, M_7C_3 and cementite fraction) three variants of intercritical annealing temperatures were selected: 795, 805 and 815 °C. The influence of time and temperature of intercritical annealing on Ms temperature values and quenched samples' hardness was investigated. The obtained results are presented in Table 2 and 3, respectively. As it can be seen, the increase of holding temperature in the two-phase region augments value of the Ms temperature. The higher intercritical austenitization temperature, the higher amount of austenite is formed, but with lower carbon concentration which has a direct impact on Ms temperature.

On the other hand, increase of annealing time causes Ms reduction, which is probably attributed to the carbides dissolution and the consequent austenite carbon enrichment. Note, that increase of both parameters, intercritical annealing temperature and time, influence the hardness increment. Although the carbon content in austenite and, ultimately, in martensite decreases with temperature, the hardness of the material is higher due to the amount of martensite formed. On the basis of the obtained results, parameters of isothermal quenching preceded by intercritical annealing will be designed.

Table 1. The influence of intercritical annealing parameters on Ms temperature in 38CrAlMo7-10 steel

Time / Temperature	1h	2h	10h
795°C	311	305	286
805°C	316		
815°C	338		

Table 2. The influence of intercritical annealing parameters on hardness (HV2) in 38CrAlMo7-10 steel

Time / Temperature	1h	2h	10h
795°C	442	464	545
805°C	536		
815°C	554		

Acknowledgments: The research was supported by Warsaw University of Technology and the National Center for Research and Development under the project no. TECHMATSTRATEG-III/0028/2019-00. Development of innovative hybrid surface layers composed of anti-wear coatings dedicated to gears for conveyor drive assemblies working in difficult operating conditions

BIBLIOGRAPHY

[1] Bleck W., Phiu-On K.: Microalloying of Cold-Formable Multi Phase Steel Grades, Mat. Sc. Forum, Vols. 500–501, 2005

MTS CONFERENCE
MATERIAL TECHNOLOGIES IN SILESIA

12-15.06.2022
Crystal Mountain***** Hotel, Wisła, Poland

Modyfikacja morfologii bainitu oraz austenitu szczątkowego w wysokowytrzymałych stalach średniomanganowych

A. Skowronek[a,*], A. Grajcar[a]

[a] Politechnika Śląska, Wydział Mechaniczny Technologiczny, Katedra Materiałów Inżynierskich i Biomedycznych
email: *adam.skowronek@polsl.pl; adam.grajcar@polsl.pl

Abstract: Praca dotyczy możliwości maksymalizacji udziału austenitu szczątkowego oraz rozdrobnienia mikrostruktury w procesie wytrzymania izotermicznego stali średniomanganowej 3,3Mn-0,17C-1,6Al-0,23Mo-0,22Si. Proces pojedynczy został zrealizowany w temperaturze 450 przez 10 min i jest porównywany z procesem podwójnym, dla którego I etap odbywa się w 450°C przez określony czas - odpowiadający 50% przemiany bainitycznej. Następnie temperatura zostaje obniżona do 400°C w celu dokończenia przemiany.

Keywords: austenit szczątkowy, stal AHSS, przemiana bainityczna, dylatometria

1. WSTĘP

Zmniejszenie grubości płytek bainitycznych ma kluczowe znaczenie dla poprawy właściwości mechanicznych wysokowytrzymałych stali obrabianych izotermicznie. Zarówno twardość, jak i udarność poprawiają się wraz ze zmniejszeniem grubości płytek, która zależy zarówno od składu chemicznego, jak i temperatury wytrzymania izotermicznego. Z tego względu najczęstszą metodą rozdrobnienia bainitu jest obniżenie temperatury etapu wytrzymania. Obszar występowania przemiany bainitycznej jest ograniczony przez temperatury początkowe przemian bainitycznej (B_s) i martenzytycznej (M_s). W ostatnim czasie prowadzone są badania w kierunku zastosowania podwójnego lub wielostopniowego wytrzymania izotermicznego. Pierwszy etap odbywa się w temperaturze nieco wyższej niż M_s stopu, natomiast temperatura kolejnego etapu (lub kolejnych etapów) podąża za obniżającą się temperaturą M_s, co spowodowane jest stabilizacją austenitu wskutek jego stopniowego wzbogacenia w węgiel. Innym argumentem za obniżeniem temperatury przemiany bainitycznej jest ewolucja morfologii austenitu szczątkowego w stalach bainitycznych, z ziarn blokowych do cienkich warstw lub filmów.

Celem pracy była analiza możliwości aplikacyjnych przedstawionej strategii obróbki cieplnej w najnowszej generacji wysokowytrzymałych stali dla motoryzacji – stalach średniomanganowych.

2. METODYKA BADAŃ

Eksperymenty przeprowadzono z wykorzystaniem stali 3,3Mn-0,17C-1,6Al-0,23Mo-0,22Si z zastosowaniem dylatometrii oraz symulatora Gleeble. Materiał został poddany pojedynczej oraz podwójnej przemianie bainitycznej. Proces pojedynczy został zrealizowany w temperaturze 450 °C (M_s stali ~ 430 °C) przez 10 min i stanowił odniesienie do procesu podwójnego, dla którego I etap przeprowadzono w 450°C przez czas odpowiadający 50 % przemiany bainitycznej. Następnie temperatura została obniżona do 400°C w celu dokończenia przemiany. Do obrazowania wykorzystano mikroskopię świetlną oraz skaningową mikroskopię elektronową. Próbki poddano następnie badaniom rentgenowskim (XRD) w celu wyznaczenia udziału austenitu szczątkowego. Zastosowano trawienie kolorowe z wykorzystaniem odczynnika Klemma. Własności mechaniczne zostały określone z wykorzystaniem badań twardości Vickersa.

3. WYNIKI BADAŃ

Jednoetapowa przemiana bainityczna przeprowadzona w temperaturze 450 °C (~ 20 °C powyżej rozpoczęcia przemiany martenzytycznej dla badanego stopu) skutkuje uzyskaniem struktury bainityczno-austenitycznej z ~ 10 % udziałem grubolistwowego martenzytu, co widoczne jest na rysunku 1a. Pojawienie się niepożądanej fazy martenzytycznej w mikrostrukturze związane jest z zachowaniem obszarów austenitycznych słabo wzbogaconych w węgiel po zakończeniu przemiany bainitycznej. Badania rentgenowskie wskazują, iż udział austenitu w stali wynosi ~14 % przy jego wzbogaceniu w węgiel ~1%. Struktura po podwójnej przemianie bainitycznej wykazuje znacznie wyższą jednorodność oraz prawie całkowite ograniczenie występowania martenzytu (>>1%), co związane jest ze znacznie szerszym zakresem przemiany bainitycznej w obniżonej temperaturze. Stężenie węgla w pozostałym austenicie szczątkowym wzrosło do ponad 1,2 %, przy zachowaniu ponad 13 % tej fazy (co wpływa na jego podwyższoną stabilność). Pomiary z wykorzystaniem wysokorozdzielczych zdjęć SEM ujawniły w materiale po obróbce podwójnej redukcję grubości płytek bainitycznych o ponad 15%, natomiast filmów austenitycznych aż o 38 % w stosunku do wariantu pojedynczego. Skutkuje to finalnie podwyższeniem twardości o 40 HV10, z wyjściowych 323 HV10 w próbce po obróbce pojedynczej.

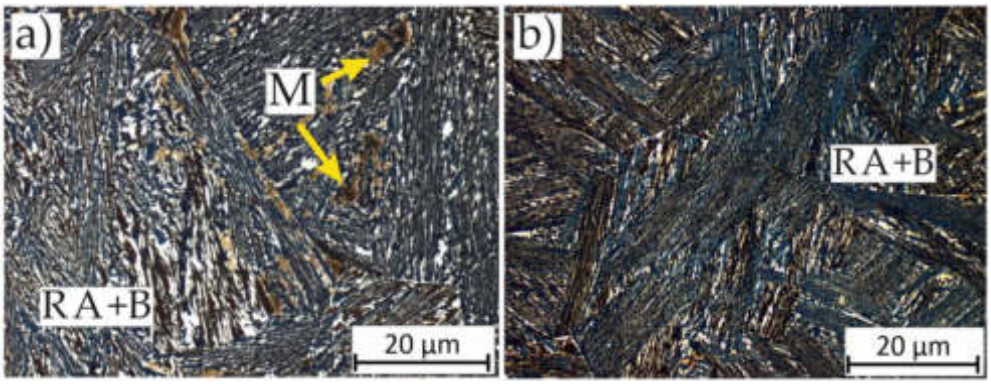

Figure 1. Ewolucja mikrostruktury przy zastosowaniu różnych wariantów obróbki bainitycznej: (a) przemiana pojedyncza w 450 C; (b) przemiana podwójna 450/400°C; M – martenzyt, RA – austenit szczątkowy, B – bainit

4. WNIOSKI

Wzbogacenie austenitu w węgiel podczas wytrzymywania izotermicznego w obszarze bainitycznym prowadzi do obniżenia temperatury M_s, a tym samym umożliwia kontynuację przemiany bainitycznej w niższej temperaturze. Pozwala to na rozdrobnienie struktury bainitycznej, co wpływa także na dodatkowe rozdrobnienie austenitu szczątkowego zwiększając jego stabilność termiczną i mechaniczną. Podsumowując, zarówno mechaniczną, jak i termiczną stabilność austenitu szczątkowego można zwiększyć, stosując dodatkowy krok podczas izotermicznego wtrzymania. Przekłada się to na wyższe właściwości mechaniczne stali średniomanganowych.

Podziękowania: Praca wykonana i finansowana w ramach grantu Narodowego Centrum Nauki, nr 2017/27/B/ST8/02864.

MTS CONFERENCE
MATERIAL TECHNOLOGIES IN SILESIA

12-15.06.2022
Crystal Mountain***** Hotel, Wisła, Poland

Preparation and characterization of one-dimensional In_2O_3 nanostructures

W. Smok[a]

[a] Silesian University of Technology, Faculty of Mechanical Engineering, Department of Engineering Materials and Biomaterials
email: weronika.smok@polsl.pl

Abstract: The aim of this work was to manufacture one-dimensional In_2O_3 nanostructures via electrospinning method with subsequent calcination. Additionally, an analysis of the morphology, structure and chemical composition of the produced PVP/$In(NO_3)_3$ nanofibers and In_2O_3 nanowires was performed using, respectively, Scanning Electron Microscopy, Raman spectroscopy, Fourier Transform Infrared Spectroscopy and Energy Dispersive X-Ray Spectroscopy.

Keywords: electrospinning, nanofibers, nanowires, indium oxide

1. INTRODUCTION

Recently, one-dimensional (1D) semiconductor metal oxide nanostructures have attracted scientists and industry attention, due to their unique electrical and optical properties. One of this type of nanomaterial is indium oxide (In_2O_3), which is very important wide band gap (3,2-3,6 eV) n-type semiconductor [1]–[3]. Moreover, it presents unusual combination of high transparency in visible region and high electrical conductivity [4]–[6] These properties make In_2O_3 an intersting material for a wide range of applictaions such as photocatalysis, innovative solar cells, novel optoelectronic devices, ultrasensitive gas sensors [7]–[10].

The above considerations indicate that 1D In_2O_3 is an extremely important nanomaterial and the method of its manufacturing significantly affects its properties. Therefore, simple, economical and universal methods of producing this material should be sought in order to ensure the best quality of nanostructures. These forms of In_2O_3 have been synthesized by various methods, including the chemical vapor deposition route, the hydro- and solvothermal method, the thermal evaporation oxidation method, and the sol–gel method. Recently, electrospinning technique has been extended to synthesis of not only organic, but also inorganic materials, such as SnO_2, TiO_2, WO_3, ZnO. Furthermore, electrospinning was proven to be a successful technique for controlling the fabrication of 1D nanostructures including nanofibers, nanowires, nanotubes and other novel structures.

Therefore, the aim of this work was to preprare 1D In_2O_3 nanostructures using electrospinning process and to study their morphology, structure and chemical composition (Fig. 1).

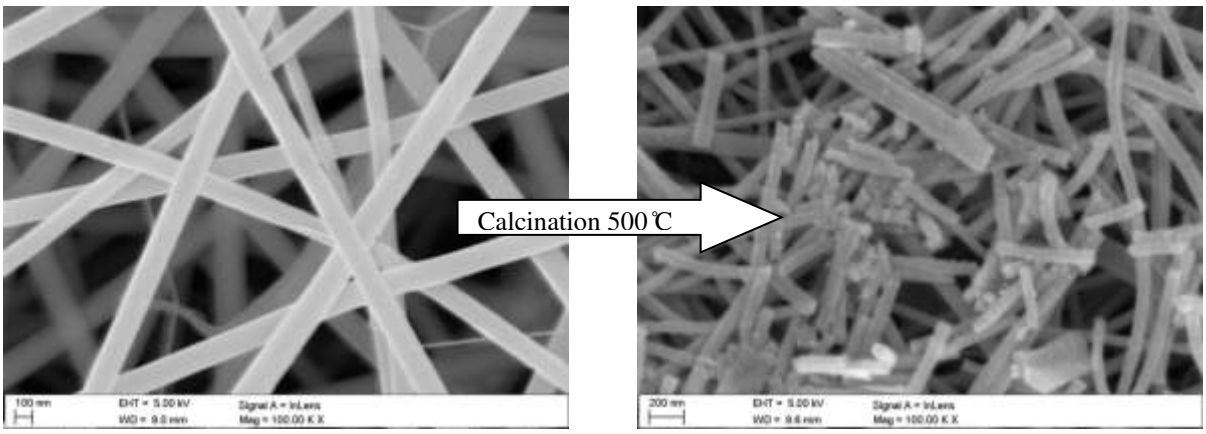

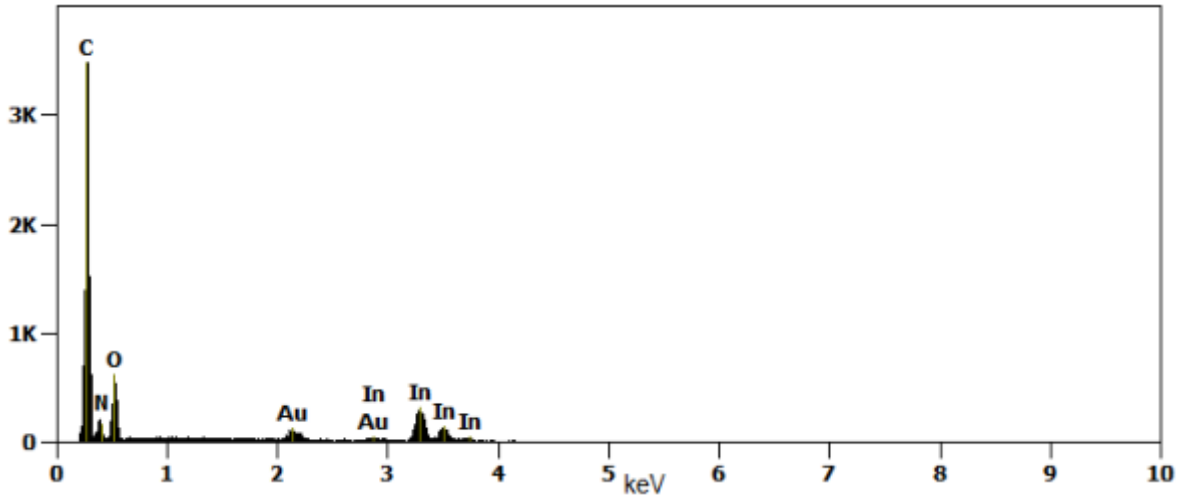

Figure 1. SEM images of 1D indium oxide-based nanostructures with EDX chemical composition analysis

BIBLIOGRAPHY

1. G. Jo *et al.*, "Structural and electrical characterization of intrinsic n-type In2O3 nanowires," *Colloids Surfaces A Physicochem. Eng. Asp.*, vol. 313–314, pp. 308–311, Feb. 2008, doi: 10.1016/j.colsurfa.2007.04.166.
2. N. Lu, C. Shao, X. Li, F. Miao, K. Wang, and Y. Liu, "A facile fabrication of nitrogen-doped electrospun In 2 O 3 nanofibers with improved visible-light photocatalytic activity," *Appl. Surf. Sci.*, vol. 391, pp. 668–676, Jan. 2017, doi: 10.1016/j.apsusc.2016.07.057.
3. W. Liu, Y. Xie, T. Chen, Q. Lu, S. Ur Rehman, and L. Zhu, "Rationally designed mesoporous In2O3 nanofibers functionalized Pt catalysts for high-performance acetone gas sensors," *Sensors Actuators, B Chem.*, vol. 298, p. 126871, Nov. 2019, doi: 10.1016/j.snb.2019.126871.
4. S. Kar and S. Chaudhuri, "Synthesis, photoluminescence and field emission properties of In2O3 nanowires," *Chem. Phys. Lett.*, vol. 422, no. 4–6, pp. 424–428, May 2006, doi: 10.1016/j.cplett.2006.03.002.
5. Z. G. Zhang *et al.*, "Recent advances in 1D micro- and nanoscale indium oxide structures," *Journal of Alloys and Compounds*, vol. 752. Elsevier Ltd, pp. 359–375, Jul. 05, 2018, doi: 10.1016/j.jallcom.2018.04.188.
6. M. Vila, C. Díaz-Guerra, and J. Piqueras, "α-Bi2O3 microcrystals and microrods: Thermal synthesis, structural and luminescence properties," *J. Alloys Compd.*, vol. 548, pp. 188–193, Jan. 2013, doi: 10.1016/j.jallcom.2012.08.133.
7. C. Feng, X. Liu, S. Wen, and Y. An, "Controlled growth and characterization of In 2 O 3 nanowires by chemical vapor deposition," *Vacuum*, vol. 161, pp. 328–332, Mar. 2019, doi: 10.1016/j.vacuum.2018.12.055.
8. S. Zhang, P. Song, Z. Yang, and Q. Wang, "Facile hydrothermal synthesis of mesoporous In2O3 nanoparticles with superior formaldehyde-sensing properties," *Phys. E Low-Dimensional Syst. Nanostructures*, vol. 97, pp. 38–44, Mar. 2018, doi: 10.1016/j.physe.2017.10.020.
9. P. Van Tong, L. Hoang Minh, N. Van Duy, and C. Manh Hung, "Porous In2O3 nanorods fabricated by hydrothermal method for an effective CO gas sensor," *Mater. Res. Bull.*, vol. 137, p. 111179, May 2021, doi: 10.1016/j.materresbull.2020.111179.
10. N. Padmanathan, H. Shao, D. McNulty, C. O'Dwyer, and K. M. Razeeb, "Hierarchical NiO-In2O3 microflower (3D)/ nanorod (1D) hetero-architecture as a supercapattery electrode with excellent cyclic stability," *J. Mater. Chem. A*, vol. 4, no. 13, pp. 4820–4830, 2016, doi: 10.1039/c5ta10407f.

MTS CONFERENCE
MATERIAL TECHNOLOGIES IN SILESIA

12-15.06.2022
Crystal Mountain***** Hotel, Wisła, Poland

Enhancement of strength-ductility synergy of SLM AlSi10Mg alloy through ECAP processing

P. Snopiński[a], S. Rusz[b]

[a] Silesian University of Technology, Faculty of Mechanical Engineering, Department of Engineering Materials and Biomaterials
email: przemyslaw.snopinski@polsl.pl
[b] Faculty of Mechanical Engineering, VSB-TU Ostrava, 17. Listopadu 2172/15, 708 00 Ostrava, Czech Republic

Abstract: To overcome the trade-off between strength and ductility of the additively manufactured AlSi10Mg alloy used in the automotive and aerospace industries, samples with a multilevel structural heterogeneity were produced using single-pass ECAP at 150 ° C and 200 ° C. The microstructure of the analyzed samples was composed of a partially ruptured Al / Si cellular network and alternatively arranged zones of elongated (pancaked) grains separated by wide zones composed of ultrafine grains. Experimental results demonstrated that the AlSi10Mg alloy sample deformed at 150 ° C exhibited a superior ultimate tensile strength (UTS) of ~541 MPa but limited ductility, while the sample deformed at 200 ° C exhibited both a high ultimate tensile strength (UTS) of ~463 MPa and an excellent elongation at break of ~16.3%. It reveals that the superior combination of strength and ductility originated from the bimodal grain size distribution, Orowan bowing, mechanical twining of the hard Si phase, and back-stress hardening. Our results shed new light on the unexploited potential in improving the mechanical properties of additively manufactured alloys.
Keywords: AlSi10Mg, ECAP, EBSD, TEM, deformation mechanisms

1. INTRODUCTION

In recent decades, the accelerated development of the traffic and transportation sector has caused significant alterations in the global climate due to the ever-increasing emissions of CO_2 [1]. Although increasing political awareness and increasing economic necessity have boosted research and development in these sectors, current technologies are still not capable of fully addressing this challenge.

One way to substantially improve energy savings and thus reduce the level of harmful emissions is significant optimizations in vehicle design, which are strongly related to the materials used. Light weighting by deploying low-density materials such as aluminium alloys to substitute high-density steel is a well-established approach to mitigate greenhouse emissions. The reduction in vehicle weight linearly results in a corresponding reduction in fuel consumption, with a general value of 0.5 liters less fuel per 100 kg of weight reduction [2]. Unfortunately, multiple operational demands and engineering criteria, in particular those promoting strength and ductility, limit the benefits of light weighting due to the restricted property portfolio of commercial aluminum alloys and require the unbeneficial utilization of a multimaterial mix, thus limiting the recyclability at the end of a product lifetime. Therefore, the trade-off between strength and ductility becomes a fundamental challenge in the manufacturing of lightweight, high-performance structural materials. Focusing on metals, the strength is mainly enhanced via microstructure refinement to the nanometer scale [3]. There are also several other well-known mechanisms for strengthening metallic materials, in addition to refining grains, including solution hardening, dislocation (cold work) hardening, and precipitation (second-phase particle) hardening. However, these strengthening mechanisms are also often accompanied by a reduction in ductility [4], which is attributed to the lack of strain hardening capacity that is primarily due to inefficient dislocation storage. The question thus arises of whether there are yet to be explored new strategies to make the next generation of lightweight metals and alloys with a 'quantum jump' in strength and ductility instead of the incremental improvements we have seen over the past several decades?

To obtain a combination of high strength and good ductility, materials with a high strain-hardening capacity are required. Strain hardening results from interactions between the bearers of various deformation mechanisms

and lattice defects within the material and progresses on multiple scales ranging from the atomic level to the level of individual grains [5] [6]. The strain hardening capacity can be enhanced by increasing the number of potential deformation mechanisms associated with different bearers, such as slip deformation (SD), mechanical twinning (MT), or the addition of a strain gradient (heterogeneous microstructural design).

Heterostructured (HS) materials are generally produced through simple thermomechanical processing routes that can be easily applied to emerging new alloys. However, current developments in additive manufacturing techniques enable the formation of a complex geometric structure with custom material properties. Intuitively, if the composition of a material changes at a different location within a product, this technique would exhibit significant potential for the fabrication of HS materials. According to Chen et al. [7] and Li et al. [8] the SLM AlSi10Mg alloy having a heterogeneous cellular network structure has an almost twice higher work hardening exponent of ~0.252 than the PM alloy ~0.127 and more than twice higher work hardening exponent than the conventional gravity-cast Al-Si alloy ~0.1 [9]. The existing microstructural heterogeneity in additively manufactured materials can promote grain refinement, as GNDs provide a continuous increase in subgrain boundary misorientations, which, in conjunction with the strong strain hardening capability, makes heterostructured materials ideal candidates to overcome the strength-ductility trade-off that is the case for homogeneous counterparts.

Consequently, in this work, we investigated a novel post-processing strategy for the SLM-fabricated AlSi10Mg alloy which opens new opportunities in the design of high-strength and ductile aluminium alloys. Then, the mechanisms responsible for high-strength AlSi10Mg samples were examined by microstructure characterizations and confirmed by hardness and tensile property measurements. The justification for the use of additively manufactured AlSi10Mg alloy lies in the fact that the unique cellular microstructure offers substantially different deformation mechanisms from conventional counterparts thus providing suitable starting points for severe grain refinement. According to studies by Zhang et al. [10] and Kim et al. [11] the basic deformation mechanism in rapidly solidified Al-Si alloys includes plastic incompatibility across the Al/Si interface (accommodated by geometrically necessary dislocations during straining) and the deformation twinning of the Si phase.

Acknowledgments: This article was completed in association with project Innovative and additive manufacturing technology—new technological solutions for 3D printing of metals and composite materials, reg. no. 319 CZ.02.1.01/0.0/0.0/17_049/0008407 financed by Structural Funds of the European Union.

BIBLIOGRAPHY

[1] D. Mayer, T. Bein, H. Buff, B. Götz, O. Schwarzhaupt, D. Spancken, Enhanced lightweight design by composites – Results of the EU project ENLIGHT, J. Reinf. Plast. Compos. (2018).
[2] Z. Wang, W. Lu, H. Zhao, C.H. Liebscher, J. He, D. Ponge, D. Raabe, Z. Li, Ultrastrong lightweight compositionally complex steels via dual-nanoprecipitation, Sci. Adv. 6 (2020) eaba9543.
[3] G.B. Schaffer, S.H. Huo, J. Drennan, G.J. Auchterlonie, The effect of trace elements on the sintering of an Al-Zn-Mg-Cu alloy, Acta Mater. (2001). https://doi.org/10.1016/S1359-6454(01)00177-X.
[4] Y. Wei, Y. Li, L. Zhu, Y. Liu, X. Lei, G. Wang, Y. Wu, Z. Mi, J. Liu, H. Wang, H. Gao, Evading the strength-ductility trade-off dilemma in steel through gradient hierarchical nanotwins, Nat. Commun. (2014).
[5] U.F. Kocks, H. Mecking, Physics and phenomenology of strain hardening: The FCC case, Prog. Mater. Sci. (2003). https://doi.org/10.1016/S0079-6425(02)00003-8.
[6] R.O. Ritchie, The conflicts between strength and toughness, Nat. Mater. (2011). https://doi.org/10.1038/nmat3115.
[7] B. Chen, S.K. Moon, X. Yao, G. Bi, J. Shen, J. Umeda, K. Kondoh, Strength and strain hardening of a selective laser melted AlSi10Mg alloy, Scr. Mater. (2017).
[8] Z. Li, Z. Li, Z. Tan, D.B. Xiong, Q. Guo, Stress relaxation and the cellular structure-dependence of plastic deformation in additively manufactured AlSi10Mg alloys, Int. J. Plast. (2020).
[9] R. Hadian, M. Emamy, N. Varahram, N. Nemati, The effect of Li on the tensile properties of cast Al-Mg2Si metal matrix composite, Mater. Sci. Eng. A. (2008). https://doi.org/10.1016/j.msea.2008.01.039.
[10] H.H. Lien, J. Mazumder, J. Wang, A. Misra, Ultrahigh strength and plasticity in laser rapid solidified Al–Si nanoscale eutectics, Mater. Res. Lett. (2020). https://doi.org/10.1080/21663831.2020.1755380.
[11] D.K. Kim, J.H. Hwang, E.Y. Kim, Y.U. Heo, W. Woo, S.H. Choi, Evaluation of the stress-strain relationship of constituent phases in AlSi10Mg alloy produced by selective laser melting using crystal plasticity FEM, J. Alloys Compd. 714 (2017) 687–697. https://doi.org/10.1016/J.JALLCOM.2017.04.264.

MTS CONFERENCE
MATERIAL TECHNOLOGIES IN SILESIA

12-15.06.2022
Crystal Mountain***** Hotel, Wisła, Poland

Possibilities of evaluating the effect of hydrogen in magnesium alloys with rare earth elements

M. Sozańska [a]

[a] Silesian University of Technology, Faculty of Material Engineering, Department of Materials Technologies
email: maria.sozanska@polsl.pl

Abstract: The article presents the possibilities of assessing the destructive effect of hydrogen in WE43 magnesium alloy containing rare earth elements (RE) under the conditions of alloy hydrogenation in the environment of 0.1M Na_2SO_4.

Keywords: magnesium alloys, hydrogen, mechanical properties, degradation, test methods

1. RESEARCH IDEA

Magnesium alloys are characterized by the lowest density of all metallic structural materials and display good mechanical properties. Therefore, they are widely used in automotive and aerospace industries. However, magnesium alloys show very poor corrosion resistance, even in dilute electrolyte solutions []. Structural components made of magnesium alloys are often subjected to mechanical load and corrosive environment contains hydrogen simultaneously. Initiation and advancement of micro cracks is very difficult to detection. In the first step material failure displays no significant indications, although it leads to essential properties changes [2-6].

The basic criterion for assessing the alloy's behaviour under complex mechanical and corrosive loads is deterioration in mechanical properties (elongation – ε, %, reduction in area – Z, %, tensile strength – Rm, MPa, time to failure –t, h) by *Slow Strain Rate Test* (SSRT) in air and in a corrosive environment (particularly with the presence of hydrogen) conditions. However, it is very often an insufficient criterion to assess the effect of hydrogen in the material [7-9].

Generally, the interaction of hydrogen in metal alloys can be divided into several sub-stages and assessed qualitatively and quantitatively at each of these stages using different test methods:

Stage 1 - HYDROGENATION (from solution - electrochemical parameters: potentiostat; in gases – physical parameters, e.g. pressure, temperature, hydrogen concentration in the alloy),

Stage 2 - TRANSPORT: diffusion and transport by dislocations,

Stage 3 – LOCATIONS:
- **trapping hydrogen on structural defects in the alloy,**
- **formation of hydrides,**
  (structural, chemical and phase composition studies in terms of micro- and substructure, e.g. SEM-TEM with techniques accompanying the chemical composition: EDS, WDS, XPS and phase: electron and X-ray diffraction),

Stage 4 – FRACTURE (cracking):
- **evaluation of stresses in the material,**
- **initiation and development of micro cracks,**
- **final destruction** (fracture),
  (shape of samples, tests of mechanical properties, e.g. *Slow Strain Rate Test* - SSRT, fatigue tests, numerical models; structural and fractographic tests).

The paper presents the possibility of assessing the interaction of hydrogen in the WE43 magnesium alloy at various levels, from the characteristics of its penetration into the alloy, through diffusion and trapping on defects

and the formation of hydrides, changes in the stress state and the initiation and development of micro cracks, up to the final destruction (Fig.1).

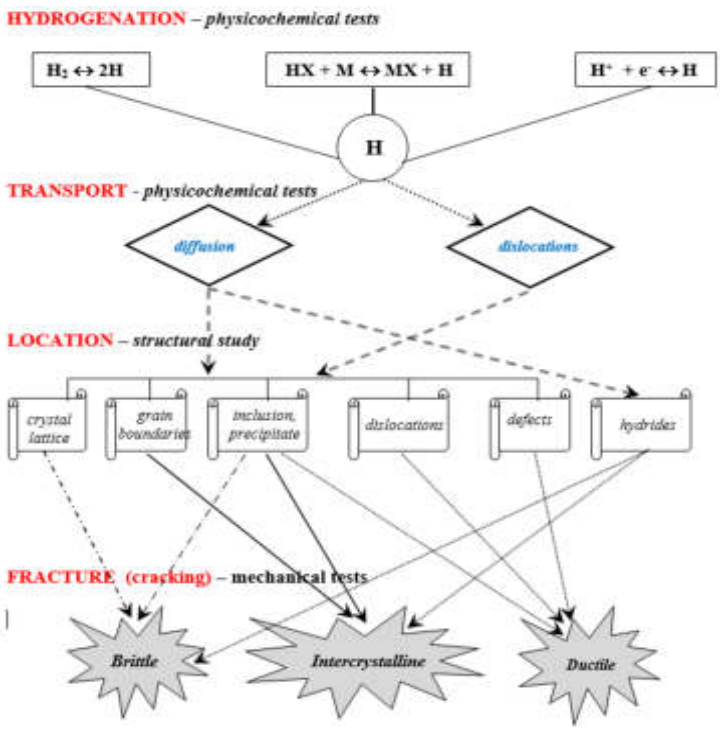

Figure 1. Scheme of hydrogen degradation processes

Acknowledgments: This work partially was supported by the National Science Centre in Poland under the research grant "*Effect of hydrogen on structure and stress corrosion cracking of selected magnesium alloys from Mg-Y-RE-Zr and Mg-Al-RE systems*" No. 2011/03/B/ST8//06387 and by Silesian University of Technology in grant BK RM3 - 11/030/BK_22/1082.

BIBLIOGRAPHY

1. R.C. Zeng, J. Zhang, W.J. Huang, W. Dietzel, K.U. Kainer, C. Blawert, K. Wei, W. Ke, Review of studies on corrosion of magnesium alloys, Transactions of Nonferrous Metals Society of China, 2006, 763–771.
2. J. Flis, Corrosion of metals and hydrogen-related phenomena - Selected topics, Elsevier, 1991.
3. J. Wang, J. Chen, E. Han, W. Ke, Investigation of Stress Corrosion Cracking Behaviors of an AZ91 Magnesium Alloy in 0.1 kmol/m^3 Na_2SO_4 Solution Using Slow Strain Rate Test, Materials Transactions, 2008, 1052–1056.
4. A. Atrens, N. Winzer, W. Dietzel, P.. Srinivasan, G.-L. Song, Stress corrosion cracking (SCC) of magnesium (Mg) alloys, in: Corrosion of Magnesium Alloys, Elsevier, 2011, 299–364.
5. N. Winzer, A. Atrens, G. Song, E. Ghali, W. Dietzel, K.U. Kainer, N. Hort, C. Blawert,A Critical Review of the Stress Corrosion Cracking (SCC) of Magnesium Alloys, Advanced Engineering Materials, 2005, 659–693.
6. A. Atrens, N. Winzer, W. Dietzel, P.. Srinivasan, G.-L. Song, Stress corrosion cracking(SCC) of magnesium (Mg) alloys, in: Corrosion of Magnesium Alloys, Elsevier, 2011, 299–364.
7. B. Chmiela, A. Mościcki, M. Sozańska, Investigation of Stress Corrosion Cracking in Magnesium Alloys, Solid State Phenomena, 2013, 89–92.
8. M. Sozańska, A. Mościcki, B. Chmiela, Investigation of Stress Corrosion Cracking in Magnesium Alloys by Quantitative Fractography Methods, Archives of Metallurgy and Materials, 62, 2017, 557-562
9. M. Sozańska, A. Mościcki, Investigation of the Susceptibility of the WE54 Magnesium-Based Alloy to Stress Corrosion Cracking, Journal of Materials Engineering and Performance vol.29, 949–963 (2020)

MTS CONFERENCE
MATERIAL TECHNOLOGIES IN SILESIA

12-15.06.2022
Crystal Mountain***** Hotel, Wisła, Poland

Badania naprężeń własnych z wykorzystaniem nowoczesnego przenośnego rentgenowskiego analizatora naprężeń Pulstec µ-X360s

L. Sozańska-Jędrasik[a], K. Radwański[a], R. Kuziak[a]

[a] Sieć Badawcza Łukasiewicz – Instytut Metalurgii Żelaza im. Stanisława Staszica, Grupa Badawcza: Badania Właściwości i Struktury Materiałów

email: liwia.sozanska-jedrasik@imz.pl

Abstrakt: W ostatnich latach zaobserwowano rosnące zainteresowanie zakładów przemysłowych badaniami stanu naprężeń w wyrobach stalowych, dającymi możliwość poprawy jakości procesów technologicznych oraz produktów końcowych. Dla oceny oraz prognozowania okresu eksploatacji wyrobów istotne znaczenie ma określenie naprężenia szczątkowego. Naprężenia własne (szczątkowe, resztkowe) są ważnym parametrem, dzięki któremu można określić jakość wyrobu. Definiowane są one jako naprężenia pozostające po procesach technologicznych, bez oddziaływania sił zewnętrznych oraz bez obecności gradientów termicznych. Każdy etap procesów technologicznych poprzez działanie obciążeń termicznych oraz mechanicznych, może być przyczyną zmiany struktury i właściwości wyrobów przemysłowych. Odkształcenie plastyczne, a także obciążenia cieplne materiału mogą wywoływać powstanie trwałych naprężeń w materiale. Naprężenia te są istotne z punktu widzenia dalszego procesu technologicznego przerobu półwyrobów oraz właściwości mechanicznych wyrobów końcowych. Przyczyną powstawania wad, na przykład podczas cięcia laserowego oraz niskiej wydajności komponentów w warunkach eksploatacyjnych mogą być duże naprężenia szczątkowe. Zniszczenie konstrukcji wykonanych z wysokowytrzymałych materiałów niejednokrotnie związane było z obecnością naprężeń szczątkowych. W czasie obróbki mechanicznej lub eksploatacji podczas oddziaływania sił zewnętrznych naprężenia szczątkowe sumują się z naprężeniami zewnętrznymi, przez co może zostać przekroczona granica sprężystości, co prowadzić może do utraty stabilności, wykrzywienia, niejednorodnego odkształcenia plastycznego, a także innych efektów. Naprężenia własne mogą zostać częściowo usunięte z wyrobu poprzez operację prostowania bądź też obróbki cieplnej. Z uwagi na znaczenie naprężeń własnych w procesie użytkowania elementów konstrukcyjnych, zaobserwowano doskonalenie metodyk pomiarowych. Metody, które pozwalają na wyznaczenie naprężeń pierwszego rodzaju (makro naprężeń) można podzielić na metody niszczące częściowo niszczące i nieniszczące.

Naprężenia szczątkowe są określane na podstawie zmian wartości odległości międzypłaszczyznowych sieci krystalicznej badanego materiału w odniesieniu do płaszczyzn krystalograficznych oraz wartości stałych sprężystości. Wartość odległości międzypłaszczyznowych (d_{hkl}) sieci krystalicznej zwiększa się, gdy składowa tensora naprężenia skierowana jest prostopadle do pierwotnej orientacji płaszczyzn krystalograficznych. Analogicznie w przypadku gdy wartość d_{hkl} zmniejsza się, składowa tensora jest skierowana równolegle do sieci polikryształu. Na podstawie zmiany wartości odległości międzypłaszczyznowej można określić charakter naprężenia. W przypadku naprężenia rozciągającego wartość d_{hkl} rośnie, natomiast w przypadku występowania naprężenia ściskającego wartość d_{hkl} maleje.

Do metod nieniszczących należy metoda pomiaru naprężeń z wykorzystaniem promieniowania rentgenowskiego opierająca się na prawie Bragga definiującym warunki dyfrakcji na płaszczyznach krystalicznych. W pracy skupiono się możliwościach badawczych oraz na metodzie *cos(α)* pomiaru naprężeń własnych za pomocą dyfrakcji rentgenowskiej z wykorzystaniem nowoczesnego rentgenowskiego przenośnego analizatora naprężeń Pulstec µ-X360s. Analizator Pulstec jest wyposażony w płaski detektor o wysokiej czułości oraz lampę chromową chłodzoną powietrzem. Badania można przeprowadzać nie tylko dla materiałów stalowych, ale również dla stopów niklu oraz stopów aluminium. Powstałe podczas pomiaru ugięte promienie rentgenowskie w zakresie od 0° do 360° wokół wiązki są rejestrowane za pomocą dwumiarowego detektora w 125 punktach i tworzą obraz pierścienia Debye'a – Scherrera.. Warunki pracy lampy rentgenowskiej to 30 kV i 1 mA. Wykorzystano lampę o anodzie chromowej ($\lambda = 2{,}291$ Å). Zastosowano długość fali Kα, rodzinę płaszczyzn

{211} oraz kąt Bragga 2θ = 156,396°. Głębokość wnikania promieniowania rentgenowskiego wynosi – w zależności od składu chemicznego stopu – od 10 mikronów. Urządzenie może być wykorzystane do badań rozkładu naprężeń (mapping) na płaskich powierzchniach (np. blach), do badań naprężeń w kołach zębatych oraz rozkładu naprężeń w głębokości. Dodatkowe wyposażenie umożliwia badanie materiałów o różnej wielkości ziarna oraz wyznaczenie udziału austenitu szczątkowego.

Keywords: naprężenia własne, metoda *cos(α)*, pierścień Debye'a – Scherrera, austenit szczątkowy

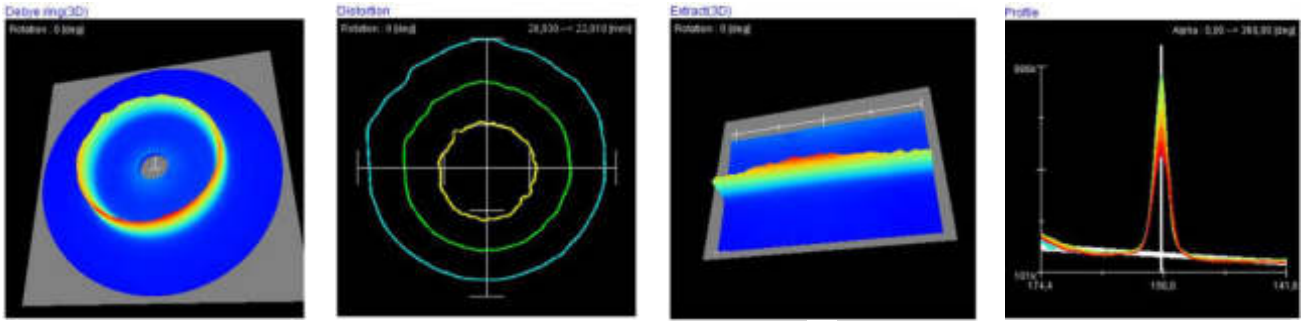

(a) (b) (c) (d)

Rys. 1. Pierścień Debye'a – Scherrera 3D (a), odkształcenie (b), widok przekroju 3D (c), profil (d) otrzymany na powierzchni blachy ze stali H800LA, naprężenie szczątkowe: -32 MPa, FWHM: 3.30º

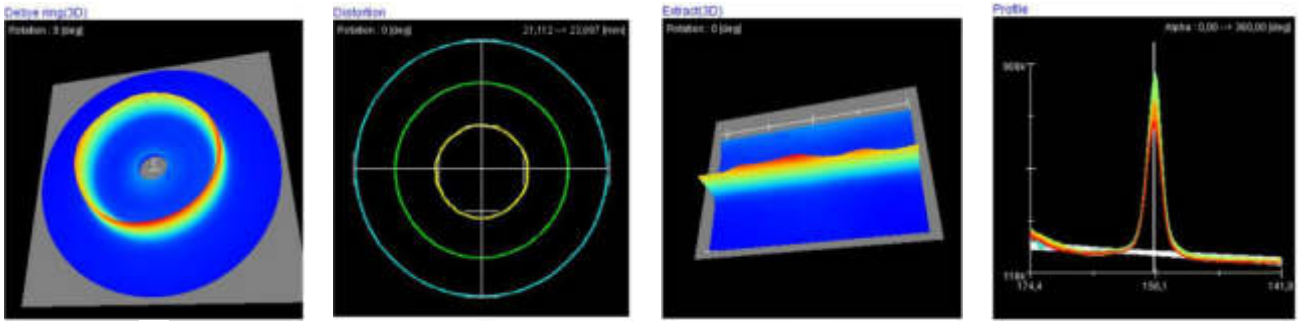

(a) (b) (c) (d)

Rys. 2. Pierścień Debye'a – Scherrera 3D (a), odkształcenie (b), widok przekroju 3D (c), profil (d) otrzymany na głębokości 300 μm na powierzchni blachy ze stali H800LA, naprężenie szczątkowe: 72 MPa, FWHM: 2.86º

LITERATURA

[1] Firma Sentenso; Rentgenowski analizator do badan naprężeń μ-360s. Instrukcja eksploatacji.
[2] S.J. Skrzypek; Nowe możliwości pomiaru makronaprężeń własnych materiałów przy zastosowaniu dyfrakcji promieniowania X w geometrii stałego kąta padania, AGH Uczelniane Wydawnictwo Naukowo – Dydaktyczne, Kraków 2002.
[3] D. Senczyk; Naprężenia własne. Wstęp do generowania, sterowania i wykorzystania, Wydawnictwo Politechniki Poznańskiej, Poznań 1996.
[4] K. Tanaka; The cos(α) method for X-ray residual stress measurement using two-dimensional detector, Bulletin of the JSME, Mechanical Engineering Reviews, Vol. 6, No.1, 2018.
[5] G. Totten; Handbook on residual stress, SEM, Bethel 2005, ISBN: 978-0871707291.
[6] F.A. Kandil, J.D. Lord, A.T. Fry and P.V. Grant; A review of residual stress measurement methods- a guide to technique selection, MPL Report MATC(A)04.
[7] J. Guo, H. Fu, B. Pan, R. Kang; Recent progress of residual stress measurement methods: A review, Chinese Journal of Aeronautics, 2021, 34(2), 54-78.
[8] P.J. Withers, HKDH Bhadeshia; Residual stress. Part I – measurement techniques, Mat. Sci. Technol. 2001, 17(4), 355-365.
[9] W. Szymański, M. Lech-Grega, M. Gawlik, A. Kokosza, A.Chochorowski; Measurement of residual stresses in hot-rolled steel sheets for laser cutting, Computer Methods in Materials Science, 2015, 15(1), 251-257.
[10] R. Bąk, T. Burczyński; Wytrzymałość materiałów z elementami ujęcia komputerowego, Wydawnictwa Naukowo-Techniczne, Warszawa, 2009, ISBN: 978-83-204-3600-6.

MTS CONFERENCE
MATERIAL TECHNOLOGIES IN SILESIA

12-15.06.2022
Crystal Mountain***** Hotel, Wisła, Poland

Właściwości mechaniczne złącza spawanego ze stali P92 po 3000 godzin wyżarzania w temperaturze 600°C i 650°C

K. Sówka [a,c], H. Purzyńska [b], M. Sroka [a], T. Puszczało [a,c], A. Zieliński [b]

[a] Silesian University of Technology, Faculty of Mechanical Engineering, Department of Engineering Materials and Biomaterials
[b] Łukasiewicz Research Network – Institute For Ferrous Metallurgy
[c] Zakłady Remontowe Energetyki Katowice S.A.

email: marek.sroka@polsl.pl , karol.sowka@polsl.pl

Streszczenie: W pracy przedstawiono wyniki badań własności wytrzymałościowych i struktury złącza spawanego stali P92 stosowanej na elementy ciśnieniowe jednostek energetycznych o nadkrytycznych parametrach pracy. Przedstawiono ocenę przydatności do dalszej eksploatacji zarówno materiału podstawowego jak i jednoimiennego obwodowego złącza spawanego gotowych wyrobów w postaci rur ze stali P92 po wyżarzaniu przez 3000 godzin w temperaturze 600 i 650°C. Porównano zmiany właściwości mechanicznych w odniesieniu do stanu struktury materiału podstawowego i materiału złącza spawanego.

Abstract: The paper presents the results of research on the strength properties and structure of a welded joint of P92 steel used for pressure elements of supercritical operating parameters power units. The paper presents an assessment of the suitability for further operation of both the basic material and the unanimous circumferential welded joint of the finished products in the form of P92 steel pipes after annealing for 3000 hours at the temperature of 600 and 650 °C. The changes in mechanical properties were compared in relation to the state of the structure of the base material and the material of the welded joint.

Słowa kluczowe: X10CrWMoVNb9-2, P92, złącze spawane jednoimienne, mikrostruktura, badania własności mechanicznych, wyżarzanie, starzenie.
Keywords: X10CrWMoVNb9-2, P92, similar welded joint, microstructure, mechanical properties testing, annealing, aging.

1. WSTĘP

Budowa w Polsce kotłów na nadkrytyczne parametry pary wymusza konieczność uruchomienia badań oraz analiz do określenia wytrzymałości poszczególnych elementów ciśnieniowych omawianych jednostek. W największym stopniu dotyczy to elementów ciśnieniowych o najwyższych parametrach pracy, jakimi są rurociągi i kolektory parowe. Dla rurociągów oraz kolektorów zbiorczych dominującym czynnikiem powodującym degradację materiału jest zjawisko pełzania. Należy porównać szereg własności mikrostruktury oraz badań mechanicznych, aby sprawdzić jak w funkcji czasu materiał ulega degradacji [1].

Stal P92 jest martenzytyczną stalą żarowytrzymałą z grupy stali o zawartości 9% chromu stosowaną na rury bez szwu wg EN 10216-2 lub wg ASTM A213 i A335 przeznaczone na urządzenia ciśnieniowe. Stal ta opracowana została w latach 90 ubiegłego wieku. W porównaniu do standardowej już stali X20CrMoV11-1 zastosowano modyfikację składu chemicznego poprzez wprowadzenie 1,8% wolframu oraz mikrododatków niobu, boru i azotu oraz obniżenie zawartości molibdenu do 0,5%. Charakteryzuje się ona dobrymi własnościami wytrzymałościowymi, korozyjnymi, spawalnością i żaroodpornością w podwyższonej temperaturze oraz wyraźnie wyższą wytrzymałością na pełzanie w porównaniu ze stalą P91 [2].

2. WYNIKI BADAŃ

Obserwacje mikrostruktury materiału złącza wykonanego ze stali P92 przeprowadzono na zgładach metalograficznych z ujawnieniem stref złącza (rys. 1). Zgłady wykonano na przekroju poprzecznym wycinków złączy poprzez szlifowanie i polerowanie mechaniczne oraz trawienie.

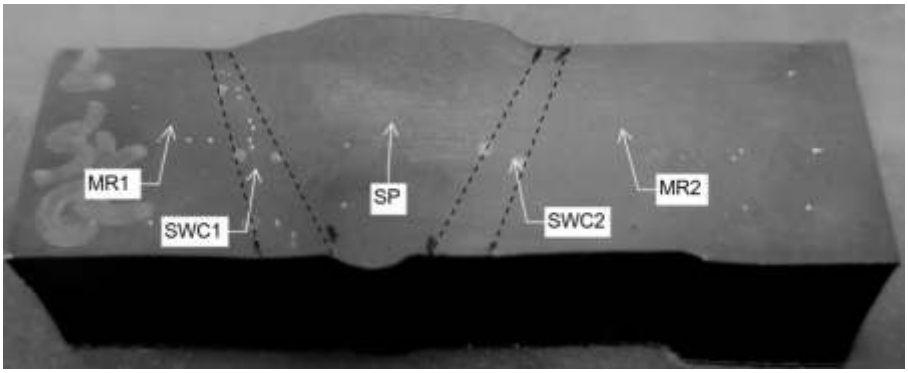

Rysunek 1. Schemat obserwacji mikrostruktury złącza

Badania mikrostruktury materiału w stanie dostawy po 3000h w temp. 600ºC oraz po 3000h w temp. 650ºC przeprowadzono na zainkludowanych zgładach wykorzystując skaningowy mikroskop elektronowy Inspect F przy powiększeniu do 5000x (rys. 2).

Obserwacje materiału rodzimego w stanie dostawy dla obu stron złącza wykazały strukturę odpuszczonego martenzytu listwowego z bardzo drobnymi wydzieleniami typu $M_{23}C_6$ po granicach ziaren byłego austenitu i listwach martenzytu, co jest prawidłowe dla stanu wyjściowego badanej stali.

Badania mikrostruktury jednoimiennego złącza spawanego po wyżarzaniu w temperaturze 600ºC wykazały bardzo zbliżoną strukturę do stanu wyjściowego tzn. strukturę odpuszczonego martenzytu listwowego z zauważalnym, jednakże bardzo nieznacznym wzrostem wielkości wydzieleń, głównie po granicach ziaren byłego austenitu.

Badania mikrostruktury jednoimiennego złącza spawanego po wyżarzaniu w temperaturze 650ºC wykazały zbliżoną strukturę do stanu wyjściowego tzn. strukturę odpuszczonego martenzytu listwowego z zauważalnym, nieznacznym wzrostem wielkości pojedynczych wydzieleń, głównie po granicach ziaren byłego austenitu, licznymi wydzieleniami na granicach ziaren byłego austenitu i listwach martenzytu. Zaobserwowano lokalnie wzrost wielkości pojedynczych wydzieleń i ich koagulację w odniesieniu do stanu wyjściowego oraz wyżarzania w temperaturze 600ºC.

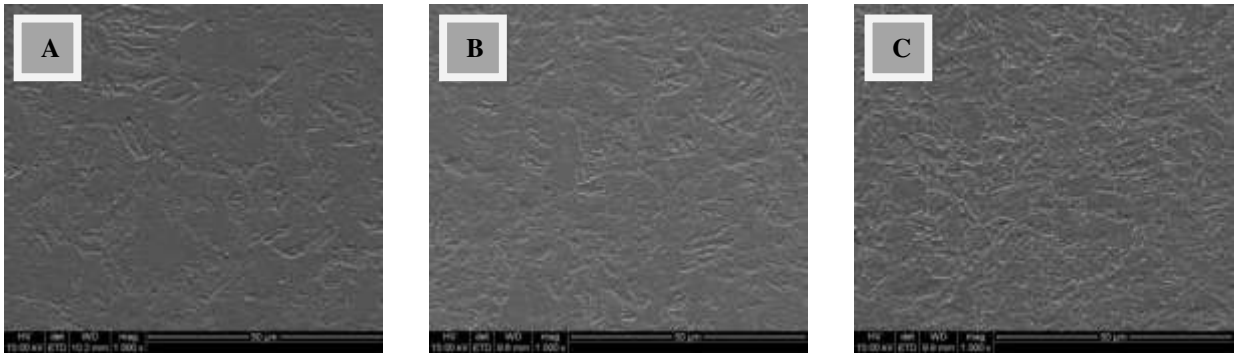

Rysunek 2. Mikrostruktura materiału rodzimego badanego złącza w stanie dostawy (A), złącza po wyżarzaniu przez 3000h w temp. 600ºC (B) oraz złącza po wyżarzaniu przez 3000h w temp. 650ºC (C).

LITERATURA

1. Zieliński, A. (2016). Trwałość eksploatacyjna żarowytrzymałych stali o osnowie ferrytycznej w warunkach długotrwałego oddziaływania temperatury. Instytut Metalurgii Żelaza im. Stanisława Staszica: s. 29.
2. Hernas A., Dobrzański J., Pasternak J., Fudali S. (2015). Charakterystyki nowej generacji materiałów dla energetyki. Wydawnictwo Politechniki Śląskiej: s. 130.

MTS CONFERENCE
MATERIAL TECHNOLOGIES IN SILESIA

12-15.06.2022
Crystal Mountain***** Hotel, Wisła, Poland

The correlation of the results after the static compression test for FC-0208 material sintered with the conventional method.

A. Stanula[a], W. Pilarczyk

[a] Silesian University of Technology, Faculty of Mechanical Engineering, Department of Engineering Materials and Biomaterials
e-mail: Agnieszka.Stanula@polsl.pl

Abstract: The article aims to find the correlation of the results after the static compression test for FC-0208 material sintered by the conventional method. It has been noticed that elements with a porous structure do not give a linear result after the static compression test. For checking these items the endurance machine Zwick / Roel Z 100 will be used, density, hardness of sinter material, SEM microscope, and EDS chemical content. The software Minitab, like data analysis, statistical and process improvement tools was used for data calculation. This investigation provides standardized rules that can be implemented within any powder metal element design.

Keywords: powder metallurgy, material FC-02028, the static compression test , statistic

1. INTRODUCTION

The concept of this paper is the part, compactly made of FC-0208 material . The research is to check a static compression test results: Module E; Yield Strength, Tensile Strength of this part. These results are presented for different densities of the compact. This article shows the way how to understand this relation. And find the potential correlation. Assuming this one is possible to achieve. In addition the hardness and SEM analysis were perform.

Powder metallurgy materials are tested for strength in the loading of tension, compression or bending, depending on the nature of the material. For example, tensile test is carried out in ductile metallic materials, while compression and bending strengths are carried out for brittle materials such as ceramic [1].

1.1. Correlation check

For checking the correlation between density and Module E; density and Yield Strength Rp0.2; density and Tensile Strength Rs – the Minitab tool was used. Minitab is a statistics package. It is a statistical analysis program. It is the leading software of choice for statistics.

Minitab Statistical Software can look at current and past data to discover trends, find and predict patterns, uncover hidden relationships between variables, and create stunning visualizations to tackle even the most daunting challenges and opportunities [2]. The example of usage of this tool is visible in Figure 1-3.

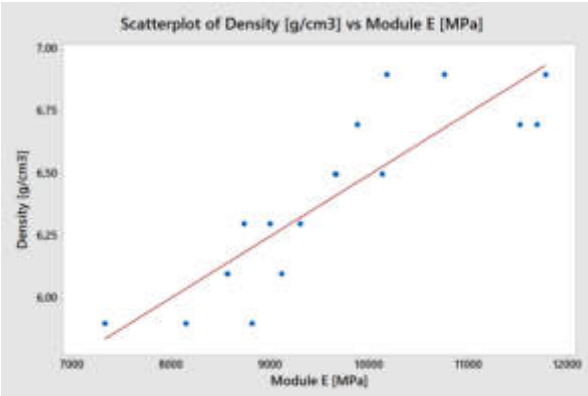

Figure 1. Correlation between density and Module Young E.
Rysunek 1. Korelacja pomiędzy gęstością a wartością Moduł Younga E.

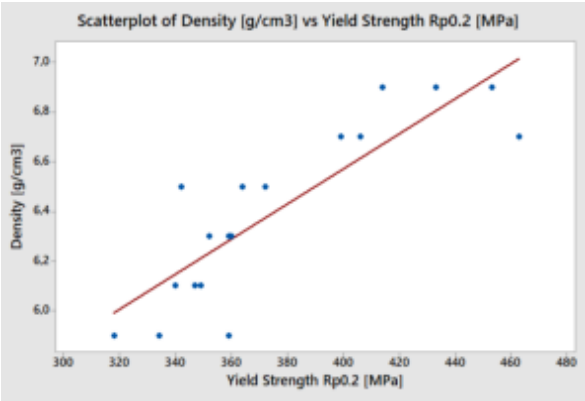

Figure 2. Correlation between density and Yield Strength Rp0.2.
Rysunek 2. Korelacja pomiędzy gęstością a umowna granicą plastyczności Rp0.2 przy ściskaniu.

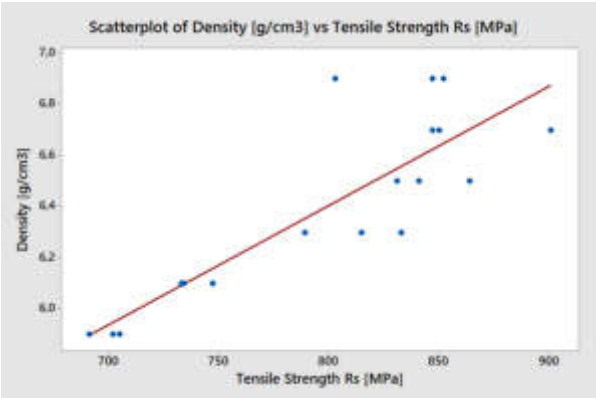

Figure 3. Correlation between density and Tensile Strength Rs.
Rysunek 3. Korelacja pomiędzy gęstością a wytrzymałością na ściskanie Rs.

BIBLIOGRAPHY

1. ISKOVYCH-LOTOTSKY, R., ZELINSKA, O., IVANCHUK, Y., VESELOVSKA, N. Development of the evaluation model of technological parameters of shaping workpieces from powder materials. Eastern-European Journal of Enterprise Technologies. 2017, vol. 85, no. 1/1, pp. 9-17.
2. www.minitab.com

MTS CONFERENCE
MATERIAL TECHNOLOGIES IN SILESIA

12-15.06.2022
Crystal Mountain***** Hotel, Wisła, Poland

Structure and properties of DLC:Ti, DLC:Si-mono, DLC:Si-multi coatings on the 30HGSNA steel substrate

M. Staszuk [a], K. Lukaszkowicz [a], A N. Wieczorek [b], Z. Brytan [a], Ł. Reimann [c], T. Tański [a], E. Skołek [d], K. Wasiak[d]

[a] Silesian University of Technology, Faculty of Mechanical Engineering, Department of Engineering Materials and Biomaterials, Konarskiego Str. 18A, Gliwice, Poland
[b] Silesian University of Technology, Faculty of Mining and Geology, Akademicka 2A, Gliwice, Poland
[c] Silesian University of Technology, Materials Research Laboratory, Konarskiego St. 18A, 44-100 Gliwice, Poland
[d] Warsaw University of Technology, Faculty of Materials Science and Engineering, Narbutta Str. 85, Warszawa, Poland
email: marcin.staszuk@polsl.pl

Abstract: The purpose of the work was to investigate the structure and physicochemical properties of DLC:Ti, DLC:Si-mono, DLC:Si-multi coatings, CVD deposited in 30HGSNA alloy steel. Structural studies were performed on a scanning electron microscope (SEM) and an atomic force microscope (AFM). Properties tests included microhardness, adhesion using the Scratch Test method, electrochemical properties tests using the potentiodynamic method, and electrochemical impedance spectroscopy (EIS). Among the coatings studied, the DLC (a-C:H:Si)-multi coating shows the best electrochemical parameters determined by the Tafel simple extrapolation method. Selected research results are presented in this study.

Keywords: alloy steel; DLC coatings; CVD; corrosion resistance

1. INTRODUCTION

The operational properties of the materials intended for machine elements very often depend not only of the material properties of the entire active cross-section but also on the properties of the surface layer. During operation, elements of machines and devices are exposed to various types of wear, including corrosive wear. Proper selection of coating technology, capable of effectively minimizing the surface degradation process of machine elements, requires understanding the influence of coatings properties on minimization of individual wear mechanisms [1-3]. Therefore, this article presents selected results from the structural and operational properties tests, in particular, the corrosion resistance of the DLC coatings produced by the CVD method on the 30HGSNA steel.

2. MATERIALS

The tests were carried out on uncoated 30HGSNA nanobainitized steel and samples with the coatings listed in Table 1.

Table 1. Designations of DLC coatings on nanobainitized 30HGSNA steel

Designation of samples	Thermal treatment	Type of coating
DLC1	nanobainitization	(a-C:H:Ti)
DLC2		(a-C:H:Si) – mono
DLC3		(a-C:H:Si) – multi

3. RESULTS

The morphology of the coatings was investigated by scanning electron microscopy (SEM) and atomic force microscopy (AFM). As a result of the research, it was found that the coatings show a diversified topography (Fig. 1). On the surface of the coatings, in particular DLC1 and DLC2, scratches were found, resulting from mapping the substrate after surface preparation prior to coating, that is, grinding and polishing. Furthermore, the DLC1 (a-C:H:Ti) coating has microdroplet and craters, which are microdroplets remnants, which is a characteristic feature of the arc spraying process. In the case of DLC2 (a-C:H:Si)-mono coatings, the heterogeneity of the morphology was manifested in the presence of areas with an increased concentration of iron and chromium.

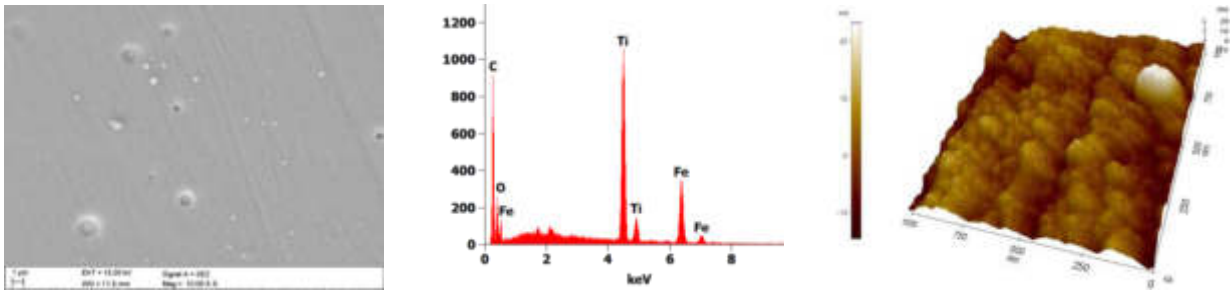

Figure 1. The DLC1 (a-C:H:Ti) coating morphology; from left: SEM image, EDS analysis, AFM image

Electrochemical tests were carried out in a 3.5% NaCl solution. Among the protective coatings, the best electrochemical parameters (high polarization resistance R_p and corrosion potential E_{kor}) demonstrated the DLC3 (a-C: H: Si)-multi coating - Table 2. In this case, the polarization resistance is almost 5 times higher (R_p = 18190 $\Omega \times cm^2$) than for uncoated nanobainitized steel (R_p = 3858 $\Omega \times cm^2$) and 3 times higher than for the same type of coating obtained with other deposition parameters, the DLC2 (a-C:H:Si)-mono. The titanium doped DLC coating Ti - DLC1 (a-C:H:Ti) has the weakest corrosion resistance in the tested environment, which may be related to a higher density of structural defects, especially open porosity.

Table 2. List of electrochemical parameters determined in the Tafel extrapolation method

Designation of samples	i_{kor}, $\mu A/cm^2$	E_{kor}, mV	R_p, $\Omega \times cm^2$	V_p, mm/**year**
uncoated	4.66	-640	3858	0.0541
DLC1 (a-C:H:Ti)	7.23	-479	3263	0.0840
DLC2 (a-C:H:Si)-mono	4.11	-493	5360	0.0477
DLC3 (a-C:H:Si)-multi	1.5	-476	18190	0.0174

Acknowledgments: The publication was made as part of TECHMATSTRATEG III/0028/2019 project: Development of innovative hybrid surface layers composed of anti-wear coatings dedicated to gears for conveyor drive assemblies working under difficult operating conditions.

BIBLIOGRAPHY

1. W. Tuszyński, R. Michalczewski, E. Osuch-Słomka, A. Snarski-Adamski, M. Kalbarczyk, A.N. Wieczorek, J. Nędza, Abrasive Wear, Scuffing and Rolling Contact Fatigue of DLC-Coated 18CrNiMo7-6 Steel Lubricated by a Pure and Contaminated Gear Oil, Materials 14(22) (2021) 7086;
2. K. Lukaszkowicz, J. Sondor, K. Balinc, J. Kubacki, Characteristics of CrAlSiN+DLC coating deposited by lateral rotating cathode arc PVD and PACVD process, Applied Surface Science 312 (2014) 126-133;
3. A.N. Wieczorek, I. Jonczy, P. Bała, K. Stankiewicz, M. Staszuk, Testing the Wear Mechanisms of the Components of Machines Used in Fossil Energy Resource Extraction, Energies 14 (2021) 2125;

MTS CONFERENCE
MATERIAL TECHNOLOGIES IN SILESIA

12-15.06.2022
Crystal Mountain***** Hotel, Wisła, Poland

Wpływ oddziaływania podwyższonej temperatury na mikrostrukturę nowoczesnej stali Thor115

J. Stroniewski, H. Purzyńska, A. Zieliński

Sieć Badawcza Łukasiewicz – Instytut Metalurgii Żelaza im. St. Staszica, 44-100 Gliwice, ul. K. Miarki 12-14 email: hanna.purzynska@imz.lukasiewicz.gov.pl

Abstract: W pracy omówiono wyniki badań mikrostruktury oraz twardości jednoimiennych oraz różnoimiennego złącza spawanego ze stali Thor15 stosowanej na elementy ciśnieniowe jednostek energetycznych o nadkrytycznych parametrach pracy. W artykule porównano obrazy mikrostruktury złączy spawanych w stanie wyjściowym spawanych przy uzyciu różnych materiałów dodatkowych w odniesieniu do pomiarów twardości. Badania mikrostruktury wykonano w oparciu o mikroskopię skaningową, natomiast badania twardości wykonano na twardościomierzu stacjonarnym w skali HV10.

Abstract: The paper discusses the results of research on the microstructure and homonymous hardness as well as the dissimilar welded joint made of Thor15 steel used for pressure elements of power units with supercritical operating parameters. The article compares the microstructure images of welded joints in the initial state, welded with the use of various additional materials in relation to hardness measurements. The microstructure tests were carried out on the basis of scanning microscopy, while the hardness tests were carried out on a stationary hardness tester in the HV10 scale.
Keywords: microstructure, THOR115 steel, annealing, creep test, hardness

1. WSTĘP

Wdrażanie nowych materiałów dla energetyki wymaga nie tylko zdobycia wiedzy w zakresie stabilności mikrostruktury w wyniku długotrwałego oddziaływania temperatury i naprężenia ale także opracowania technologii wykonywania elementów konstrukcyjnych z wykorzystaniem technologii spawania. Szczegółowa analiza zmian mikrostruktury, właściwości mechanicznych oraz zastosowanie metod ilościowej analizy obrazu mikrostruktury tych stali po długotrwałym oddziaływaniu podwyższonej temperatury i naprężenia umożliwi opisanie i opracowanie modeli zmian w procesie wydzieleniowym, które z kolei pozwolą oszacować ich stopień wyczerpania a więc czas dalszej bezpiecznej eksploatacji elementów ciśnieniowych wykonanych z tej stali.

Przedstawiono wstępne wyniki badań dwóch jednorodnych złączy stali Thor115 spawanych przy użyciu dwóch materiałów dodatkowych: SNi6082 (ozn. A) i EPRI P87 (ozn. B) oraz jedno różnorodne złącze stali Thor115 i stali T/P92 (ozn. C), spawane materiałem dodatkowym SNi6082. Wybrane złącza spawane zostały zbadane w stanie wyjściowym, przy czym zostaną również zbadane po długotrwałym wyżarzaniu w podwyższonej temperaturze. Porównanie próbek w stanie dostawy oraz po długotrwałym wyżarzaniu i pełzaniu, obejmujące materiał podstawowy, strefę wpływu ciepła oraz spoinę, pozwoli opracować charakterystyki materiałowe zawierające wyniki badań mechanicznych, mikrostruktury materiału oraz prób pełzania, co w efekcie końcowym umożliwi oszacowanie trwałości eksploatacyjnej, a tym samym czas dalszej bezpiecznej eksploatacji elementów pracujących w podwyższonej temperaturze wykonanych z nowoczesnej stali Thor115.

Tablica 1. Nominalny skład chemiczny stali THOR115

C	Mn	Si	Cr	Mo	Ni	Cu	V	Nb	N
0,09	0,47	0,15	11,30	0,52	0,16	0,08	0,24	0,04	0,002

2. WYNIKI BADAŃ

Badania mikrostruktury przeprowadzono na dwóch jednorodnych złączach spawanych wykonanych ze stali T115 przy użyciu dwóch materiałów dodatkowych SNi6082 (złącze ozn. A) oraz EPRI P87 (złącze ozn.B). Złącza po spawaniu poddane były obróbce cieplnej. W mikrostrukturze strefy wpływu ciepła (ozn. SWC1 oraz SWC2) złącza ozn. A oraz złącza ozn. B można wyróżnić dwa obszary SWC o strukturze drobnoziarnistej z licznymi o zróżnicowanej wielkości wydzieleniami. Wydzielenia obserwowano głównie na granicach ziaren byłego austenitu, na granicach listew oraz wewnątrz ziaren.

Mikrostruktura spoiny złącza ozn. A oraz złącza ozn. B jest zbliżona. Badania mikrostruktury przeprowadzono również na złączu różnorodnym ze stali Thor115 i T/P92 spawanego materiałem dodatkowym SNi6082 (złącze ozn. C). Materiał podstawowy stali Thor115 charakteryzuje się mikrostrukturą odpuszczonego martenzytu z licznymi wydzieleniami, występującymi głównie na granicach ziaren byłego austenitu, listwach martenzytu oraz wewnątrz listew. W stanie wyjściowym materiał podstawowy stali P92 charakteryzuje się mikrostrukturą z dominującym udziałem odpuszczonego martenzytu listwowego.

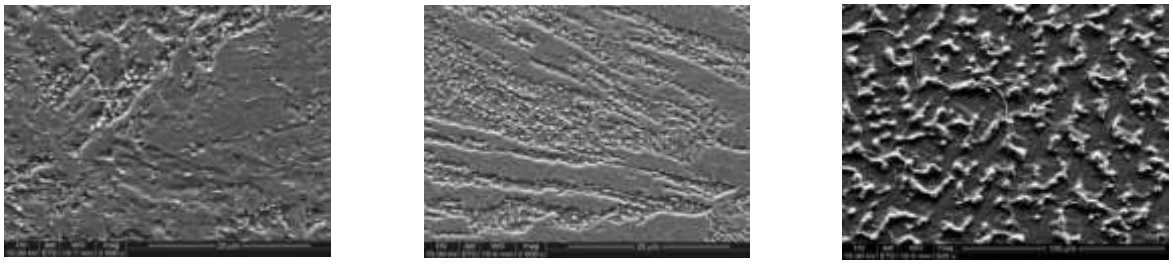

a) b) c)

Rys. 1. Obrazy elementów mikrostruktury materiału spoiny jednoimiennego złącza spawanego ze stali Thor115/Thor115 ozn. A w stanie dostawy obserwowanej w skaningowym mikroskopie elektronowym na trawionym poprzecznym zgładzie metalograficznym: a) MR b) SWC c) SP

a) b) c)

Rys. 2. Obrazy elementów mikrostruktury materiału rodzimego jednoimiennego złącza spawanego ze stali Thor115/Thor115 ozn. B w stanie dostawy obserwowanej w skaningowym mikroskopie elektronowym na trawionym poprzecznym zgładzie metalograficznym: ozn. MR1.a) MR b) SWC c) SP

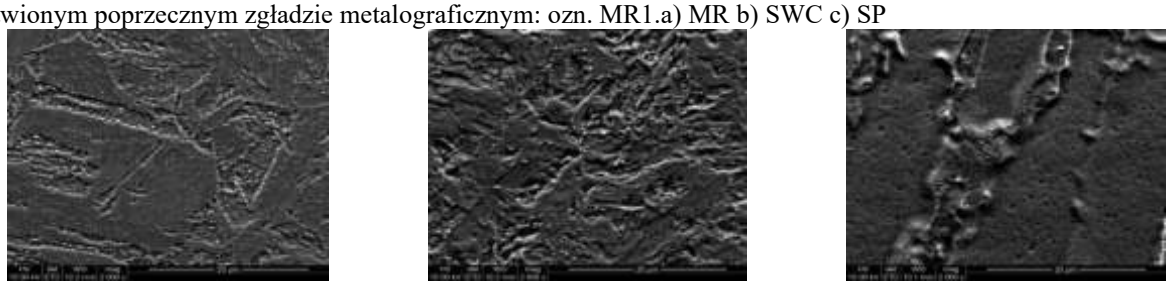

a) b) c)

Rys. 3. Obrazy elementów mikrostruktury materiału rodzimego jednoimiennego złącza spawanego ze stali Thor115/Thor115 ozn. B w stanie dostawy obserwowanej w skaningowym mikroskopie elektronowym na trawionym poprzecznym zgładzie metalograficznym: ozn. MR1.a) MR b) SWC c) SP

Pomiary twardości na złączach zostały przeprowadzone zgodnie z wymaganiami norm PN-EN ISO 15614-1 oraz PN-EN 12952-6 PN EN ISO 6507-1 i PN-EN ISO 9015-1. Powyższe normy określają maksimum twardości stali martenzytycznych na poziomie 350 HV10. Twardość materiału podstawowego złącza ozn. A wynosi średnio 210 HV10. Twardość materiału podstawowego złącza ozn. B wynosi średnio 205 HV10. Twardość złącza spawanego ozn. C wynosi 207 HV10 dla materiału podstawowego stali Thor115 oraz 222 HV10 dla materiału podstawowego stali T/P92.

BIBLIOGRAPHY

1. Dobrzański J. Monografia, Materiałoznawcza interpretacja trwałości stali dla energetyki, Wydawnictwo Open Access Library, 3, 2011, ISBN 978-83-63553-43-2
2. Zieliński A.: Trwałość eksploatacyjna żarowytrzymałych stali o osnowie ferrytycznej w warunkach długotrwałego oddziaływania temperatury. Wydawca: Instytut metalurgii Żelaza im. St. Staszica, Gliwice 2016,monografia habilitacyjna
3. Urzynicok M., Kwieciński K., Fabrication experience of new high oxidation material Thor115, SIM, Kraków, 2021

MTS CONFERENCE
MATERIAL TECHNOLOGIES IN SILESIA

12-15.06.2022
Crystal Mountain***** Hotel, Wisła, Poland

The effect of carbon content on microstructure and phase composition of hot-dip galvanised wires

H. Suchánek[a], P. Gogola[a], Z. Gabalcová[a], M. Kusý[a]

[a]Slovak University of Technology in Bratislava, Faculty of Materials Science and Technology in Trnava, Institute of Materials Science.
email: henrich.suchanek@stuba.sk

Abstract: The experimental observations were designed to analyse the effect of hot dip galvanizing (HDG) parameters such as bath temperature and immersion time. Alloy layer thickness, morphology and phase composition were investigated by optical microscopy (OM), scanning electron microscopy (SEM) and x-ray diffraction (XRD) techniques. An initial experiment of hot dip galvanising at 450°C was carried out on a 4N5 purity Fe substrate, i.e. 0 wt.% of C. It has served as a benchmark to identify possible divergence of experimental results obtained with the current laboratory set-up from data already published in literature. Subsequently, high carbon substrates were galvanised and studied. Generally, regardless of carbon content, increasing immersion time during HDG causes an increase of total alloy layer thickness. Bath temperature variation (440, 450 and 460°C) shows less influence on the total alloy layer thickness. Different carbon content of the substrate leads to differences in morphology and phase composition of the alloy layer.

Keywords: Hot-dip galvanising, phase composition, intermetallic alloy layer, high carbon substrate

1. INTRODUCTION

Hot-dip galvanised (HDG) layers prepared on a 0.98 wt.% C steel substrate were investigated in detail. Currently, several literature sources are focused on HDG including pure zinc baths, or zinc alloy baths. However, these are mainly focused on low carbon steel substrates. On the other hand, the continuous hot-dip galvanising of wires uses high carbon steel substrates in most cases. HDG in these cases is performed often in a bath consisting of pure Zn because it has several advantages for the final applications [1-7].

2. RESULTS

Figure 1 shows a typical microstructure of a steel wire hot dip galvanised at 450°C for 30 seconds. In total, up to four different layers can be distinguished via SEM and EDX analysis. The names of the individual layers proceeding outwards from the steel are: delta (δ), delta mix (δ_{mix}), zeta (ζ), and eta (η).

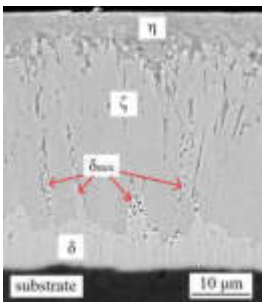

Fig. 1 Microstructure of Zn coating on a steel substrate galvanised in pure zinc at 450°C for 30 seconds and etched in 0.2% nital

Results of thickness measurements allowed the determination of a parabolic character of the growth of total alloy layer. It was observed that with increasing immersion time the total alloy layer thickness has increasing tendency. Relationship between the thickness of the total alloy layer and reaction time was fitted with the empirical power-law [8]. The value of the power-law exponent *n* indicates that the growth evolution is governed by volume diffusion (n = 0.5) [8].

Series of XRD patterns taken from the experiment of a controlled removal of Fe-Zn coating formed on a steel wire is shown in fig. 2. This experiment confirmed that the hot dip galvanized layer is composed of η – Zn based solid solution which is gradually replaced with ζ-$FeZn_{13}$ intermetallic phase. α-Fe solid solution and Fe_3C were determined in the steel substrate of the wire.

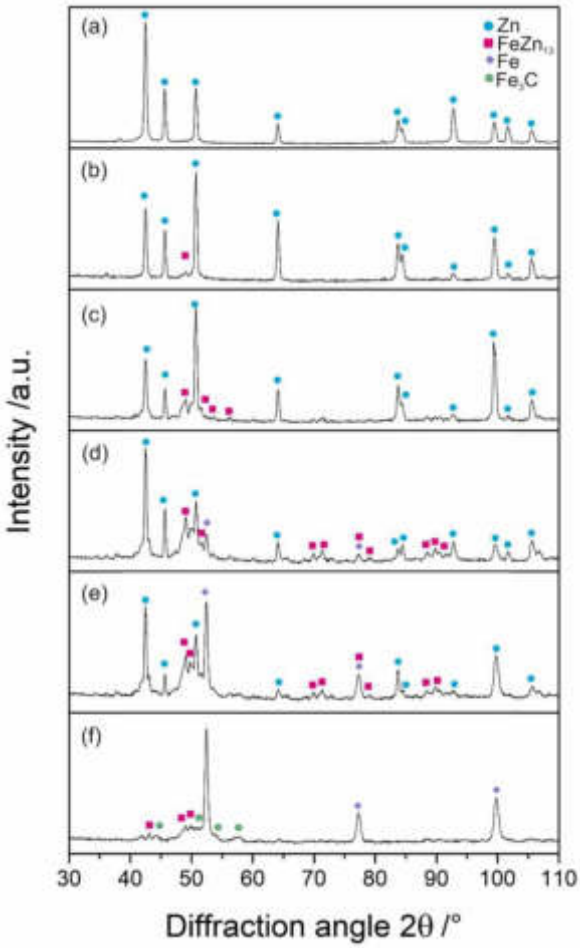

Fig. 2 Series of XRD patterns taken during step-wise chemical stripping of Zn coating layer

BIBLIOGRAPHY

1. Jie L, Hongbo L and Zhihua C 2017 J. Constr. Steel Res. 136 110–27.
2. Singh R P, Mousumi M and Verma M K 2016 Eng. Fail. Anal. 70 290–304.
3. Kuklik V and Kudlacek J 2014 Žárové Zinkování (Ostrava: Asociace českých a slovenských zinkoven) p 208.
4. Shibli S M A, Meena B N and Remya R 2015 Surf. Coat. Tech. 262 210–5.
5. Dallin G W 2015 Galvanizing 2015. Galvinfo Center – A Program of the International Zinc Association November 2015 p 8
6. Bicao P, Jianhua W, Xuping S, Zhi L and Fucheng Y 2008 Surf. Coat. Tech. 202 1785–8
7. Bakhtiari A, Toroghinejad M R and Ashrafizadeh F 2014 Metall. Mater. Eng. 20 41–52.
8. YAO, Y. and others: Interfacial structure and growth kinetics of intermetallic compounds between Sn-3.5Ag solder and Al substrate during solder process. Journal of Alloys and Compounds 682 (2016) 627 - 633

MTS CONFERENCE
MATERIAL TECHNOLOGIES IN SILESIA

12-15.06.2022
Crystal Mountain***** Hotel, Wisła, Poland

Rola asymetrii prędkości oraz geometrii walców w aspekcie krzywizny pasma walcówki

B. Sułek[a,b],*, J. Krawczyk[c] M. Lijewski[a], M. Majewski[a]

[a] Sieć Badawcza Łukasiewicz – Poznański Instytut Technologiczny, Centrum Obróbki Plastycznej, ul. Jana Pawła II 14, 61-139 Poznań,
[b] AGH Akademia Górniczo-Hutnicza, Szkoła Doktorska, al. A. Mickiewicza 30, 30-059 Kraków
[c] AGH Akademia Górniczo-Hutnicza, Wydział Inżynierii Metali i Informatyki Przemysłowej, al. A. Mickiewicza 30, 30-059 Kraków
*Autor do korespondencji: Bartosz.sulek@pit.lukasiewicz.gov.pl

Abstrakt:
Głównym celem badań było określenie wpływu asymetrii walcowania na zimno na geometrię uzyskiwanych pasm taśmy ze stali S235 dla różnych wartości gniotów. Badanie przeprowadzono metodą elementów skończonych przy wykorzystaniu programu Simufact Forming 2016. W ich trakcie testowano wpływ asymetrii kinetycznej (prędkości walców roboczych), geometrycznej (różnorodne średnice walców) oraz asymetrii wynikającej z zastosowania obu tych czynników jednocześnie. Przeprowadzone badania miały na celu określenie takich wartości współczynników asymetrii prędkości walców oraz asymetrii geometrycznej, które pozwalają na uzyskanie dla różnych gniotów prostego pasma walcówki przy jednoczesnym obniżeniu sił podczas walcowania. Na podstawie tych wyników stworzono mapy procesowe, dla poszczególnych gniotów i materiału S235 określające, przy jakich parametrach asymetrii prędkości oraz średnic walców możliwe będzie uzyskanie poprawnego pasma walcówki. W celu weryfikacji wyników przeprowadzono próby laboratoryjnej na walcarce typu DUO.
Słowa kluczowe: Walcowanie asymetryczne, symulacje MES, asymetria kinetyczna, asymetria geometryczna, stal S235.

1. WPROWADZENIE

Walcowanie asymetryczne stanowi modyfikację walcowania blach i taśm w skali przemysłowej. Polega na wprowadzeniu do procesu walcowania umyślnej i kontrolowanej asymetrii uzyskiwanej poprzez zastosowanie różnych prędkości obrotowych walców, różnych średnic walców roboczych, zróżnicowaniu warunków tarcia dla obu walców, czy poprzez różnorodną temperaturę po obu stronach wsadu. Technologia ta posiada wiele zalet, do który zalicza się m.in. poprawa jakości geometrii poprzecznej i wzdłużnej wyrobów, obniżenie sił występujących podczas walcowania i zmniejszenie sprężystego ugięcia elementów klatki walcowniczej, zwiększając tym samym trwałość elementów walcarki oraz umożliwiając stosowanie większych gniotów w jednym przepuście. Proces ten posiada jednak wady, do których można zaliczyć wyginanie się pasma po wyjściu z kotliny walcowniczej. Wartość tej krzywizny zależna od wartości zastosowanych parametrów asymetrii walcowania [1]. Niniejsze opracowanie stanowi próbę lepszego poznania wpływu asymetrii walcowania, na przebieg procesu, geometrię walcówek, a także mikrostrukturę i właściwości mechaniczne materiału dla cienkich blach walcowanych na zimno.

2. MATERIAŁ DO BADAŃ

Materiałem do badań laboratoryjnych były taśmy płaskie o wymiarach 50 x 150 x 2 mm (szerokość x długość x grubość) ze stali S235 wycięte wzdłuż kierunku walcowania. Materiał poddano statycznej próbie rozciągania w celu określenia jej właściwości wytrzymałościowych, na podstawie których dobrano materiał do badań symulacyjnych (rys. 1a).

a) *b)*

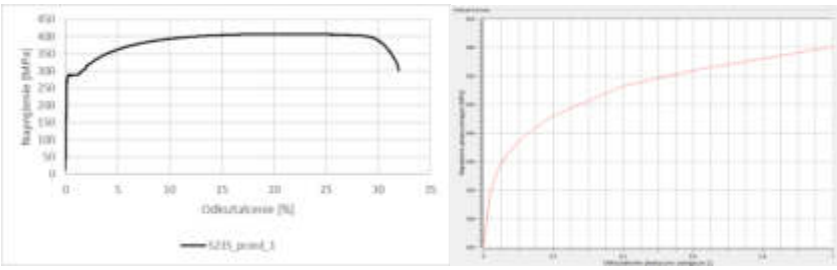

Rysunek 1. Dane materiałowe: a) krzywa zależności naprężenia od odkształcenia dla stali S235, b) krzywa płynięcia stali S235 z biblioteki programu Simufact 2016.

Do badań symulacyjnych wykorzystano stal S235 z biblioteki programu Simufact Forming 2016. Materiał ten był możliwie zbliżony do rzeczywistego materiału, dla którego prowadzono badania rzeczywiste. Krzywa płynięcia zastosowanego materiału przedstawiona została na rysunku 1b.

3. SKRÓT WYNIKÓW BADAŃ

Wstępne badania symulacyjne wykazały wpływ poszczególnych typów asymetrii (stosowanych osobno oraz jednocześnie), na krzywiznę pasma walcówek, a także na siły występujące podczas procesu. Na podstawie uzyskanych wyników stworzono mapy procesu walcowania dla różnych gniotów, pozwalające na określenie, przy jakich parametrach asymetrii możliwe jest uzyskanie dopuszczalnej krzywizny walcówki wraz z jednoczesnym obniżeniem sił procesu. Przeprowadzone badania laboratoryjne pozwoliły na określenie stopnia zbieżności pomiędzy wynikami rzeczywistymi a symulacyjnymi. Uzyskane wstępne wyniki pozwoliły na opracowanie modelu symulacyjnego walcowania asymetrycznego, mającego w przyszłości umożliwiać ustawienie poprawnych parametrów wejściowych dla symulacji walcowania asymetrycznego cienkich blach na zimno.

a) *b)* *c)* *d)*

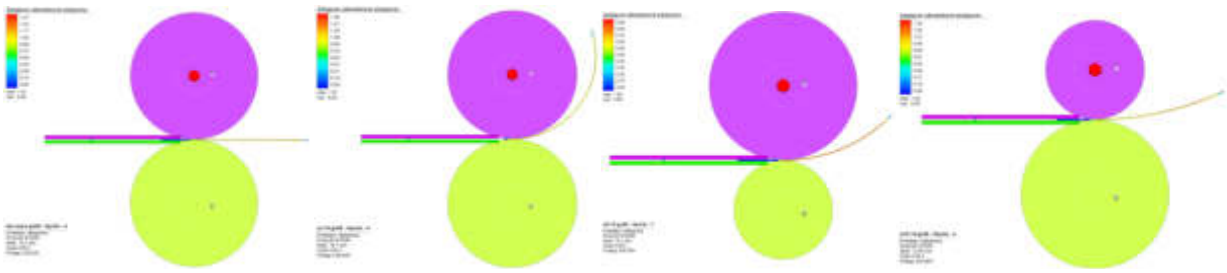

Rysunek 2. Przykładowe wyniki badań: a) wynik walcowania bez asymetrii b) wynik walcowania z asymetrią prędkości $a_V=V_g/V_d=1,5$ c) wynik walcowania z asymetrią geometrii $a_D=D_d/D_g=1,5$ d) wynik z podwójną asymetrią

4. SPOSTRZEŻENIA OGÓLNE

Podczas przeprowadzonych prac określono dla poszczególnych gniotów zakres wartości różnych typów asymetrii, pozwalających na otrzymanie dopuszczalnej krzywizny pasma walcówki przy jednoczesnym obniżeniu sił walcowniczych. Wyniki przeprowadzonych symulacji wykazały, że zastosowanie jednego typu asymetrii znacząco wpływa na obniżenie sił podczas walcowania, ale powoduje krzywienie się pasma w stopniu dyskwalifikującym produkt. Zastosowanie natomiast dwóch typów asymetrii umożliwia uzyskanie walcówki o dopuszczalnej krzywiźnie, przy jednoczesnym spadku sił walcowniczych.

Podziękowania: Praca finansowana przez Ministerstwo Edukacji i Nauki w ramach V edycji doktoratów wdrożeniowych.

LITERATURA

1. Anna Kawałek, Konrad Laber, Kirill Ozhmegov *Analiza zmian parametrów geometrycznych i energetyczno-siłowych w procesie walcowania blach przy różnych rodzajach asymetrii* Obróbka Plastyczna Metali vol. XXIX nr 3 (2018), s. 229–242

MTS CONFERENCE
MATERIAL TECHNOLOGIES IN SILESIA

12-15.06.2022
Crystal Mountain***** Hotel, Wisła, Poland

High Temperature Oxidation Behavior of TiAlCrYSi Bond Coatings Obtained Using CHC-PVD Method on ɣ-TiAl

R. Swadźba[a], B. Mendala[b], L. Swadźba[b], U. Schulz[c], N. Laska[c], Peter-Philipp Bauer[c]

[a]Łukasiewicz Research Network - Institute for Ferrous Metallurgy, Gliwice, Poland, rswadzba@imz.pl
[b]Silesian University of Technology, Katowice, Poland
[c]German Aerospace Center (DLR), Institute of Materials Research, Linder Hoehe, D-51147 Cologne, Germany

Abstract: The paper deals with high temperature oxidation behavior of EB-PVD TBCs on a 48-2-2 TiAl alloy with a TiAlCrYSi bond coating. The samples were subjected to the cyclic oxidation test at 900 °C in 1-hour cycles up to 1000 cycles. Special focus was paid to STEM investigations of the interfacial phenomena occurring in the TBCs. The pre-oxidation treatment resulted in formation of a thermally grown oxide with outer Cr-rich γ-Al_2O_3 as well as nanometric TiO_2, Y_2O_3 and $Y_3Al_5O_{12}$ and inner α-Al_2O_3 that grew during the oxidation test at 900 °C. Yttrium segregation to α-Al_2O_3 grain boundaries was evidenced using STEM.

Keywords: coatings, TiAl, oxidation, TBC

1. Introduction

γ-TiAl intermetallics have recently been successfully applied on low pressure turbine blades of modern aircraft engines due to their low density, high specific strength and creep resistance, all of which make them excellent alternatives for Ni-based superalloys. The next milestone achieved in the field of these materials was the application of additive manufacturing technology for production of turbine blades1,2. However, the application of TiAl intermetallics is limited to maximum temperature between 750 – 850 °C due to their low high temperature oxidation resistance3,4. This is the motivation for development of novel protective coatings that will allow for increasing the operational temperature of TiAl intermetallics.

2. Materials and Methods

This work concerns the application of Closed Hollow Cathode - Physical Vapor Deposition (CHC-PVD) method for the deposition of TiAlCrYSi bond coatings for Thermal Barrier Coatings (TBCs) on γ-TiAl 48-2-2 alloy for high temperature oxidation protection. In the CHC-PVD process, the samples were placed within the hollow cathode with diameter of 80 mm and length of 160 mm and nominal composition Ti-54Al-14Cr-0.5Si-0.5Y (at. %). Prior to coating deposition the samples were subjected to argon ion bombardment using 150 V bias voltage in order to remove contamination from their surfaces. The coating deposition power was 500 W and the argon pressure was maintained at 0.5 mbar Ar for 4 hours. After deposition of the bond coating the samples were pre-oxidized at 900 °C for 2 hours in pure O2 atmosphere and coated with 7YSZ using EB-PVD method. The coated samples were subjected to the cyclic oxidation test at 900 °C in 1 hour cycles based on which mass change curves as a function of time were prepared. The study involved the detailed analysis of the coating's growth mechanism, initial microstructure as well as phase transformations using high resolution Transmission and Scanning Transmission Electron Microscopy (HRTEM and STEM) as well as Scanning Electron Microscopy (SEM) and high temperature X-ray diffraction (HT-XRD).

3. Results and Discussion

In the as-deposited state the obtained CHC-PVD TiAlCrYSi bond coating was found to be characterized by a columnar („Type T") microstructure that contained both amorphous and crystalline regions. It has been found using HRTEM that the latter were composed of a strongly textured, hexagonal C14 Ti(Al,Cr)2 Laves phase. The coated alloy was subjected to the cyclic oxidation test at 900 °C with 1 hour cycles and the lifetime of 1000 cycles

was achieved without any spallation of the YSZ top coating. The microstructure of the coating was investigated after 100, 500 and 1000 cycles. It was found that the initially amorphous bond coating transforms to a mixture of ɣ-TiAl and C14 Ti(Al,Cr)2 Laves phase during pre-oxidation and YSZ deposition (Fig. 1a). Due to depletion in Al during the high temperature oxidation the bond coating transformed to a continuous layer of the Laves phase. Detailed microstructural investigations using STEM allowed to characterize the thermally grown oxide (TGO) scale (Fig. 1b), which was found to be composed of nanometric layers of titania, equiaxed (Al,Cr)2O3 and columnar α-alumina. These investigations provided microstructural evidence for the Cr effect on the formation of Al2O3 during pre-oxidation treatment. Yttrium was found to segregate to the grain boundaries of alumina oxide scale during high temperature oxidation, indicating the occurrence of the reactive element (RE) effect. Upon further high temperature oxidation the TGO grew in the form of columnar α-Al2O3 and maintained excellent adhesion between the ceramic top coating and the TiAlCrYSi bond coating.

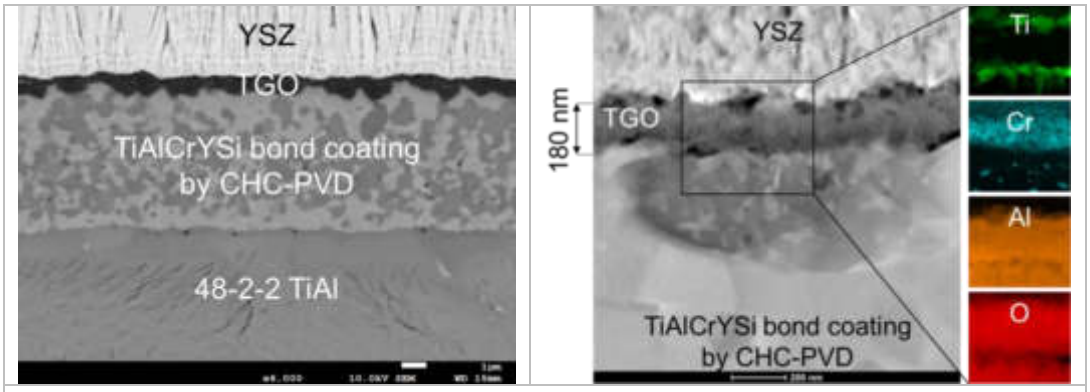

Fig. 1: Microstructure of the TiAlCrYSi bond coating deposited on 48-2-2 TiAl by CHC-PVD method (a) and (b) STEM-HAADF image and EDS mapping of the Thermally Grown Oxide (TGO) in the as-deposited condition.

Acknowledgments: This work was performed in the Framework of the TiAlMET Research Project 2016/23/G/ST5/04128, funded by National Science Centre, Poland and SCHU 1372/6, funded by DFG-Deutsche Forschungsgemeinschaft (German Science Foundation) within the Beethoven 2 program.

BIBLIOGRAPHY

1. Kim, Y. W. & Kim, S. L. JOM, 2018, 70, 553–560.
2. Bewlay, B. P., Nag, S., Suzuki, A. & Weimer, M. J. Materials at High Temperatures, 2016, 33, 549–559.
3. Schütze, M. JOM, 2017, 69, 2602–2609.
4. Pflumm, R., Friedle, S. & Schütze, M. Intermetallics, 2015 56, 1–14

MTS CONFERENCE
MATERIAL TECHNOLOGIES IN SILESIA

12-15.06.2022
Crystal Mountain***** Hotel, Wisła, Poland

Heat treatment of nickel-based superalloy with monocrystalline structure based on experiments with CMSX-4 superalloy

A. Szczotok[a]

[a] Silesian University of Technology, Faculty of Materials Engineering, Department of Materials Technology
email: agnieszka.szczotok@polsl.pl

Abstract: The article summarises the results of research conducted into the heat treatment of the CMSX-4 nickel-based superalloy. Reference is made to a paper [1] proposing to estimate the relative volume of eutectics (γ+γ') in monocrystalline CMSX-4 nickel superalloy in the as-cast state by quantitative metallography. The values of relative volume of the eutectic (γ+γ') and the average value of the plane cross-sectional area of the eutectic areas (γ+γ'), determined for the as-cast state of the analysed superalloy may constitute a reference point for the heat treatment of this superalloy, as the heat treatment parameters, especially temperature and supersaturation time. Based on the results of the study on the effect of 8-step homogenisation under supersaturation and 2-step ageing on the dendritic microsegregation of the CMSX-4 superalloy with monocrystalline structure described in [2], experimental solution heat treatment processes were planned to optimise the microstructure of the CMSX-4 superalloy, which would result in shorter time and lower cost of this process. The article describes selected results of the carried out experiments.

Keywords: nickel-based superalloy, heat treatment, experiment.

1. INTRODUCTION

Due to the strong casting segregation of the microstructure of components made of Ni-based superalloys, it is necessary to carry out their heat treatment process to obtain an optimal and advantageously homogeneous γ/γ' structure [3; 4]. Due to the non-uniform distribution of the strengthening phase γ' and the eutectic (γ+γ') formed during crystallization, time-consuming heat treatment efforts are made to homogenize the microstructure in order to improve the high-temperature properties of the superalloy. Typically, the specific heat treatment for γ' supersaturation and ageing is performed after homogenisation to achieve an optimum γ' size and its cubic morphology [5].

The range of supersaturation temperatures is theoretically limited by the solvus temperature of the γ' phase and the solidus of the given superalloy. The small (sometimes only a few degrees Celsius) difference between the γ' phase solvus temperature and the superalloy melting onset temperature (solidus) makes heat treatment of γ' phase-reinforced superalloys challenging as it makes full supersaturation difficult [6].

In the monocrystalline nickel superalloy CMSX-4, about 16 wt.% is made up of the hard-to-melt metals, including Ta, Re, W or Mo, which contribute to slowing down the diffusion rate of alloying elements in the superalloy matrix, and thus slowing down the diffusive homogenisation of the chemical composition of the superalloy matrix during homogenisation annealing.

Figure 1 shows a typical dendritic microstructure of the CMSX-4 superalloy in the as-cast state recorded by optical microscopy (a) and scanning electron microscopy (b). Such a structure with visible islands of eutectic (γ+γ') is subject to heat treatment in order to eliminate them at best and reduce them at worst.

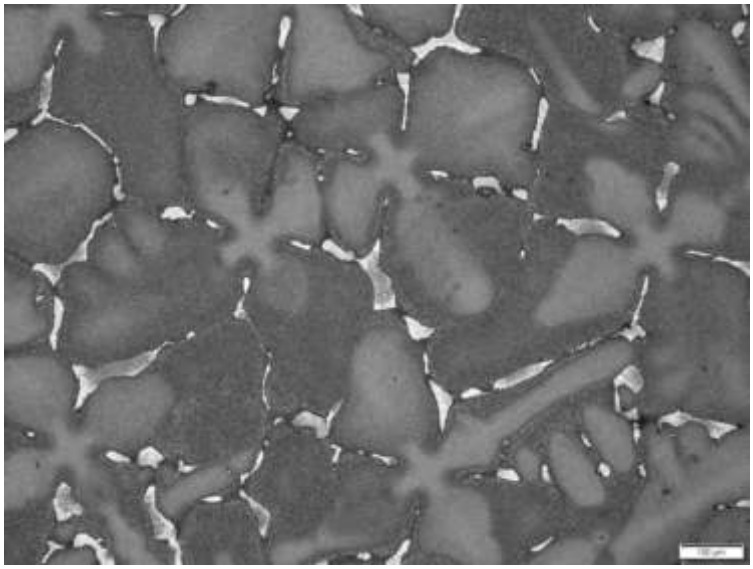

a)

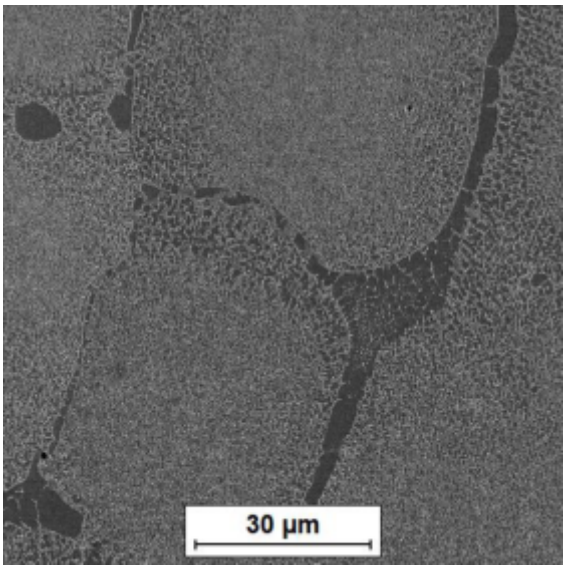

b)

Figure 1. Typical dendritic microstructure of the CMSX-4 superalloy in the as-cast state recorded by light microscopy (a) and scanning electron microscopy (b).

ACKNOWLEDGMENTS
This work was supported by Silesian University of Technology in grant RM3 - 11/030/BK_22/1082.

BIBLIOGRAPHY

1. A. Szczotok, On γ-γ' eutectic quantitative evaluation in the as-cast CMSX-4 nickel-based superalloy, Solid State Phenomena (Trans Tech Publications, Switzerland) 197 (2013) 203-208.
2. A. Szczotok, B.Chmiela, Effect of heat treatment on chemical segregation in CMSX-4 nickel-base superalloy, Journal of Materials Engineering and Performance 23/8 (2014) 2739-2747.
3. A. Heckl, R. Rettig, R.F. Singer, Solidification characteristics and segregation behavior of nickel-base superalloys in dependence of different rhenium and ruthenium contents, Metallurgical and Materials Transactions A 41A (2010) 202-211.
4. B. Wilson, Solution heat treatment response of CMSX-4, Journal of Undergraduate Research 3/7 (2002) 1-4.
5. D. Goldschmidt, Einkristalline Gasturbinenschaufeln aus Nickelbasis-Legierungen. Teil II: Wärmebehandlung und Eigenschaften, Materialwissenschaft und Werkstofftechnik 25 (1994) 373-382.
6. B. Geddes, H. Leon, X. Huang, Superalloys: alloying and performance, 1st ed. ASM International, Materials Park, Ohio, 2010.

MTS CONFERENCE
MATERIAL TECHNOLOGIES IN SILESIA

12-15.06.2022
Crystal Mountain***** Hotel, Wisła, Poland

Możliwości zastosowania lokalnego źródła energii do zasilania laboratorium prób pełzania

M. Szulc[a], J. Loska[a], H. Purzyńska[a]

[a] Łukasiewicz Research Network – Institute for Ferrous Metallurgy, Research Group: Materials Research for Power Engineering
email: michal.szulc@imz.pl

Streszczenie: W pracy zdefiniowano warunki techniczne umożliwiające zasilanie laboratorium prób pełzania z lokalnego źródła energii. Przedmiotem analizy jest laboratorium prób pełzania składające się z blisko stu maszyn jednopróbkowych, w których próbki nagrzewane są w trójstrefowych piecach, oraz czterech dwukomorowych maszyn wielopróbkowych, w których wymagany rozkład temperatury utrzymywany jest z użyciem szesnastu grzałek w każdej komorze. Regulacja temperatury we wszystkich piecach maszyn do badań pełzania odbywa się z zastosowaniem samodzielnych regulatorów dwupołożeniowych, wykorzystujących jako elementy wykonawcze przekaźniki elektroniczne. Obciążenie sieci elektrycznej grzałkami włączanymi w sposób nieskoordynowany powoduje nieoptymalne wykorzystanie lokalnego źródła zasilania, a także może być przyczyną jego niestabilnej pracy. Zastosowanie dodatkowego sterownika nadrzędnego, szeregującego włączenia grzałek, przy jednoczesnym uwzględnieniu zdefiniowanych ograniczeń, ustabilizuje obciążenie sieci i pozwoli na użycie źródeł zasilania o znamionowych mocach porównywalnych z mocą laboratorium. W oparciu o identyfikację urządzeń nagrzewających, będących częścią maszyn do prób pełzania, znajdujących się w laboratorium, opracowano dynamiczne modele nagrzewania próbki. Bazując na tych modelach, a także wykorzystując dane archiwalne zgromadzone podczas prowadzenia prób, zbadano wpływ opóźnień w sterowaniu mocą grzałek na utrzymanie zadanej wartości temperatury próbki. Badania przeprowadzono w odniesieniu do wymagań normy PN-EN ISO 204 w zakresie dopuszczalnej odchyłki między wskazywaną i wymaganą temperaturą oraz dopuszczalnego maksymalnego jej gradientu na próbce, jakie muszą być spełnione podczas prowadzenia próby pełzania.

Abstract: The paper defines the technical conditions for powering the creep laboratory from a local energy source. The subject of the analysis is the creep laboratory consisting of nearly one hundred single-sample machines, in which the samples are heated in three-zone furnaces, and four two-chamber multi-sample machines, in which the required temperature is maintained with the use of sixteen heaters in each chamber. Temperature control in all creep testing machines furnaces is performed with the use of independent two-position controllers, using solid-state relays as actuators. The load of the electric network with heaters switched on in an uncoordinated manner causes the suboptimal use of the local power source, and may also cause its unstable operation. The use of an additional upper-level controller, scheduling the switching on of the heaters, while taking into account the defined limitations, will stabilize the network load and allow the use of power sources with rated power comparable to the power of the laboratory. Based on the identification of the heating devices that are part of the creep testing machines located in the laboratory, dynamic models of sample heating were developed. Based on these models, as well as on the basis of archival data collected during the tests, the influence of delays in controlling the heater power on maintaining the sample temperature setpoint was investigated. The research was carried out in relation to the requirements of the PN-EN ISO 204 standard in terms of the permitted deviation between the corrected measured and the specified temperature and permitted maximum temperature variation along the test piece, which must be met during the creep test.

Słowa kluczowe: sterowanie, identyfikacja, optymalizacja, symulacja, job-shop

1. WSTĘP

Układy zasilania energetycznego projektowane są z uwzględnieniem odpowiedniego zapasu zapewniającego dostarczenie energii również w szczytowym momencie zapotrzebowania na moc. Jest to łatwo realizowalne

w publicznej sieci energetycznej, gdzie duża liczba odbiorników zapewnia stosunkowo małe zmiany obciążenia sieci w odniesieniu do jego średniej wartości. W przypadku zasilania układu z lokalnych źródeł energii, gdzie moc źródła jest porównywalna z mocą odbiorników, częste zmiany obciążenia, w szczególności w sytuacji dwustanowej pracy odbiorników, stanowią poważną przeszkodę w zapewnieniu znamionowych parametrów zasilania (Rys. 1). Takie awarie są dużym zagrożeniem technologicznym i wymagają systemowego przeciwdziałania. Zmniejszenie chwilowych skoków mocy układu nie tylko pozwoli na zastosowanie lokalnych, w tym odnawialnych źródeł energii, ale również wpłynie korzystnie na efektywne ich wykorzystanie.

Laboratorium prób pełzania funkcjonuje w oparciu o zasady przedstawione w normie PN-EN ISO 204 „Próba pełzania przy jednoosiowym rozciąganiu". Zgodnie z normą wymaga się, aby próby przeprowadzane były nieprzerwanie w stałej temperaturze, przy stałym naprężeniu i przy stabilnych warunkach otoczenia [1]. W zależności od badanego materiału i rodzaju próby, jej czas wynosi od kilkudziesięciu godzin, do kilkudziesięciu lat. Każde przerwanie próby w trakcie jej trwania wpływa na dokładność wyników, a także może doprowadzić do przedwczesnego jej zniszczenia. Ze względu na czas przeprowadzanych prób, a także unikatowość materiału poddawanego próbie, wymaga się od laboratorium wysokiej niezawodności i odporności na zakłócenia pochodzące z zewnątrz, w tym w szczególności zabezpieczenia przed zanikami napięcia zasilania. Jest ono realizowane w postaci zasilaczy awaryjnych UPS oraz spalinowego agregatu prądotwórczego [2].

2. WYNIKI I PODSUMOWANIE

Przedstawiony problem bliski jest tematyce znanej pod nazwą: „job shop scheduling". W przypadku zagadnienia dotyczącego laboratorium prób pełzania, poszukuje się algorytmu szeregującego włączenia grzałek, minimalizującego wahania mocy w dopuszczalnych granicach umożliwiających prawidłową pracę agregatu prądotwórczego, przy jednoczesnym uwzględnieniu wpływu tego szeregowania na utrzymanie zadanych wartości temperatury w poszczególnych strefach grzewczych pieców [3]. Rozwiązanie tego problemu charakteryzuje się wysokim stopniem trudności ze względu na sumaryczną liczbę zadań poddanych procesowi szeregowania, zmienną liczbę maszyn, w ramach których się odbywa, a także bardzo krótki czas potrzebny na wypracowanie kolejnego sterowania. Z uwagi na trwające próby pełzania, końcowe testy muszą być poprzedzone badaniami i testami symulacyjnymi. Powoduje to konieczność identyfikacji obiektu, jakim jest System Prób Pełzania, stworzenia dobrze zwalidowanego modelu tego systemu, a następnie budowy symulatora.

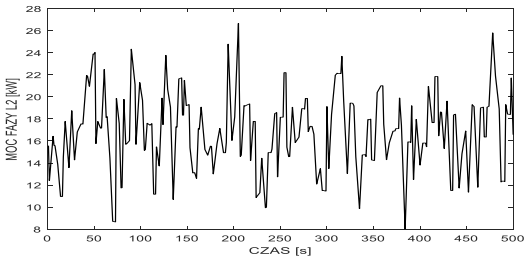

Rysunek 1. Obciążenie fazy L2 podczas prób pełzania

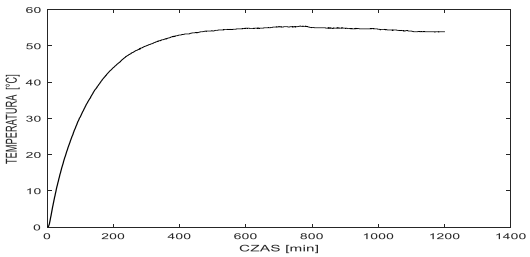

Rysunek 2. Odpowiedź obiektu na skok 3% mocy

Wstępne badania odpowiedzi na wymuszenie okresowe prostokątne, a także odpowiedzi na skok jednostkowy, wskazują na dużą bezwładność obiektu, jakim jest piec maszyny do prób pełzania (Rys. 2). Zmiany sygnału wejściowego charakteryzujące się dużą szybkością w porównaniu z częstotliwością graniczną rozpatrywanego obiektu nie są przenoszone na jego wyjście. W rezultacie opóźnianie sygnału sterującego mocą pieca w szerokim zakresie, w odniesieniu do szerokości impulsu włączenia grzałki, nie zakłóca sygnału wyjściowego. Można wnioskować, że algorytm sterowania nadrzędnego, pomimo wniesienia dość znacznego opóźnienia w pętlę sprzężenia zwrotnego nie będzie destabilizował układu, przy jednoczesnym minimalizowaniu skoków obciążenia sieci elektrycznej. W dalszej części badań zostaną sprawdzone algorytmy deterministyczne i stochastyczne, w celu wdrożenia w istniejącym systemie.

LITERATURA

1. PN-EN ISO 204:2018-11 - Metale – Próba pełzania przy jednoosiowym rozciąganiu – Metoda badania
2. J. Dobrzański, J. Loska, M. Szulc, A. Zieliński: Sprawozdanie nr S0-0628 pt.: Testowanie i ocena nowej metodyki zbierania i archiwizacji danych z prób pełzania z wykorzystaniem zaprojektowanego i wykonanego stanowiska badawczego (2007)
3. Nayak, A., K. Kim, and S. Lee. Modeling Job Shop Scheduling for Peak Electricity Load Constraint, 2020

MTS CONFERENCE
MATERIAL TECHNOLOGIES IN SILESIA

12-15.06.2022
Crystal Mountain***** Hotel, Wisła, Poland

Numerical analysis of static tensile test of the sample made of polyethylene reinforced by halloysite nanoparticles

A. Śliwa*, M. Bonek

Silesian University of Technology, Faculty of Mechanical Engineering, Department of Engineering Materials and Biomaterials
*email: agata.sliwa@polsl.pl

Abstract:
This work presents the results of computer simulation of one of the most common strength tests, which is a static tensile test. The sections used in a numerical analysis are so-called "dumbbells", typical for plastic samples. The analysis results were referenced to the actual tensile test of the samples made of polyethylene reinforced by halloysite nanoparticles. The material was produced with the high-pressure injection method. The computer simulation results were referenced to literature properties of the industrially used polyethylene to compare the results obtained with those commonly considered typical for the above-mentioned material. The above results that the stress values and deformation values obtained with computer simulation are similar to the actual results. Computer simulation and modelling is an interdisciplinary field necessary for the development of science and technology, having an important role in materials engineering and is to improve the ability to predict results and to optimise solutions.

Keywords: Computational materials scienc, Finite Element Method, static tensile test, polietylen, halloysite nanoparticle, nanocomposites.

1. INTRODUCTION

At present, composite materials represent a group of materials subject to constant improvement and continued research, mainly due to unlimited possibilities of combining the particular components used for their fabrication and due to outstanding properties of the input material after modifying the percentage content of its particular constituent materials.

The Finite Element Method (FEM) is a tool used in engineering and scientific computations, allowing to perform computer simulations identifying the effect of various phenomena and processes on the elements made from specific materials subject to the research.

2. INVESTIGATION METHODOLOGY COMPUTER SIMULATION

Figures 1 and 2 show samples before rupture and after the stretching process. Boundary conditions were applied to the geometrical model, by immobilising one end of the sample, which is reflected in a static tensile test by a holding part fitted to the fixed tensile machine jaws; the force was also applied acting on the sample in the axis Y, corresponding to the average force acting on the examined samples during the static tensile test described earlier with the value of 1.3 kN, so that the simulation reflects, as far as possible, the conditions of the test performed with the testing machine (Fig. 3).
Figure 4 shows the distribution of the stresses reduced in the sample subject to simulation, and their value reaches approx. 28-31 MPa; they exceed the value of normal stresses, which results from combining all the constituent stresses existing in the loaded element according to the von Mises hypothesis.

Fig.1.The sample before the static tensile test

Fig. 2. Samples after the fracturing in the static tensile test

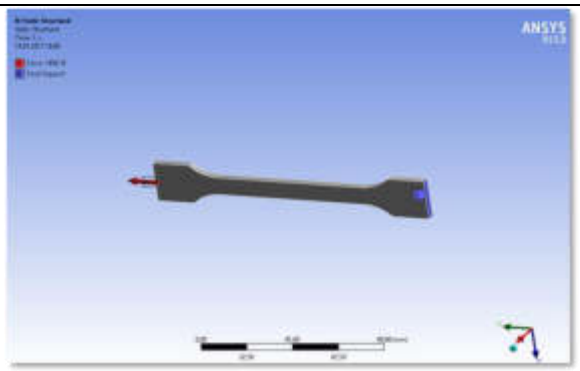

Fig. 3. The boundary conditions for analyzed sample: A- the tensile force; B- immobilisation of the sample

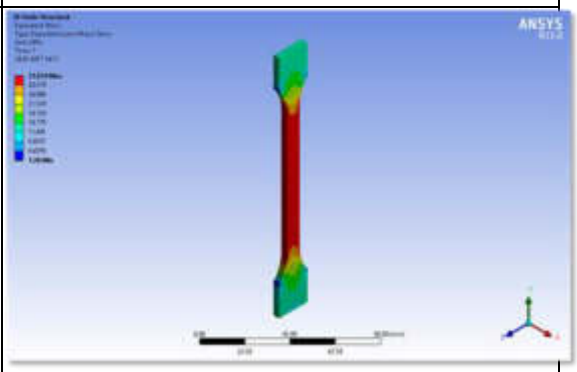

Fig. 4. Distribution of the reduced stress in the Y axis of the sample

3. CONCLUSIONS

It can be concluded in the light of the above results that the stress values and deformation values obtained with computer simulation are similar to the actual results.The highest concentration of material stresses and deformations takes place in the test part of the sample, which confirms the test assumptions providing that a sample should be broken in the middle part of the so-called dumbbell.

BIBLIOGRAPHY

1. Herranz G., Matula G., Romero A. Effects of chromium carbide on the microstructures and wear resistance of high speed steel obtained by powder injection moulding route; Powder Metall., 60, 120–130. (2017)
2. Śliwa A., Sroka M., Bloch K.; . G., Al Bakri Abdullah M. M., Sandu A. V. Finite element method application for the determination of hardness for magnesium alloys . Rev. Chim., 69, 324–327. (2018)

MTS CONFERENCE
MATERIAL TECHNOLOGIES IN SILESIA

12-15.06.2022
Crystal Mountain***** Hotel, Wisła, Poland

Study of morphology and structure of electrospun hybrid nanowires

T. Tański[a], M. Zaborowska[a]

[a] Silesian University of Technology, Faculty of Mechanical Engineering, Department of Engineering Materials and Biomaterials, Konarskiego 18a, 44-100 Gliwice, Poland
e-mail: marta.zaborowska@polsl.pl

Abstract: The aim of this work was to obtain, using hybrid methods combining the sol-gel technique of preparing spinning solutions, electrospinning from solutions to obtain an intermediate product in the form of polymer-ceramic nanofibers and high-temperature thermal treatment, which resulted in ceramic one-dimensional nanostructures. The obtained nanomaterials were tested with the use of advanced research techniques, analyzing their morphology, structure and the influence of the production parameters used on the optical properties of nanostructures. The morphology were analyzed using scanning electron microscope (SEM) followed by chemical composition examination using X-ray Energy Dispersive Spectroscopy (X-ray Energy Spectroscopy). Moreover, transmission electron microscopy (TEM) was used to determine morphology and structure, with the special emphasis on crystal structure using selected area electron diffraction (SAED) and high-resolution transmission electron microscope technique (HRTEM). Fourier-Transform Infrared Spectroscopy (FTIR) was used to examine the chemical bonds and structure of hybrid nanowires. The optical properties were determined based on absorbance in the function of electromagnetic radiation wavelengths graphs and the values of optical band gaps were calculated using Tauc formula.

Keywords: electrospinning, hybrid nanofibers, photocatalysis, one-dimensional nanostructures

1. INTRODUCTION

In recent years, the growing interest of hybrid ceramic nanofibers around the world is more and more visible. Within 30 years, the number of scientific publications in the field of electrospun nanofibers has increased more than 7,000 times, with the last 10 years of nanotechnology development accounting for over 66% of all publications on this topic. Moreover, hybrid ceramic nanofibers account for 6% of all scientific works on the electrospinning method, and the use of ceramic one-dimensional nanostructures in the field of photocatalysis is less than 0.55% of the total (Fig. 1).

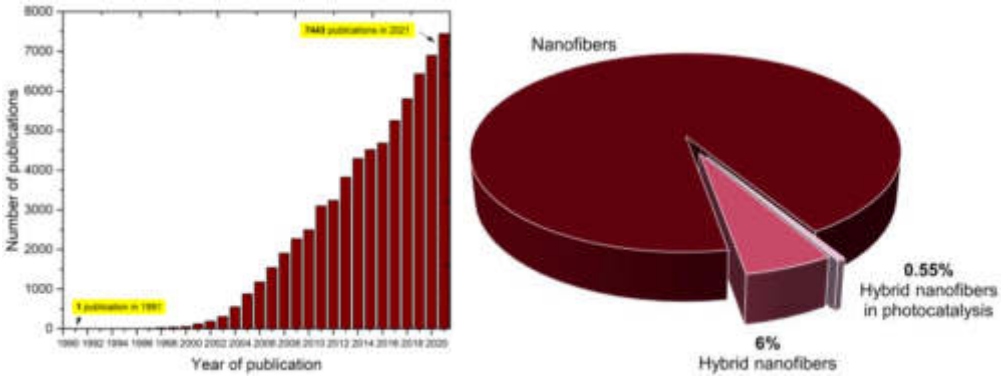

Figure 1. The growing interest in the field of electrospun nanofibers and their use in photocatalytic water treatment (source: Scopus)

However, it is ceramic nanofibers that have great potential to revolutionize the processes of photocatalytic water purification from organic pollutants [1]. While nanoparticles have a high tendency to agglomerate, which lowers their specific surface area and thus the active surface for adsorption of contaminant particles, one-dimensional nanostructures can overcome this problem. The diameters of electrospun nanofibers depend mainly on the type of polymer material and ceramic precursor used, the concentration of spinning solutions and the parameters of the manufacturing process. Therefore, the electrospinning method from solutions is currently one of the most versatile method of obtaining one-dimensional nanostructures with the desired morphology. What's more, electrospinning is a fully reproducible and scalable method of producing nanofibers while maintaining high-quality material (Fig. 2).

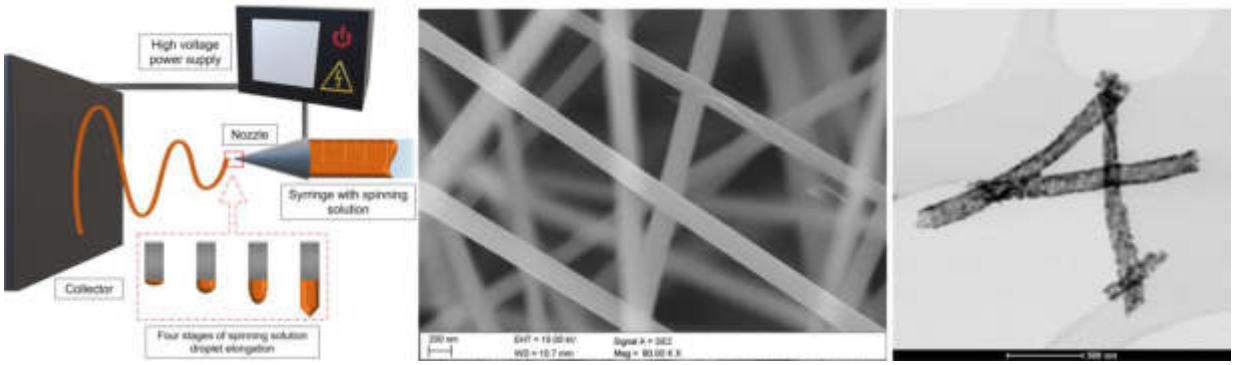

Figure 2. (From the left side): Scheme of electrospinning setup, SEM image of as-spun polymer-ceramic nanofibers and TEM image of calcined ceramic nanowires

There are two possible scenarios for the production of hybrid nanofibers with the use of electrospinning. In the first scenario, a spinning solution containing solvents, a polymeric material, and a ceramic salt precursor is electrospun into nanofibers. Then, such obtained nanofibers are subjected to a high-temperature thermal treatment process in order to produce ceramic nanowires. The second scenario excludes the calcination process, and the as-spun nanofibers become the final material with the desired properties [2,3].

Zinc oxide, next to titanium dioxide, is one of the most widely researched and described in the literature photocatalytically active materials. However, more and more often the ZnO crystal lattice is modified with foreign ions and/or atoms in the form of dopants in order to improve its photocatalytic properties. First of all, its optical properties are modified, with particular emphasis on the absorption range of electromagnetic radiation, which in undoped ZnO structures is limited to a narrow ultraviolet range. It is assumed that rare earth metals can significantly improve optical properties, including reducing the width of the optical ZnO band gap, due to their unique properties [4,5].

Acknowledgments: The scientific work was financed from the budget for science in the years 2020 - 2024, as a research project under the “Diamond Grant” program (No. DI2019 014949).

BIBLIOGRAPHY

1. Xing, Y., Cheng, J., Li, H., Lin, D., Wang, Y., Wu, H., & Pan, W. (2021). Electrospun Ceramic Nanofibers for Photocatalysis. Nanomaterials, 11(12), 3221.
2. Esfahani, H., Jose, R., & Ramakrishna, S. (2017). Electrospun ceramic nanofiber mats today: Synthesis, properties, and applications. Materials, 10(11), 1238.
3. George, G., Senthil, T., Luo, Z., & Anandhan, S. (2021). Sol-gel electrospinning of diverse ceramic nanofibers and their potential applications. In Electrospun Polymers and Composites (pp. 689-764). Woodhead Publishing.
4. Cerrato, E., Gionco, C., Berruti, I., Sordello, F., Calza, P., & Paganini, M. C. (2018). Rare earth ions doped ZnO: Synthesis, characterization and preliminary photoactivity assessment. Journal of Solid State Chemistry, 264, 42-47.
5. Cerrato, E., Zickler, G. A., & Paganini, M. C. (2020). The role of Yb doped ZnO in the charge transfer process and stabilization. Journal of Alloys and Compounds, 816, 152555.

MTS CONFERENCE
MATERIAL TECHNOLOGIES IN SILESIA

12-15.06.2022
Crystal Mountain***** Hotel, Wisła, Poland

Deformation degree impact on the properties of Ta_2O_5 coating on NiTi alloy

A. Taratuta[a], J. Lisoń[a], M. Antonowicz[a], Z. Paszenda[a], M. Basiaga[a]

[a] Silesian University of Technology, Faculty of Biomedical Engineering, Department of Biomaterials and Medical Devices Engineering
email: anna.taratuta@polsl.pl

Abstract: NiTi alloy is characterized by its superelasticity, which makes it used for minimally invasive implants such as self-expanding stents and cardiac occlusion implants. Despite good biocompatibility in the environment found in the bloodstream, there is still a risk of releasing toxic Ni ions, thrombus formation, or excessive endothelial overgrowth. In addition, this alloy is not well visible in the X-ray beam. Therefore, it was proposed to deposit a thin layer of tantalum pentoxide (Ta_2O_5) on the NiTi alloy by Atomic Layer Deposition Method. In order to minimize the permeation of nickel ions into body, electropolishing was performed prior to coating, which increased the thickness of the titanium oxide (TiO_2) layer on the alloy surface. The tolerable deformation of Ta_2O_5 layer with different thicknesses and biocompatibility in terms of stress corrosion resistance in artificial plasma environment were investigated. Scanning Electron Microscope (SEM) observations enabled the surface of the layer subjected to different deformations to be evaluated. The results obtained allow us to determine the maximum degree of deformation that the tested coating can be subjected to without excessive damage to its morphology or changing the material properties.

Keywords: NiTi alloy, Atomic Layer Deposition, Tantalum pentoxide

1. INTRODUCTION

Shape memory alloys (SMAs) based on NiTi alloy have been widely used in biomedical engineering due to their superelasticity. They are used for guide wires, stents, implants for cardiac occlusion and dental arch wires. Despite its relatively good biocompatibility, it has been found that the release of toxic Ni ions can lead to hypersensitivity to this element and even carcinogenicity in the human body. Moreover, for minimally invasive procedures, implant insertion under the light of X-rays is used. In these cases, fluoroscopically visible markers are required due to the high radio-opaque nature of the NiTi alloy [1].

Many researchers have attempted to improve the properties of NiTi alloy. The most promising research direction seems to be the coating of NiTi alloy. However, due to the nature of shape memory alloy implants, i.e., high strain rates, this presents quite a challenge [2].

The biocompatibility of the implant is a prerequisite to minimize the risk of inflammation. The excellent biocompatibility of tantalum is related to the formation of a self-assembling surface oxide layer. Intentional oxidation of tantalum with chemicals has been shown to improve its biological properties [3].

A promising thin film deposition method is Atomic Layer Deposition (ALD), which can produce layers with uniform, controlled thickness. Due to the self-limiting reaction, ALD exhibits several advantages, including precise thickness control, low defect density, hole-free structure, excellent step coverage, and uniformity over a large area [4, 5]. The fundamental problem of using coatings on shape memory materials is to manufacture it in such a way, and to select such properties, that it will not be damaged when introduced into the patient's body.

2. MATERIALS AND METHODS

A superelastic NiTi alloy (55.6% Ni) designed for implant applications was used. The chemical composition of the alloy meets the requirements of ASTM 2063-18. Rectangles of size 5x90mm were cut from the sheet with thickness g = 0.3mm.

All of the specimens prepared in this way were electropolished in a 3.5-mol solution of H_2SO_4. Part of them were treated by ALD process. 400 process cycles were performed at 300°C. The carrier and purge gas was high purity nitrogen (N_2).

For electrochemical testing, a special holder was used to allow gradual bending of the plates. The corrosion resistance test was conducted in 37°C, in Phosphate Buffered Saline (PBS) environment. The degree of nickel ion permeation into solution after a certain strain was also measured. Furthermore, Scanning Electron Microscope (SEM) observations of the specimen surface before and after deformation were made. Tantalum Ethoxide $Ta(OC_2H_5)_5$ and water (H_2O) were used as precursors.

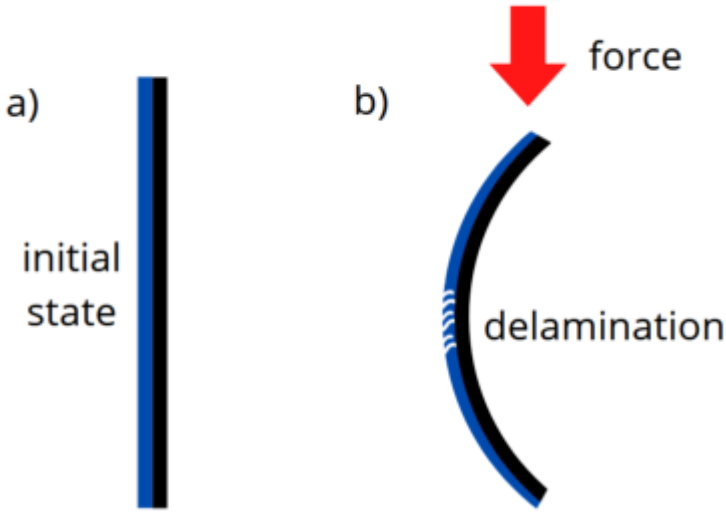

Figure 1. Scheme of deformation method of NiTi alloy (black) and delamination of Ta_2O_5 coating (blue), lateral view

3. RESULTS

The results of the corrosion resistance tests allowed us to determine the strain rate at which the applied Ta_2O_5 layer breaks. Increased nickel permeation into solution was demonstrated after destruction of the Ta_2O_5 coating. SEM observations allowed estimation of the size and shape of delamination.

Acknowledgments: Research funded by statutory activities of Department of Biomaterials and Medical Devices Engineering, Faculty of Biomedical Engineering, Silesian University of Technology, no. 07/020/BK_22/0073.

BIBLIOGRAPHY

1. S. Guo, Y. Shi, R. Wu, H. Liu, Q. Meng, G. Liu, X. Cheng, X. Zhao, Deformation behavior of a novel sandwich-like TiNb/NiTi composite with good biocompatibility and superelasticity, Materials Science and Engineering: A, Volume 794, 2020
2. A. Abbas, H. Hung, P. Lin, K. Yang, M. Chen, H. Lin, Y. Hanb, Atomic layer deposited TiO2 films on an equiatomic NiTi shape memory alloy for biomedical applications, Journal of Alloys and Compounds, Volume 886, 2021
3. M. Vaidulych, P. Pleskunov, J. Kratochvíl, H. Mašková, P. Kočová, D. Nikitin, J. Hanuš, O. Kylián, J. Štěrba, H. Biederman, A. Choukourov, Convex vs concave surface nano-curvature of Ta2O5 thin films for tailoring the osteoblast adhesion, Surface and Coatings Technology, Volume 393, 2020
4. M. Leskelä, M. Ritala, Atomic layer deposition (ALD): From precursors to thin film structures, Thin Solid Films, 409, Issue 1 (2002) 138-146.
5. R. W. Johnson, A. Hultqvist, S. F. Bent, A brief review of atomic layer deposition: from fundamentals to applications, Materials Today, 17, Issue 5 (2014) 236-246.

MTS CONFERENCE
MATERIAL TECHNOLOGIES IN SILESIA

12-15.06.2022
Crystal Mountain***** Hotel, Wisła, Poland

Zastosowanie metod inteligencji obliczeniowej do projektowania składu chemicznego stali o założonej twardości po chłodzeniu z temperatury austenityzowania

J. Trzaska

Politechnika Śląska, Wydział Mechaniczny Technologiczny, Katedra Materiałów Inżynierskich i Biomedycznych
email: jacek.trzaska@polsl.pl

Streszczenie: W artykule opisano hybrydową metodę obliczania składu chemicznego stali o wymaganych wartościach twardości po ciągłym chłodzeniu z temperatury austenityzacji. Do obliczeń wykorzystano algorytm genetyczny i sztuczne sieci neuronowe.

Abstract: The article describes a hybrid method of calculating the chemical composition of steel with required values of hardness after continuous cooling from the austenitizing temperature. A genetic algorithm and artificial neural networks were used for the calculations.

Słowa kluczowe: obróbka cieplna, stal, sztuczne sieci neuronowe, algorytm genetyczny

1. WPROWADZENIE

Właściwie dobrany skład chemiczny powinien zapewnić uzyskanie wymaganych własności stali oraz ograniczyć koszty jej wytworzenia. W projektowaniu składu chemicznego stali istotną rolę mogą odgrywać metody obliczeniowe i modele własności. Istotnych informacji na temat struktury i własności stali uzyskanych po chłodzeniu ciągłym z temperatury austenityzowania dostarczają wykresy CTPc (Czas-Temperatura-Przemiana). Wykresy CTPc wykorzystywane są do doboru warunków obróbki cieplnej oraz do obliczania parametrów modeli przemian fazowych [1, 2]. W pracy [3] opisano model umożliwiający obliczenie wykresu CTPc stali konstrukcyjnych i maszynowych na podstawie składu chemicznego. Do opracowania modelu wykorzystano sztuczne sieci neuronowe.

Wyraźnie widocznym trendem w modelowaniu, również w obszarze inżynierii materiałowej, jest stosowanie metod hybrydowych. Połączenie w modelu sztucznych sieci neuronowych i algorytmów genetycznych umożliwia rozwiązywanie zadań optymalizacyjnych. Sztuczne sieci neuronowe są w tym przypadku stosowane do obliczania wartości funkcji przystosowania poszczególnych chromosomów. Chromosomy są zakodowaną postacią wartości zmiennych decyzyjnych i tworzą zbiór potencjalnych rozwiązań. Przy odpowiednim zdefiniowaniu warunków zadania wartość przystosowania odpowiada wartości optymalizowanej funkcji celu. Pozwala to na identyfikację wartości zmiennych niezależnych spełniających określone kryteria.

W artykule przedstawiono przykład zastosowania sztucznych sieci neuronowych i algorytmu genetycznego do obliczania składu chemicznego stali o wymaganej twardości po chłodzeniu z temperatury austenityzowania.

2. METODA I PRZYKŁAD OBLICZEŃ

Przedstawiona w artykule metoda umożliwia obliczenie składu chemicznego stali o założonej twardości uzyskanej po chłodzeniu w sposób ciągły z temperatury austenityzowania dla pięciu szybkości chłodzenia. Metodę obliczania składu chemicznego, w tym zakres stężeń masowych pierwiastków, w którym może być poszukiwane rozwiązanie przedstawiono szczegółowo w pracy [4]. Funkcję celu opisującą różnicę między twardością wymaganą i obliczoną dla pięciu szybkości chłodzenia, przedstawia równanie (1). Do obliczenia wartości funkcji celu zastosowano model twardości opracowany z wykorzystaniem sztucznych sieci neuronowych [3], a do poszukiwania jej wartości minimalnej wykorzystano klasyczny algorytm genetyczny z binarnym kodowaniem chromosomów,

selekcją metodą ruletki oraz operatorami genetycznymi krzyżowania jednopunktowego i mutacji. Średni błąd bezwzględny twardości stali chłodzonej w sposób ciągły z temperatury austenityzowania modelu neuronowego, który zastosowano w obliczeniach, jest równy 33 HV.

$$f_{HV}(x) = \sum_{i=1}^{5} w_{HVi} \cdot \left| \frac{(HVo_i - HV_{min}) - (HVz_i - HV_{min})}{HV_{max} - HV_{min}} \right| \quad (1)$$

gdzie: i – indeks szybkości chłodzenia (i=1,2,…,5),
x - wektor zmiennych niezależnych (stężenia masowe pierwiastków, temperatura austenityzowania),
w_{HVi} – współczynnik wagowy definiujący istotność twardości dla szybkości chłodzenia opisanej indeksem i,
HVo_i, HVz_i – odpowiednio: twardość obliczona i założona,
HV_{min}, HV_{max}, – minimalna i maksymalna twardość przyjęta na podstawie analizy danych empirycznych.

Zastosowanie metody hybrydowej wykorzystującej algorytmy genetyczne do wielokryterialnej optymalizacji składu chemicznego stali i sztuczne sieci neuronowe do obliczenia wartości funkcji przystosowania wymagało opracowania odpowiedniego programu komputerowego. Program został napisany w języku C++. Użytkownik definiuje pięć szybkości chłodzenia oraz oczekiwaną twardość po chłodzeniu z temperatury austenityzowania. Program umożliwia ograniczenie zakresu stężeń pierwiastków, w którym jest poszukiwane rozwiązanie oraz zmianę podstawowych parametrów algorytmu genetycznego. Wymaganym wartościom twardości może zostać przypisany współczynnik (w_{HVi}) wskazujący na ich istotność w poszukiwanym rozwiązaniu.

Przykład wyników obliczeń w postaci stężeń masowych pierwiastków przedstawiono w tabeli 1. W tabeli 2 zestawiono informacje na temat wymaganej twardości dla pięciu szybkości chłodzenia, twardość obliczoną oraz średni błąd bezwzględny. Średni błąd bezwzględny obliczono jako sumę modułów różnicy między twardością wymaganą i obliczoną dla pięciu szybkości chłodzenia.

Ze względu na ograniczoną objętość publikacji przedstawiono jedynie podstawowe założenia oraz wybrane wyniki obliczeń. Więcej informacji można znaleźć w pracy [4].

Tabela 1. Przykład wyników obliczeń
Table 1. Example of calculation results

Numer rozwiązania	Stężenie masowe pierwiastka, %							Temperatura austenityzowania, °C
	C	Mn	Si	Cr	Ni	Mo	V	
1	0,29	1,13	0,35	0,27	0,83	0,00	0,07	860
2	0,32	0,52	0,35	0,50	0,54	0,16	0,04	860
3	0,32	0,85	0,46	0,24	0,02	0,16	0,09	875

Tabela 2. Wymagane i obliczone wartości twardości
Table 2. Required and calculated hardness values

Szybkość chłodzenia, °/s	70	20	10	4	2
Twardość wymagana HV	500	400	300	280	200
Twardość obliczona HV (rozwiązanie nr 1, błąd 14 HV)	493	400	304	285	218
Twardość obliczona HV (rozwiązanie nr 2, błąd 8 HV)	500	395	302	279	222
Twardość obliczona HV (rozwiązanie nr 3, błąd 10 HV)	498	400	306	284	220

BIBLIOGRAFIA

1. J. Pacyna, Projektowanie składów chemicznych stali, Wydawnictwo Wydziału Metalurgii i Inżynierii Materiałowej AGH, Kraków, 1997.
2. J. Trzaska, Examples of simulation of the alloying elements effect on austenite transformations during continuous cooling, Archives of Metallurgy and Materials 66 (2021) 331–337.
3. J. Trzaska, A new neural networks model for calculating the continuous cooling transformation diagrams. Archives of Metallurgy and Materials 63/4 (2018) 2009-2015.
4. J. Trzaska, Metodologia prognozowania anizotermicznych krzywych przemian fazowych stali konstrukcyjnych i maszynowych, Wydawnictwo Politechniki Śląskiej, Gliwice, 2017.

MTS CONFERENCE
MATERIAL TECHNOLOGIES IN SILESIA

12-15.06.2022
Crystal Mountain***** Hotel, Wisła, Poland

Zastosowanie technologii laserowych do łączenia rur dwuwarstwowych

M. Urbańczyk[a], J. Adamiec[b], R. Ciokan[c]

[a] Sieć Badawcza Łukasiewicz – Instytut Spawalnictwa, ul. Błogosławionego Czesława 16-18, 44-100 Gliwice
[b] Katedra Metalurgii i Recyklingu, Wydział Inżynierii Materiałowej, Politechnika Śląska, ul. Krasińskiego 8, 40-019 Katowice
[c] Wspólna Szkoła Doktorska, Politechnika Śląska, ul. Akademicka 2a, 44-100 Gliwice
email: michal.urbanczyk@is.lukasiewicz.gov.pl

Abstract: Wytwarzanie energii elektrycznej to jeden z najważniejszych elementów gospodarki. Nowoczesne materiały i innowacyjne technologie stanowią dziś kluczowy element rozwoju energetyki, stając się gwarancją bezpieczeństwa energetycznego.

Artykuł przedstawia wyniki badań dotyczących zastosowania technologii laserowych do łączenia doczołowego rur dwuwarstwowych (*composite tubes*) stosowanych w przemyśle energetycznym, min. w spalarniach śmieci.

Badania były realizowane na rurach dwuwarstwowych z gatunku 3R12/4L7 i Sanicro 38/4L7 firmy Sandvik. W ramach badań opracowano parametry spawania laserem warstwy wewnętrznej (4L7 (P265GH) – 1.0425) oraz napawania hybrydowego (laser + MAG) i laserowego proszkowego warstwy zewnętrznej (3R12 – 1.4301, Sanicro 38 – 2.4858).

Badania wykazały, że możliwe jest zastosowanie technologii laserowych do łączenia rur dwuwarstwowych. Stosując metodę spawania laserowego do łączenia rur ze stali 4L7 (warstwa wewnętrzna) o grubości 6,53 mm można uzyskać jakościowe złącza doczołowe z równomiernym licem i prawidłowo uformowaną granią spełniając wymagania poziomu jakości B wg normy PN-EN ISO 19319-1.

Zastosowanie procesu napawania hybrydowego laser + MAG i laserowego proszkowego do warstwy zewnętrznej rury (Sanicro 38 i 3R12) o grubości 1,42 mm pozwoliło na uzyskanie napoiny o odpowiednim kształcie lica spełniające wymagania poziomu jakości B wg normy PN-EN ISO 12932.

Przeprowadzone badania metalograficzne makroskopowe nie wykazały niezgodności spawalniczych w obszarze spoiny i SWC, a uzyskane napoiny charakteryzowały się równomiernym kształtem bez rozprysków.

Keywords: laser, hybryda, HLAW, rura dwuwarstwowa, 3R12/4L7, Sanicro 38/4L7, rura kompozytowa

1. Wprowadzenie

Wzrost zapotrzebowania na energię elektryczną, podnoszenie sprawności spalarni śmieci oraz przepisy dyrektyw Unii Europejskiej m.in. 2014/68/UE powodują konieczność modernizacji europejskiego przemysłu a zwłaszcza energetyki. W tym celu przedsiębiorstwa energetyczne zmuszone są do podejmowania działań w zakresie projektowania, wytwarzania i eksploatacji urządzeń energetycznych [1].

Dotychczas najbardziej rozpowszechnionym w energetyce procesem zwiększającym trwałość elementów kotłów jest ich napawanie stopami na bazie niklu [2, 3].

Innym rozwiązaniem, pozwalającym chronić elementy kotłów przed agresywnym oddziaływaniem produktów spalania jest stosowanie rur dwuwarstwowych, nazywanych kompozytowymi (z ang. *composite tube*) [3].

Rura dwuwarstwowa jest stosowana tam, gdzie warunki na zewnątrz i wewnątrz rury wymagają właściwości materiału, których nie może spełnić tylko jeden materiał. Rura taka składa się z dwóch różnych stopów połączonych metalurgicznie w celu uzyskania dobrych właściwości przenoszenia ciepła. Jeden stop jest używany do wytrzymania korozji, podczas gdy drugi często jest materiałem o podwyższonej odporności na pełzanie [4].

W przemyśle energetycznym coraz częściej stosuje się obok nowych materiałów konstrukcyjnych nowe rozwiązania technologiczne w zakresie technologii łączenia np. spawanie laserowe lub hybrydowe (laser + MAG), co powoduje wzrost efektywności produkcji oraz jakości wyrobów [5].

1.1. Materiały

W badaniach wykorzystano rury dwuwarstwowe firmy Sandvik z gatunku 3R12/4L7 oraz Sanicro 38/4L7 o wymiarach ø 63,5×6,53 mm. Skład chemiczny materiału podstawowego zestawiono w tablicy 1.

Tabl. 1 Skład chemiczny rur dwuwarstwowych 3R12/4L7 i Sanicro 38/4L7 [6]

	C	Si	Mn	Cr	Ni	Mo	Cu	Ti
4L7 (P265GH)	0,18	0,30	0,69	0,14	0,25	0,04	0,030	0,005
3R12 (AISI304)	0,008	0,36	1,11	18,22	10,04	0,24	0,26	0,004
Sanicro 38 (Alloy 825)	0,012	0,15	0,47	19,92	38,24	2,57	1,61	0,75

1.2. Wyniki badań

Proces spawania rur dwuwarstwowych był prowadzony w dwóch etapach. W pierwszej kolejności warstwa wewnętrzna rury (4L7) została wykonana wiązką promieniowana laserowego (bez materiału dodatkowego), celem uzyskania spoiny czołowej z pełnym przetopem (rys. 1a). Drugim etapem procesu spawania było napawanie hybrydowe z wykorzystaniem materiału dodatkowego w postaci drutu (rys. 1b) oraz laserowe proszkowe (rys. 1c) warstwy zewnętrznej (3R12, Sanicro 38).

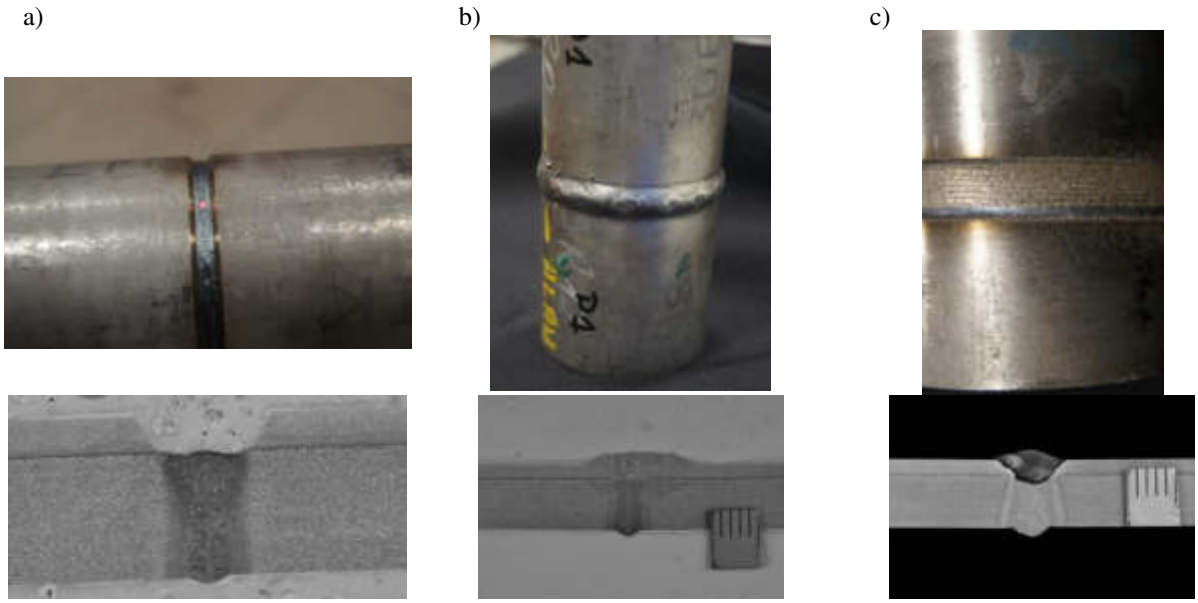

Rys. 1. Widok złączy po procesie spawania, napawania oraz makrostruktura uzyskanych połączeń: a) warstwa wewnętrzna spawana laserem, b) napawanie hybrydowe warstwy zewn., c) napawanie laserowe proszkowe warstwy zewn.

LITERATURA

1. Dyrektywa Parlamentu Europejskiego i Rady 2014/68/UE z dnia 15.05.2014 r. Dz. Urzędowy L189/164, 2014.
2. A. Hernas, „Żarowytrzymałość stali i stopów", Wydawnictwo Politechniki Śląskiej, Gliwice, 1999.
3. Adamiec J.: High temperature corrosion of power boiler components cladded with nickel alloys. Materials Characterization 60 1093÷1099, 2009,
4. Sandvik 3R12/4L7, "Composite tubes for recovery boilers and other boiler applications", Sandvik Materials Technology, 2012,
5. Ciokan R., Urbańczyk M. Lisiecki A.: Opracowanie technologii spawania złączy doczołowych rur kompozytowych z wykorzystaniem metod laserowych. Biuletyn Instytutu Spawalnictwa, 2021, nr 1,
6. http://www.materials.sandvik/contensets/1a283c301e094421b1feac664-f21029e/s-12126-eng-2003-02

MTS CONFERENCE
MATERIAL TECHNOLOGIES IN SILESIA

12-15.06.2022
Crystal Mountain***** Hotel, Wisła, Poland

Heat treatment in welding processes of ferritic stainless steels

G. Walczyk [a], M. Roszak [b]

[a] School of Doctors, Silesian University of Technology, Faculty of Mechanical Engineering, Department of Engineering Materials and Biomaterials, Staltech S.C. Giemza i wspólnicy, Łazy
email: grzewal517@student.polsl.pl
[b] Silesian University of Technology, Faculty of Mechanical Engineering, Department of Engineering Materials and Biomaterials
email: marek.roszak@polsl.pl

Abstract:
The article presents the results of the analysis of heat treatment operations used in the welding processes of ferritic stainless steels. Analysis covering preheat operations, interpass temperature maintenance and post welding heat treatment operations. The analysis of available publications was the basis for determining the significant problems occurring during the welding process of ferritic stainless steels, indicating the importance of heat treatment operations. The results of the analysis of available research related to the phenomenon of grain growth in ferritic stainless steels are presented.

Keywords: ferritic stainless steels, heat treatment, thermal processes, welding.

1. INTRODUCTION

The process of joining metals by welding methods causes the unfavorable phenomenon, which is internal stress in the weld, which is the result of mixing the melted parent material and the base material with a heat source. Too high internal stress may significantly reduce the resistance of the welded joint to dynamic loads. to eliminate internal stresses arising as a result of welding, heat treatment of welds is applied, including: preheating, interpass temperature and stress relief annealing.

2. CHARACTERISTICS OF FERRITIC STAINLESS STEELS

Ferritic stainless steels with low carbon content (maximum about 0.12% C) and high chromium content up to 30% are characterized by high resistance to pitting corrosion arising in environments containing chloride ions [1], no hardened structure, high formability, good plasticity and less hardening as a result of metal working in relation to stainless steels with austenitic structure [1].

There are the following groups of ferritic stainless steels [3]: first generation steels (about 0.12% C) with limited weldability and a tendency to the growth of ferrite grains, second-generation steels (from 0.02% to 0.08% C) in which the growth phenomenon was hindered by the introduction of carbide-forming elements (niobium, titanium) and third generation steels characterized by a high amount of chromium from 25 to 30%, molybdenum up to about 4% and reduction of carbon to about 0.02% [3].

3. HEAT TREATMENT OPERATIONS OF FERRIC STAINLESS STEELS

One of the main research areas in the field of designing the technology of joining ferritic stainless steels by welding methods are heat treatment processes including (fig. 1): preheating used in welding ferritic stainless steels of the first and third generation, in which a partial martensitic transformation takes place and used in the temperature range of 200 - 300ºC and even up to 400ºC [1,2], interpass temperature used too welding ferritic

stainless steels of the first and third generation in order to avoid the formation of a hardened zone associated with an increased brittleness of these steels [1,2].

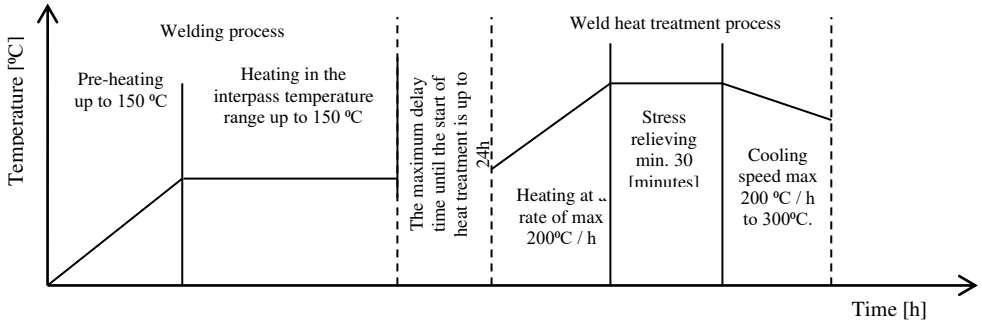

Figure 1. Schematic diagram of the welding process together with heat treatment operations (own elaboration)

Research by M.O.H. Amuda and S. Mridha [5] showed that a significant reduction of the interpass temperature through the use of an additional process of cooling the welds with nitrogen is able to significantly inhibit the phenomenon of ferrite grain growth.

Post-weld heat treatment, used in depend the chromium content and the percentage of ferritic structure can be in the range from 680 ° C to 1050 ° C realize in order to limit the phenomenon of loss of plastic properties. During the annealing of the welds, the stresses are relaxed and the martensite in the weld structure is tempered [2]. Heat treatment of ferritic stainless steels at 900ºC reduces the resistance to intergranular corrosion [4].

4. PROBLEMS RELATED TO HEAT TREATMENT OPERATIONS DURING WELDING FERRITIC STAINLESS STEELS

The use of heat treatment of ferritic stainless steels during the welding process is related to the need to prevent such unfavorable phenomena as:

- The separation of the sigma σ phase in the case of steels containing from 20 to 70% of chromium, resulting from long-term annealing at temperatures from 500ºC to 800ºC, increasing the hardness of steel and their welds [1-4].
- Growth of ferrite grains as a result of diffusion of alloying elements formed in the temperature range from 600ºC to 900ºC, and also as a result of the lack of phase changes that could inhibit the size growth of ferrite grains [1-4].
- High probability of a decrease in resistance to inter-crystalline corrosion called sensitization or sensitization as a result of the welding process and / or post-welding heat treatment at around 900ºC [4], followed by slow cooling in the temperature range from 400ºC to 600ºC, consisting in the formation and diffusion chromium carbides and nitrides from the matrix to the grain boundaries [1,2,4].

Acknowledgments: The study was created as part of the doctoral studies at the Joint Doctoral School covered by the program of the Ministry of Science and Higher Education "Implementation doctorate".

BIBLIOGRAPHY

1. J. Łobanowski, Stale odporne na korozję i ich spawalność, Wydawnictwo Politechniki Gdańskiej, Gdańsk, 2020
2. E. Tasak, A. Ziewiec, Spawalność materiałów konstrukcyjnych. Tom 1 spawalność stali, Wydawnictwo JAK, Kraków, 2009.
3. M. Wróbel, S. Nowak, Stale ferrytyczne odporne na korozję, „Inżynieria Materiałowa" , Vol. 134, 2003. ,
4. M. Blicharski, Zmiany mikrostruktury w połączeniach spawanych różnoimiennych materiałów stosowanych w energetyce. Przegląd Spawalnictwa, 3, 2013.
5. M.O.H. Amuda, S. Mridha, Grain refinement and hardness distribution in cryogenically cooled ferritic stainless steel welds. Materials and Design, 47, 2013.

MTS CONFERENCE
MATERIAL TECHNOLOGIES IN SILESIA

12-15.06.2022
Crystal Mountain***** Hotel, Wisła, Poland

Technology of production of high-strength double-layer 42CrMo4 / NANOS-BA® clad plates in a one-stage process using isothermal annealing

B. Walnik, D. Woźniak, M. Adamczyk, A. Nieszporek

Łukasiewicz Research Network - Institute for Ferrous Metallurgy, Research Group: Manufacturing Technology and Application of Products
email: bartlomiej.walnik@imz.pl

Abstract:

The paper presents the results of semi-industrial tests of manufacturing by hot rolling and heat treatment of double-layer clad plates made of steel 42CrMo4 and NANOS-BA®. The studies on the microstructure and mechanical properties were carried out on samples taken from 42CrMo4/NANOS-BA® clad plates after a two-stage and one-stage process. The results of the project indicate the formation of strong bonds between the layers of bonded materials as a result of their hot rolling and heat treatment with isothermal annealing for the manufacturing technologies used. The two-stage technology enables the production of a wider range of products, while the one-stage technology allows for a significant reduction in the time and cost of their production compared to the two-stage technology.

Keywords: high-strength clad plates, hot rolling bonding, nanobainitic steel

1. INTRODUCTION

The paper presents the results of tests to produce 42CrMo4/NANOS-BA® clad plates in the process of hot rolling and heat treatment. The base material was the commercial non-weldable 42CrMo4 steel, while the steel applied was the experimental non-weldable NANOS-BA® steel. The project is a continuation of the research carried out by Łukasiewicz Research Network – Institute of Ferrous Metallurgy (Łukasiewicz-IMŻ) on the possibility of producing high-strength double-layer clad plates [1-2]. The main purpose of the project was to develop a manufacturing technology that enables the combination of two non-weldable steels into one high-strength product with properties suitable for use in the construction, mining or defence industries [3-4]. The paper presents the results of attempts to optimise the developed two-stage manufacturing technology with the omission of the intermediate stage – intermediate annealing. The production of high-strength 42CrMo4 / NANOS-BA® clad plates in a modernised one-stage process allows to reduce the costs associated with the need to perform energy-consuming and time-consuming soft annealing at 690°C for 4 hours with subsequent cooling with the furnace to ambient temperature (approx. 48 hours), while maintaining high strength of connections between the steels.

2. METHODOLOGY

The microstructure tests were carried out at Łukasiewicz-IMŻ on microsections taken from high-strength 42CrMo4 / NANOS-BA® clad plates in the condition after hot rolling with integrated isothermal annealing at 210°C for 120 hours. Observations of the microstructure in the range of magnifications up to 10,000x were carried out in selected areas in the base material and the welding plane using an Inspect F scanning electron microscope (SEM).

3. STUDY RESULTS

The microstructure of carbide-free lower bainite and austenite, characteristic for this steel, was obtained in the original material of the NANOS-BA® steel. Figure 1 presents the microstructure within the welding plane area of the 42CrMo4 / NANOS-BA® steel. Tests of the produced joints for all variants of hot rolling with integrated heat treatment implemented as part of the project did not show any cracks, delamination, signs of weld failures or other

discontinuities in the base material and the welding plane of both steels. As a result of the tests, permanent connections between steels 42CrMo4 and NANOS-BA® were obtained.

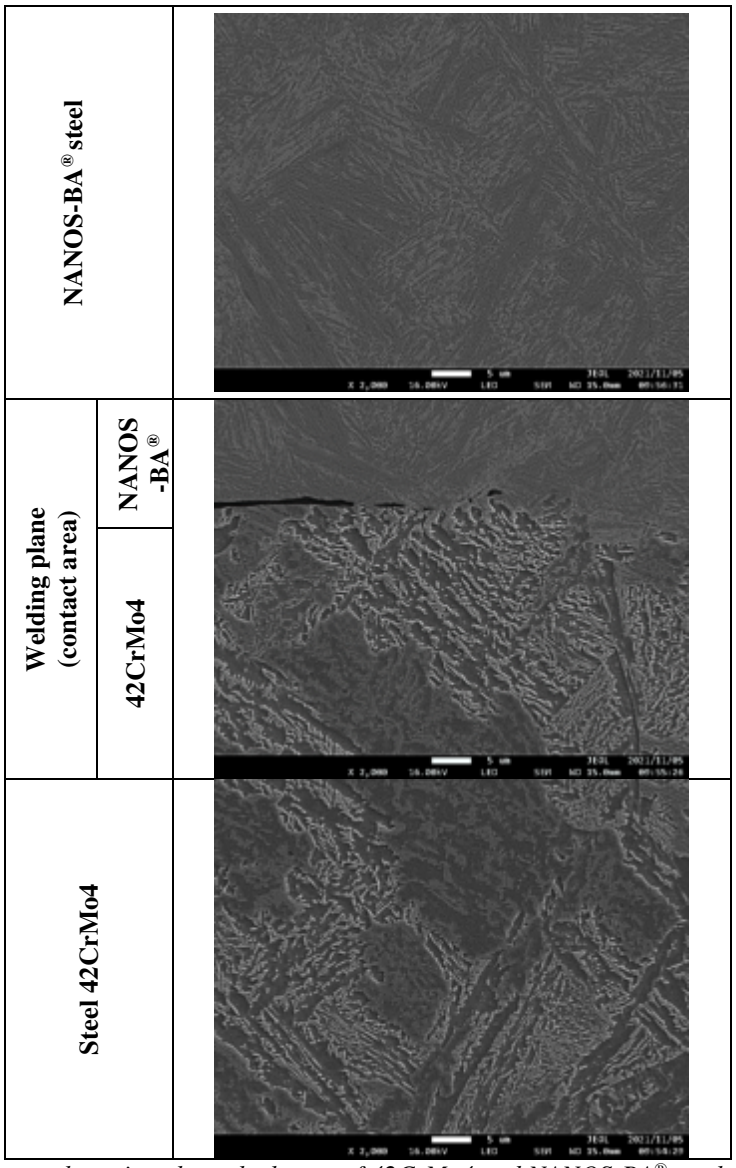

Figure 1. Microstructure at the point where the layers of 42CrMo4 and NANOS-BA® steels are joined after a one-stage process, SEM, microsection etched with 4% Nital

BIBLIOGRAPHY

1. B. Walnik, D. Woźniak, M. Adamczyk, Badania właściwości mechanicznych i mikrostruktury eksperymentalnych blach warstwowych walcowanych na gorąco. Hutnik - Wiadomości Hutnicze, Vol. 86, No. 10, 2019, pp. 309 – 314.
2. B. Walnik, D. Woźniak, A. Nieszporek, M. Adamczyk, Study on mechanical properties and microstructure of 42CrMo4/ NANOS-BA® High-strength clad plates after the process of hot rolling and two-stage heat treatment with isothermal transformation. Journal of Mettalic Materials, Vol. 73 (1) (2021), pp. 22-31
3. B. Walnik, J. Marcisz, A. Iwaniak, J. Wieczorek, Badania zużycia ściernego nanostrukturalnej stali bainitycznej. Prace Instytutu Metalurgii Żelaza, 69 (3)(2017), pp. 55-60
4. J. Marcisz, B. Walnik, W. Burian, A. Iwaniak, J. Wieczorek, D. Paluch, Odporność na zużycie erozyjne nanostrukturalnej stali bainityczno-austenitycznej. Prace Instytutu Metalurgii Żelaza, Vol. 1 (2015), pp. 14-21

MTS CONFERENCE
MATERIAL TECHNOLOGIES IN SILESIA

12-15.06.2022
Crystal Mountain***** Hotel, Wisła, Poland

Microstructure and properties of bainitic tool steel

K. Wasiak[a], Ł. Szczepanek[a], M. Węsierska-Hinca[a], G. Łukaszewicz[a], K. Chmielarz[a], E. Skołek[a]

[a] Warsaw University of Technology, Faculty of Materials Science and Engineering
email: krzysztof.wasiak@pw.edu.pl

Abstract: The microstructure consisting of ferritic bainite, residual austenite and undissolved alloy carbides was studied in K360 tool steel subjected to austempering heat treatment. The hardness, compresive strength, fracture toughness and dry sliding wear of bainitic microstructure have been investigated and compared with those obtained after conventional quenching and tempering heat treatment. The bainitic microstructure exhibits high strength and high toughness due to the refinement of the microstructure. The bainitic microstructure and the martensitic microstructure present different wear mechanisms under the same sliding wear process. For a higher load the bainitic steel exhibits better wear resistance in comparison to tempered martensite as a consequence of fine microstructure and carbon enriched austenite, which undergo martensitic transformation during friction (TRIP effect).
Keywords: K360, bainite, tool steel, fracture toughness, wear resistance

1. INTRODUCTION

Properly carried out heat treatment of tool steels allows to obtain high hardness and wear resistance, as well as sufficient toughness. Typical heat treatment of tool steels consists of quenching and single or multiple tempering. Tempering helps to lower the residual stresses and increase the plasticity and toughness. It also lead to carbides precipitation from retained austenite, which may be undesirable due to sensitization of the steel to fracture. Multiple tempering is used to temper the secondary martensite, which appears during cooling of unstable retained austenite after first tempering – to avoid brittleness of heat treated tool. Notwithstanding, the improvement in fracture toughness comes at the expense of hardness, strength and wear resistance. Extending the lifetime of the tools, however, it requires a compromise between these properties.
To meet the current needs of the industry, new heat treatment technologies dedicated to tool steels are developed. Among them are subzero treatments, used to improve the properties of dies for at least eight. Placed between quenching and tempering, allow to reduce amount of retained austenite by martensitic transformation, lead to uniform distribution of fine secondary carbides and reduce residual stresses [1]. This in turn allows to increase the hardness and wear resistance of the tools, but on the other hand it can result in reduction of toughness. Nevertheless, this leads to an increase in the service life of the tools. A great interest in subzero treatments in the context of improving the mechanical properties of tool steels reflects the needs of the industry for new material solutions in the area of tool materials. The predominance of research on sub-zero treatments over other treatments should be an incentive to explore as yet unknown areas. Especially considering the successes of unconventional heat treatments, which allow obtaining a nanostructure in steels.
Bhadeshia et al. [2] and Caballero et al. [3] developed isothermal treatment of structural steels at low temperature within the range of bainitic transformation, which lead to obtain a carbide-free microstructure, composed of bainitic ferrite and retained austenite, in steels containing approximately 2 wt.% of silicon. This type of microstructure is called nanobainite and exhibit a favourable combination of mechanical and service properties. The wear resistance of nanobainitic steel is superior to the microstructure containing tempered martensite with comparable or even higher hardness values.
This paper presents the possibility of using bainitization to shape the properties of the BÖHLER K360 ISODUR 8%Cr cold work tool steel. The hardness, compresive strength, fracture toughness and dry sliding wear of bainitic

microstructure have been investigated and compared with those obtained after conventional quenching and tempering heat treatment.

2. RESULTS

2.1. Microstructure

As a result of austempering of K360 tool steel the carbide-free bainitic microstructure was obtained in the matrix. The bainitic ferrite nucleates preferentially at the grain boundaries of prior austenite and at the carbides. Sub-units grow towards the grain interior, dividing it into smaller blocks. As transformation progresses, subsequent plates nucleate on the tips of the previous ones *Figure 1*.

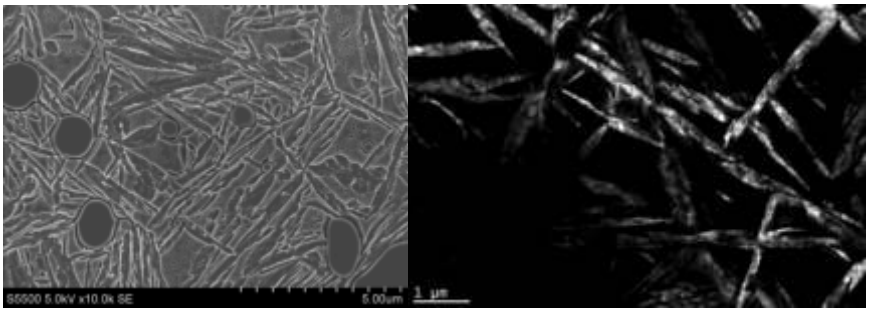

Figure 1 Microstructure of the K360 tool steel after austempering.

The bainitic microstructure exhibits lower hardness in comparison to the martensite, but the fracture toughness and wear resistance is higher due to the refinement of the microstructure and carbon enriched austenite, which undergo martensitic transformation under strain (TRIP effect) *Figure 2*.

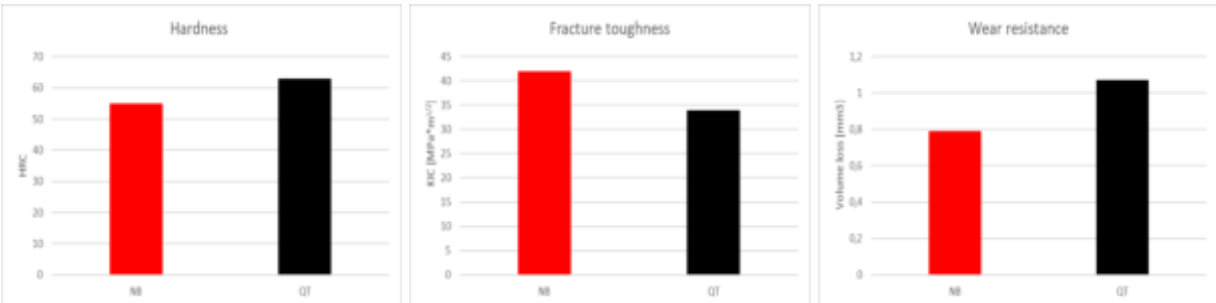

Figure 2 Properties of the K360 tool steel after bainitization (NB) and quenching and tempering.

Acknowledgments:
The results presented in this work have been obtained within the project NanoCarbain (contract no. LIDER/12/0040/L-9/17/NCBR/2018). The project is financed by the National Centre for Research and Development under the LIDER IX program.

BIBLIOGRAPHY

[1] J. Sobotova, P. Jurci, I. Dlouhy, The effect of subzero treatment on microstructure, fracture toughness, and wear resistance of Vanadis 6 tool steel, Mater. Sci. Eng. A. 652 (2016) 192–204. https://doi.org/10.1016/j.msea.2015.11.078.
[2] H.K.D.H. Bhadeshia, D. V. Edmonds, Bainite in silicon steels: New composition-property approach Part 1, Met. Sci. 17 (1983) 420–425. https://doi.org/10.1179/030634583790420646.
[3] P. Brown, Design of novel high strength bainitic steels : Part 1, (2000).

MTS CONFERENCE
MATERIAL TECHNOLOGIES IN SILESIA

12-15.06.2022
Crystal Mountain***** Hotel, Wisła, Poland

Structure and properties of friction stir welded joints of magnesium alloy AZ91

A. Węglowska[a], K. Mroczka[b], St. Dymek[b], C. Hamilt[b], D. Miara[e]

[a]Łukasiewicz Research Network - Institute of Welding, Gliwice, Poland
email: aleksandra.weglowska@is.lukasiewicz.gov.pl
[b] Cracow University of Technology, Department of Materials Engineering, Faculty of Materials Science and Physics, Krakow, Poland
email: kmrocz@gmail.com,
[c] AGH University of Science and Technology in Krakow, Department of Surface Engineering and Materials Characterization Krakow, Poland,
email: gmdymek@cyfronet.pl
[d] Mechanical and Manufacturing Engineering, Miami University, USA
email: hamiltbc@miamioh.edu
[e] Łukasiewicz Research Network - Institute of Welding, Gliwice, Poland
email:damian.miara@is.lukasiewicz.gov.pl

Abstract: Results of friction stir welding of cast AZ91 magnesium are presented in this paper. Joints were produced in butt-weld configuration with different welding parametersTensile tests as well as micro-hardness tests were performed. The microstructures of the welds were characterized through light and electron microscopies (SEM-EBSD, TEM). Results of torques and forces measurements recorded with the LowStir device was presented. Numerical modeling of FSW process was carried out.
Keywords: Friction Stir Welding, magnesium alloy, microstructure, micro-tensile test, hardness

1. INTRODUCTION

Due to the highly specific strength, ductility and low density, magnesium alloys are widely used in the automotive, aerospace and ship building industries [1]. Conventional fusion welding of lightweight alloys produces welds which suffer from defects such as hot cracking, residual stress, porosity etc. The solid-state processes, such as Friction Stir Welding (FSW), can substantially eliminate or reduce these disadvantages and improve the joint quality [2]. The microstructure that evolves during FSW results from the simultaneous interaction of material flow, plastic deformation and exposure to elevated temperature [3]. Heat is generated at the work pieces, both due to the friction between the work pieces and the rotating tool shoulder and pin, and also by the severe plastic deformation of the work pieces. Magnesium FSW joints, free from defects, are formed with optimal welding parameters (tool rotation speed, traverse speed and axial pressure) which generate the required heat input and material flow [2]. During the process an onion ring structure, as a result of a different material flow can be identified [4]. Stir zone (SZ) and thermomechanical affected zone (TMAZ) undergo intense plastic deformation with a rise in temperature, which lead to a phenomenon of dynamic recrystallization and reduction in the grain size [3]. These zones are composed of an α-Mg phase with β-$Mh_{17}Al_{12}$ precipitates localized around the grain boundaries [3]. The micro-hardness is inhomogeneously distributed in welds [2]. Some studies showed that the more refined grains obtained in SZ lead o increase of micro-hardness [5, 6], according to Hall-Petch parameter (H_v). Although other results showed [3, 7] that micro-hardness in the SZ is lower than in base material due to the presence of the β-$Mg_{17}Al_{12}$ phases.

2. EXPERIMENTAL METHODOLOGY

Joints were produced in butt-weld configurations with 6 mm thick workpieces utilizing two different tools and various welding parameters. Tensile tests as well as micro-hardness tests were performed. The hardness distribution on the weld cross-section in the distance of 2,45 mm from the weld face presents fig. 1. Table 1

reveals the results of the micro-tensile test for locations relevant to the micro-hardness track. The results of the micro-hardness distribution test showed differences in properties that may affect the performance of the joints. The microstructures of the welds were characterized through light and electron microscopies (SEM-EBSD, TEM). Some regions with different phase compositions (different content of $Mg_{17}Al_{12}$) were discerned within the weld - fig 2. These regions were harder than the parent material. Within the central part of welds, a homogeneous microstructure contains precipitates partly distributed within grain boundaries in the weld nugget. Influence of the shape of working part of pin as well as the linear welding speed on the course of forces and torque acting on the tool during the welding process was performed with the use LowStir device. Numerical modeling of FSW process of magnesium alloy was carried out.

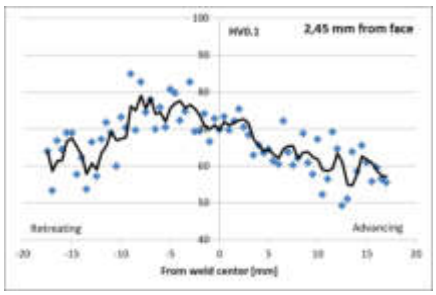

Figure 1. Hardness distribution on cross-section 2,45 mm from weld face

Table 1. Micro-tensile test results (MPa) for locations in distance 2,45 mm from weld face

Strona natarcia			Środek zgrzeiny	Strona spływu		
162 ± 20,7	235 ± 12,3	297 ± 4,2	277 ± 3,6	272 ± 5,4	195 ± 5,0	133 ± 8,8

Figure 2. Light microscopy microstructure on the cross-section of placed nearby weld face

Acknowledgments: The research was carried out as part of a project (no. UMO-2018/31/B/ST8/01594) financed by the National Science Center (Polish government unit).

Bibliography

1. P.K. Sahu, S. Pal: Influence of metallic foil alloying by FSW process on mechanical properties and metallurgical characterization of AM20 Mg alloy. Mater. Sci. Eng. A, 684, 442–455, 2017.
2. L. Yajie, Q. Fengming, L. Cuirong, W. Zhisheng: A Review: Effect of Friction Stir Welding on Microstructure and Mechanical Properties of Magnesium Alloys. Metals, 7, 524, 2017.
3. A. Kouadri-Henni, L. Barrallier: Mechanical properties, microstructure and crystallographic texture of magnesium AZ91-D alloy welded by friction stir welding (FSW). Metall. Mater. Trans. A, 45, 4983–4996, 2014.
4. M.N. Avettand-Fènoël, A. Simar: A review about friction stir welding of metal matrix composites. *Mater. Charact. 120*, 1–17, 2016.
5. J. Chen, H. Fujii, Y. F. Sun, Y.Morisada, Y., K. Kondoh:. Optimization of mechanical properties of fine-grained non-combustive magnesium alloy joint by asymmetrical double-sided friction stir welding. J. Mater. Process. Technol. 242, 117–125, 2017.
6. J. Chen, H. Fujii, Y. F. Sun, Y. Morisada, K. Kondoh: Effect of grain size on the microstructure and mechanical properties of friction stir welded non-combustive magnesium alloys. Mater. Sci. Eng. A. 549, 176–184, 2012.
7. O. S. Salih, H. Ou, W. Sun, D. G. McCartney: A review of friction stir welding of aluminium matrix composites. Mater. Des. 86, 61–71, 2015.

MTS CONFERENCE
MATERIAL TECHNOLOGIES IN SILESIA

12-15.06.2022
Crystal Mountain***** Hotel, Wisła, Poland

Laser and electron beam remelting of Re plasma spraying

M.St. Węglowski[a], J. Dworak[a], P. Śliwiński[a], S. Dymek[b], I. Kalemba-Rec[b], A. Wrona[c], K. Kustra[c]

[a] Łukasiewicz – Institute of Welding, [b]Łukasiewicz – Institute of Non-Ferrous Metals, [c]AGH University of Science and Technology, Faculty of Metals Engineering and Industrial Computer Science
email: marek.weglowskie@is.lukasiewicz.gov.pl

Abstract:
One of the most popular thermal spraying technologies is plasma spraying, which allows for the formation of coatings with a desired chemical composition and thickness. However, such coatings can be characterized by numerous imperfections associated with the nature of the process itself. The reduction of porosity is possible only by remelting the coating using different heat sources such as laser or electron beams. By adjusting the technological parameters especially power and travelling speed, it is possible to precisely control the depth of the remelted material and thus the properties of final coatings. The paper presents the laser and electron remelting processes of plasma spraying coatings in relation to microstructure of coatings.

Keywords: plasma spraying, laser beam remelting, electron beam remelting, rhenium

1. INTRODUCTION

The coatings obtained in atmospheric plasma spraying are characterized by specific microstructure as well as imperfections. In order to improve properties and eliminate material discontinuous laser or electron beam remelting processes can be applied. Li C. et al.[1] applied CO2 laser remelting to plasma-sprayed nanostructured Al2O3–13 wt%TiO2 coatings deposited on an AZ91D magnesium alloy substrate. Ge Y. et al [2] employed the LB remelting to modified of plasma sprayed micro-structured Al–Si based and 1 wt.% nano-structured Si3N4 coating fabricated on an AZ31B magnesium alloy. Ciubotariu C.R. et al. [3] applied LB remelting process to improve the HVOF-sprayed Stellite 6 wear resistant coatings. Wang D. [4] revealed that the laser remelting process allows to improve hot corrosion resistance of MCrAlY coating prepared by plasma spraying. Utu D. et al. [5] employed the EB surface treatment to remelting the CoNiCrAlY coatings (0.7–1 mm) with 8 wt.% Al content were sprayed onto a copper substrate (5 mm thick) using the HVOF-spraying technique. Hamatani H. et al. [6] applied EB remelting to reduce or remove low coating cohesive strength and low interface strength between the substrate and coating. The main goal of the research was to present the effects of remelting processes of plasma sprayed coatings in relation to microstructure.

2 EXPERIMENTAL PROCEDURE

The materials used in this procedure was Ni20%Cr + 20%Re alloy. The procedure consisted of 2 stages. During the first stage, manufactured powders with rhenium was plasma sprayed on an austenitic stainless steel (AISI 316Ti) substrate. The surface of the substrate was prepared by abrasive blasting using corundum abrasive. The plasma spraying parameters: current 530 A, arc voltage 690 V, shielding gas flow rate (Ar) 54 l/min, plasma gas flow rate (H2) 9 l/min, transport gas flow rate (Ar): 5 l/min, spraying distance 140 mm, travelling speed 400 mm/s. The second stage was laser and electron beam remelting that were carried out using a laser Yb:YAG TRUMPF Trudisk 12002 r as well as electron beam machine model XW150:30/756 (Cambridge Vacuum Engineering). Laser remelting at the following parameters was conducted: P=1,9 kW, v=0.3 m/min, Ar as shielding gas. For electron beam process the following parameters were applied: U=60kV, I=28 mA, v=0.5 m/min.

EB remelting in vacuum was carried out. The microstructures of the etched samples were investigated by light and scanning electron microscopy.

3 RESULTS

The cross-section images of the plasma sprayed coatings NiCr + Re are shown in Figure 1. The microstructure is characterized by high porosity and contains a lot of cracks and have typical plasma sprayed lamellar structure. In turn, Figures 2a, 2b illustrates the cross-sections of coatings after laser and electron beams remelting, respectively. As shown in Figure 2 remelting effectively reduces the presence of pores and microcracks resulting in much denser coating. After laser remelting the lamellar structure of the plasma sprayed coating was replaced by fine homogenous microstructure.

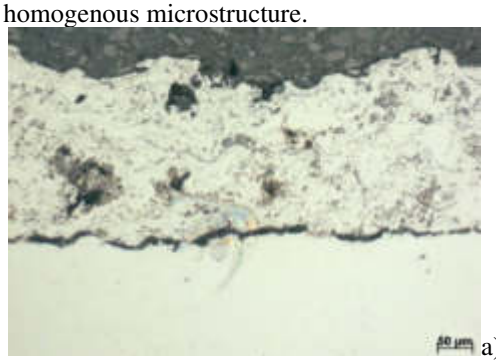

a)

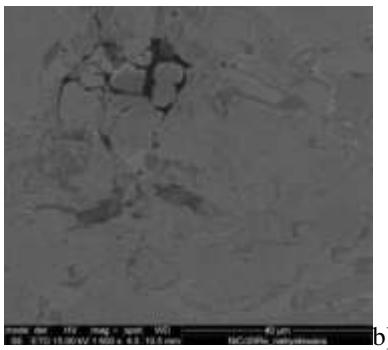
b)

Figure 1. The cross-section images of plasma-sprayed coating, a) LM, b) SEM

a)

b)

Figure 2. The cross-section images of plasma-sprayed coating after a) laser, b) electron, beam remelting

Acknowledgments: The financial support of the National Science Center, Poland, is gratefully acknowledged, grant no. UMO-2018/29/B/ST8/01206.

BIBLIOGRAPHY

1. C. Li, Y. Wang, et al., Laser surface remelting of plasma-sprayed nanostructured Al 2O 3–13 wt%TiO 2 coatings on magnesium alloy J. Alloys Compd, 503 (2010) 127-132.
2. Y. Ge, W. Wang, Study on laser surface remelting of plasma-sprayed Al–Si/1 wt% nano-Si3N4 coating on AZ31B magnesium alloy, Appl Surf Sci., 273 (2013) 122–127 C.R. Ciubotariu, Optimization of the laser remelting process for HVOF-sprayed Stellite 6 wear resistant coatings, Opt Laser Technol, 77 (2016) 98-103.
3. D. Wang, Effects of Laser Remelting on Microstructural Characteristics and Hot Corrosion Behavior of MCrAlY Coating Prepared by Plasma Spraying, Mater. Sci. Forum, 971 (2019) 70-76.
4. D. Utu, W. Brandl, et al., Morphology and phase modification of HVOF-sprayed MCrAlY-coatings remelted by electron beam irradiation, Vacuum, 77 (2005) 451-455.
5. R. Franke, I. Haase, Friction and wear behaviour of electron beam surface treated aluminium alloys AlSi10Mg(Cu) and AlSi35, Wear, 269 (2010) 921-929.
6. H. Hamatani, Y. Miyazaki, Optimization of an electron beam remelting of HVOF sprayed alloys and carbides, Surf. Coat. Tech., 154 (2002) 176-183.

MTS CONFERENCE
MATERIAL TECHNOLOGIES IN SILESIA

12-15.06.2022
Crystal Mountain***** Hotel, Wisła, Poland

Innovative heat treatment leading to formation of nanocrystalline multiphase microstructure in high-alloy tool steel

M. Węsierska-Hinca[a], K. Jurko, K. Chmielarz. K. Wasiak, W. Świątnicki

[a] Warsaw University of Technology, Faculty of Materials Science and Engineering
email: monika.wesierska.dokt@pw.edu.pl

Abstract: Nanostructurization by bainitic phase transformation is a revolutionary method of improving the mechanical properties of a wide range of steels. It can be applied as a single process or as a part of the innovative multistage heat treatment. While implementing the latter to the tool steel allows obtaining a new type of complex microstructure consisting of very hard carbides in a tough, nanocrystalline matrix comprising bainitic ferrite, martensite and retained austenite. In the present work, the influence of process parameters on multiphase microstructure evolution was investigated in high carbon steel, containing enhanced concentration of silicon and carbide forming elements. By controlling the amount of particular components in the microstructure it is possible to change the mechanical and service properties of steel.
The kinetics of phase transformations that occurred during the process was analyzed using dilatometric tests. The phase composition and morphology of phase constituents were determined by observations with the scanning electron microscope (FE-SEM Hitachi S-5500) and transmission electron microscope (TEM), accompanied by magnetic measurements. The study was completed with mechanical tests, including hardness measurements, uniaxial compression tests, impact and fracture toughness tests.

Keywords: tool steel, nanobainite, tempering, carbides, retained austenite

1. INTRODUCTION

The tool steels are widely used in applications demanding high hardness, compressive strength and enhanced wear resistance, such as dies, stamps, and matrix. Required properties are usually achieved due to the conventional heat treatment consisting of quenching combined with single or multiple tempering. However, the main flaw of this treatment is limited fracture toughness and the risk of deformation or even cracks that can occur as a result of stresses induced to the structure during martensitic transformation.
Thus the promising solution is to introduce the isothermal stop in the temperature range of bainitic transformation to the process (B). Formation of the desired fraction of nanocrystalline bainitic plates in the structure separated by austenite films increases toughness and plasticity of the steel. Moreover, the carbides present after austenitization can act as additional nucleation sites leading to evolution of acicular ferrite morphology. Enhanced concentration of silicon and aluminium retards cementite precipitation. As a result, the application of partial bainitization affects the fragmentation of the microstructure, dividing the primary austenite grain with bainitic ferrite sheaves. Afterwards, the element is subjected to an interrupted quench to a temperature between the martensite start (Ms) and martensite finish (Mf) temperatures of the retained austenite in order to introduce very fine plates of martensite to the steel (Q). Subsequently, the tempering step is carried out, leading to the reduction of the brittleness of martensite, stabilization of the retained austenite and the precipitation of very fine and well-dispersed alloy carbides (T). The time, temperature and number of the tempering steps should be selected in such a way that the diffusion of the alloying elements is sufficient for the formation of precipitates, which result in secondary hardness of the steel, whereas the diffusion of carbon from martensite and bainitic ferrite enables thermal stabilization of the retained austenite, avoiding martensitic transformation during cooling.

The scheme of the designed BQ&T (Bainitization -Quenching &Teempering) heat treatment method with microstructure evolution is presented in Figure 1.

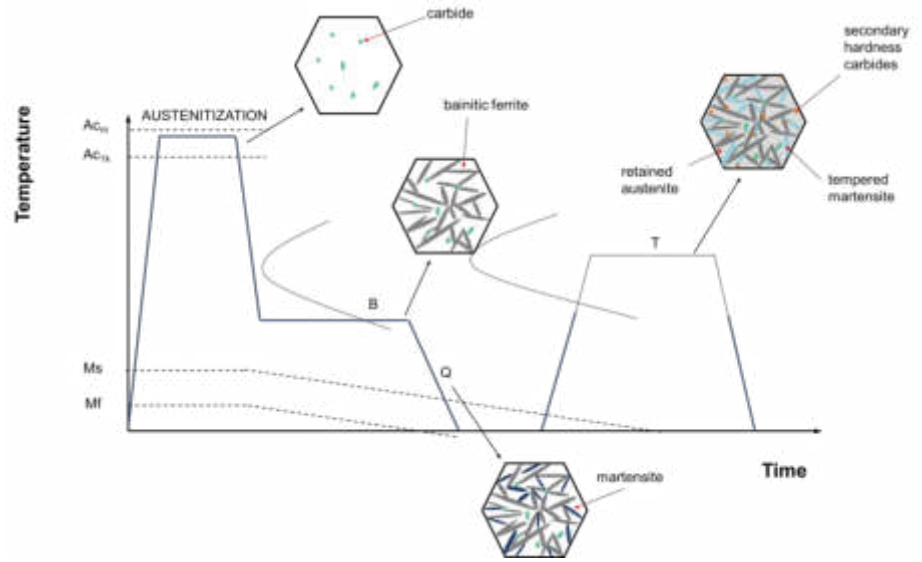

Figure 1. Scheme of the innovative BQ&T heat treatment for tool steels

2. RESULTS

The BQ&T heat treatment was implemented into K360 cold-working steel with the chemical composition (% wt.): 1.56% C, 0.33% Mn, 0.90% Si, 0.84% Al, 8.99% Cr, 2.81% Mo, 1.19% V, 0.45% Nb, 0.24% Ni, 0.18% W. The samples were subjected to two variants of partial bainitization: 20% and 60% of advancement of bainitic transformation in order to verify the influence of bainitic ferrite on microstructure evolution and mechanical properties of steel. Afterwards quenching to the room temperature was carried out, followed by tempering at 500^0C, where secondary hardness occurs. The obtained results were compared to the conventionally treated samples.

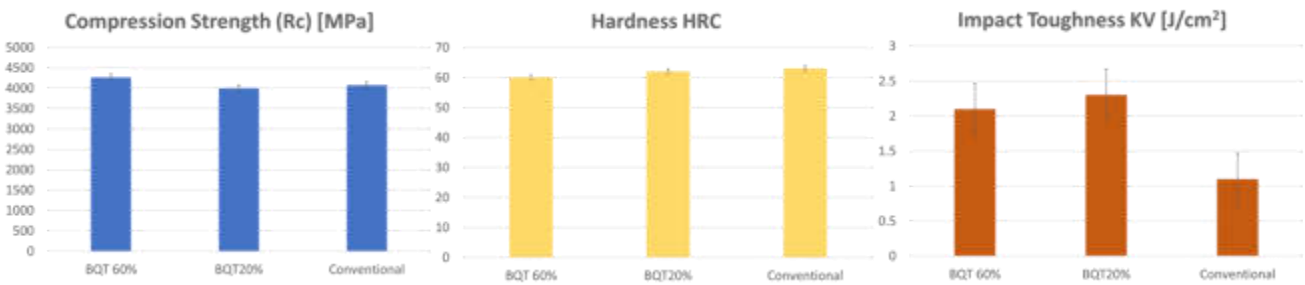

Figure 2. Comparison of mechanical properties of K360 steel subjected to BQT and conventional heat treatments.

The multiphase microstructure consisting of carbides, bainitic ferrite, martensite and retained austenite (above 20% vol.) indicates very high hardness and compression strength, comparable to the steel after conventional heat treatment. However, the introduction of bainite results in increase of impact and fracture toughness of samples. Moreover, the samples after BQT treatment, despite similar surface properties, exhibit enhanced wear resistance. Refinement of microstructure and higher grain disorientation lead to crack path deflection, whereas carbon enriched austenite accommodate stress and delay crack propagation due to the TRIP effect. The increase of bainite fraction augments strengthening effect, as bainitic ferrite is less prone to tempering and indicates higher mechanical stability in elevated temperatures.

Acknowledgments: This research is funded by the National Centre for Research and Development under the LIDER IX program, project NanoCarbain (contract no. LIDER/12/0040/L-9/17/NCBR/2018).

MTS CONFERENCE
MATERIAL TECHNOLOGIES IN SILESIA

12-15.06.2022
Crystal Mountain***** Hotel, Wisła, Poland

Influence of heat treatment on the properties of selected materials produced by the arc welding

A.N. Wieczorek[a] S. Marciniak[b], A. Gołaszewski[b]

[a] Silesian University of Technology, Faculty of Mining, Safety Engineering and Industrial Automation
[b] NanoStal Sp. z o.o
email: andrzej.n.wieczorek@polsl.pl

Abstract: The article discusses the possibility of increasing the plastic properties of Tubrodur 35 G M material with a composition of 0.21% C, 0.80% Si, 1.29% Mn, 1.34% Cr obtained with the use of arc welding methods. As a result of the conducted research, it was found that it was possible to obtain a significant increase in the impact toughness of the sample after heating it in the so-called the intercritical range in relation to the thermally improved variant.

Keywords: heat treatment, arc welding, additive methods

1. INTRODUCTION

Rapid prototyping with arc welding methods with the use of wire is in line with the global trend of searching for quick and effective methods of increasing the functional properties of materials obtained with the use of additive methods by means of heat treatment [1,2]. The demand for rapid prototyping methods [3,4] is related to the development of new technologies in the automotive, aviation and machine building industries.

1.1. Results

The conducted tests used dilatometric tests, light and electron microscopy (Fig. 1), tests of mechanical properties (microhardness, impact strength, static tensile test) and functional properties, such as resistance to wear by friction. In this study, it was shown that it is possible to produce a carbide-free banite structure in a ferritic matrix and improved plastic properties of the material obtained by arc methods based on Tobrodur 35 G M wire with the use of intercritical annealing.

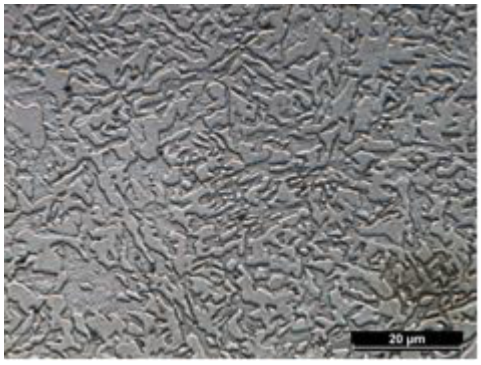

Figure 1. Microstructure of the sample from Tobrodur 35 G M wire after annealing in the intercritical range.

Acknowledgments:
The presented results were obtained as part of the grant for ground-breaking research 06/020/SDU/10-21-01 financed by the Rector of the Silesian University of Technology.

BIBLIOGRAPHY

1. Bhadeshia H. K. D. H.: Bainite in steels, Third edition. Maney Publishing, Wakefield, UK, 2015, ISBN: 978-1-909662-74-2
2. Dossett J., Totten G.E.: Steel Heat Treating Fundamentals and Processes. Introduction to Surface Hardening of Steels. ASM Handbook, Vol. 4A. Revised by Michael J. Schneider, The Timken Company, and Madhu S. Chatterjee, 2013.
3. Herzog D., Seyda V., Wycisk E., Emmelmann C. "Additive manufacturing of metals". Acta Materialia, 2016, p. 371–392.
4. Murr L.E., Martinez E., Amato K.N., Gaytan S.M., Hernandez J., Ramirez D.A., Shindo P.W., Medina F., Wicker R.B. "Fabrication of metal and alloy components by additive manufacturing: examples of 3D materials science". Journal of Materials Research and Technology, 2012, p. 42–54.

MTS CONFERENCE
MATERIAL TECHNOLOGIES IN SILESIA

12-15.06.2022
Crystal Mountain***** Hotel, Wisła, Poland

Kompozyty polimerowe wzmacniane mączką z łupin orzechów jako alternatywa dla wytworów z drewna

A. Włodarczyk-Fligier[a], M. Polok-Rubiniec[a]

[a]Politechnika Śląska, Wydział Mechaniczny Technologiczny, Katedra Materiałów Inżynierskich i Biomedycznych
email: anna.wlodarczyk@polsl.pl

Abstrakt: W artykule przedstawiono wyniki badań: twardości, wytrzymałości na rozciąganie wytworzonych polimerowych materiałów kompozytowych o osnowie polipropylenowej PP z napełniaczem naturalnym z mączki łupin orzechów laskowych o różnym udziale % i różnej frakcji.

Słowa kluczowe: materiały WPC, polipropylen, napełniacz naturalny

1. WSTĘP

Zaletą kompozytów WPC w stosunku do typowych polimerów jest upodobnienie ich wyglądu do naturalnego drewna, przy zachowaniu między innymi wysokiej odporności na działanie czynników środowiskowych. Obecnie poszukuję się zastępstwa dla mączki drzewnej i dobrą alternatywą jest mączka z łupin orzechów różnego gatunku. Pozwala ona na zmniejszenie chłonności wody oraz polepszenie własności użytkowych, co umożliwiłoby ich zastosowanie m.in. na elementy ogrodowe (deski tarasowe, balustrad, place zabaw, pokrycia dachowe itp.) [1 - 3].

1.1. Materiał do badań

Badania wykonano na polimerowych materiałach kompozytowych o osnowie z polipropylenu PP Moplen HP400R z napełniaczem naturalnym z mączki łupin orzecha laskowego o udziale 30 i 50% i frakcji 0-200 µm oraz 315-443 µm. Oznaczenia badanych materiałów zestawiono w Tabeli 1.

Tabela 1. Oznaczenia badanych materiałów.

Mąka z łupin orzecha laskowego, frakcja µm	Zawartość mączki z łupin orzecha laskowego w osnowie polipropylenowej PP, %		
	0	30	50
0-200	PP	A2	A4
315-443	PP	C2	C4

Wykorzystane łupiny z orzechów laskowych, jako napełniacz przed wytłoczeniem były poddane rozdrobnieniu w sposób dwuetapowy: I etap odbył się na młynie młotkowym SchutteBuffalo, a II etap na młynie turbinowym. Po rozdrobnieniu otrzymaną mączkę przesiewano przez sita o różnej wielkości oczek w celu uzyskania różnej wielkości frakcji mączki. Przesiane mączki następnie poddano suszeniu w temperaturze ok. 80°C przez ok. 4h i mieszano z granulatem poliolefinowym.

Takie mieszaniny poddano jednokrotnemu wytłaczaniu homogenizującemu przy użyciu wytłaczarki dwuślimakowej przeciwbieżnej Goöttfert, stosunku L/D= 25 wyposażonej w głowicę do wytłaczania pręta o średnicy na wyjściu ø 3mm.

Warunki procesu wytłaczania, jakie dobrano do otrzymanych mieszanin PP/mączka z łupin z orzechów laskowych: temperatura I strefy: 180°C, temperatura II strefy: 200°C, temperatura III strefy: 210°C, temperatura

głowicy: 215÷220°C, ilość obrotów: 2-4 obr/min. Po wytłoczeniu granulat poddano wtryskiwaniu, efektem końcowym było uzyskanie próbek badawczych w kształcie wiosełek znormalizowanych typu A1 wg PN-EN ISO 527-1. Proces wtryskiwania przeprowadzono na wtryskarce Battenfeld Plus 35/75 wyposażonej w system sterowania Unilog B2 o stosunku L/D 17.

1.2. Metodologia

Twardość badanych polimerowych materiałów kompozytowych przeprowadzono przy użyciu twardościomierza Zwick metodą kulkową pod obciążeniem badawczym 358N w temperaturze otoczenia 22°C zgodnie z wytycznymi normy PN-EN ISO 2039-1.

Statyczną próbę rozciągania wykonano na uniwersalnej maszynie wytrzymałościowej firmy Zwick/Roell Z020 wg normy PN-EN ISO 527-1:1998, przy prędkości badawczej 5mm/min, w temperaturze otoczenia 22°C.

1.3. Omówienie badan

Wprowadzenie do osnowy PP mączki z łupin orzechów laskowych spowodowało zauważalny wzrost twardości badanego kompozytu polimerowego. Wraz ze wzrostem zawartości napełniacza w osnowie znacząco wzrasta twardość wytworzonego materiału. W porównaniu do samej osnowy PP jego twardość wynosi 58,1 HB, gdzie w przypadku próbki A2 twardość wzrosła do 63,1 HB, A4 69,6 HB, a w przypadku mączki o większej frakcji wzrosła w przypadku próbki C2 do 72,2 HB, a próbki C4 do 76,4 HB (Tabela 2).

Tabela 2. Twardość badanego kompozytu polimerowego wzmacnianego mączka z łupin orzecha laskowego.

PP	A2	A4	C2	C4
58,1 HB	63,1 HB	69,6 HB	72,2 HB	76,4 HB

Wprowadzenie do osnowy polimerowej badanego napełniacza w postaci mączki z łupin orzecha laskowego spowodowało zmianę jego własności wytrzymałościowych. Wraz ze wzrostem zawartości mączki w kompozycie zmniejszyła się wartość wytrzymałości na rozciąganie Rm. Zawartość 50% zawartości napełniacza w osnowie PP spowodowała spadek wytrzymałości Rm kompozytu do wartości ok. 15 MPa w obu przypadkach wielkości frakcji napełniacza (Tabela 3)

Tabela 3. Statyczna próba rozciągania badanego kompozytu polimerowego wzmacnianego mączką z łupiny orzecha laskowego.

PP	A2	A4	C2	C4
30,85 MPa	21,6 MPa	14, 45 MPa	20,29 MPa	15,48 MPa

WNIOSKI

Wytworzone kompozyty polimerowe charakteryzują się znacznym wzrostem twardości oraz spadkiem wytrzymałości na rozciąganie wraz ze wzrostem zawartości naturalnego napełniacza w osnowie polipropylenowej. W badanych próbkach wytrzymałość materiału jest liniowo zależna od zawartości napełniacza. Własności mechaniczne wytworzonych kompozytów w dużej mierze zależą od zdolności wkomponowania się napełniacza z mączki w mikrostrukturę osnowy.

BIBLIOGRAFIA

1. M. Carus, A. Eder, L. Dammer, H. Korte, L. Scholz, R. Essel, E. Breitmayer, Wood-Plastic Composites (WPC) and Natural Fiber Composites (NFC); Conduct on European and Global Markets 2012 and Future Trends: Huerth, Niemcy, 2015.
2. I. Kruszelnicka, D. Ginter-Kramarczyk, M. Michalkiewicz, A. Kloziński, S. Zajchowski, P. Jakubowska, J. Tomaszewska, Kompozyty polimerowo-drzewne w technologii zawieszonego złoża ruchomego, Polimery (2014) 739-746.
3. A. Włodarczyk-Fligier, M. Polok-Rubiniec, Studies of resistance of PP/natural filler polymer composites to decomposition caused by fungi, Materials, 14 (2021) 1-18

MTS CONFERENCE
MATERIAL TECHNOLOGIES IN SILESIA

12-15.06.2022
Crystal Mountain***** Hotel, Wisła, Poland

The influence of the hybrid surface modification on electrochemical and physicochemical properties of Ti6Al4V alloy

A. Woźniak[a], M. Adamiak[a]

[a] Materials Research Laboratory, Silesian University of Technology, Konarskiego 18a Str., 44-100 Gliwice, Poland
email: anna.wozniak@polsl.pl

Abstract: The article describes the idea of the surface modification of the titanium alloy Ti6Al4V by laser texturing and deposition thin zinc oxide layer ZnO by Atomic Layer Deposition method (ALD). It was focused on physicochemical and electrochemical properties, especially corrosion resistance and electrochemical impedance spectroscopy in simulated human body environments. Additionally, the wear properties were too investigated. Based on the results obtained it can be concluded that the hybrid surface modification shows significant effects on the properties of the Ti6Al4V alloy. In effect surface modification by deposited zinc oxide, the corrosion behavior of Ti6Al4V alloy was improved. Additionally, laser texturing provides better wear properties compared to the material in its initial state.

Keywords: Ti6Al4V, ALD method, ZnO layer, layer texturing, corrosion

1. INTRODUCTION

Titanium and its alloys, especially pure titanium (Ti Grade II and Ti Grade IV) and Ti-6Al-4V alloy (Ti Grade V) are the most common metallic biomaterials for long-lasting implantation in the dental and orthopedic applications [1,2]. Titanium and its alloys are characterized by more favorable mechanical properties, relatively low elastic modulus, a low specific weight (strength-to-density ratio), and better corrosion resistance compared to the other metal biomaterials for long-term implant i.e. stainless steel 316L or cobalt-based alloy. Good corrosion resistance is associated with the ability to spontaneously form a thin and stable protective oxide layer, which constitutes a compact and dense kinetic barrier for extensive corrosion. However, the passive layer does not fully guarantee corrosion protection, because it can include some defects (inclusions and discontinuity—weak spots), which could become the initial areas of corrosion. Additionally, mechanical stress results in depassivation, bare metal exposure, repassivation and corrosion [3]. This is an important aspect, given that the human body environment is an aggressive corrosive environment. After surgical investigation, an implant can be surrounded by blood, as well as both dead and living bone tissue. Hence, the implanted material is exposed to a biochemically dynamic environment that tends to react causing corrosion/ionization. The corrosion resistance of titanium and its alloys is weakened in the presence of proteins from the albumin group and reactive oxygen species (ROS), such as hydrogen peroxide H_2O_2 [4]. The limitation of using titanium and its alloy in medical applications is also poor wear resistance, which is generally inferior to that of other metallic biomaterials. Based on the results of tribological and fretting resistance of three biomaterials – stainless steel SU304, cobalt-based alloy Co-39Cr-6Mo, and titanium alloy Ti6Al4V presented by Iwabuchi et al. [5] it can be concluded, that the Ti6Al4V alloy shows the best fretting resistance in Hanks' solution. But the wear rate of Ti-alloy becomes great in the sliding. This property is caused by the strong affinity of Ti to the Al_2O_3 ball, and the abrasion appears by the roughened surface of Al_2O_3. Similar results were presented by Beak et all [6] – it was found that the Ti6Al4V alloy is characterized by a lower wear resistance compared to most biomaterials. The poor wear resistance of the titanium and its alloy is associated with high chemical reactivity of titanium, and insufficient stability of the surface oxide layer. As a result of the exposure of the base material, titanium tends to crush material particles and scratch the friction surface, thereby increasing component wear (Fig. 1).

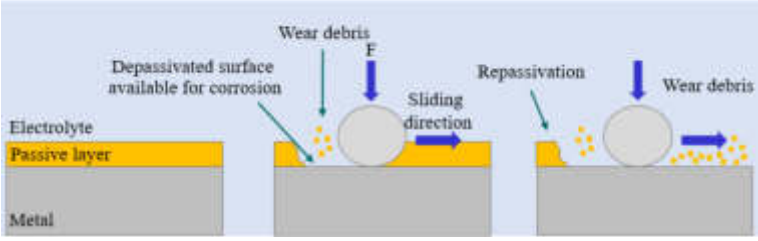

Figure 1.Scheme wear degradation in electrolyte environmental of metal biomaterials

In vivo corrosion and tribological wear of titanium, materials can, therefore, lead to the release of particles in the form of TiO_2, inorganic metallic salts, as well as free metal ions to the intraarticular joint space. In addition to material weakening during the corrosion process, there is a risk of the tissue reacting, promoting the release of corrosion products from the implant inside the body. Ions are deposited in the surrounding tissues leading to metallosis and cytotoxic effect in the implant cavity generating necrosis and complete implant failure [7]. Unfortunately, and contrary to popular belief, released titanium degradation products may cause serious side effects such as inflammation, pain, cytotoxicity, allergy, genotoxicity, and carcinogenicity. Additionally, titanium dioxide TiO_2 can alter the viability and behavior of multiple bone cells, which may result in bone resorption, aseptic implant loosening, and disrupt implant retention. Therefore, modifications of the surface properties of the titanium implants are still recognized as an important way to improve widely understood biocompatibility [8]. Currently, one of the most popular surface biomaterials modification methods is the Atomic Layer Deposition (ALD) method, which allows the deposition of extremely conformal and high-quality barrier layers with controllable thickness, even on complex three-dimensional surfaces. Among the many different types of coatings, currently used for biomedical purposes, very common are metal oxide coatings, such as TiO_2, Al_2O_3, ZrO_2, SnO_2, or ZnO, which are designed to increase not only the corrosion resistance of titanium alloy but also to changing the wetting angle, and in effect may cause decrease bacterial adhesion [9]. Additionally, in order to improve tribological properties, additional methods of treatment are considered, such as laser texturing [10]. Therefore, in the presented work we focused on the hybrid modification by the laser texturing, and ALD method. The aim of the presented work was to instigate the influence of the hybrid coating on the chosen properties, such as the value of contact angle, surface free energy (SFE), corrosion resistance, and wear resistance of Ti6Al4V alloy samples manufacturing by selective laser melting.

BIBLIOGRAPHY

[1] I. Ivlev, J. Vacek, P. Kneppo, Multi-criteria decision analysis for supporting the selection of medical devices under uncertainty, European Journal of Operational Research, 247 (2015) 216–228.
[2] C. Yan, L. Hao, A. Hussein, P. Young, Ti–6Al–4V triply periodic minimal surface structures for bone implants fabricated via selective laser melting, Journal of the Mechanical Behavior of Biomedical Materials, 51 (2015) 61–73.
[3] T. Hryniewicz, R. Rokicki, K. Rokosz, Corrosion and surface characterization of titanium biomaterial after magnetoelectropolishing, Surface and Coatings Technology, 203 (2009) 1508–1515.
[4] S.R. Sousa, P. Moradas-Ferreira, B. Saramago, L.V. Melo, M.A. Barbosa†, Human Serum Albumin Adsorption on TiO2 from Single Protein Solutions and from Plasma, Langmuir. 20 (2004) 9745–9754.
[5] A. Iwabuchi, J.W. Lee, M. Uchidate, Synergistic effect of fretting wear and sliding wear of Co-alloy and Ti-alloy in Hanks' solution, Wear. 263 (2007) 492–500.
[6] B.D. Beake, T.W. Liskiewicz, Comparison of nano-fretting and nano-scratch tests on biomedical materials, in: Tribology International, Elsevier Ltd, 2013: pp. 123–131.
[7] S. Raikar, P. Talukdar, S. Kumari, S.K. Panda, V.M. Oommen, A. Prasad, Factors affecting the survival rate of dental implants: A retrospective study, Journal of International Society of Preventive and Community Dentistry. 7 (2017) 351–355.
[8] J.C.M. Souza, S.L. Barbosa, E. Ariza, J.P. Celis, L.A. Rocha, Simultaneous degradation by corrosion and wear of titanium in artificial saliva containing fluorides, Wear. 292–293 (2012) 82–88.
[9] A. Woźniak, W. Walke, A. Jakóbik-Kolon, B. Ziębowicz, Z. Brytan, M. Adamiak, The Influence of ZnO Oxide Layer on the Physicochemical Behavior of Ti6Al4V Titanium Alloy, Materials (Basel). 14 (2021)
[10] B.S. Yilbas, H. Ali, A. Al-Sharafi, H. Al-Qahtani, Laser processing of Ti6Al4V alloy: wetting state of surface and environmental dust effects, Heliyon. 5 (2019) e01211.

MTS CONFERENCE
MATERIAL TECHNOLOGIES IN SILESIA

12-15.06.2022
Crystal Mountain***** Hotel, Wisła, Poland

Carbon coatings produced on nanobainite steel by RFCVD method

K. Wunsch, M. Tarnowski, K. Kulikowski, E. Skołek, J.R. Sobiecki

Warsaw University of Technology, Faculty of Materials Science and Engineering
email: robert.sobiecki@pw.edu.pl

Abstract: The article presents the initial research results on the influence of the process temperature and the composition of the gas atmosphere on nanohardness and adhesion to the substrate of carbon coatings produced by the RFCVD method on nanobainite steel before and after hardening. It has been shown that the coatings produced on steel after prior hardening show higher nanohardness and adhesion to the substrate. The coating obtained at a temperature of 100ºC and a nitrogen flow of 80 sccm shows the highest adhesion to the substrate.

Keywords: carbon coating, RFCVD method, nanohardness, nanobainite steel.

1. INTRODUCTION

Carbon coatings, including DLC (diamond-like-carbon) and a-C (amorphous carbon), are well known for their very high hardness and beneficial tribological properties, especially in terms of lowering the friction coefficient[1]. PACVD is one of the most promising methods for producing high quality carbon coatings on steels [2] and other metallic/polymer materials [3]. The papers aims to present properties and characterization of carbon coatings produced via RFCVD method on 35HGS steel of nanobainitic microstructure, what is not yet reported in the worldwide literature.

2. EXPERIMENTAL METHOD

The substrate was 35HGS steel with a nanobainite structure before and after hardening. The coating production process was carried out with the following parameters: t = 20min, P = 600W, p = 10^{-2}hPa, composition atmosphere CH_4 = 80sccm, H_2 in the range of 0-80 sccm, N_2 in the range of 0-80sccm, temperature in the range of 50-250°C Sputtering was carried out prior to the main process to clean and activate the surface of the samples t = 3 min., P = 600W, p =10^{-1}hPa, atmosphere: Ar=10 sccm, H_2=20 sccm. The coating adhesion and critical forces were tested on the CSM Instruments Scratch-test device. During the test, the normal force, frictional force, penetration depth and the acoustic emission signal related to cracking and decohesion of the layers were recorded. The length of the scratch 5 mm, the load from 1 to 30N. The adhesion analysis of the coatings was carried out by means of microscopic observations of the scratches using the Nikon Eclipse LV150N microscope. The nanoindentation tests were carried out on the NanoTest Alpha device using the following parameters: number of measurement points 9, maximum load 2mN, initial load 0.03mN, loading time 10s, unloading time 10s, dwell period 5s.

3. RESULTS

Fig. 1 shows the nanohardness results of carbon coatings produced on nanobainite substrates without (NB) and after hardening (M) in comparison to the nanohardness of the substrate. We can see that carbon coatings significantly increase the nanohardness of the nanobainintic substrate. It can also be seen that the nanohardness of the coatings produced on the hardened substrates is higher than on the non-hardened nanobainite substrate.

The adhesion tests showed that the absence of nitrogen or hydrogen in the reaction mixture results in a significant reduction in the adhesion of the coatings to the substrate, what is more, the coating produced without nitrogen in the atmosphere was destroyed after opening the working chamber. Figure 2a shows the image of the

scratch for the coating produced in the atmosphere of CH_4=80sccm and N_2=20sccm, while the fig. 2b shows the image of the scratch for the coating produced in the atmosphere of CH_4=80sccm N_2=20sccm H_2=20sccm.

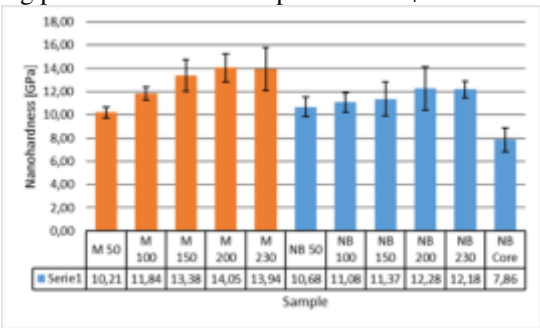

Fig. 1 Nanohardness of carbon coatings produced in RFCVD process.

a)
b)

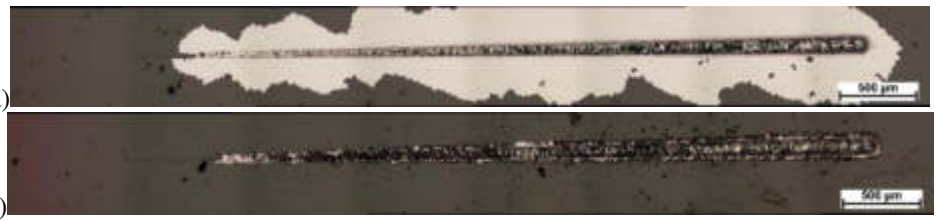

Fig. 2 Scratch images for the coating produced in the atmosphere of CH_4=80sccm and N_2=20sccm, (a) CH_4=80sccm N_2=20sccm H_2=20sccm (b)

The adhesion tests of carbon coatings both without and after hardening (Fig. 3a), showed that the highest critical force Lc1 is characteristic for a coating produced at a temperature of 100ºC. Increasing the temperature causes a reduction of the critical force until the coating obtained at a temperature of 250°C is completely peeled off. Lc1 values are much higher for coatings produced on hardened substrates. Therefore, the research on the influence of the gas atmosphere composition on the adhesion of coatings was carried out at a temperature of 100° C. It turned out that the coating produced with a nitrogen flow of 80 sccm (Fig. 3b) showed the best adhesion.

a)

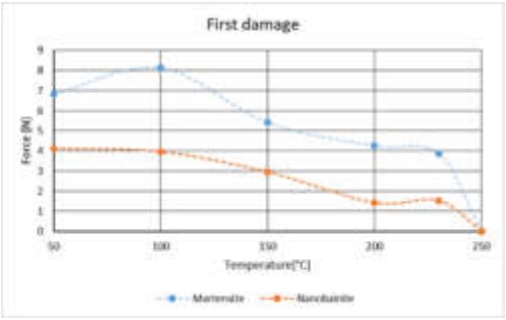

b)

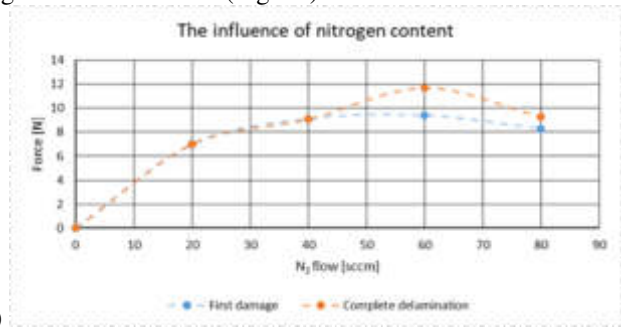

Fig.3 The results of coatings adhesion: influence of temperature (a), influence of nitrogen coating (b).

Acknowledgments: The financial support of the National Centre for Research and Development, Poland, is gratefully acknowledged, grant TECHMATSTRATEG-III/0028/2019.

BIBIOGRAPHY

1. J. Marciniak, Z Paszenda, W. Walke, M. Basiaga, J. Smolik, DLC coatings on martensitic steel used for surgical instruments, Archives of Materials Science and Engineering, 28 (5), 2007, 285-288.
2. K. Kyzioł, S. Jonas, K. Tkacz-Śmiech, K. Marszałek, A role of parameters in RF PA CVD technology of a-C:N:H layers, Vacuum 82 (10), 2008, 998-1002.
3 M. Tarnowski, K. Kulikowski, T. Borowski, B. Rajchel, T. Wierzchoń, Influence of amorphous carbon layers on tribological properties of polyetheretherketone composite in contact with nitrided layer produced on Ti6Al4V titanium alloy, Diamond and Related Materials 75, 2017, 123-130.

MTS CONFERENCE
MATERIAL TECHNOLOGIES IN SILESIA

12-15.06.2022
Crystal Mountain***** Hotel, Wisła, Poland

Właściwości wlewków ciągłych odlanych ze stali wytwarzanych z zastosowaniem samoredukcyjnego kompozytu

A. Żak[a], M. Adamczyk[a], M. Borecki[a], M. Rachwalski[b], P. Górny[b]
[a] Sieć Badawcza Łukasiewicz – Instytut Metalurgii Żelaza, email: artur.zak@imz.pl
[b] Cognor S.A. Oddział Ferrostal Łabędy w Gliwicach, email: marian.rachwalski@ferrostal.com.pl

Streszczenie:

W pracy przedstawiono wyniki badań i ocenę jakości wlewków ciągłych odlanych ze stali w gatunkach B500B i S235JR, które zostały wytworzone z zastosowaniem samoredukcyjnego kompozytu. Celem uzyskania pełnej charakterystyki doświadczalnych partii wlewków przeprowadzono analizę makrostruktury, mikrostruktury, wtrąceń niemetalicznych oraz geometrii wlewków i nieciągłości wewnętrznych.
Dla zoptymalizowania technologii ciągłego odlewania stali, wykorzystaniem programu ProCAST wykonano numeryczną symulację procesu COS obejmującą wyznaczenie zmian temperatury i udziału fazy stałej na przekroju poprzecznym w kolejnych fazach odlewania oraz symulację fizyczną procesu COS pozwalającą na wyznaczenie temperatur krytycznych, w tym zakresów temperatur występowania obniżonej plastyczności stali. Fizyczną symulację procesu ciągłego odlewania wykonano z wykorzystaniem symulatora Gleeble 3800. Uzyskane wyniki badań metaloznawczych oraz symulacji numerycznych i fizycznych procesu ciągłego odlewania pozwoliły na zoptymalizowanie technologii odlewania stali wyprodukowanych z zastosowaniem samoredukcyjnego kompozytu.

Słowa kluczowe: wlewek ciągły, makrostruktura i mikrostruktura wlewka COS, samoredukcyjny kompozyt

1. WPROWADZENIE

W przemyśle hutniczym na różnych etapach produkcyjnych powstaje duża ilość odpadów w postaci zgorzeliny stanowiącej potencjalne źródło żelaza. W Stalowni Ferrostal Łabędy powstaje rocznie około 1100 ton zgorzeliny. Opanowanie technologii zawracania żelazonośnych odpadów pozwala na ograniczenie ilości odpadów jak i zmniejszenie zużycia surowców. W ramach projektu POIR- INNOSTAL realizowanego przez firmę Ferrostal Łabędy i Sieć Badawczą Łukasiewicz–IMŻ opracowano technologię redukcji tlenków żelaza w łukowym piecu elektrycznym z wykorzystaniem reakcji aluminotermicznej różnoważącej w znacznym stopniu endotermiczną reakcję redukcji tlenków żelaza węglem. Równolegle z wprowadzeniem nowej technologii wytapiania stali wykonano badania właściwości wlewków ciągłych odlanych ze stali, których wytopy prowadzono z zastosowaniem samoredukcyjnego kompozytu. Badania wykonano na wlewkach ciągłych z doświadczalnych wytopów przemysłowych stali w gatunkach B500B i S235JR. Wytopy ze stali w gatunku S235JR zostały odlane we wlewki kwadratowe o przekroju 120 x 120 mm. Wytopy ze stali w gatunku B500B odlano we wlewki o przekroju kwadratowym 100 x 100 mm [1]. Proces odlewania prowadzono metodą dozatorową.

W celu zoptymalizowania technologii COS przeprowadzono symulacje numeryczne odlewania stali wykorzystaniem programu ProCAST obejmujące wyznaczenie zmian temperatury i udziału fazy stałej na przekroju poprzecznym w kolejnych fazach odlewania. Dla wyznaczenia zakresów temperatur występowania obniżonej plastyczności stali przeprowadzono fizyczną symulację procesu ciągłego odlewania z wykorzystaniem symulatora Gleeble 3800 [2].

2. ZAKRES I METODYKA BADAŃ

Zakres wykonanych badań obejmował:

- badania makrostruktury na przekroju poprzecznym i wzdłużnym,
- analizę makrosegregacji pierwiastków stopowych i domieszkowych na przekroju poprzecznym wlewka,
- analizę wtrąceń niemetalicznych,
- analizę mikrostruktury wlewków,
- symulacje numeryczne odlewania stali wykorzystaniem programu ProCAST,
- symulacje fizyczne procesu COS za pomocą symulatora Gleeble 3800w celu wyznaczenia temperatur krytycznych,
  w tym zakresów występowania temperatur obniżonej plastyczności stali.

Badania metalograficzne wykonano na odcinkach o długości około 300 mm pobranych z wlewków odlanych w środkowej fazie odlewania wytopów. Z odcinków wlewków wycinano tarcze poprzeczne, które po sfrezowaniu i oszlifowaniu trawiono w 50 % wodnym roztworze kwasu solnego w temperaturze otoczenia. Analizę wtrąceń niemetalicznych

prowadzono za pomocą mikroskopu skaningowego Inspekt F. Badania mikrostruktury na zgładach wytrawionych nitalem wykonano za pomocą mikroskopu świetlnego Olympus.

3. WYNIKI BADAŃ

Przykładowe wyniki badań makrostruktury wlewków z wytopów doświadczalnych na tarczach poprzecznych zamieszczono na rysunkach 1a i 1b. We wszystkich badanych wlewkach występuje zbliżony rodzaj makrostruktury. W warstwie zewnętrznej, która obejmuje naskórek wlewka występuje mieszana strefa drobnych kryształów równoosiowych i kolumnowych. We wlewku ze stali S235JR wysokość tej strefy jest równa około 13 mm, natomiast we wlewkach ze stali B500B wynosi około 10 mm. Poniżej naskórka występuje strefa kryształów kolumnowych o średniej wysokości około 30 mm. W środkowej części wlewka występuje strefa kryształów równoosiowych. W osi wlewków widoczny jest obszar porowatości/pustki środkowej o wysokości około 3 ÷ 8 mm. Przeprowadzona ocena makrostruktury wlewków odlanych ze stali z dodatkiem kompozytu wskazuje, że zastosowanie kompozytu nie powoduje obniżenia jakości wewnętrznej wlewków ciągłych. Porównanie uzyskanych wyników badań mikrostruktury i wtrąceń niemetalicznych z wynikami badań wlewków ze stali B500B wytworzonych według standardowej technologii, tj. bez stosowania kompozytu zawierającego zgorzelinę [2] wskazuje, że wlewki z wytopów doświadczalnych charakteryzują się zbliżoną budową mikrostruktury i rodzajem wtrąceń niemetalicznych. W badanych wlewkach głównym rodzajem wtrąceń niemetalicznych są złożone tlenko-siarczki zawierające Si, Al, Mn, Mg, Ca i Si oraz globularne siarczki manganu.

Na rysunku 2 zamieszczono zmian plastyczności stali B500B w funkcji temperatury odkształcenia uzyskany w próbach symulacji fizycznej wykonanych za pomocą symulatora Gleeble,

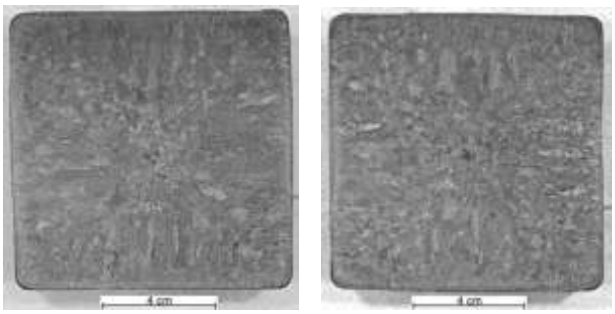

a) b)

Rys. 1. Makrostruktura przekroju poprzecznego wlewków ze stali B500B, a) z wytopu stali z dodatkiem kompozytu, b) z wytopu stali bez dodatku kompozytu

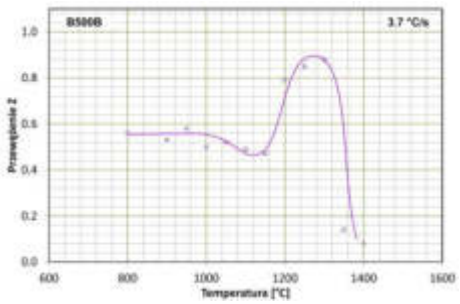

Rys. 2. Zmiana plastyczności stali B500B w funkcji temperatury odkształcenia, określona na próbkach chłodzonych ze stanu ciekłego do temperatury odkształcenia

Pracę wykonano w ramach programu POIR 2014-2020, działanie 1.2-INNOSTAL, nr umowy:POIR.01.02.00-00-0163/16

LITERATURA

1. A. Mazur, Z. Łapczyński, A. Żak, B. Walnik, Sprawozdanie z pracy badawczej IMŻ nr B0-1656-11 „Fizyczna i numeryczna symulacja procesu ciągłego odlewania stali z uwzględnieniem zmian w procesie wytapiania stali", czerwiec 2019, materiał niepublikowany
2. A. Żak, J. Marcisz, B. Walnik, M. Adamczyk, Sprawozdanie z pracy badawczej IMŻ nr B0-1656-10-02, "Opracowanie zaleceń technologicznych do ciągłego odlewania wlewków ze stali wykonanej z zastosowaniem kompozytów żelazonośnych", czerwiec 2019; materiał niepublikowany

MTS CONFERENCE
MATERIAL TECHNOLOGIES IN SILESIA

12-15.06.2022
Crystal Mountain***** Hotel, Wisła, Poland

The heat generated analysis during static and dynamic deformation of high manganese steels

M.B. Jabłońska

[a] Silesian University of Technology, Faculty of Materials Engineering, Department of Technology of Materials
email: Magdalena.jablonska@polsl.pl

Abstract: The aim of the work is the explanation and description of properties and some structural aspects occurring in high manganese steels with TWIP effect during static and dynamic deformation, taking into account the heat generated during the deformation. The steels with SFE in a range which defined the main deformation mechanism as twinning was deformed by the standard tensile tests as well as by the tensile with high strain rates on flywheel machine. During the tensile tests the temperature distribution was analysed with a thermal imaging camera as well as was calculated by the numerical modelling. On the base of these results the temperature distribution during dynamic tensile tests was calculated only on the base of by the numerical modelling. Moreover a 2D finite element thermo-mechanical model of uniaxial tensile tests will be developed to determine local strain in samples conducted static and dynamic deformation. Obtained results allow presenting the influence of heat generated on the main deformation mechanism regarding strain rate and chemical composition.

Keywords: steels, deformation, strain rate, properties

1. INTRODUCTION

Steels for light-weight construction have been developed to satisfy the requirements of passive safety, weight reduction, and energy saving as well as economic mass production by the automotive industry. Hence, the development of strong, tough, and ductile new steels for automotive applications is an essential topic in steel research. In this approach, twinning-induced plasticity steels (TWIP) with up to 30 wt.% Mn, 5 wt.% Al and >0.4 wt.% C content have shown an interesting combination of ductility and strength with the reduction in mass density. A literature study and own investigations became a basis for formulation of assumptions, that the hardening of a high-manganese austenitic steels while maintaining its high plasticity under conditions of dynamic deformation depends on its ability to generate deformation twins and on evolution of the dislocation structure which are connected by the heat generated [10].
The literature defined that associated deformation energy is predominantly dissipated via defect motion, leading to a distinct thermomechanical response. In metals, this can result in local temperature increases of up to several hundred Kelvin. Chen et al. measured overall temperature increases in Fe–Mn–C steels due to the Portevin–LeChatelier effect of about 110°C [11]. The temperature can affect on the dominant deformation mechanism.

2. RESULTS

It has been proved that application of the accepted plan of studies on properties, including static and dynamic tensile tests, allows for obtaining a characteristics of mechanical and plastic properties of the steel, which may be useful in application of the steel for structural elements under dynamic loads. The temperature distribution during static tensile tests measured by the experimental method reveals increasing the temperature in breaking zone up to

120ºC and 220ºC (Fig.1). During the dynamic tensile tests the temperature growth could be higher than 250ºC (Fig1.). This situation can change the dominant deformation mechanism from twinning to the dislocation glide.

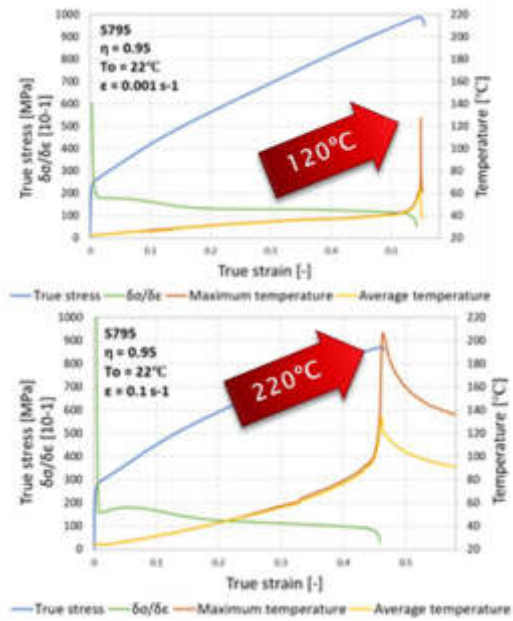

Fig.1. True stress – true strain curves and the local temperature distribution in MnAl steel during tensile tests.

Acknowledgments: The work supported by the Polish Ministry of Science and Higher Education within the framework of the project Effect of the heat generated during deformation at high strain rates on the structure and properties of high manganese steels with twinning as the dominant deformation mechanism - UMO-2019/35/B/ST8/02184

BIBLIOGRAPHY

1. D. Barbier, N. Gey, S. Allain, N. Bozzolo, and M. Humbert, Mater. Sci. Eng. A 500, 196 (2009).
2. F.G. Caballero and H.K.D.H. Bhadeshia, Curr. Opin. Solid State Mater. Sci. 8, 251 (2004).
3. M. Calcagnotto, Y. Adachi, D. Ponge, and D. Raabe, Acta Mater. 59, 658 (2011).
4. B.C. De Cooman, O. Kwon, and K.G. Chin, J. Mater. Sci. Technol. 28, 513 (2012).
5. M. Calcagnotto, D. Ponge, and D. Raabe, ISIJ Int. 48, 1096 (2008).
6. B.C. De Cooman and J.G. Speer, Steel Res. Int. 77, 634(2006).
7. Y. Toji, H. Matsuda, M. Herbig, P.-P. Choi, and D. Raabe,Acta Mater. 65, 215 (2014).
8. F.G. Caballero, H.K.D.H. Bhadeshia, J.A. Mawella, D.G.Jones, and P. Brown, Mater. Sci. Technol. 17, 517 (2001).
9. L. Yuan, D. Ponge, J. Wittig, P.P. Choi, J.A. Jiminez, and D.Raabe, Acta Mater. 60, 2790 (2012).
10. M.B. Jabłońska, Structure and properties of a high-manganese austenitic steel strenghtened in the result of mechanical twinning in processes of dynamic deformation, Wydawnictwo Politechniki Śląskiej, Gliwice, (2016).
11. A. Eisenlohr, I. Gutierrez-Urrutia, D. Raabe, Acta Materialia, Volume 60, Issue 9, Pages 3994-4004, (2012). .

MTS CONFERENCE
MATERIAL TECHNOLOGIES IN SILESIA

12-15.06.2022
Crystal Mountain***** Hotel, Wisła, Poland

Effect of laser alloying on corrosion of commercially pure titanium grade

Z. Brytan[a], T. Tański[a], M. Wiśniowski[b],

[a] Silesian University of Technology, Faculty of Mechanical Engineering, Department of Engineering Materials and Biomaterials, ul. Konarskiego 18a, 44-100 Gliwice, Poland
[b] BOS Innovation and Technology Center, aleja Roździeńskiego 188H, 40-203 Katowice, Poland
email: zbigniew.brytan@polsl.pl

Abstract: The purpose of the present work is to evaluate the corrosion behaviour of CP titanium grade 1 subjected to laser surface alloying (LSA) by Fe-Cr powder. The scope of the LSA process of titanium grade 1, that is α phase alloy, was the development of mixed α/β microstructure in the alloyed layer, thus β-stabilisers such as Fe and Cr were used in the form of ferrochromium powder (the ratio of element Fe/Cr was 75/25). The LSA was realized by a high-power direct-diode laser (HPDDL) with varying laser power (1 and 2kW) and scanning speed (0.2 and 0.5m/min) and a constant powder feed rate of 1.5 g/min. In the presented study, selected LSA processing conditions demonstrated the ability to improve the corrosion resistance of titanium alloy in a chloride-containing environment.

Keywords: CP titanium grade 1, LSA, HPDDL, corrosion

1. INTRODUCTION

Laser surface alloying (LSA) is a well-known metal surfacing process that uses a laser beam as the source of energy. Depending on the chemistry of the processed alloy and the resulting cooling rate, significant changes in the morphology of the structure occur, e.g., expanding ranges of equilibrium phases and/or the formation of new intermetallic phases. The fast cooling rate of the molten material in the LSA can result in a surface layer with improved mechanical, physical and chemical properties. LSA, e.g., was successfully used to improve erosion wear resistance of Ti6Al4V applied for rotors and fan blades of modern turbofan engines [1]. The corrosion resistance of the LSA surface also changes, it does not necessarily improve, which is due to the more complex and heterogeneous structure of the surface layer, and the presence of secondary phase precipitates that can form corrosion cells accelerating the corrosion rate. When an appropriate LSA strategy is selected, laser type/process conditions/alloying material, the corrosion resistance of titanium alloys can be improved. An example of this is laser gas alloying with the nitrogen of β titanium alloy [2]. The development of laser techniques, and in particular the high-power direct-diode lasers (HPDDL), opens new possibilities for surface modification and improvement of material properties, also for Ti alloys. Compared to other kinds of lasers (solid state YAG and gas lasers), the HPDDL have particularly advantageous characteristics for the LSA [1]. It is related to the rectangular laser beam spot of the multimode and the uniform intensity of laser radiation that is very profitable in the case of laser surface treatment (remelting and alloying). The above features ensure that the processed surface is heated uniformly, so uniform penetration depth and uniform thickness of the surface layer can be achieved, which is not the case with the circular laser beams of YAG and gas lasers.

Titanium alloys are commonly divided into three groups, depending on the main phases present: alloys α, α-β and alloys β, sometimes also subgroups of almost-α grades are derived. Unalloyed Commercially Pure (CP) titanium is represented by four distinct grades, where grade 1 is the highest purity grade. The CP titanium family is a class of α alloys that differs by the amount of O and Fe in each alloy. The mechanical properties of titanium are greatly dependent on the content of O, N, H and Fe. They increase the hardness, yield point and tensile strength of the material while simultaneously reducing the elongation. Titanium Grade 1 shows high plastic properties, formability, and thus excellent cold deformability and low mechanical properties, compared to other CP grades. Moreover, it exhibits excellent corrosion resistance in highly oxidizing to mildly reducing environments, including chlorides.

2. MATERIALS AND METHODS

CP titanium grade 1 was subjected to laser surface alloying (LSA) with Fe-Cr powder. The scope of the LSA process of titanium grade 1 (α alloy) was the development of α/β microstructure at the alloyed layer, thus β-stabilisers such as Fe and Cr were used in the form of ferrochromium powder (Fe/Cr ratio was 75/25). The LSA was realised by a high-power direct-diode laser (HPDDL) with varying laser power (1 and 2kW) and scanning speed (0.2 and 0.5m/min), a constant powder feed rate of 1.5 g/min in an Ar protective atmosphere. The microstructure was studied by optical and scanning microscopy with the support of EDS analysis. The corrosion resistance of the LSA surface was evaluated in 3.5% NaCl solution using a standard electrochemical method and Tafel analysis.

3. RESULTS

LSA of titanium grade 1 with Fe-Cr results in a complex structure in the surface layer. Starting from the base material that is fully α phase a very narrow HAZ may be distinguished and a sharp crystallisation front is formed. The next zone is a proper melting zone, where the molten alloying elements (Fe-Cr) were fully mixed with titanium. The microstructure in this zone is composed of the martensitic matrix of ca. 70%Ti, 20%Cr and 10%Fe - at.% of β phase and small secondary precipitates (of acicular and spheroidal shape) of α phase and probably FeTi and ternary Laves phases type $Ti(Fe_{1-x}Cr_x)_2$)) [3]. The upper zone of the remelted area shows some non-fully dissolved powder particles (Fe-Cr) that protrude from the surface, considerably increasing surface roughness. Between non-fully melted powder particles and α/β matrix also transient zones exist, and various secondary precipitates (intermetallics, nitrides) appear.

The corrosion resistance of LSA titanium grade 1 in 3.5% NaCl (Table 1) was decreased when compared polarisation resistance (R_p) to the untreated sample. The (R_p) value of the LSA surface decreased two or three times. When analysing LSA samples, the higher polarization resistance is obtained when higher laser beam power (2kW) and faster scanning speed (0.5m/min) are applied. Such processing parameters ensure higher energy input to the melting zone, thus higher dilution rate of alloying power, more uniform distribution of alloying elements and more uniform microstructure. LSA also shifts the corrosion potential (E_{cor}) to more positive values. Generally, the corrosion potential in the corrosion thermodynamics describes the difficulty level of corrosion. The higher the corrosion potential, the better the anticorrosion properties. Ultimately, based on the corrosion potential, LSA improved the corrosion resistance of the surface

Table 1. Electrochemical parameters of LSA titanium grade 1 with FeCr in a 3.5% NaCl solution

Sample	Laser power, kW	Scanning speed, m/min	Powder feed rate, g/min	I_{cor}, nA ·cm^{-2}	E_{cor}, mV	R_p, kΩ ·cm^2
Grade 1	-			73	-84	164
LSA with FeCr	1	0.2	1.5	150	-78	43
	2	0.5		135	-67	67
	2	0.5	3.0	108	-48	85
	1	0.2		162	-44	43

4. CONCLUSIONS

The corrosion resistance of LSA titanium grade 1 is related to process parameters that determine the dilution rate of alloying powder and the resulting microstructure. In the presented study, selected LSA processing conditions demonstrated the ability to improve the corrosion resistance of the titanium alloy in a chloride-containing environment.

BIBLIOGRAPHY

1. A. Lisiecki, A. Klimpel, Diode laser surface modification of Ti6Al4V alloy to improve erosion wear resistance, Archives of Materials Science and Engineering, Volume 32 Issue 1, (2008) 5-12.
2. C. W. Chan, S. Lee, G. Smith, G. Sarri, et. al, Enhancement of Wear and Corrosion Resistance of Beta Titanium Alloy by Laser Gas Alloying with Nitrogen, Applied Surface Science, 367, (2016) 80-90.
3. S. Wanga, et. al, Thermodynamic modeling of Ti-Fe-Cr ternary system, Calphad, vol 56 (2017), 160-168, https://doi.org/10.1016/j.calphad.2016.12.007.